Università degli Studi di Cagliari

Ph.D. DEGREE

Earth and Environmental Sciences and Technologies

Cycle XXXIV

Valorisation of organic residues through hydrothermal carbonization

Scientific Disciplinary Sector ICAR/03

Ph.D. Student: Gianluigi Farru

Supervisor: Giovanna Cappai

Final exam. Academic Year 2020 – 2021

Thesis defence: April 2022 Session

I wish the reader a delightful read. I hope they will enjoy the work proposed as much as I loved producing it and that they find it as interesting as I do.

Contents

Introduction

In recent years, our planet has been facing severe environmental threats with consequences for the health of plants, animals, and humans. Environmental degradation and climate change impact the global social and economic balance, raising the concern worldwide and changing the point of view of governments and people towards environment protection, energy production and applications, soil and water health, waste management and various other fields. A clear sign is the recent outcome of the 26th Conference of the Parties (COP26), the global climate summit, gathering 197 nations that recognised the seriousness of the environmental conditions and agreed to a new environmental pact. Several challenges have been pointed out.

To overcome these challenges, various tools have been introduced by governments. In Europe, the European Green Deal is thought to transform the EU into a resource-efficient and competitive economy by reducing net greenhouse gases (GHG) emissions by 2050 and decoupling economic growth from the reckless exploitation of natural resources facilitating waste re-entry into the circular economy. Another challenge is increasing the soil carbon in agriculture, restoring degraded land, and ensuring that soil ecosystems are healthy by 2050.

In concrete, the EU will increase funding for research into environmental technologies to meet these new challenges recognising that good practices and new technologies are essential.

Globally, the only food sector produces more than one-third of global anthropogenic GHG emissions, derived from the 11-19 billion tons of emissions per year estimated by the Intergovernmental Panel on Climate, and incorrect waste management pushes the food supply chain to the top of the list of GHG emitters, as reported by the United Nations Agriculture Agency during the COP26 climate conference in Glasgow in 2021.

Worldwide, organic waste, such as food waste, biomass, agricultural residues, etc., are generated in large quantities and only partially reused for production purposes. Traditional waste management methods have highlighted limits in terms of environmental compatibility or applicability, or added value of the recovered products (Alibardi et al., 2020; Muntoni, 2019).

In recent years, some studies (Ferrentino et al., 2021; Rezaee et al., 2020) focused on integrating several biomass conversion technologies to optimise different treatment systems. Several biochemical, thermochemical and physicochemical processes, along with various technologies, are available to convert biomass and, in general, organic residues into energy and value-added materials.

This strategy may be desirable from an environmental and economic perspective, particularly in light of the concepts of circular economy and biorefinery, allowing to rationalise the exploitation of natural resources and use processes that have little and controlled impact on the environment.

Anaerobic digestion (AD) is a widely used biochemical conversion process, capable of recovering energy from organic waste (e.g., food waste, sewage sludge, and municipal solid waste (MSW)), and reducing environmental pollutants and GHG emissions. Through the activity of different groups of microorganisms, lipids, polysaccharides, and proteins are converted into CH_4 and CO_2 by hydrolysis, acidogenesis, acetogenesis, and methanogenesis. The two main products of AD, biogas and digestate, play an increasingly important role in the future of the global circular economy, improving resource recovery and nutrient recycling (Rezaee et al., 2020).

However, the traditional use of sewage sludge digestate as an organic soil improver is becoming increasingly limited for environmental and economic reasons: first, the nutrients contained in digestate can percolate to groundwater, causing pollution; secondly, gaseous emissions into the atmosphere may occur, in particular CO_2 and nitrogen compounds, caused by the decomposition of the non-recalcitrant carbonaceous components of the digestate, which represents a loss of energy, linked to the energy content of the digestate itself (Pecchi & Baratieri, 2019). In fact, digestate still contains a high amount of organic matter that can be exploited for energy production through thermochemical conversion processes, such as hydrothermal carbonization (Ferrentino et al., 2021). The hydrothermal carbonization process allows recovering energy from wet raw materials, e.g., digestate, wastewaters, or biomass. Given the high moisture content, the processes of dehydration and separation of the produced liquid and solid phases, necessary for direct use as fuel, require a high amount of energy, and, therefore, the HTC process is a better option.

Although known for some time, in recent years, the process has again aroused great and widespread interest as it is suitable for the full recovery of the chemical value of the residual material, especially with high humidity content. Furthermore, HTC is characterised by greater flexibility in terms of enhancement options compared with more commonly used systems. In fact, hydrochar, in addition to immobilising carbon in a stable form, can be used as a fuel with reduced CO_2 emissions, as a soil improver for agricultural use, and as an adsorbent for the removal of pollutants. The process water can instead be treated by anaerobic digestion owing to the organic load derived from the hydrolysing capacity of the HTC, even for complex organic compounds. This flexibility of use is consistent with the principles of the circular economy, and the aforementioned enhancement options fully meet some critical and global issues of the agricultural sector.

In the framework of the doctoral course "Earth and Environmental Sciences and Technologies" held at the University of Cagliari, this work is the result of three years of experimental activities, literature study, and comparison and discussion with international colleagues and researchers. The main activities have been carried out in Cagliari; however, a six-month period was spent in Potsdam (Germany) at the Leibniz Institute (ATB) under the supervision of Dr Judy Libra, where it was possible to learn several methods and meet skilled and competent researchers to share opinions and discuss the obtained results. This manuscript reports on the experimental activities carried out according to the intended aims of the PhD project, despite the recent pandemic (COVID-19) caused by the SARS-CoV-2 virus, which delayed experimental activities and forced a re-planning of work.

In this work, the HTC treatment of different organic feedstocks is presented. In detail, the valorisation of specific residues is investigated, converting them into new materials. Solid and liquid products are tested to be used in different applications to exploit their energy content, apply on soil as ameliorant, or be transformed into unharmful materials for easier management.

This work consists of eight chapters in which a particular feedstock is presented, and the results of its valorisation are discussed. Each chapter is presented in the form of journal publication, and it is anticipated by a general introduction of the main topic and the scientific question that the chapter faces.

The main structure of the thesis is as follow:

- Chapter 1 – *State of the Art*

  This chapter presents a brief overview of the general knowledge of the thermochemical processes, the advantages and disadvantages, and the theory behind the hydrothermal carbonization process. This section summarises the crucial aspects of the HTC process, the parameters and conditions that affect the resulting products, and the possible applications investigated by several authors, giving a helpful tool for understanding the obtained results presented in the following chapter.

- Chapter 2 – *Hydrothermal carbonization of hemp digestate: influence of operating parameters*

  This chapter reports the experimental work done in collaboration with Sardegna Ricerche (regional research centre in Sardinia) on the HTC treatment of hemp and digestate from anaerobic digestion of hemp. In the discussion, the results of the carbonization of both the

materials are presented, suggesting a feasible valorisation way for digestate and comparing with hemp straw.

- Chapter 3 – *Hydrothermal carbonization of agro-industrial waste: a sustainable option towards GHC reduction and waste valorisation*

  The experimental work conducted on grape marc and residues of grape marc after ethanol-solution extraction is presented in Chapter 3. The results and discussion propose an alternative application of grape marc instead of typical uses. The energetic valorisation of hydrochar and process water from grape marc is discussed, along with the possible applications on soil.

- Chapter 4 – *Valorisation of Spent Coffee Grounds through hydrothermal carbonization*

  This chapter explores the valorisation of spent coffee grounds, a wet and widely produced organic residue. The carbonization and the exploitation of solid and liquid HTC products are tested and discussed. In particular, the use of hydrochar as solid fuel or as soil amendment is deeply investigated. Moreover, in this chapter, a post-treatment for hydrochar is tried out and reported.

- Chapter 5 – *Benefits and limitations of using hydrochars from organic residues as replacement for peat on growing media*

  This chapter presents the results of the experimental work based on the feasibility of using HTC products as suitable materials for plant growth. This work was realised in collaboration with the Biochar research group at the Leibniz Institute – ATB (Leibniz Institute for Agricultural Engineering and Bio-economy e.V.) led by Dr Judy Libra in Potsdam (Germany). Germination tests conducted on hydrochar from cow manure digestate, spent coffee grounds, and grape marc are reported. In addition, the inhibiting effects on germination caused by process water when used in fertigation are discussed and different bioassay and parameters are tested to be feasible indexes for soil applications.

- Chapter 6 – *Cigarette butts: a valuable raw material? A preliminary evaluation of their potential recovery as a solid fuel*

  The carbonization of cigarettes butts and residues of HEETS (heat-not-burn tobacco product) is reported in this chapter. In detail, the current management of this kind of residues and their potential valorisation/treatment via HTC is presented here.

- Chapter 7 – *Valorization of PPE waste produced during COVID-19 pandemic through Hydrothermal Carbonization (HTC): a preliminary study*

  In Chapter 7, the carbonization and disinfection of PPE, such as facial masks, derived by the ongoing COVID19 pandemic, is reported suggesting HTC as a suitable treatment for their safe handling and sustainable management. This work was realised in collaboration with the Biochar research group at the Leibniz Institute – ATB led by Dr Judy Libra in Potsdam (Germany) and Dr Kyoung Ro (USDA-ARS, Florence, SC - USA).

- Chapter 8 – *Process waters characterisation for their valorisation and suitable treatment*

  Chapter 8 summarises the results obtained on the process water characterisation and biological treatments. Some of the results have already been reported in the previous chapters, but they are presented here in a different key to discuss the issues deriving from their nature and possible valorisation.

Finally, the conclusions summarise the most interesting findings for each material tested, contributing to the global understanding of the HTC process and suggesting feasible applications for the new materials produced and, therefore, possible valorisation paths based on the data previously discussed for all the organic feedstocks treated. Moreover, the future needs and challenges and the limitations of the process deriving from the experimental activities are discussed.

An additional section (Supplementary materials) reports all the partial and preliminary results not covered in the manuscript, along with the pictures of the devices and materials used in this works.

Chapter 1

State of the Art

This chapter summarises the state of the art of the thermochemical processes commonly applied to convert biomass and organic materials into added-value by-products. In detail, the discussion focuses on the hydrothermal carbonization process describing the overall features and characteristics, the applications and the knowledge achieved to date.

1.1   Definitions

In the last decades, several new thermochemical technologies have been proposed to be suitable treatments for the production of solid materials. Scientific literature reports numerous publications where thermal processes are applied on diverse feedstocks using different operative conditions. However, this has resulted in a vast number of different terms to indicate the resulting solid product that may cause confusion and that it is due to a lack of standardised definitions for the processes and their products (Libra et al., 2011). Sometimes, these terms depend on the generating process and their applications. Some of these terms found in the literature are reported in Table 1.1 and their common definition used in this work. Therefore, it is essential to distinguish between terms such as biochar, charcoal, and hydrochar, where their final fate is the main difference between these materials. Charcoal is a carbon-rich solid product prepared from the carbonization of natural organic materials and is used for energetic purposes (i.e., energy production by combustion), whereas biochar is a synonym for charcoal when used on soil applications (e.g., soil improvement and carbon capture and storage). On the other hand, hydrochar is similar to biochar but is hydrothermally produced. Typically, biochar is produced as a solid product in a dry carbonization process like pyrolysis, while hydrochar is produced as a solid-liquid mixture. However, biochar and hydrochar differ significantly in their physical and chemical properties.

Table 1.1 – *Common terms and definitions used to indicate thermal processes-derived solid products.*

Term	Definition	Source
Coal	Sedimentary rock, generally used as solid fuel	-
Char	A solid decomposition product of a natural or synthetic organic material	(IUPAC, 1997)
Coke	A solid high in content of the element carbon and structurally in the non-graphitic state. It is produced by pyrolysis of organic material that has passed, at least in part, through a liquid or liquid-crystalline state during the carbonization process	(IUPAC, 1997)
Charcoal	Char obtained from wood, peat, coal or some related natural organic materials; usually used for cooking purposes	(Fitzer et al., 1995; IUPAC, 1997)
Biochar	Term used in the fields of soil and agricultural sciences to indicate a char, generally produced via pyrolysis, which is applied to soil with the intent to improve soil properties	(Lehmann & Joseph, 2009; Libra et al., 2011)
Pyrochar	Char produced from pyrolysis or torrefaction (biochar)	(Arauzo et al., 2020)
Hydrochar	Regardless of its application, char produced from hydrothermal carbonization	(Libra et al., 2011)

1.2   Thermochemical conversion processes

Thermochemical conversion technologies include several processes such as combustion, gasification, and pyrolysis, which aim to transform the inputs, generally residues, into by-products for the recovery of energy, materials, and chemical compounds with higher value. Technically, combustion is the most straightforward process, and it is widely used to generate energy, burning waste (e.g., urban waste) or biomass. However, combustion produce emission (such as CO_2, CO, NOx, SOx) and the overall efficiency of heat generation from organic materials is often low due to their generally high water and ash content (A. Kumar et al., 2009). Indeed, both have a great influence on combustion properties and calorific value. The higher the humidity, the more energy is

required to remove the water and, therefore, less energy is recovered (Bartlett et al., 2019). Processing wet materials is generally not economical for technologies like combustion because a high level of energy is consumed for drying. Other processes, such as hydrothermal treatments, are more efficient in eliminating the pricey drying step, making them an attractive solution (A. Kumar et al., 2009).

1.3   Pyrolysis

Pyrolysis is a thermochemical decomposition process that converts organic materials into a carbon-rich solid residue, a bio-oil, and gas (CO, CO_2, CH_4, and H_2) by heating in an oxygen-free environment (Demirbaş, 2001; Mohan et al., 2006). Depending on the reaction time, temperature, and heating rate, the pyrolysis process can be sub-divided into slow, intermediate, fast, and flash pyrolysis. (A. Ahmed et al., 2018; Onay & Kockar, 2003).

Slow pyrolysis is commonly used to produce biochar for agricultural purposes, with bio-oil and synthesis gas as by-products (Onay & Kockar, 2003). Typically, it is carried out at atmospheric pressure, with heat supplied by partial combustion of the feed by external heaters or by hot gas recirculation. Typical yields of biochar, bio-oil, and synthesis gas are 35%, 30%, and 35% of the dry biomass of the feedstock, respectively. However, the heat flux, pyrolysis temperature, processing time, gas conditions, feed density, and particle size influence the yield and properties of the biochar. Of these factors, the peak temperature (highest temperature) during pyrolysis is critical to determining the yield and quality of the biochar. The pyrolysis of vegetative materials begins as early as 190 °C. At temperatures above 250 °C, carbohydrates lose mass at a significant rate and release CO_2 and CO. The efficiency of biochar yield decreases significantly with the increase of pyrolysis temperature, especially after exceeding the temperature of 480 °C (Song & Guo, 2012). During slow pyrolysis, the biomass is heated in the temperature range of 300 - 650 °C with residence times from several minutes to a couple of hours and low heating rates, about 10-30 °C/min (Kambo & Dutta, 2015; Onay & Kockar, 2003).

In contrast to slow pyrolysis, fast or flash pyrolysis operates at a higher temperature for a shorter time. The material is rapidly heated, evaporates, and condenses into a dark brown mobile liquid (bio-oil) with a calorific value of about half the calorific value of conventional fuel oil. While it is associated with the traditional pyrolysis processes used to produce biochar, fast pyrolysis is a more advanced process that must be carefully controlled to obtain high liquid yields. Firstly, very high heating rates need to be provided, requiring finely ground biomass. Subsequently, the temperature

should be carefully controlled to around 500 °C. Rapid cooling of the pyrolysis vapours to obtain bio-oil is also important. The main product (bio-oil) is obtained with a yield of up to 80% of the dry feedstock, along with the by-product and gas used in the process, so there are no waste streams. For optimal performance of chemicals and food additives, vapour residence times of several hundred milliseconds are required, while fuels can tolerate vapour residence times of up to about 2 seconds. Longer residence times may significantly reduce the organic yield (Bridgwater, 2000; Onay & Kockar, 2003).

Intermediate pyrolysis occurs between the slow and fast pyrolysis reaction conditions, including moderate operating temperatures up to 500 °C, feedstock residence times of 0.5 - 25 min, and vapour residence times of 2 – 4 s. The product distribution generated by this process is typically 40 – 60% pyrolysis liquids, 20 – 30% non-condensing vapours, and 15 – 25% biochar, with the pyrolysis liquids and vapours being further converted into electricity, heat, and transport fuels. In particular, the biochar obtained by intermediate pyrolysis is dry and has a brittle texture as it contains less tar and therefore less toxic compounds, which makes it suitable for downstream uses such as solid fuel, soil additive and fertiliser (A. Ahmed et al., 2018; Kebelmann et al., 2013).

1.4 Gasification

Gasification is a process of partial combustion and takes place at high temperatures in the presence of an oxidizing agent (also called a gasifying agent, such as oxygen, air, vapour). Heat is supplied to the gasifier directly or indirectly, increasing the gasification temperature to 600 - 1200 °C for a short residence time between 10 – 20 s (Kambo & Dutta, 2015). Oxidising agents are usually air, water vapour, nitrogen, carbon dioxide, oxygen, or combinations. With a high-temperature oxidising agent, the large polymeric biomass particles decompose into lighter particles and eventually into permanent gases (CO, CH_4, H_2, and lighter hydrocarbons), ash, char, tar, and fine pollutants, where char and tar are the result of incomplete biomass conversion.

In order to obtain the desired gas composition and the minimum amount of impurities, the gasification operating conditions should be optimised. The main operating conditions regarding the quantity and composition of the gaseous product and its impurities are the biomass flow rate, the type and properties of the biomass, the flow rate of oxidising agents, the type and quantity of catalysts, the design of the gasifier, and the gasification temperature. Gasification temperature is one of the most important factors influencing the composition and properties of the gas in the product. Higher temperature results in increased gas yield due to higher conversion efficiency. At

temperatures above 750 - 800 °C, the endothermic nature of the H_2 production reaction (steam reforming and gas-water reactions) causes the H_2 content to increase and the CH_4 to decrease with increasing temperature. At temperatures above 850 - 900 °C, both steam reforming and Boudouard reactions dominate, increasing CO content. High temperature also promotes tar destruction and reforming, leading to a decrease in tar content and an increase in gas yield (A. Kumar et al., 2009). The primary product of gasification is a mixture of gases (>85 %). Moreover, the process ends with a small amount of biochar (less than 10%). Biochar produced in the gasification process contains large amounts of alkali metals and alkaline earth metals (such as Ca, K, Si, Mg) and polyaromatic hydrocarbons (PAHs), which are highly toxic compounds produced as a result of high-temperature reactions (Kambo & Dutta, 2015).

1.5   Hydrothermal processes

Hydrothermal processing is an outstanding method of converting wet organic materials into valuable products. Indeed, it offers the advantage of directly handling high-moisture materials, excluding an energy-intensive pre-treatment step, like drying. Hydrothermal conversion is a thermochemical process involving the thermal transformation of biomass in water under sub or supercritical conditions (critical point: T_c = 374 °C, p_c = 22.1 MPa), where the physical properties of the water change in a series of complex reactions. The process converts the feedstocks into solid hydrochar, liquid bio-oil (or process water), and/or gas. The desired products are obtained by changing the process conditions (temperature, pressure, holding time, and catalyst type). Depending on the desired by-products, changing the process conditions, hydrothermal processing can be divided into hydrothermal carbonization (HTC), hydrothermal liquefaction (HTL), and hydrothermal gasification (HTG).

Hydrothermal liquefaction involves the thermochemical conversion of organic materials into a liquid known as bio-oil (or biocrude) as the main product under subcritical conditions. To maintain the water in the liquid state, HTL requires specific operative conditions (temperature = 280 - 370 °C, pressure = 5 - 20 MPa, holding time = 5 - 60 min). Unlike other processes such as pyrolysis, HTL produces low-oxygen oil. In fact, HTL is considered a very energy efficient process as it works at lower temperatures than pyrolysis (López Barreiro et al., 2013). Often, to optimise the HTL process and minimise the formation of undesirable products, catalysts can be used, but that can be costly (Tran, 2016). However, compared to pyrolysis, HTL has the advantage of directly working on wet feedstock, reducing operational costs of equipment and storage (Dimitriadis & Bezergianni, 2017).

At higher temperatures (above 350 °C), the gaseous phase (enriched in H_2 and CH_4) is the main product of hydrothermal processes (M. Kumar et al., 2018). In particular, the hydrothermal gasification (or supercritical water gasification, SCWG) can operate at low-temperature zone 350 - 500 °C (with an increase in CO and CH_4 efficiency) and at high-temperature zone 500 - 700 °C (formation of H_2 and CO_2 occurs). Temperature is one of the most important parameters influencing product yield during the hydrothermal gasification of organic feedstocks, notably when the reaction is carried out without a catalyst. In contrast, the influence of the holding time on individual gas yields is dependent on the effects of the other parameters like pressure, temperature, solid content, and the type of feedstock (Okolie et al., 2019). As for HTL, the main advantage of HTG is to avoid the expensive pre-treatment of drying the feedstock, compared to traditional gasification (M. Kumar et al., 2018; Okolie et al., 2019).

1.6 Hydrothermal carbonization

Hydrothermal carbonization converts biomass into a solid product (hydrochar, HC) with high yields at relatively low temperature and saturated pressure (in the subcritical state of water). This artificial coalification process is also referred to as hot compressed water treatment, subcritical water treatment, wet torrefaction, and hydrothermal treatment. The resulting liquid phase (process water, PW) contains most of the dissolved organic compounds in the form of carbon with a minimal amount of gas. The type of feedstock affects the process as well as the input solid content and the operative conditions of the process (Libra et al., 2011; Shen, 2020). In the process, very little gas (1 – 5%) is generated, and most organics remain as or are transformed into solids (50 - 80%) (Libra et al., 2011). The gas formed during hydrothermal carbonization consists mainly of carbon dioxide (CO_2), and its concentration is around 70 - 90%, depending on the substrate (Ramke et al., 2009). Published studies show that the amount of gaseous products increases with increasing reaction temperature; at the same time, the fraction of carbon monoxide (CO) decreases while methane (CH_4) and hydrogen (H_2) increases (Ramke et al., 2009). Finally, it is worth to be noted that the total amount of carbon lost as CO_2 is low compared to the TOC present in the process water.

Table 1.2 compares all the thermochemical processes described above regarding the process conditions and the mass distribution of solid, liquid, and gaseous products. Not all data were included due to the complexity of reaction mechanisms occurring in individual processes. The reaction pathways and kinetics, even for pure materials, are not fully understood due to the

formation of many intermediates through parallel and consecutive reactions (Libra et al., 2011; Shen, 2020).

Table 1.2 - Thermochemical Process parameters comparison (adapted from Bridgwater, 2000; Kambo and Dutta, 2015; Kebelmann et al., 2013; Libra et al., 2011; López Barreiro et al., 2013; Okolie et al., 2019; Song and Guo, 2012).

Process type	Product distribution [%wt]			Temperature [°C]	Holding time
	Solid	*Liquid*	*Gas*		
Slow pyrolysis	35	30	35	300 - 650	minutes to several hours
Fast/flash pyrolysis		< 80		near 500	< 2 [s]
Intermediate pyrolysis	15 - 25	40 - 60	20 - 30	up to 500	2 - 4 [s]
Gasification	< 10	< 5	> 85	600 - 1200	10 - 20 [s]
HTC	50 - 80	5 - 20	1 - 5	180 - 250	5 [min] - [d]
HTL		*ambiguous*		280 - 370	5 - 120 [min]
HTG				350 - 700	

1.6.1 Reaction mechanisms

Several chemical reactions occur during HTC, including hydrolysis, dehydration, decarboxylation, decarbonylation, demethoxylation, condensation, polymerisation, and aromatisation (Funke & Ziegler, 2010; Libra et al., 2011). The first step of the hydrothermal carbonization process reaction is hydrolysis. Hydrolytic reactions lead to breaking mainly ester and ether bonds of biomacromolecules after adding 1 mole of water. Typically, vegetative residues mainly consist of cellulose, hemicellulose, and lignin. These components are highly interlocked, chemically bonded by non-covalent forces, and cross-linked, providing structure and rigidity to the plant (Kambo & Dutta, 2015). Cellulose is highly hydrolysed under hydrothermal conditions at about 220 °C hemicellulose readily hydrolyses between 180 – 200 °C, and hydrothermal degradation of most lignin can be accomplished in the middle of 180 - 220 °C due to the high content of ether bonds (Basso et al., 2016; Libra et al., 2011). Dehydration (dewatering) during hydrothermal carbonization

can involve chemical reactions and physical processes that remove water molecules from the feedstock without changing the chemical composition. Chemical dehydration causes significant biomass carbonization by reducing the H/C and O/C ratio (Funke & Ziegler, 2010). Chemical dehydration dominates the main water loss from biomass in the HTC process and is generally more intense than decarboxylation. Significant decarboxylation can only occur after some water has been formed by the chemical dehydration process. This chemical loss of water from biomass under subcritical water conditions can be understood as an assimilative dehydration process along with a condensation reaction to produce a solid residue (T. Wang et al., 2018). During the HTC process, due to the presence of subcritical water, the reaction mechanism is initiated by the hydrolysis of biomacromolecules, resulting in the formation of oligosaccharides, hexoses (glucose and fructose), pentoses (xylose) and lignin fragments. Dehydration converts hexose and pentons into furfural compounds (Kambo & Dutta, 2015). In addition, HTC treatment partially eliminates carboxyl groups. Carboxyl and carbonyl groups quickly degrade above 150 °C, yielding CO_2 and CO, respectively. One possible source of carbon dioxide is formic acid (formed in great amounts during the degradation of cellulose) that produces mainly CO_2 and H_2O. Other possible sources could be the formation of CO_2 during the condensation reaction and the cleavage of intramolecular bonds. Another assumption is that H_2O acts as an oxidising agent at temperatures above 300 °C, and that additional CO_2 is formed by the thermal destruction of such oxidised units (Funke & Ziegler, 2010). Higher temperatures can lead to dehydration, decarboxylation and condensation at the same time with oxygen and hydrogen contents decreasing (T. Wang et al., 2018). Some fragments resulting from the degradation of biomacromolecules under hydrothermal conditions are highly reactive. Unsaturated, easily polymerisable compounds are formed as a result of the elimination of carboxyl and hydroxyl groups. Free radical mechanisms can occur but are more likely to be dominant under supercritical and low-density conditions (Funke & Ziegler, 2010). Under subcritical conditions, free radicals are efficiently saturated with the water present and the hydrogen provided by aromatisation. In the case of the highly reactive lignin fragments, it has been reported that the polymerisation was completed in a few minutes above 300 °C, whereas it took months at room temperature. The polymerisation that produces a solid precipitate is generally considered an undesirable side reaction and is therefore largely minimised in other hydrothermal processes (Funke & Ziegler, 2010). All the above-mentioned reactions are dominated by the operative conditions. For instance, the holding time is an essential factor in hydrochar formation since a long holding time increases the severity of the reaction. Long holding times can result in polymerisation of the dissolved fragments in the liquid

phase and can lead to the formation of a secondary char with a polyaromatic structure. In the case of lignocellulosic materials, secondary char formation depends mainly on the holding time since the dissolved monomers require intensive polymerisation (T. Wang et al., 2018). Although hemicellulose consists of carbohydrates, it is able to form aromatic structures under both non-aqueous and hydrothermal conditions. Alkaline conditions seem to favour the formation of aromatic structures. Aromatic structures show high stability under hydrothermal conditions and, therefore, can be considered the basic building blocks of the obtained HTC carbon. The condensation of the cross-linking of aromatic rings is also the principal constituent of natural coal, which may explain the good agreement between natural coalification and hydrothermal carbonization. Aromatisation appears to be highly temperature-dependent (Funke & Ziegler, 2010). However, different studies report conflicting results, concluding that further investigations are needed and confirming that several mechanisms are still unknown. Figure 1.1 summarises the main paths reactions occurring during the hydrothermal degradation of lignin, cellulose, and hemicellulose.
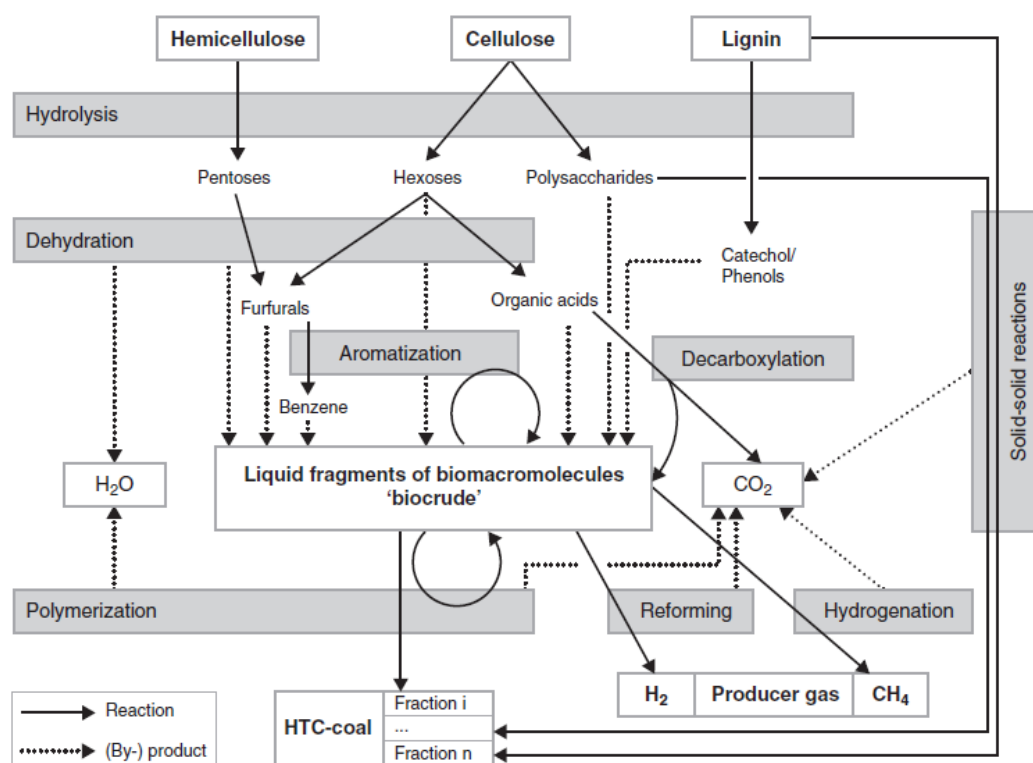

Figure 1.1 - Main reaction pathways of hydrothermal carbonization for cellulose, hemicellulose, and lignin (Kruse et al., 2013).

1.6.2   Process parameters

The HTC process requires understanding the influence of process parameters such as surrounding medium, temperature, holding time, pressure, pH, and input solid content and composition. Referring to various sources, the effects of each process parameter are discussed in more detail. Hydrothermal carbonization is carried out in the presence of subcritical liquid water. Water is considered a harmless environment for most organic reactions. Beyond the critical point, the properties of the water can be changed without any phase change. Supercritical condition refers to a zone of high temperature and pressure at a critical point where water plays the role of both a reactant and catalyst. Under these conditions, water properties such as viscosity, density, and dielectric constant are rapidly changed. As a solvent, supercritical water is characterised by high miscibility and absence of phase boundaries (A. Kumar et al., 2009). Typically, HTC works with a 75 – 90% water content or even higher. The amount of external heat needed for HTC depends on the design of the process but is expected to be significantly lower than for dry pyrolysis, especially considering the high heat-exchange capacity of water. Hydrothermal carbonization of organic dry matter with water content lower than 40% is unlikely to have any energetic advantage compared to dry pyrolysis (Libra et al., 2011). In early experiments, it was observed that the biomass above the surface of the liquid does not carbonize, which is also strongly emphasised in the case of water pyrolysis experiments. This is why Funke and Ziegler (2010) suggest that the solid material should always be submerged during the process. It is possible to carbonize the biomass in both oil and water; however, the carbonization process is accelerated by water than oil. Water is a suitable heat carrier and accumulator to avoid local temperature peaks that may result from exothermic reactions. Furthermore, the importance of hot water as a reactant, solvent and catalyst for organic compounds in natural systems has been recognised to facilitate hydrolysis, ionic condensation and cleavage (Funke & Ziegler, 2010).

Temperature is a key parameter of the HTC process because it is probably the major determinant of the properties of water. The primary role of temperature is to provide decay heat for the biomass bond's fragmentation. It is worth noting that biomass conversion efficiency increases with increasing temperature; however, the higher the temperature, the lower the solid yield recovered. This is generally due to the additional energy supplied by the temperature, which improves the breaking of the biomass bond (Nizamuddin et al., 2017). Above the critical point, the reaction mechanism changes from ionic to free-radical reactions in the region of supercritical water.

However, an increase in temperature alters the viscosity of the water, allowing easier penetration into porous media and thus further degradation of the biomass (T. Wang et al., 2018).

Jung and Kruse (2017) applied the general Arrhenius type kinetic equation (Equation 1.1) to model the hydrochar mass yield, carbon, and oxygen content in HTC experiments, using three regulatory parameters, A, B, and C (Román et al., 2018).

$$A \cdot t^B \cdot \exp\left(\frac{-C}{T}\right) = \frac{O_{feed} - O_t}{O_{feed} - 6} \tag{1.1}$$

The total conversion was defined as the achievement with an oxygen content of HTC carbon of 6 w% (6 is the oxygen content of the sub-bituminous coal, taken as reference) since no specific carbon product could be determined (Funke & Ziegler, 2010). The above equation is based on the coalification model (Equation 1.2) reported by Ruyter (1982).

$$f = 50 \cdot t^{0.2} \cdot \exp\left(\frac{-3500}{T}\right) \tag{1.2}$$

Where t and T are time (s) and temperature (K), respectively, O_{feed} is the oxygen content of the raw material and O_t is the oxygen content after t reaction time.

Table 1.3 presents the HTC of various organic residues to hydrochars from several sources and reveals information about process temperature, holding time, surrounding medium and solid yield provided from the process. In the table, a few studies have been reported in order to provide an example of the variability of parameters. It can be easily seen that the process parameters differ for individual feedstock; however, the temperature range of 180 – 250 °C can be assumed as the most significant in the process.

Compared to pyrolysis and gasification, HTC is considered a slow process. Reported holding times range from a few minutes to several hours (even days). However, the reaction time only affects the hydrolysis reactions up to a specific time range, beyond which it has no particular effect on the process. It is generally observed that the longer reaction times result in a greater amount of solid product (Nizamuddin et al., 2017), which may be due to condensation and polymerisation phenomena, resulting in the formation of a secondary char (Lucian et al., 2018), as shown in Figure 1.2. As the holding time in the HTC process increases, cellulose and hemicellulose are transformed, resulting in the formation of microspherical particles that can positively affect the surface area and porosity (Kambo & Dutta, 2015). In the studies conducted by Gao et al. (2013), the extension of the holding time from 30 minutes to 24 hours at the temperature of 240 °C resulted in different

characteristics of the hydrochar surface. The results showed that a shorter holding time causes cracks on the hydrochar surface, with no carbon microspheres forming until the holding time exceeds six hours. Times exceeding 24 hours caused aggregation of microspheres on the hydrochar surface (T. Wang et al., 2018).

Table 1.3 - HTC of different organic residues to hydrochars.

Feedstock	Temperature [°C]	Holding time [h]	Surrounding medium	Mass yield [%]	Reference
Water hyacinth	240	0.5 – 24.0	water	38.00	(Gao et al., 2013)
Opuntia ficus-indica	180 - 250	0.5 – 3.0	water	43.00 - 66.00	(Volpe et al., 2018)
Polyvinyl chloride	220 - 280	0.5 - 1.5	water	30.90 - 41.30	(Ning et al., 2020)
Faecal sludge	220	0.5	water, acetic acid, lithium chloride, borax, zeolite	69.80 - 77.00	(Koottatep et al., 2016)
Pulp and paper mill sludge	180 - 260	0.5 - 5.0	water, hydrogen chloride, sodium hydroxide	up to 53.00	(Mäkelä et al., 2016)
Tobacco stalk	180 - 260	2.0	water	43.00 - 80.00	(Cai et al., 2016)
	260	1.0 – 12.0		41.00	
Food waste	200 - 300	1.0	water	5.25 - 7.00	(Saqib et al., 2018)
Corn stover	180 - 260	4.0	water	44.17 - 67.90	(Y. Zhang et al., 2019)
	220	1.0 – 24.0	water	48.75 - 58.59	
	220	4.0	water, hydrogen chloride	32.86 - 33.29	
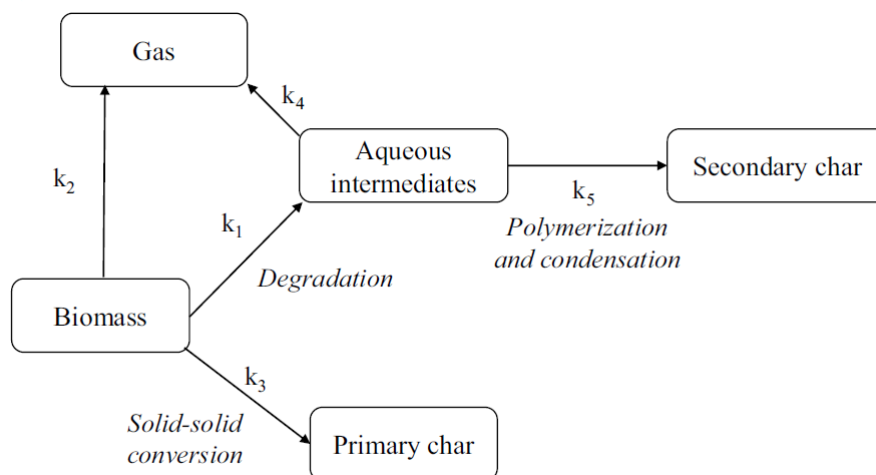
Figure 1.2 - Simplified reaction paths of hydrothermal carbonization (Ischia & Fiori, 2020).

Severity reaction factors are proposed by different authors to assess biomass degradation and conversion to understand the combined effects of temperature and holding time. Reaction severity (R_0) is a function of the combined effect of processing temperature and residence time based on the Equation 1.3.

$$R_0 = t \cdot \exp\left[\frac{T - 100}{14,75}\right] \tag{1.3}$$

Where R_0 and t (holding time) are measured in min, and T is the temperature (°C). 100 °C is used as reference. This severity factor equation has been used by other researchers to describe the HTC process applied to various biomass feedstocks (Román et al., 2018; T. Wang et al., 2018).

In hydrothermal processes, solid material is surrounded by water during the reaction, which is kept in the liquid state, allowing the pressure to increase with the vapour pressure in high-pressure reactors. As with dry pyrolysis, reaction temperature and pressure determine product decomposition. At process temperatures of up to 220 °C and corresponding pressures of up to 20 bar, very little gas is produced (1 - 5%), and the most organic matter remains or is converted into a solid (Libra et al., 2011). The pressure effect on HTC greatly influences the formation of the hydrochar. High pressures lead to high temperatures, so the biomass composition breaks down quickly. Hence, the effect of increased pressure is to increase the hydrochar formation in the HTC process (Nizamuddin et al., 2017). Typically, the reaction pressure is not controlled by the process and is autogenous at the saturated vapour pressure (subcritical water) corresponding to the reaction temperature (Kambo & Dutta, 2015). By increasing the temperature, the pressure in the reactor increases isotropically. Solids are distributed only based on gravitational forces, however,

natural convection during heating periods is possible in the case of small-size reactors without agitation (Funke & Ziegler, 2010). The dielectric constant of water is a function of temperature and a strong function of pressure. At normal temperature and pressure, the dielectric constant of water is relatively high (> 80) due to the strong hydrogen bonding effect in water. With elevated temperature and pressure, it drops to 5 at the critical point (Shen, 2020).

Pressure has a positive effect on the density of the solvent or medium; the higher the pressure, the higher the density. Therefore, a higher degree of extraction and disintegration of biomass is achieved by using high-density solvents. The pressure in the reactor can be raised either directly or by adding fluids such as nitrogen. The reaction inside the reactor is influenced by pressure, according to Le Chatelier's principle. The direction in which the equilibrium shifts at higher pressure, from solid to liquid or vice versa, is decided according to this principle. At the same time, it is a fact that the shift is in a direction that has fewer moles. For example, in both decarboxylation and dehydration reactions, depression occurs at higher pressure (Nizamuddin et al., 2017).

In the HTC process at high temperatures, the pressure inside the reactor is significantly high (45 MPa), which makes the process complex, dangerous, and expensive. The use of additives (e.g., salts or acids) has been recommended by several authors in order to catalyse the process reactions, improving the properties of the hydrochar and reducing the pressure and temperature of the reaction. However, the choice of catalyst should be made very carefully as it can be expensive and cause corrosion in the reactor (Kambo & Dutta, 2015).

It should be noted that manipulating the pH of the water has a significant effect on the mechanism of cellulose reaction in water. Alkaline conditions are often used to liquefy biomass (Libra et al., 2011). Compared to acidic and neutral conditions, alkaline conditions provide the highest reaction rates, while glucose degradation reactions are strongly enhanced by acidic conditions. In acidic pH (3 to 7), the reaction rate is independent of the concentration of H^+ and OH^-. The different kinds of used acid play a fundamental role; for example, small amounts of Arrhenius acid generally catalyse dehydration. It should also be noted that a high pH value usually results in higher H/C ratios of the solid product (Funke & Ziegler, 2010). Organic acids act as a crucial intermediate in the complex pathway reaction, catalysing the decomposition of macromolecules and the formation of hydrochar. Therefore, changes in pH during the hydrothermal process can significantly impact the characteristics of the hydrochar and, consequently, the formation of compounds dissolved in the process water. The HTC process is generally considered autocatalytic for forming organic acids such as formic, acetic, lactic and levulinic acids from biomass, resulting in a drop in pH (T. Wang et al.,

2018). However, the addition of acids or bases can be used as a catalyst during processing, accelerating the reactions or leading reaction path to obtain the desired final compounds (T. Wang et al., 2018).

Although the literature is full of examples of the effect of temperature and holding time on hydrochar yield for various organic materials, there is little research into the effect of solid loading on the field (Volpe et al., 2018). For example, at close to zero solid content, biomass can be almost completely dissolved, leaving a small solid residue. On the other hand, a higher biomass-to-water ratio is unlikely to increase the concentration of monomers in the liquid phase because the holding time is long enough to achieve equilibrium in the solution. Moreover, high solid content facilitates polymerisation reaction positively affecting the hydrochar formation (Funke & Ziegler, 2010). So far, however, the influence of solid content on the yield is not well understood in the literature, and the available data is too rare to achieve reasonable conclusions (Volpe et al., 2018). Figure 1.3 schematically summarises the HTC process highlighting the most affecting conditions and the resulting products due to the reaction occurring during the process.
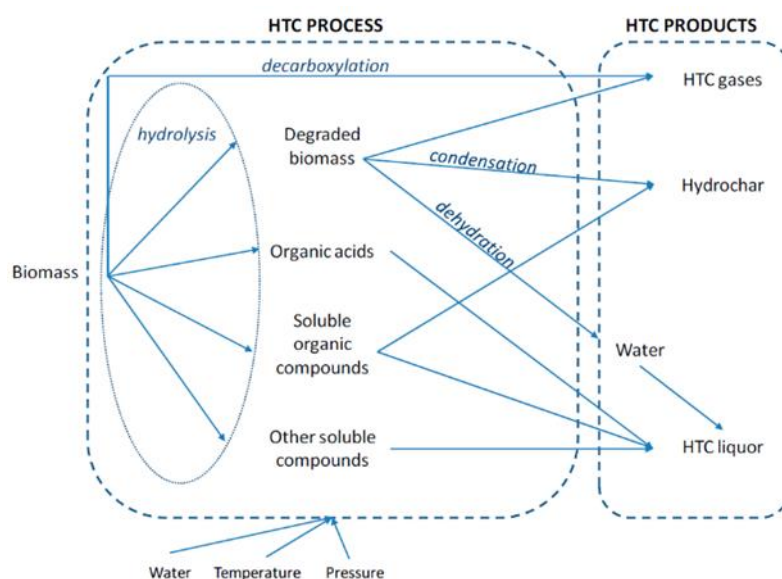
Figure 1.3 - The HTC process and its products (Langone & Basso, 2020).

1.6.3 Applications

Hydrochar represents a promising material with enormous potential for use in a wide range of industrial and environmental applications (Sharma et al., 2019). Hydrochar can be used as a viable alternative to fossil fuels (Sharma et al., 2019). In fact, compared to the feedstock, it is characterised by a higher energy content (higher calorific value) and lower ash, ensuring better combustion (Maniscalco et al., 2020a). Energy recovery is not the only advantageous use of hydrochar. It seems

to be an excellent candidate for applications like microbial electrochemical technologies (MET) for biomass processing, CO_2 fixation, soil or water bioremediation, and wastewater treatment (Schievano et al., 2019), as a substrate for microbial growth or as a primary material.

Hydrochar can be potentially applied in electrochemical technologies, like batteries and supercapacitors. Due to HC properties (surface area, polarity, porosity, aromaticity, and stability), supercapacitors demonstrated longer life and power density, while rechargeable batteries showed lower cycle stability, higher energy density and lower discharge-charge rate (Masoumi et al., 2021). Research into the possible use of biomass-derived materials for the production of supercapacitors focused on the use of the HTC process as a pre-treatment. It has been studied by Ding et al. (2012) hydrochar combined with nickel, improving by almost 150% its specific capacity compared to that of a composite material of activated carbon and nickel. The excellent performance of the hydrochar-nickel composite has been attributed to its porous structure, characterised by a relatively high pore volume. Char is known to be a good adsorbent material for carbon sequestration, particularly CO_2, or as a carbon sink in soils for climate change mitigation. The advantage of using hydrochar is that the HTC process does not produce harmful gases and is environmentally sustainable compared with other thermal processes (Fang et al., 2018). In addition, as for carbon sequestration, it is necessary to produce hydrochar with O/C and H/C ratios of 0.4 and 0.6, respectively, typical of low polarity, which are generally highly refractory to microbial degradation (Tasca et al., 2019). The result of carbon sequestration in soil is a reduction in greenhouse gas (GHG) emissions and thereby a decrease in the effect of global warming and pollution mitigation. Hydrochar is able to adsorb several other organic/inorganic contaminants thanks to the presence of oxygen-rich functional groups that increases hydrochar adsorption capacity (Kambo & Dutta, 2015). Like biochar, HC may efficiently remove from soil or water persistent organic pollutants (POPs), such as furans, pesticides, chlorinated aromatic hydrocarbons, dioxins, halogenated ethers, and heavy metals (Ambaye et al., 2021; Kambo and Dutta, 2015). Recently, hydrochar properties in enhancing biogas yield from anaerobic digestion of sewage sludge and swine manure, as an additive to AD, were investigated, highlighting even better properties in the digestate, such as better dewatering characteristics and improved soil amendment properties (S. Xu et al., 2020). In addition, hydrochar can be applied as catalyst for enzymatic and heterogeneous catalytic reactions; However, it is often chemically activated to enhance sorption potential. Its utilisation in biotechnological processes (such as enzyme immobilisation) may enhance the economic feasibility of industrial-scale applications (Masoumi et al., 2021). Although most types of hydrochar, especially those derived from vegetative residues,

have a low nutrient content and cannot be used as the only substrates, it can be added to the soil as a soil improver, reducing the amount of fertiliser that is lost through surface leaching. Hydrochar, in fact, thanks to its high porosity, has an excellent water retention capacity, and nutrients are absorbed by the surface pores, which then slowly release into the soil, favouring absorption by plants (Fang et al., 2018). Several studies have shown how hydrochar can improve the physicochemical properties of soil, including pH, water retention capacity, cation and anion exchange capacity, and nutrients. The studies conducted by Bargmann et al. (2014) on the growth of different plants showed how hydrochar improved growth for beans and barley but inhibited leeks development, attributing the negative effect on plant growth to the decomposition activity of hydrochar that immobilised nitrogen in the soil (Fang et al., 2018). The use of hydrochar as a soil improver is subject to numerous experimental works in order to test its actual validity, as it could be a valid substrate as a partial substitute for peat.

Regarding the process water, it can be recirculated into the HTC process or further treated. However, in the context of maximising energy recovery and resources, process water should be valued (Langone & Basso, 2020). Only few experiments on the use and valorisation of process water are present in the scientific literature and mainly focus on their recirculation in the process, such as in the studies conducted by Stemann et al. (2013), Kabadayi Catalkopru et al. (2017), and Kambo et al. (2018). The recirculation of process water in HTC is mainly applied in the industrial treatment of dried biomass. Typically, when treating dry biomass, water is added to the HTC system with a liquid-to-solid ratio ranging from 0.2 to 30. Recirculation is a practical operation that reduces both the consumption of fresh water and the cost related to the treatment of process water, increasing the overall efficiency of the system. In addition, process water recirculation helps reduce the wastewater produced, as well as recover heat and reduce external heat demand by up to ten times. Moreover, recirculating, the pressure, and the temperature required by the process are reduced due to the increase of organic acids concentrations formed in the process water that are able to catalyse the reactions involved. Hydrochar solid yield, together with its carbon and energetic content, and the dewatering properties are improved by PW recirculation (Stemann et al., 2013). In fact, degraded sugar compounds from biomass polymers in process water could be deposited in the porous structure of hydrochar, further increasing the solid's overall energy density (Kambo et al., 2018). However, the recirculation option is practical and only convenient with relatively dry feedstocks, and further treatment of the process water is still required after a number of recirculation cycles (Langone & Basso, 2020). Other interesting options have been proposed to

valorise the process water. Process water contains fairly high concentrations of carbon, phosphorus, nitrogen, potassium, as well as calcium and magnesium, making these waters suitable for agricultural applications, e.g., in fertigation (Smith & Ross, 2016). In addition, reaction temperatures above 120 – 180 °C provide complete sanitisation in terms of biological-health risks. The use as a nutrient culture medium for algae growth has been studied by Biller et al. (2012) and Yao et al. (2016) to reduce algae cultivation costs and increase the overall sustainability of the process. However, it is known that process water contains specific compounds, such as phenols, organic acids, and furans, which can, instead, have toxic or inhibiting effects on plant development. Recently, the toxicity of the process water on seeds has been studied, the tests of which have shown that the inhibition and delay of germination depend on the species (e.g., concentrated process waters inhibited the germination process of corn, lettuce, and tomato seeds as reported by Fregolente et al. (2019). However, the process water delayed the seeds germination at lower concentrations but did not inhibit it completely. It was concluded that process water, when applied in specific quantities, can be used as fertiliser to provide the nutrients necessary for the initial growth of the plant and to promote the elongation of roots and shoots.

So far, few other solutions have been proposed for the treatment and valorisation of HTC process water. Treating lignocellulosic biomass, process water is predominantly characterised by phenolic compounds and furan derivatives, which can be interesting raw materials for producing biodiesel and in green chemistry (Xiao et al., 2012). In addition, HTC process water can also be used as substrate for anaerobic digestion (AD). Several research groups have studied the exploitation by AD of the relatively high residual carbon content for different organic residues such as primary sewage sludge (Danso-Boateng, 2015), spent malts from breweries (Poerschmann et al., 2014), orange pomace (Erdogan et al., 2015), food waste (Zhao et al., 2018), rice straw (T. Wang et al., 2018), and agricultural residues (Oliveira et al., 2013). The AD application could help energetically support the thermal needs of the HTC process, generating a positive energy balance (Langone & Basso, 2020). In addition, the digested liquid can be easily treated at a wastewater treatment plant (Tasca et al., 2019). Generally, HTC process water and sewage sludge meet anaerobic digestion needs in terms of nitrogen and micronutrient requirements. Due to the relatively high residual carbon content, the process water could be further used as an external carbon source in conventional nitrification and denitrification processes. However, this aspect has not yet been deepened. The treatment and valorisation of HTC process water by recovering resources, mainly nitrogen and phosphorus, has great potential (Marin-Batista et al., 2020). In particular, phosphorus is an essential nutrient for all

living organisms and agriculture and an important element in numerous industrial applications. Almost 100% of the phosphorus used in Europe has to be imported, and it is becoming increasingly difficult to supply the necessary quantities as the world's phosphate mineral resources are limited. Within the circular economy, research is focusing on the recovery of P from urban wastewater, sludge, and other waste. HTC can facilitate nutrient recovery, although its extraction depends on the type of feedstock treated. Becker et al. (2019) proposed a combination of HTC treatment of AD of sewage sludge and mechanically dehydrated municipal sludge with a nutrient recycling strategy via phosphate and nitrogen precipitation as struvite. Finally, the extraction of certain organic compounds, such as acetic acid, from process waters could be of considerable interest in organic syntheses and green chemistry (Langone & Basso, 2020).

Chapter 2

Hydrothermal carbonization of hemp digestate: influence of operating parameters

The results of the carbonization of hemp and hemp digestate are presented in this chapter. This work was conducted in collaboration with Sardegna Ricerche. A preliminary version of this chapter has been presented at XI International Symposium on Environmental Engineering – SIDISA 2021, in Turin (Italy). The conference paper has been selected for the potential publication at the international journal Biomass Conversion and Biorefinery. A modified version of this chapter is at present under review.
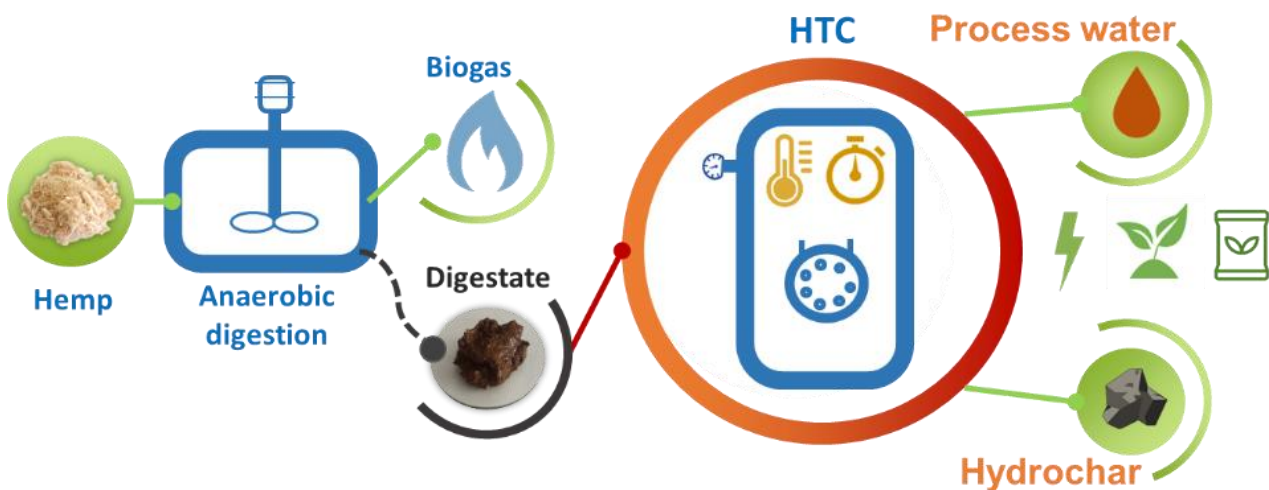
2.1 Abstract

In the last decade, great attention has been given to hydrothermal carbonization (HTC) as a suitable process for residual biomass valorisation, able to convert organic waste into useful materials or energy carriers. Based on the use of water as a solvent/reaction medium, it is considered particularly appropriate for the upgrading of wet biomasses since no drying pre-treatment is required. However, the involved conversion reactions that biomass components undergo are influenced by the characteristics of the treated residue along with the HTC process conditions, particularly in terms of temperature and holding time.

In this paper, the potential valorisation of hemp digestate via HTC was investigated. The study was aimed at evaluating the effect of reaction temperature and holding time on the yield and composition of produced hydrochar and on the process water characteristics. Three temperatures (180, 200, and 220 °C) were investigated along with three holding times (1, 3, and 6 h) and the obtained solid and liquid phases were characterised. Results show that the investigated operating parameters affect both the solid yield and the hydrochar and process water composition. By increasing process severity conditions through an increase in temperature and/or holding time, a drop in solid yield and an increase in carbon content were achieved for the produced hydrochar, which showed suitable properties in view of its use as a fuel. Process water characteristics suggest a potential valorisation in terms of nutrient recovery or biogas production by anaerobic digestion.

2.2 Introduction

The current depletion of fossil fuels is increasing the importance of biomass as a source for both biofuels or raw materials to be used in manufacturing processes. To fully exploit the potential of biomass as resource, a biorefinery concept needs to be applied, integrating different valorisation processes aimed at providing multiple products, with a greater recovery yield, and hence an overall increased efficiency (Ferreira, 2017; Rajesh Banu et al., 2021). A possible strategy towards the sustainable production of bioenergy and bioproducts is the integration of biological processes with thermochemical conversion methods (Parmar & Ross, 2019).

Among bio-technologies, anaerobic digestion (AD) is known as a simple and robust valorisation process aimed at biogas production from several categories of organic waste. The residual non-degraded fraction is converted into digestate, typically used as soil fertiliser, whose increasing production, as well as some environmental concerns related to land application, are rising interest

in alternative valorisation technologies (Cao et al., 2020; Ro et al., 2010; Sheets et al., 2015; D. Zhang et al., 2018).

Hydrothermal carbonization (HTC) is a wet thermochemical process that takes place at relatively low temperatures (generally in the range 180 – 250 °C) and residence times (up to several hours) under autogenous pressure, using subcritical water to convert biomass into highly dense carbonaceous materials. HTC is particularly suitable for biomass valorisation since it can be applied on humid feedstocks without any dewatering or drying pre-treatment. In addition, due to the high process temperature, complete disinfection from pathogens is ensured (Ducey et al., 2017; Funke & Ziegler, 2010; Libra et al., 2011). Within a biorefinery approach, HTC represents a very attractive option since any biomass can be processed, being the applied aqueous conditions particularly advantageous for organic residues with very high water content, such as digestate. Therefore, HTC is gaining interest as a viable route for digestate enhancement, and several studies indicate it can be applied to convert digestate into exploitable materials and sustainable energy sources, capable of adding value to the AD process (Hitzl et al., 2015; Parmar & Ross, 2019). The two main by-products of the process are a peat-like carbonaceous solid (hydrochar) and a liquid fraction (process water) enriched by the most soluble compounds formed during the involved reactions. The solid hydrochar properties allow to consider it as biofuel (M. Ahmed et al., 2021; Akarsu et al., 2019; Belete et al., 2021; Cao et al., 2019, 2020; Libra et al., 2011; Merzari et al., 2020), soil amender (Belete et al., 2021; Celletti et al., 2021; de Jager et al., 2020; Merzari et al., 2020) adsorbent for pollutant removal and the production of nanostructured materials (Libra et al., 2011; Niinipuu et al., 2020). At the same time, the high presence of organics and nutrients in process water suggests the opportunity to recycle it back into AD allowing for additional energy recovery through biogas production (Qiao et al., 2011; Wirth et al., 2015) or applying nutrient recovery/fertigation (Hitzl et al., 2015).

The final quality of the produced solid and liquid by-products is significantly influenced by both the initial characteristics of the feedstock and the adopted operating conditions. According to the type of feedstock, organic carbon will be differently speciated and could be differently affected by the thermochemical degradation reactions, whose extent will also be influenced by the severity of the process, especially in terms of temperature and residence time. It is known that an increase in reaction severity leads to a higher release of volatile compounds and ashes, resulting in a lower solid yield and higher carbon densification in the produced hydrochar. In particular, HTC temperature is known to boost dehydration reactions that reduce the H/C and O/C ratios, whose extent seems more marked for longer residence times (M. Ahmed et al., 2021; Maniscalco et al., 2020a).

In this work, the possibility to convert digestate from the AD of hemp into valuable products was studied. Cannabis sativa L., commonly named hemp, is a crop applied in several agro-industrial sectors (e.g. construction, food/animal feed, paper, textile), characterised by a high biomass production and root elongation, which in turn allow for a CO_2 capture capacity of about 2.5 t CO_2/ha and the protection of soils from erosion while requiring low inputs in terms of fertiliser or pesticides (Tang et al., 2016; Żuk-Gołaszewska & Gołaszewski, 2018). The manifold use of hemp as well as the European and Italian regulations and incentives promoting in the last two decades hemp industry, has boosted hemp cultivation, entailing the need to properly manage the produced hemp straw residues.

Within the scope of a broader study on hemp cultivation and utilization (Asquer et al., 2019), experimental tests were conducted in which the residual hemp straw was employed to produce biogas through anaerobic digestion. In this study, the obtained digestate was used as feedstock for an HTC process aimed at achieving further biomass valorisation, by producing hydrochar to be potentially used as solid fuel and process water to be eventually considered for energy recovery through biogas production or for nutrient recovery. HTC experimental tests were carried out at different temperatures (180, 200, and 220 °C) and durations (1, 3, and 6 h) to assess the influence of the adopted operating conditions on the solid and liquid by-products, that was evaluated on the basis of mass yields, composition and High Heating Value of the produced hydrochar and composition and biogas production potential of the resulting process water.

2.3   Materials and Methods

The anaerobic digestion tests were conducted in a pilot plant having a reactor with a working volume of 0.96 m^3. The reactor was mixed and heated at the temperature of 39.0 ± 0.5 °C. Seven samples of digestate were collected over a period of one year in order to compose a representative portion of the produced substrate. Throughout the tests duration, different operational conditions were adopted (Asquer et al., 2019). However, in the time of the considered digestate samples, the hydraulic retention time (HRT) was maintained within a range of 25 ÷ 48 days, and the feeding mixture was composed of hemp straw and recirculated digestate with a ratio ranging from 3.4 to 4.8 wt/wt. The total (TS) and volatile (VS) solids content in the feeding mixture were 14.3 (±1.1) %wt and 70.3 (±0.9) %wtdb, respectively. The TS and VS values in the digestate were 12.3 (±1.1) %wt and 67.9 (±0.8) %wtdb, respectively.

Digestate was hydrothermally treated at temperatures of 180, 200 °C and a holding time of 1, 3, and 6 hours. For each couple of conditions, triplicate tests were carried out to assure replicability. Moreover, three runs at 220 °C for 1h were carried out to better investigate the effect of temperature. Hydrothermal carbonization was performed in a 1.5 L pressurised reactor (Berghof, BR-1000) equipped with an electric jacket for temperature control, a stirred shaft, and a data logging unit (Berghof, BTC-3000). For each run, the reactor was filled with around 1 L of digestate without any pre-treatment. The gas produced during the process was evacuated from the reactor and collected in gas bags for characterisation.

For the sake of comparison, HTC tests were also conducted on a representative sample of hemp straw before the digestion treatment. In this case, distilled water was added to achieve 13% of solid content in the 1 L hemp mixture, which was treated at 180, 200, and 220 °C keeping the holding time constant at 1 h.

The carbonized sludge was separated through a filter press into its solid and liquid phases, namely hydrochar and process water (Figure 2.1). The latter was filtered at 0.45 µm and stored in plastic bottles at 4 °C for subsequent analyses, while hydrochar was oven-dried at 105 °C to evaluate the humidity and stored in plastic bags for further characterisation. In each step, the amount of liquid and solid was estimated to evaluate the phases' repartition and obtain a final mass balance. Each sample was named with a code representing the feedstock (the initial letter), the temperature and the holding time, separated by underscores. For instance, a sample of digestate treated at 200 °C for 3 hours is referred to as D_200_3, while a sample of hemp processed at 180 °C for 1h is named H_180_1.

Hydrochars were characterised in terms of elemental composition (C, H, N, S, O) and ash content. Carbon, hydrogen, and nitrogen were evaluated through a CHNS analyser (LECO, TRUSpec) in accordance with ASTM D5373-16, while ashes were measured through a thermogravimetric analyser (LECO, TGA701) according to ASTM D7582-15. Higher heating values (HHV) were measured with a calorimetric bomb (LECO, AC500), and calculations for obtaining the oxygen content were made following EN 14918:2009.

Composite samples of process water obtained from triplicates test were characterised in terms of pH, electrical conductivity (EC), total organic carbon (TOC) through TOC analyser (Shimadzu, TOC-VCSH), chemical oxygen demand (COD), anions (Cl^-, NO_2^-, NO_3^-, SO_2^-) via ionic chromatography (Dionex, ICS-90), macronutrients concentration (P, K, Ca) through ICP-OES (Perkin Elmer, Optima7000), and the total phenols via spectrophotometric measurements using the Folin-

Ciocalteu method. The concentration of volatile fatty acids (VFA) (acetic, propionic, butyric + iso-butyric, valeric + iso-valeric, hexanoic + iso-hexanoic, heptanoic) was determined using a gas chromatograph with flame-ionization detection (model 7890B, Agilent Technology) equipped with a capillary column (HP-FFAP, 25 m, inner diameter 0.32 mm, Agilent Technology), as reported in Asunis et al. (2019). In addition, the acute inhibition on nitrifying bacteria caused by PW was assessed through the standard method described by Ficara&Rozzi (Ficara & Rozzi, 2001). Biochemical Methane Potential tests (BMP) have been carried out according to the standard norm (UNI1601755EIT), adopting a food-to-microorganism ratio of 0.5 gCOD/gCOD in order to prevent inhibition (Pagés-Díaz et al., 2020). A blank test containing only inoculum was also carried out. No nutrient solution was added. The reactors were shaken continuously and kept at 35°C ±1°C for the entire duration of the experiment. Biogas production was measured by liquid displacement. The biogas was injected through a valve in a gas chromatograph (model 7890B, Agilent Technology) equipped with a thermal conductivity detector (TCD) and two stainless columns packed with HayeSep N (80/100 mesh) and Shincarbon ST (50/80 mesh) connected in series, as reported in Asunis et al. (2019). The BMP test ended after 28 days, when the daily methane volume was less than 1% of the cumulative assessed methane volume.

Finally, the effect of operating variables on the final properties of the produced hydrochars was interpreted through one-way ANOVA. Tukey's HSD statistical test was applied to verify whether the hydrochar characteristics were significantly different; results are expressed with the compact letter display (CLD) method.
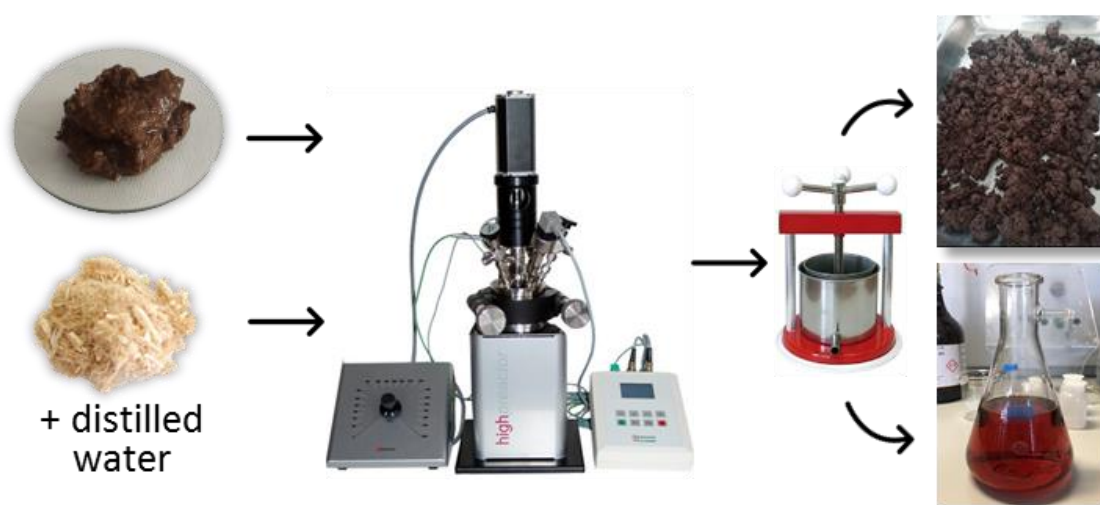

Figure 2.1 - Experimental setup and scheme of the operational steps

2.4   Results and Discussion

The products obtained after hydrothermal carbonization carried out at different temperatures and durations exhibited different properties. The solid yield of the hydrochars decreased with higher temperatures and longer holding time, as reported in Table 2.1, where statistically significant differences among the obtained hydrochar are reported. Temperature seems to be the parameter that has more influence on the solid yield while holding time plays a secondary role, as reported in similar studies (Funke & Ziegler, 2010; Libra et al., 2011). The maximum value (88.69%) for digestate hydrochars was assessed at 180 °C for 1 h, while a minimum value of 72.83% was measured at 220 °C for 1 h. Lower solid yields are reported for hemp hydrochars; at 180 °C, around 80% of the input mass was recovered, while at 220 °C, the solid yield decreased to 60%. The higher hydrochar yield obtained when hemp digestate was used as feedstock is consistent with the transformation occurring on hemp during anaerobic digestion. Hemp digestate is a by-product of a biological treatment in which organic compounds are hydrolysed and subsequently converted into biogas, that makes the produced digestate depleted in insoluble fraction and therefore less prone to further mass loss.

The composition of the produced hydrochars is shown in Figure 2.2 and Figure 2.3, respectively. In Table 2.2, different letters indicate a significant difference between the hydrochars at $p < 0.05$. According to the preliminary characterisation, all the parameters considered in the produced hydrochar were significantly different from the feedstock ($p < 0.001$). The carbon content in hydrothermally-treated samples increased with respect to the feedstock, while ash and oxygen content were reduced, indicating that they were released in the liquid and gaseous phases. As for the effect of operating conditions, higher temperatures seem to produce a significant increase in carbon concentration, while no statistically significant effect can be evidenced by increasing retention time. Hydrogen and sulphur do not present statistically significant variation at the different operating conditions adopted. Ash content is significantly lower at lower temperatures and lower residence time for digestate hydrochars. On the contrary, an increased temperature produced a lower ash content in hemp hydrochar.

Table 2.1 - Average solid yields of the hydrochars produced via HTC of hemp digestate at different temperatures and holding time and standard deviations. Significant differences (p < 0.05) among tests are represented by different upper-case letter labels for digestate and lower-case letters for hemp.

Sample	Solid yield [%]	CLD
D_180_1	88.69 (±0.68)	A
D_180_3	86.87 (±0.70)	A B
D_180_6	85.68 (±0.64)	B
D_200_1	85.78 (±1.43)	B
D_200_3	78.33 (±1.05)	C
D_200_6	73.51 (±0.85)	D
D_220_1	72.83 (±1.08)	D
H_180_1	79.67 (±1.56)	a
H_200_1	65.23 (±0.57)	b
H_220_1	60.06 (±0.65)	c
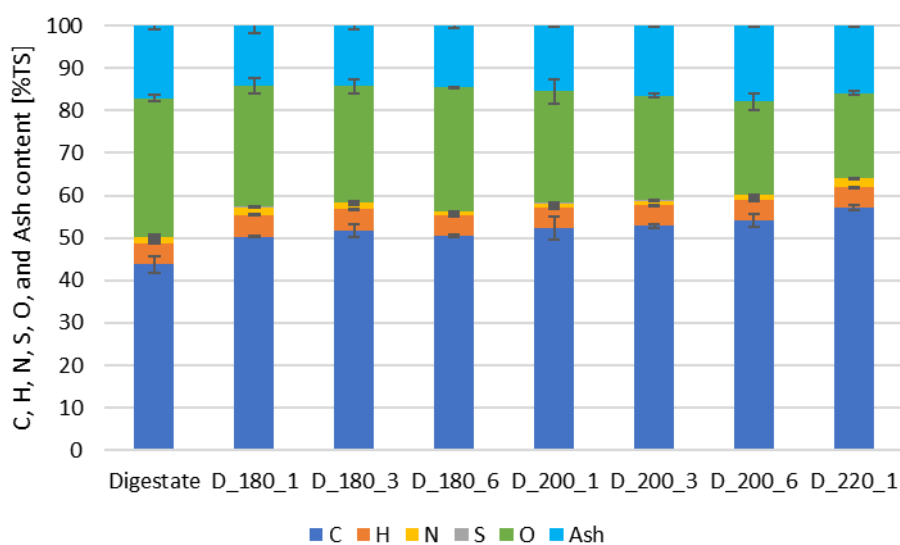
Figure 2.2 - Average composition of digestate and the produced hydrochars in terms of C, H, N, S, O, and Ash. Values reported on dry basis.
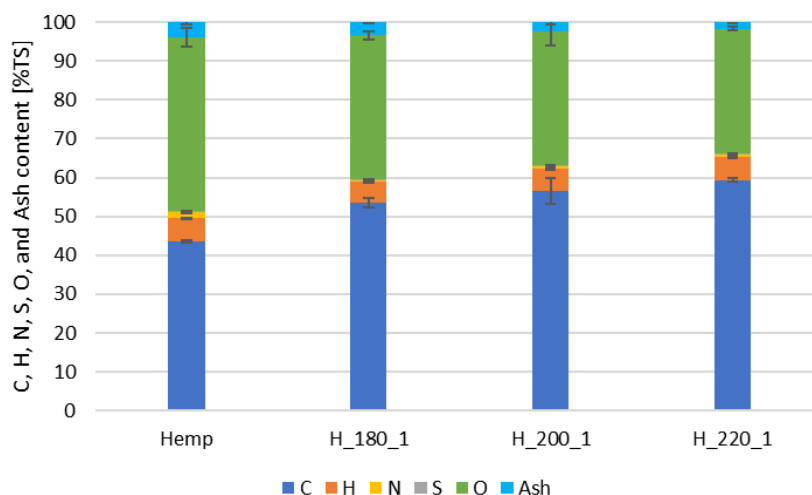
Figure 2.3 - Average composition of hemp and the produced hydrochars in terms of C, H, N, S, O, and Ash. Values reported on dry basis.

The higher heating values measured for the different hydrochars are shown in Figures 2.4 (digestate) and 2.5 (hemp). All the hydrochars reveal much higher HHV than the two feedstocks, with an increase between 15.6 and 22.2% in the case of digestate and between 16.5 and 26.0% in the case of hemp. An increase in temperature and/or holding time seem to produce a slight increase in HHV. However, no statistically significant variation was seen for digestate hydrochar (Figure 2.4). Comparing the obtained HHVs with typical solid fuels, digestate and hemp reported values similar to wood pellet (18.45 MJ/kg), wood chips (18.76 MJ/kg), and lignite (19.75 MJ/kg) as reported by Plaisant et al. (2012), but lower than coal (19 – 30 MJ/kg).

The carbonization grade was assessed through the Van Krevelen's diagram (Figure 2.6 and Figure 2.7), which highlights the changes caused by the dehydration reaction. Compared to the feedstocks, all the samples show a reduction of both the atomic ratios H/C and O/C, which place them in the typical areas of peat and lignite.

Table 2.2 Tukey's HSD test results on hydrochars from digestate and hemp. Tests connected by the same letters are not significantly different.

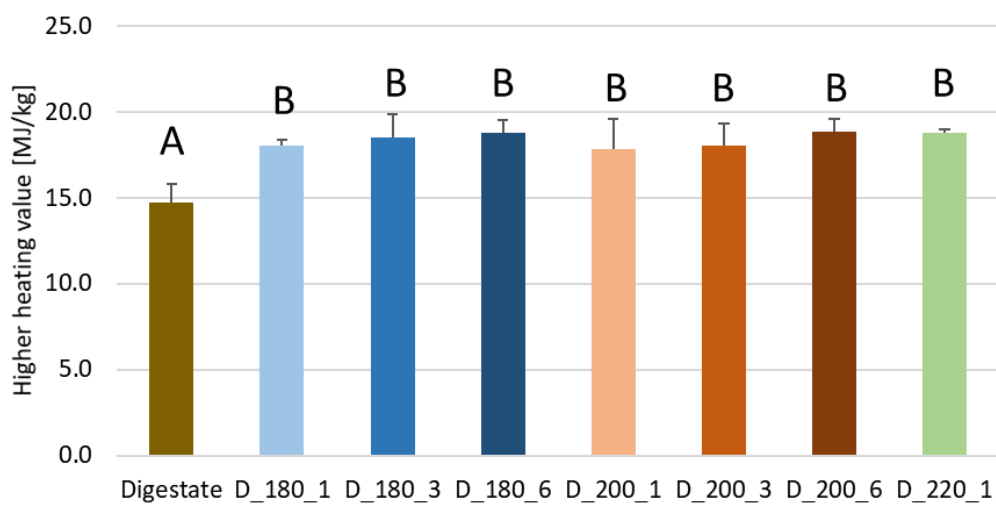|	C		H	N		S	O		Ash	
D_180_1	A		A	A		A	A		A	
D_180_3	A	B	A	A	B	A	A		A	B
D_180_6	A		A		C	A	A		A	B
D_200_1	A	B	A	B	C	A	A	B	A	B
D_200_3	A	B	A	B	C	A	A	B		B	C
D_200_6		B	C	A	B	C	A		B	C		C
D_220_1		C	A	A		A		C	A	B	C
H_180_1	a		a	a		a	a		a	
H_200_1		b	a	a	b	a		b	a	b
H_220_1		c	a		b	a		c		b

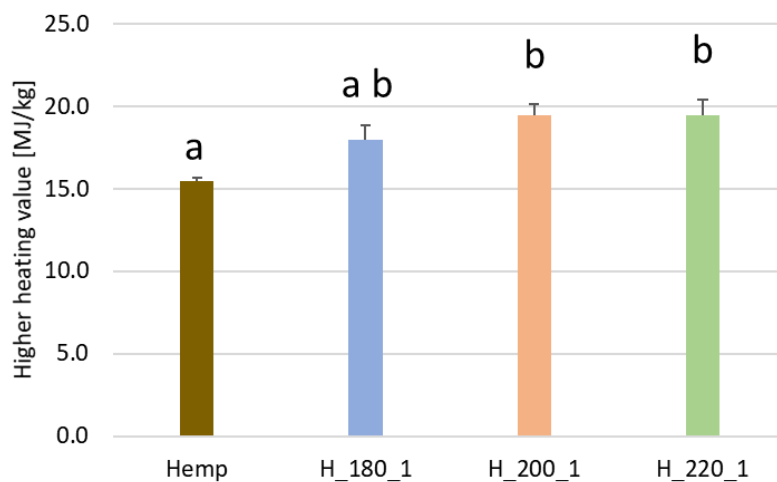*Figure 2.4 - Average higher heating values of the samples of digestate and hydrochars.*

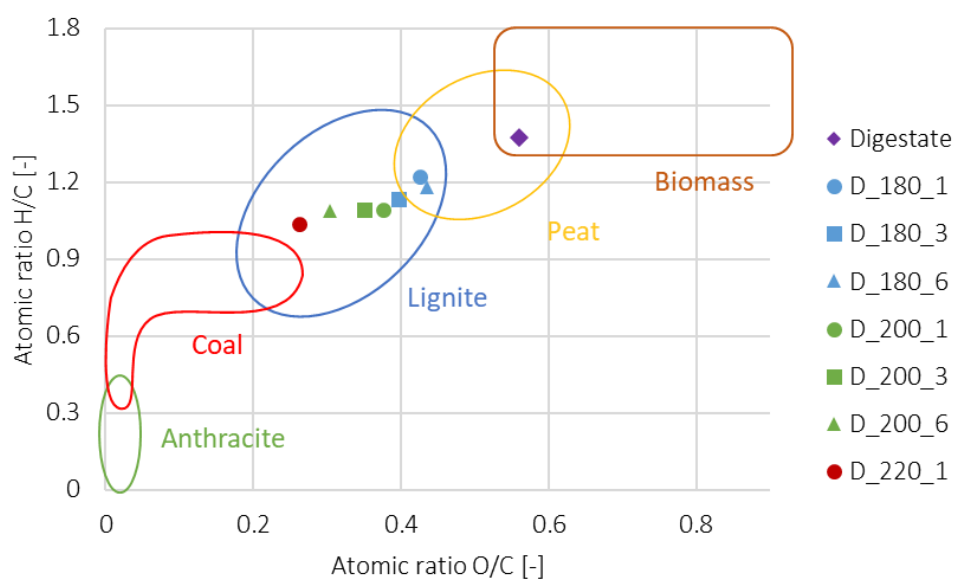*Figure 2.5 - Average higher heating values of hemp and HC from hemp.*

Figure 2.6 - Van Krevelen's diagram for hemp digestate and related hydrochars.
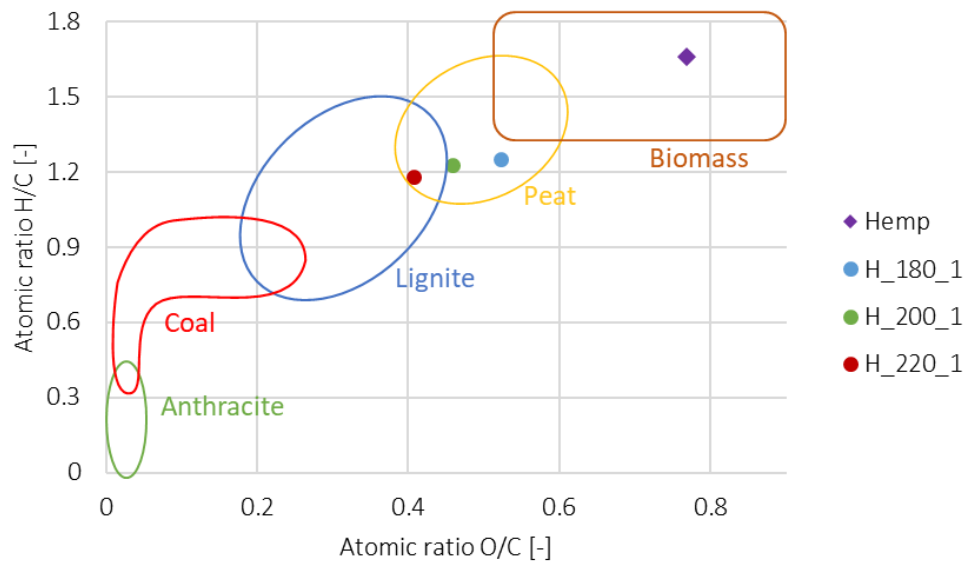
Figure 2.7 - Van Krevelen's diagram for hemp and related hydrochars.

Table 2.3 reports the characterisation of the process water samples. Hydrothermal treatment promoted acidification in the liquid phase, in which higher temperatures and longer holding times seem to produce a larger pH reduction. The pH of the digestate used as a feedstock was 8.50 (±0.25), while the pH of the produced process water ranged between 7.90 and 6.78. The initial pH of the hemp used as HTC feedstock was 5.33 (±0.12), and it dropped to acidic pH values ranging between 3.69 and 3.53 after HTC. No particular trend was found for EC in the digestate hydrochar with values around 25 mS/cm compared with the initial EC of digestate of 20.43 (±0.03) mS/cm. In contrast, much lower values are reported for hemp hydrochars ranging from 9.03 to 8.33 mS/cm, starting from an initial value of hemp of as much as 4.23 mS/cm. For both digestate and hemp samples, TOC and COD decreased in the liquid phase as the severity of the process increased; this is consistent with the intrinsic characteristics of the HTC, based on a series of reactions generally promoted by an increase in process temperature and duration. After an initial step based on hydrolysis, with the dissolution of the solid into the liquid, there is a phase in which the dissolved carbon particles recondense in the solid portion, increasing the final carbon content in the solid phase and the nutrients content in the liquid phase (Langone & Basso, 2020; Libra et al., 2011).

The organic content in process waters, particularly in terms of volatile fatty acids (VFA), suggests their potential valorisation in anaerobic digestion processes to produce biogas. Lower TOC and COD concentrations were found in process water from hemp digestate treatment, which is consistent with the assessed higher solid yield. The macronutrients (P, K, Ca) content in process water, resulting from the dissolution of the solid material in the produced liquid phase, may suggest the use of PW

in fertigation or their recovery for the production of fertilisers. However, process water contains high concentrations of phenols that may have adverse effects when PW is directly used on soil. The higher the temperature, the higher the concentration of total phenols, while a longer holding time seems to reduce the amount of these compounds.

Figure 2.8 and Figure 2.9 show the values of the inhibiting concentration for the different PW samples produced from hemp digestate and hemp at the different process conditions. At constant temperature, toxicity increases as the residence time increases (from 1 to 3 h) and then decreases to 6 h. The lowest toxicity stands out in the case of the D_180_6. With a constant holding time of 1 h, the toxicity decreases with increasing process temperature (from 180 to 200 °C) and then increases to 220 °C for digestate; in contrast, for hemp samples, the higher the temperature, the higher the inhibition. There are no significant differences between the process waters from H_180_1 and H_200_1, while the sample produced at 220 °C shows more significant toxicity.
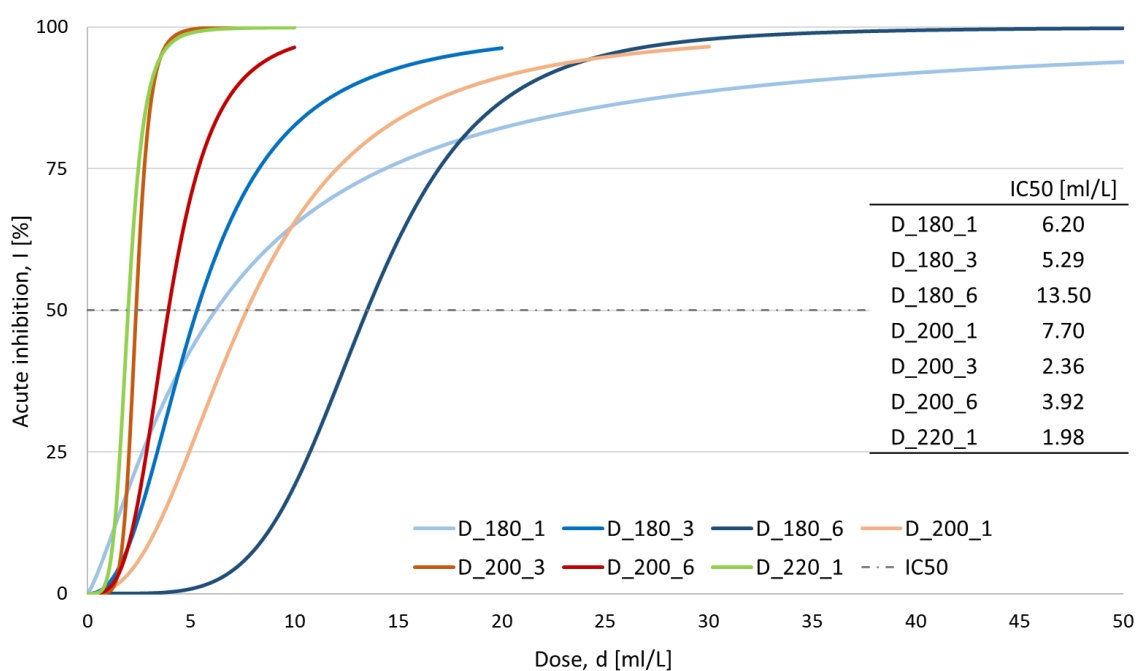
Figure 2.8 - Dose-inhibition curves of the toxicity test on process water derived from hemp digestate.

Table 2.3 - Process water characterisation

Sample	pH [-]	EC [mS/cm]	TOC [g/L]	COD [g/L]	Cl^- [mg/L]	$N\text{-}NO_3^-$ [mg/L]	SO_4^- [mg/L]	P [mg/L]	K [mg/L]	Ca [mg/L]	Total phenols [mg/L]
D_180_1	7.62	26.35	9.36 (0.06)	24.21 (0.76)	2970.71	4.88	-	32.4	5741.0	194.7	1565.3
D_180_3	7.55	26.82	9.24 (0.07)	23.71 (0.57)	5206.68	50.87	172.37	42.6	6474.0	244.1	1435.4
D_180_6	7.42	27.23	8.99 (0.11)	23.13 (0.35)	4374.97	47.61	174.88	36.1	6259.0	173.9	1445.4
D_200_1	7.91	26.50	6.95 (0.08)	19.24 (0.76)	4342.33	-	-	17.4	4759.0	54.8	1825.0
D_200_3	7.81	26.69	7.89 (0.02)	21.06 (0.29)	4756.48	53.04	325.11	19.3	5718.0	212.5	1835.0
D_200_6	7.38	27.93	7.15 (0.03)	19.90 (0.70)	4769.17	40.44	178.53	9.6	6920.0	415.0	1405.4
D_220_1	7.34	28.67	8.80 (0.13)	23.38 (0.70)	3970.50	-	171.34	33.4	6688.8	409.6	2014.8
H_180_1	3.69	9.03	12.31 (0.18)	29.85 (0.50)	1029.95	137.93	44.69	33.2	1768.0	351.5	1476.0
H_200_1	3.55	8.95	11.31 (0.13)	27.11 (0.35)	962.74	115.06	46.25	40.6	1805.0	323.1	1907.6
H_220_1	3.53	8.33	9.32 (0.08)	23.05 (0.76)	1048.68	133.92	31.23	16.5	1599.0	397.1	2083.4
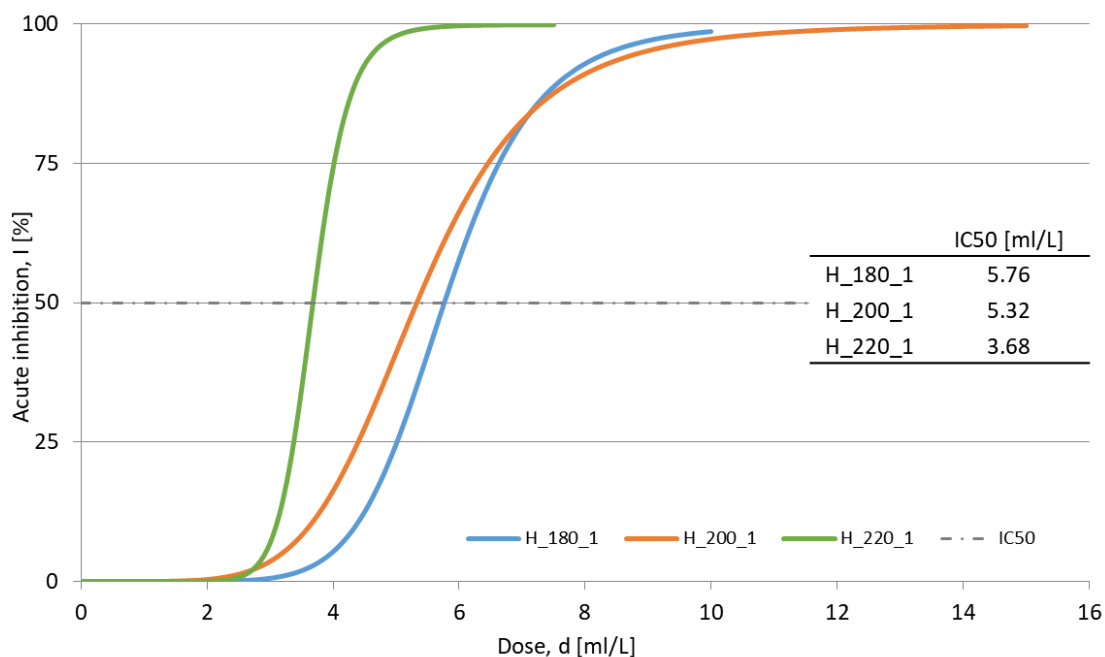
Figure 2.9 - Dose-inhibition curves of the toxicity test on process water derived from hemp

In Figure 2.10, the concentration of total phenols in PW from HTC of hemp and hemp digestate is presented together with IC50 values. The inhibition on nitrifying bacteria is stronger in PW from hemp when higher amount of total phenols are present, with an increase with temperature. Total phenols may contain compounds which can have toxic effect on aerobic bacteria. However, according to the figure, different compounds could be formed in PW from hemp digestate since a diverse trend was found, especially in samples generated at 180 °C. Considering the holding time, toxicity increased at 3h compared to 1h and then decreased at 6h. Regarding samples treated at 1h and different temperatures, PWs from D showed increased concentration of phenols which correspond at higher toxicity, except for D_180_6. The higher amount pf total phenols and the higher inhibition was found in D_220_1 and H_220_1.
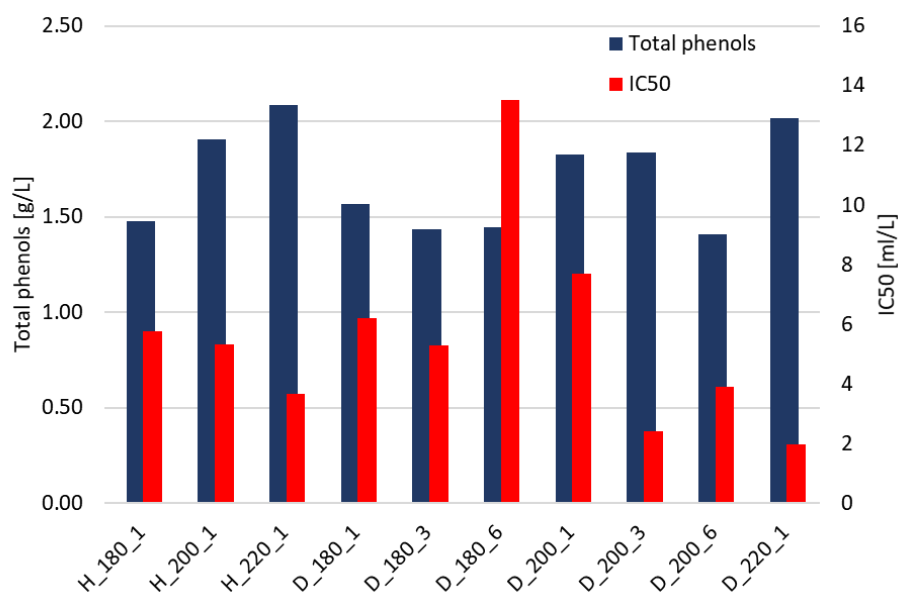
Figure 2.10 - Concentration of total phenols and IC50 in PW samples form HTC of hemp and hemp digestate.

2.4.1 Energetic valorisation

The specific cumulative methane production yield (SMY) assessed through BMP test of the PW is shown in Figure 2.11a for hemp and Figure 2.11b for digestate. The results are provided as mlCH$_4$ produced per initial gCOD in PW. The methane production yield was greatly affected by the HTC temperature. Specifically, when the HTC temperatures kept at 180 °C, higher SMY were obtained for both digestate and hemp, than those obtained for higher temperatures. After 28 days, SMY reached 75.8, 63.5, and 50.9 mlCH$_4$/gCOD for digestate and 113.6, 82.3, and 76.3 mlCH$_4$/gCOD for hemp, at 180, 200, and 220°C, respectively. Increasing the retention time of the HTC process on digestate from 1 to 6 hours has a milder effect on the SMY, with an increase of 16% and 15% at 180 °C and 200 °C, respectively. Similar results were also found by Erdogan et al. (Erdogan et al., 2015; Stökle et al., 2021) working on HTC PW from orange peels and chicory roots. This result could be linked to the higher concentration of inhibitors, such as phenols, in the PW when increasing the HTC temperature (see Table 2.3), as also underlined by the aerobic inhibition curves (Figure 2.10). Moreover, other compounds formed during the HTC process, and not specifically identified, could have had an inhibitory effect against AD. This aspect is relevant considering that more than 50% of soluble TOC has not been identified.
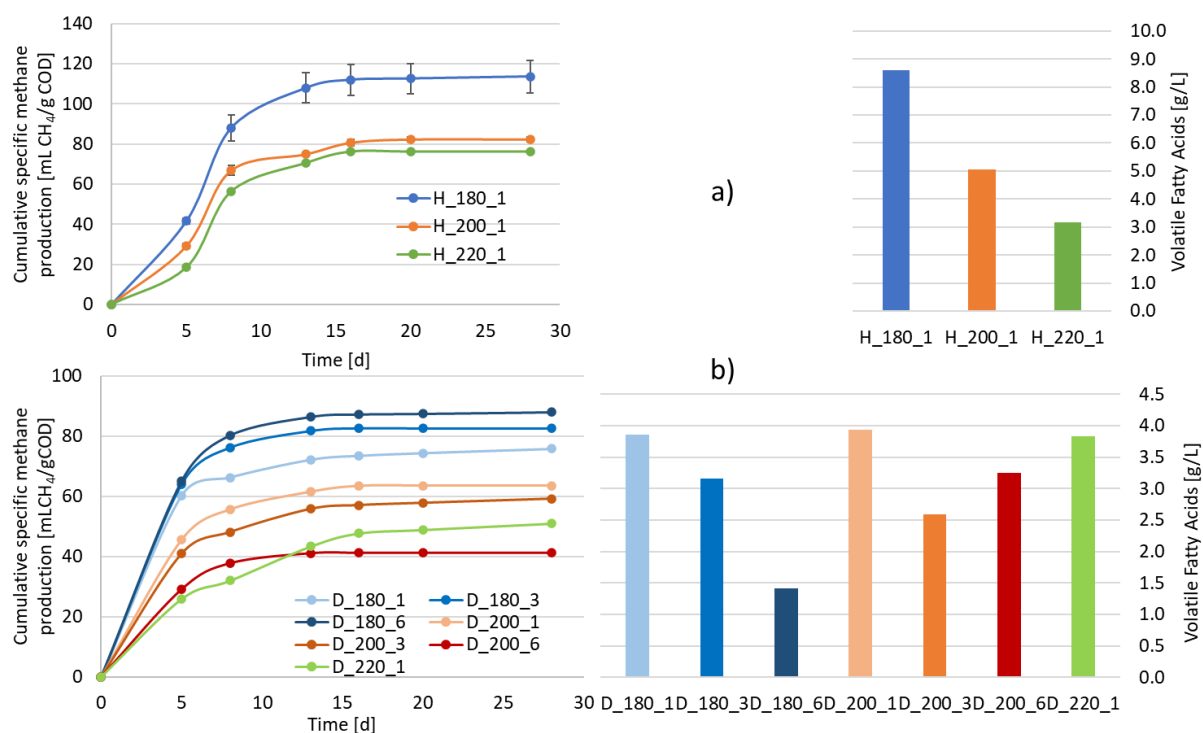
Figure 2.11 – Specific cumulative methane production yield and volatile fatty acids concentration for PW samples of a) hemp and b) hemp digestate.

2.5   Conclusion

Anaerobic digestion is a technology commonly used for the energy valorisation of residual biomass, but it produces a digestate that requires appropriate valorisation in the perspective of sustainable management. The integration of AD with HTC has been recently proposed as an interesting approach for increasing the overall recovery of energy and added value products from the hemp supply chain.

The characterisation of the hydrochars produced through hydrothermal carbonization of hemp digestate suggests that this process applied to wet feedstocks may produce added-value products. The properties of the produced hydrochar were improved compared to the input material, particularly in terms of carbon and energy content. As far as the effect of process conditions is considered, an increase of process severity with reference to higher temperatures and longer holding times resulted in a decreased solid yield and a higher carbon enrichment. The Van Krevelen's diagram showed an achieved carbonization grade similar to peat or lignite, which, along with the increase in HHV, provide good perspectives for hydrochar's use as fuel. Moreover, the hydrochars characteristics, such as high pH, peat-like properties, and complete disinfection, make them potentially suitable as soil amendments. Process water may be used for nutrient recovery, irrigation

in agriculture, or energy recovery via AD. Accordingly, hydrothermal carbonization may be a suitable process for hemp digestate valorisation.

The results of this study can provide useful information on the potential integration of HTC with AD in the management of residual biomass of agro-industrial origin.

Chapter 3

Hydrothermal carbonization of agro-industrial waste: a sustainable option towards GHG reduction and waste valorisation

This chapter presents the results of the hydrothermal carbonization on GM and GM after extraction in ethanol. A preliminary version of this chapter has been presented and the 18th International symposium on waste management and sustainable landfilling – Sardinia 2021, in Sardinia (Italy). Furthermore, it has been selected for the publication in the special issue entitled "Waste Management and Climate Change" on STOTEN (international journal of Science of the Total Environment) and, currently, it is under review.
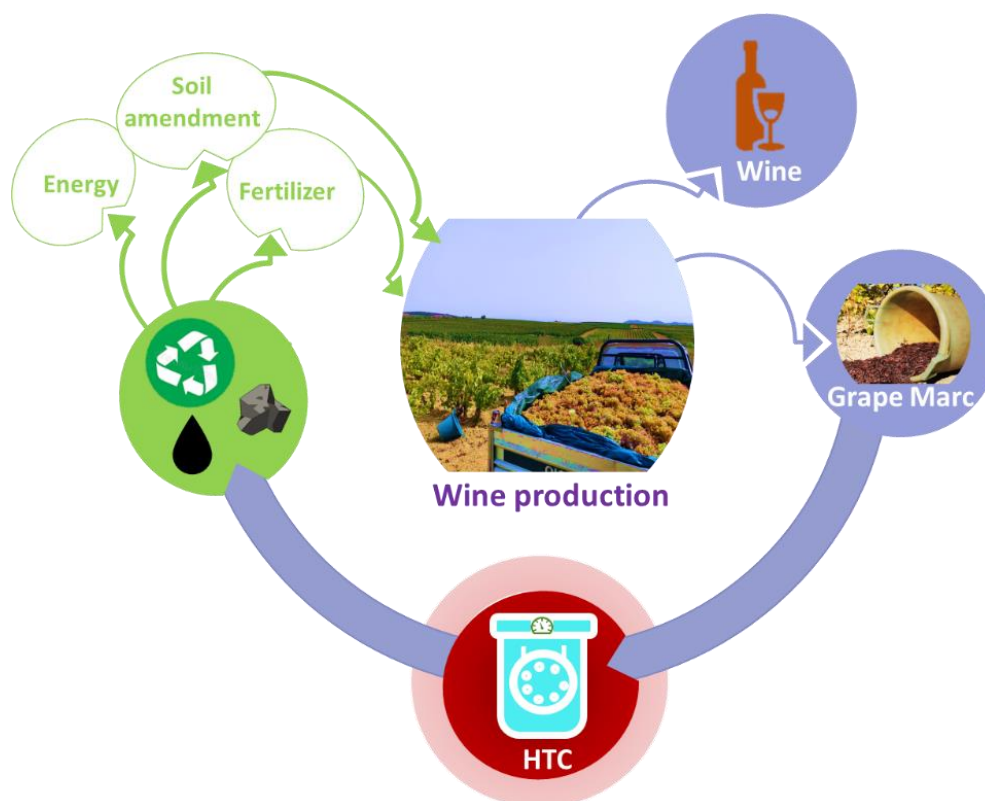
3.1 Abstract

The agro-industrial sector yields a high contribution to greenhouse gas emissions; therefore, proper waste management is of crucial importance to reduce the carbon footprint of the food chain. Hydrothermal carbonization (HTC) is a promising thermochemical process for converting organic materials into added-value products that can be used in different applications. In this work, grape marc and extracted grape marc were hydrothermally treated at 220 °C for one h. The resulting hydrochar and process water were investigated to test suitable enhancement and management options. The results show that hydrochars, particularly those obtained from previously extracted grape marc, can be used as amendments for partially substituting peat, sustaining plant growth, and saving the consumption of natural substrates such as peat. In addition, energy can be recovered from both hydrochar by combustion and from process water through anaerobic biological processes to produce biogas. HTC process waters were found to be suitable for biological treatment, but attention must be paid to the presence of inhibiting compounds that induce acute toxic effects in aerobic conditions. HTC applied to agricultural residues like grape marc may be a feasible and proper process for their valorization, addressing the need for renewable energy sources and restoring the carbon content of the soil that could increase the overall sustainability and resilience of the agro-industrial sector.

3.2 Introduction

The food supply chain is one of the foundations of human society. Its intrinsically positive role, however, has often been jeopardized by economic, environmental, and social issues, such as vulnerability to natural calamities, availability of food uneven and not always consistent with the density of human population, ownership by a few of large portions of fertile land, overuse of land and water and related morphological and hydrographic impacts, threats to ecosystems and loss of biodiversity, use of pesticides to increase productivity. In the last decades, similarly to other pivotal sectors such as industrial and energy production, urbanization and mobility, etc., the food supply chain has also raised concerns due to the contribution to the climate change emergency. Globally, the food sector yields more than one-third of global anthropogenic greenhouse gas emissions, deriving from the 11-19 billion tons of emissions per year estimated by the Intergovernmental Panel on Climate change (Crippa et al., 2021). Such recent studies confirm earlier findings of Gilbert (2012) and although land use and production, including fertilizers use, are still the main contributors, they

point out the increasing role of retail, packaging, transport, "cold chain" activities, processing, and related energy consumption and waste production. Reducing the food chain carbon footprint is, thus, central to limiting climate change, and proper waste management is of particular importance (Karl & Tubiello, 2021). In fact, on the one hand, incorrect waste management is pushing the food supply chain to the top of the list of greenhouse gas emitters, as reported by the United Nations Agriculture Agency during the COP26 climate conference in Glasgow in 2021. On the other hand, the organic nature of most of the residues produced along the food supply chain is suitable for innovative processes aimed at recycling, or even upcycling, organic waste and by-products in a waste biorefinery framework, consistent with the principles of the circular bioeconomy.

In this sense, it is important to develop processes and approaches that aim to recover both material and energy resources, in a flexible way and in accordance with the needs of the market and the local context. In the case of waste of agro-industrial origin, it is also important that the recovery of resources addresses the problems listed above, such as the need for renewable energy sources and soil improvers, the first because the food chain is becoming more and more energy-intensive, the second to preserve and restore the carbon content of the soil, sequestrating the carbon and storing it over the long term (Fryda et al., 2018).

Despite the pandemic situation and the related effects on the global markets, 260 million hectolitres of wine were produced in 2020 worldwide, which is in line with the yearly average production of the last decade. For every quintal of grapes, about 70 litres of wine and 18 kg of grape marc are produced (Muhlack et al., 2018). Accordingly, over 6 million tons of grape marc are produced globally every year (OIV - International Organisation of Vine and Wine Intergovernmental Organisation, 2021).

Managing such a large amount of residual biowaste, rich in water (around 60% by weight) and organic matter (up to 900 g/kg) and characterized by an acidic pH (3-6), and a high content of lignin and polyphenols is a challenge that must be faced consistently with the dictates of current environmental and economic policies. Furthermore, management options must consider the seasonality of production since approximately 75% of solid waste is generated during the harvest period.

Grape marc is sometimes used as a by-product, e.g., for ruminant animal feeding, although some adverse effects can be ascribed to the presence of substances such as polyphenols (Muhlack et al., 2018). If grape marc is managed as a biowaste, biological treatment such as anaerobic digestion, with reported methane yields spanning within a wide range of values (113 - 420 L CH_4/kgVS), or

composting and subsequent use on soil, are currently the most common management methods. The relatively high heating value of grape marc (19 - 22 MJ/kg) would allow an energy enhancement through direct combustion (Muhlack et al., 2018); however, the high water content makes pre-drying necessary.

This study aims to evaluate alternative valorization options, which combine the recovery of materials and energy through the application of hydrothermal carbonization. HTC is a wet thermochemical process that rapidly converts organic substrates into added-value by-products. Under autogenous pressures and temperatures generally ranging from 180 to 250 °C, a coal-like solid material known as hydrochar and process water are produced, whose characteristics suggest a wide range of potential applications (Libra et al., 2011). Since during the process, water is involved as both the reaction medium and catalyst, HTC is particularly suitable for wet biomass valorization without any dewatering or drying pre-treatment.

The HTC technology is considered particularly sustainable, as it fully embraces the principles of the circular economy and the need to identify waste management systems capable of guaranteeing lower climate-altering emissions. In its most typical application, biomass-derived hydrochar is used as a fuel for renewable energy production, acting as a neutral combustible and energy-dense carbon source. Being a carbon-enriched solid, hydrochar combustion involves lower CO_2 emissions per unit of energy developed, further offsetting CO_2 emissions. The chemical-physical characteristics of hydrochar make its application interesting also as a soil amendment, able to improve fertility as well as water retention and carbon sink (Funke & Ziegler, 2010; Libra et al., 2011; T. Wang et al., 2018). The different possibilities of char use yield evident positive effects in terms of avoided exploitation of non-renewable resources.

The specific objective of this work is to assess i) the potential application of the hydrochar produced via HTC from grape marc as a soil improver and solid fuel, and ii) the biological treatability (anaerobic and aerobic) of the process water in view of energetic valorization or disposal. Additionally, it was intended to study the application of HTC to the treatment of both raw grape marc (GM) and of the same residual biomass after extraction of polyphenols (GM_Ext), compounds that can find application in different production sectors.

To achieve the study's objective, HTC tests were carried out at a temperature of 220 °C for one h. After the HTC treatment, the obtained by-products were physically and chemically characterized. To verify the feasibility of hydrochar as a soil improver or peat substitute, germination tests were carried out in different mixture ratios (5, 25, 50%), and phytotoxicity and inhibition of plant growth

were evaluated. Respirometric tests verified the stability of the material. In addition, a biomethane potential test (BMP) was applied to process water to assess its energetic content and, consequently, evaluate anaerobic digestion as a possible way for its valorization. At the same time, acute toxicity tests on nitrifying bacteria were carried out to explore the possible PW treatment in aerobic treatment plants.

3.3   Materials and methods

3.3.1   Feedstock

The grape marc of Cannonau wine production, consisting of skins, seeds and stems, was collected in southern Sardinia (Italy) during the 2019 harvest season and stored in vacuum plastic bags at -20 °C for further analyses and experiments. As feedstock material for the HTC process, both GM and extracted GM (GM_Ext), produced within the framework of a parallel study aimed at recovering polyphenols through ethanol:water extraction (Perra et al., 2021), were used.

3.3.2   Hydrothermal carbonization

The hydrothermal carbonization tests were carried out in a stainless-steel pressurized reactor of 1.5 L of inner volume (Berghof, BR-1000). The reactor was equipped with an electric jacket for heating, a thermocouple for the continuous monitoring of the inside temperature, a stirred shaft and a data logging unit connected to a computer where the main operating parameters (inner temperature and autogenic pressure) were continuously recorded. GM and GM_Ext were both treated at 220 °C for 1 h with a temperature increase of 2 °C/min. The solid material with its humidity content was placed in the reactor together with distilled water to achieve a solid content of 10%. After the input material preparation, the reactor was sealed, and the controller was set to the desired temperature and holding time. Once continuous reactor operation at 220 °C was observed for 1 h, it was turned off and cooled to room temperature overnight. Before unsealing it, the final inner pressure was noted and the gas released evaluated through a column gas meter, based on water displacement method, to estimate the volume produced. To assure a mass balance as precise as possible, all the output materials were carefully weighed before and after each step. The carbonized sludge resulting from the HTC process was separated through a press filter obtaining the solid (hydrochar, HC) and the liquid (process water, PW) phases. The hydrochar was stored in vacuum plastic bags at 4 °C while the process water was vacuum filtered at 0.45 μm and stored in plastic bottles at 4 °C. All tests were

carried out three times to ensure replicability. According to the feedstocks, the hydrochars were named HC_GM and HC_GM_Ext and the process water samples PW_GM and PW_GM_Ext.

3.3.2.1   Hydrochar

The hydrochars produced were characterized in terms of humidity, ash content, elemental composition, density, surface chemistry and higher heating value (HHV). The residual humidity in hydrochar after separation from the liquid phase was estimated by heating three samples (randomly selected from the total mass) to 105 °C, while the ash content was measured keeping the dried samples at 550 °C. In both cases, samples were kept in oven until a constant weight was achieved. Further analyses were conducted on dried and milled samples. Elemental composition was estimated using a CHN analyser (CHN628, LECO) and oxygen by difference. The higher heating value (HHV) was measured in a calorimetric bomb (AC500, LECO) and the surface chemistry was investigated through infrared spectroscopy (ATR-FTIR, 6300FV, Jasco). The characterization was conducted on representative dried samples, milled and homogenized. The potential use of hydrochar as soil amendment to sustain plant growth was assessed through germination test as well as respirometric test, according to the methods described in 2.3 and 2.4 sections.

3.3.2.2   Process water

The liquid phase from the HTC runs was characterized in terms of pH and electrical conductivity (EC), total organic carbon (TOC) (TOC-V CSN, Shimadzu), and chemical oxygen demand (COD). The potential energy recovery from PW through anaerobic digestion, as well as the potential inhibition exerted within aerobic processed, were evaluated according to the methods described in Sections 2.5 and 2.6, respectively.

3.3.3   FT-IR analysis

GM, GM_Ext, HC_GM and HC_GM_Ext in form of homogenized powders, as well as a selection of specific parts – milled seeds (GM_{seeds}) and whole pieces of stems (GM_{stems}) and skin (GM_{skin}) - of dried grape marc before milling, underwent FT-IR analysis by a Jasco FT-IR6300A spectrometer equipped with an ATR PRO ONE (diamond crystal) in the 4000-400 cm^{-1} spectral range, ris. 4.0 cm^{-1}, 50 scans. Spectra measurements were repeated at least 5 times on different aliquots/parts of the samples in order to provide representative spectra for the heterogeneous material.

3.3.4 Germination test

According to the standard test UNI EN 16086-2:2012-01, Sphagnum peat, previously sieved at 10 mm, was mixed with GM, HC_GM, and HC_GM_Ext with a ratio of 5, 25, and 50%. Moisture was checked and adjusted with the "fist test", adding water until squeezing the material with the fist did not produce leaching. Around 50 g of each mixture were placed in 3 square Petri dishes and 10 seeds of cress (*Lepidium sativum L.*) were sown at the top of the dish. In addition, 3 more Petri dishes filled with only peat were used as a control. One drop of water was added on each seed. Petri dishes were closed with parafilm and stored in an oven at 25 °C for 72 h for incubation with an inclination of 70 – 80° (seeds at the top). After 72 h of incubation, the Petri dishes were opened, the germinated seeds were counted, and the length of the seedlings was measured. The germination rate was defined as the percentage of germinated seeds on the total number of seeds. Finally, the results were validated with statistical tests, such as ANOVA and Tukey's HSD test through the statistical software JMP (v. 15, SAS). The samples were named with the codes formed by the initials of the material mixed with the peat and the used amount; to give an example, the sample with the mixture containing peat and 5% hydrochar from grape marc was labelled HC_GM_5%. According to the standard test, different parameters were calculated: average germination rate (AGR), coefficient of variance for germination rate (CVR), average root length per plant (ARLP), coefficient of variance for root length (CVR), average hypocotyl length per plant (AHLP), coefficient of variance for hypocotyl length (CVH), root length index (RI), and Munoo-Liisa vitality index (MLV).

3.3.5 Assessment of material stability

Several methods have been proposed to measure biomaterial stability (Sánchez Arias et al., 2012). Among them, respirometric methods based on oxygen consumption are more broadly recommended and deemed as the most suitable methods. Electrolytic respirometry is based on the Warburg manometric respirometer and is usually referred to as the Sapromat® system. This system has been extensively applied to estimate O_2 consumption for various purposes/fields: biodegradability of waste and wastewater, toxicity, and inhibition tests, modelling and kinetics of biodegradation, respiration of polluted soils, compost and biologically pretreated waste stability. In this context, 10 g of pre-humidified HC were placed in a 500 ml glass reaction bottle, connected with an oxygen generator and a pressure control gauge, in a water bath (20 °C). The CO_2 produced by aerobic microorganisms is absorbed by NaOH pellets. The tests were run in triplicate.

The HC stability was assessed in relation to RA_4 (total oxygen consumption after 4 days), which is the recommended parameter for the estimation of compost stability by the European Union in the "Working Document on the Biological Treatment of Biowaste" (European Commission, 2001). The results are given in mg O_2/gTS (Binner et al., 2012).

3.3.6 Assessment of Biochemical Methane Potential (BMP)

The BMP test is a standard test for determining biogas production from an organic substrate using methanogenic bacteria as the inoculum under optimal batch conditions. This test was applied to the PW produced during HTC for assessing the possibility of conversion into biogas. According to the standard norm (UNI1601755EIT), BMP tests were conducted in brown glass bottles, where methanogenic sludge was mixed with PW derived from the HTC runs. The amount of sludge and sample was set to allow gas to form in the headspace of the bottles and ensure a food-microorganism ratio (F/M) of 0.5 gCOD/gCOD according to the literature (Boulanger et al., 2012; Pagés-Díaz et al., 2020). Methanogenic sludge added with D-glucose was used to assess the specific methanogenic activity (SMA, data not shown). A blank test was also tested with only inoculum. No nutrient solution or pH buffer was added to the bottles. The initial pH value was around 7.0 for all samples. All the tests were performed in triplicate. Before the bottles were sealed with airtight caps, the mix was purged with nitrogen to guarantee anaerobic conditions. The sealed bottles were placed in a thermostated shaker (T = 39 ± 1 °C) and kept for 36 days. An average period of 3 days was adopted, slightly shorter at the beginning of the test and longer at the end, to purge the gas produced and accumulated in the reactors to avoid the onset of high inner pressure. Partial and cumulative biogas production was measured over time. The volume produced was measured through a water-displacement method using a volumetric column, and the gas samples were analysed using a GC-FID (7890B, Agilent Technologies) equipped with a thermal conductivity detector (TCD) and two stainless columns packed with HayeSep N (80/100 mesh) and Shincarbon ST (50/80 mesh) connected in series.

The methane yield at 36 days was calculated as follows (Equation 3.1):

$$BMP = (V_{CH_4,s} - V_{CH_4,blank})/COD_s$$ (3.1)

Where $V_{CH4,s}$ is the volume of methane produced from the PW measured at the end of the test, $V_{CH4,blank}$ is the volume of methane produced from the inoculum measured at the end of the test, COD_s is the mass of soluble COD of the added PW.

The modified Gompertz equation, based on a sigmoid function, was used to calculate the kinetic parameters for the CH_4 production process, according to Equation 3.2 (Pagés-Díaz et al., 2020).

$$Y(t)CH_4 = Y_{max}CH_4 exp\left\{-exp\left[\frac{R_{max} \cdot e}{Y_{max}CH_4}(\lambda - t) + 1\right]\right\}$$ (3.2)

where: $Y(t)CH_4$ is the cumulative production yield of CH_4 at time t, $Y_{max}CH_4$ is the maximum theoretical production yield R_{max} is the maximum production rate, λ is the duration of the lag phase, t is the time and 'e' is the Neperian number. The experimental data were fitted through Eq. (2) using the TableCurve 2D® software (v. 5.01, Systat Software Inc.) through least-squares non-linear regression. The coefficient of determination R^2 was used to evaluate the quality of data fitting for each experimental dataset.

3.3.7   Assessment of acute toxicity

A pH-stat titration unit (ANITA, Ammonium NITrification Analyser) was used to assess the acute inhibiting effect of HTC process water on the ammonium-oxidizing bacterial community in activated sludge, as described in Ficara & Rozzi, (2001). The tests were carried out in a glass vessel containing 1 L of unacclimated activated sludge (total suspended solids, TSS, 4 g/L) drawn from the Oristano wastewater treatment plant (Italy). The maximum ammonium-oxidizing capacity of nitrifying biomass was measured in the presence of ammonium as the only substrate, considering the stoichiometric relationship between ammonium oxidation and acidity production, and used as reference. Known volumes of PW_GM and PW_GM_Ext were subsequently added to the activated

sludge. The resulting nitrifying activity was compared with the reference and the corresponding inhibition was calculated for each dosage. At the end of the test, nitrification was fully inhibited by allylthiourea to detect the presence of interferences. A dose-response curve was plotted for both PW_GM and PW_GM_Ext, and the IC50 (that is the amount of PW that causes 50% acute inhibition of sludge activity) was determined.

3.4 Results and discussion

3.4.1 Characterization of feedstock and products

The main properties of the two materials used as feedstock for the HTC runs are shown in Table 3.1. All parameters were evaluated on a dry basis by weight, apart from the humidity that was measured on a wet basis. The general characterization parameters do not show significant differences determined by the phenolic compounds removal process.

Table 3.1 - Main properties of grape marc and extracted grape marc. STD is reported in brackets.

Feedstock	Code	Humidity [%]	Volatile matter [%]	Ash [%]	C [%]	H [%]	N [%]	O [%]
Grape marc	GM	6.17 (0.07)	87.49 (0.95)	12.51 (0.95)	49.00 (0.15)	6.09 (0.08)	2.08 (0.13)	30.32 (0.17)
Grape marc (extracted)	GM_Ext	7.40 (0.56)	87.68 (1.61)	12.32 (1.61)	49.63 (0.29)	5.94 (0.08)	2.09 (0.13)	30.02 (0.48)

After the HTC tests, a solid yield (Y) of 62.28% (±0.69) was found for GM_Ext, while a slightly lower value of 59.59% (±0.52) was obtained in the tests on GM. This is consistent with the extraction process previously applied to GM_Ext, which may have involved the removal of soluble compounds from the solid matrix.

Characterization of the hydrochars produced from GM and GM_Ext is shown in Table 3.2. In comparison to the feedstock, the ash content in the produced HCs was lower and consequently the volatile matter higher, aspect of interest in view of the use of HC as a fuel. Regarding the elemental composition, carbon was concentrated by the carbonization process, while nitrogen and oxygen were reduced. No noticeable variation in terms of hydrogen content was found. Comparable characteristics were observed for both feedstocks.

To assess potential modifications induced by HTC on the surface chemical structure of the materials, ATR-FTIR spectra were investigated. In Figure 3.1a, the spectrum of the GM powder and those of selected seeds, stems, and skin, are compared for starting material characterization. Since a close match was found for over five replicates of the spectrum for each kind of sample, only one replicate is presented in the charts.

The spectrum of GM consists of the typical peaks reported for polyphenolic lignocellulosic and flavonoid compounds found in grape marc (Casazza et al., 2016), together with a contribution of amines reasonably present in the mixture as the result of biogenic decarboxylation processes of amino acids (Ansorge, 2009). Details on the peaks attribution are reported on the spectra. In summary, the typical peaks related to lignin and polyphenols - OH (υOH 3300s-br when secondary H-bonding are present, *δOH 1378m,* υPhO 1263s), C-H (aliphatic CH: υ 2980-2850mw, *δ/ρ* 1400-1300m; aromatic CH: *δ* 650-720m), C=C (aliphatic C=C: υ 1650m; aromatic C=C: υ 1540m) and C-O (υC=O 1750m; υC-O 1026s; υC-O-C 1130m), as well as those typical for amines (υNH 3313m and 3271m; δNH 1600m-br; υCN 1063s), are present (Fan et al., 2012). GM_{seeds} and GM_{stems} spectra are dominated by the peaks related to the lignocellulosic moiety while polyphenols are far less represented due to the negligible anthocyanine content, as reported by Pinelo et al. (2006). Furthermore, in agreement with the highest amounts of tannins and gallates contained in seeds with respect to the other fractions, a relevant C=O and C-O-C stretching vibrations contribution in GM_{seeds} spectra appears. As expected, skin demonstrated to be the richest fraction of grape marc being characterized by complex FTIR spectra where the typical peaks related to the different polysaccharides and polyphenols, as well as amines, are present. Figure 3.1b compares the GM with the HC_GM spectra and points out a significant modification of the chemical composition and structure of the sample occurred during the HTC process. Indeed, in agreement with the loss of oxygen and nitrogen found in the samples after HTC, the peaks related to the phenolic moieties of polyphenols and their intermolecular secondary interactions, as well as those of possible carboxylic groups and NH_2 stretching vibrations (υNH 3271 and 3313 cm^{-1}) are mainly reduced. Correspondingly, peaks typically related to unsaturated aromatic and aliphatic C=C bonds (1650-1598 cm^{-1}) and aromatic CH in bonds (719 cm^{-1}) increased. A close match was found for GM and GM_Ext, as well as the derived hydrochars.

The main characteristics of the process water are reported in Table 3.3. The treatment led to an acidic pH and an electrical conductivity (EC) value of around 12 mS/cm for both the PW, typical features of the liquid phase from HTC (Funke & Ziegler, 2010; Libra et al., 2011). The total organic

carbon (TOC) accounted for 9.69 g/L for PW_GM and 7.68 g/L for PW_GM_Ext; similarly, the soluble COD was higher in GM than GM_Ext, with values higher than 30 gO$_2$/L. The combined analysis of the characteristics of HC and process water suggests that the preliminary extraction treatment slightly enhances the fixation of carbon in the HC, limiting its release into the PW.

Table 3.2 - Average solid yield and composition of HC obtained during HTC test. STD is reported in brackets.

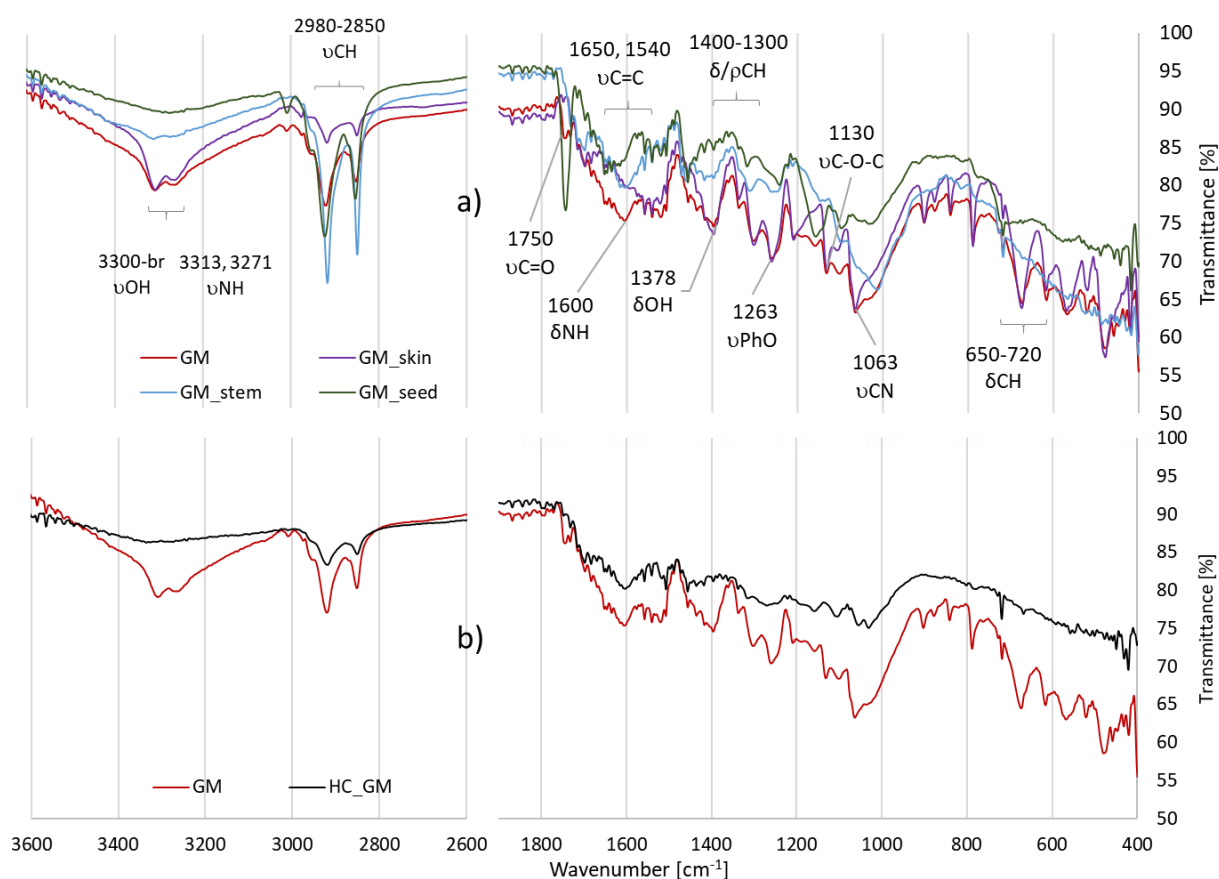| Sample	Solid yield (Y) [%]	Volatile matter [%]	Ash [%]	C [%]	H [%]	N [%]	O [%]
HC_GM	59.59 (0.52)	95.04 (0.85)	4.96 (0.85)	61.60 (0.60)	6.14 (0.15)	1.85 (0.11)	25.45 (0.78)
HC_GM_Ext	62.28 (0.69)	95.63 (0.13)	4.37 (0.13)	62.46 (0.29)	6.28 (0.12)	1.68 (0.07)	25.21 (0.22)

Figure 3.1 - FTIR spectra of a) GM and its components (stem, skin, seed) and b) GM and the derived hydrochar (HC_GM).

Table 3.3 - Process water characterization. STD is reported in brackets.

Sample	pH [-]	EC [mS/cm]	TOC [g/L]	COD [gO$_2$/L]
PW_GM	4.40 (0.02)	12.52 (0.88)	9.69 (0.33)	33.28 (0.42)
PW_GM_Ext	4.37 (0.08)	11.37 (0.16)	7.68 (0.48)	31.08 (0.97)

The product mass distribution in the solid, liquid and gas phases observed after the HTC treatment is reported in Table 3.4. The response to the conditions of the HTC process was similar for the two types of grape marc, regardless of the preliminary extraction. The solid content at the beginning of the HTC test was 90% and 10%, respectively. The treatment resulted in a dramatic reduction of the solid phase for the benefit of a modest gasification and, above all, of a liquid phase, which has become the predominant mass fraction. This was likely due to both to dehydration reactions and solid mass solubilisation, the latter resulting in an increased density of the liquid solution.

Table 3.4. Solid, liquid and gas mass fractions after HTC treatment. STD is reported in brackets.

Phase	GM [%wt]	GM_Ext [%wt]
Solid (Hydrochar)	6.05 (0.07)	6.32 (0.08)
Liquid (Process water)	92.85 (0.13)	92.78 (0.05)
Gas	1.10 (0.06)	0.90 (0.03)

The results of the characterization analyses of the phases that result from the HTC treatment were used to perform mass balances for the elements carbon and nitrogen according to Equation 3.3.

$$M_{IN} = M_{HC\ OUT} + M_{PW\ OUT} + M_{GAS\ OUT} = M_{OUT} \tag{3.3}$$

The carbon distribution in the HTC products is presented in Figure 3.2, where the gas phase was considered as a complement to 100. Most of the carbon is present in the solid phase, to a higher extent in the sample derived from GM_Ext while the carbon dissolved in the liquid phase is higher for the samples derived from GM. In contrast, nitrogen behaviour is almost uniformly distributed in the solid and liquid phases, as far as the latter is counted as a complement to 100 and assuming zero nitrogen in the gaseous phase (Figure 3.3).
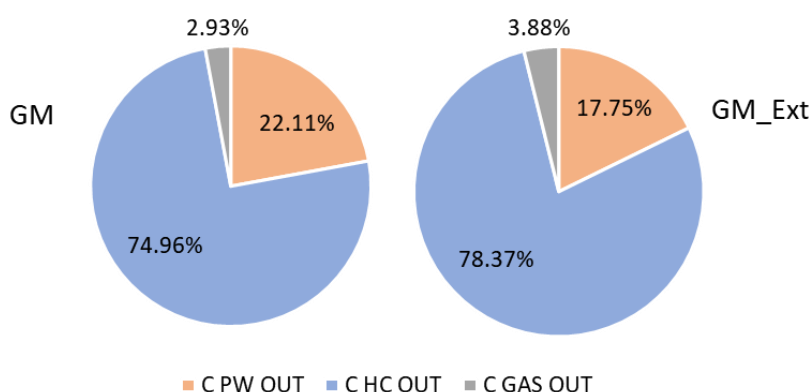
Figure 3.2 - Carbon distribution in the HTC products from GM (left) and GM_Ext (right).
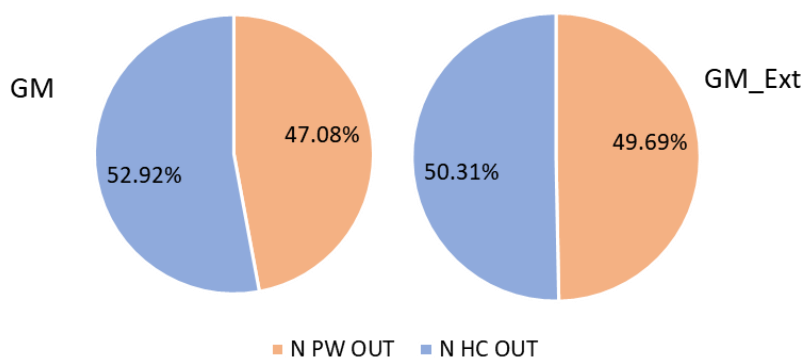

Figure 3.3 - Nitrogen distribution in the HTC products from GM (left) and GM_Ext (right).

3.4.2   Potential valorisation of HC

3.4.2.1   Assessment of the energetic valorisation of HC

In Figure 3.4 the Van Krevelen's diagram is represented, a tool that considers the atomic ratio H/C and O/C to define the grade of carbonization of a material. The feedstocks GM and GM_Ext fall within the typical area of peat, while the obtained HC, as expected, appertain to the lignite region as a consequence of the higher grade of carbonization.

Van Krevelen's diagram provides interesting information about the transformation induced by the process, underlying that the carbonization decreased both the atomic ratios H/C and O/C, that is mostly ruled by dehydration and partially by decarboxylation reactions typically occurring during HTC (Funke & Ziegler, 2010; Libra et al., 2011). This fact is also supported by the FTIR analyses, which single out a reduction in the number of carboxylic and hydroxyl groups due to HTC. The diagram is

usually used to define the quality of a solid fuel paired with the assessment of the higher heating value (HHV) data. The HHV of the samples is shown in Figure 3.5 along with the HHV of some common-use solid fuels. Through the HTC process, the energy content of the hydrochar (around 27 MJ/kg) was increased compared to the feedstock (around 19 MJ/kg), exceeding the values associated with the solid fuels considered.
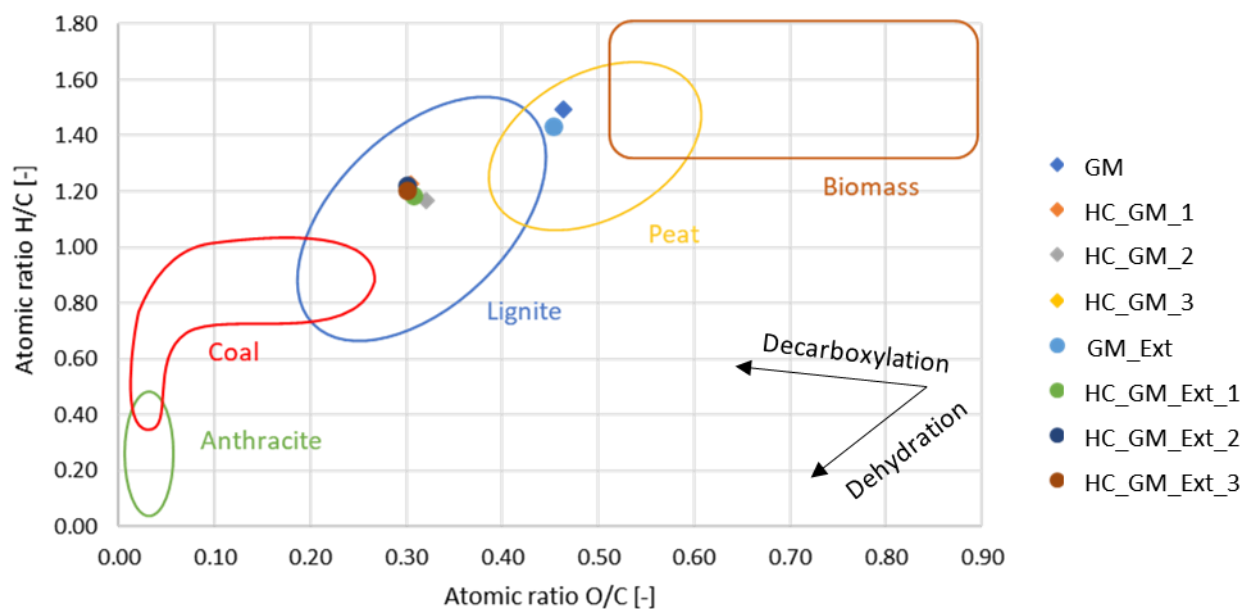

Figure 3.4 - Van Krevelen's diagram of the feedstock (GM and GM_Ext) and the related hydrochars.
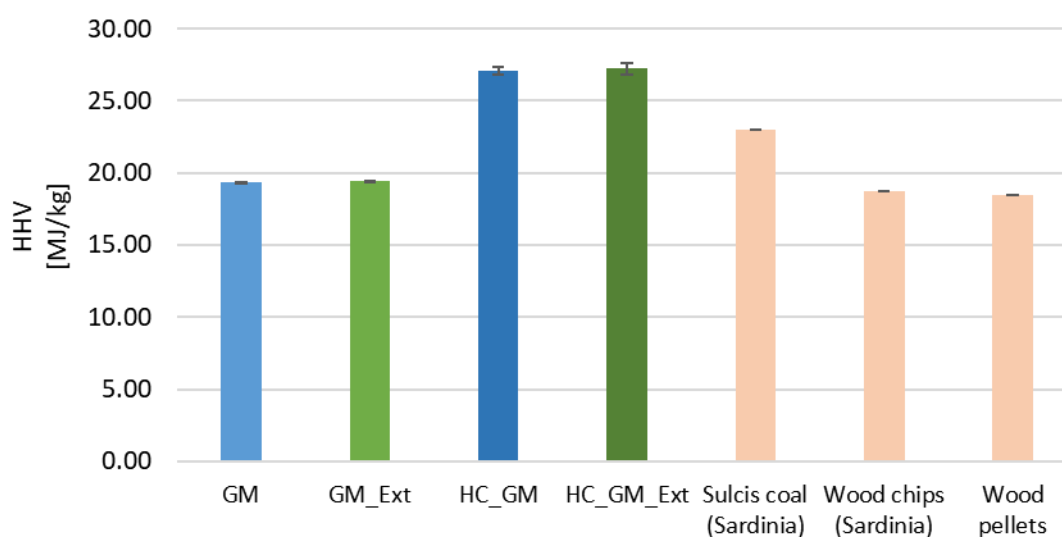

Figure 3.5 - HHV of feedstocks, hydrochar and some solid fuels of common use.

3.4.2.2   Assessment of the potential use of hydrochar as soil amendment

The results of the germination tests are shown in Table 3.5. The worst scenario is related to the raw GM. When GM and HC_GM results are compared on the basis of the RI and Munoo-Liisa vitality index (which takes into account both the germination and growth aspects normalized by the control), hydrothermal carbonization is able to produce a better material as substrate for the germination and growth of seedlings. In fact, the results show that replacing peat with an equivalent quantity of HC, despite the slightly lower germination rate, leads to longer seedlings compared to the use of GM. Indeed, it is possible to say indirectly that the extraction process also has positive effects as the best result is associated to HC_GM_Ext. On the other hand, the higher the concentration of hydrochar, the lower the germination rate, with a high inhibition effect in the samples with 50% peat substitution, especially. However, the presence of hydrochar in a percentage below 25% does not affect the germination significantly, but only the growth of the seedlings. In details, the sample HC_GM_Ext_5% achieved very high RI and MLV values. In contrast, all the other samples have shown inhibition of germination and growth resulting in a lower MLV (less than 80%, which is considered the inhibition threshold as reported in Maunuksela et al., (2012)). The lack of inhibition associated to HC_GM_Ext might be due to the preliminary ethanol extraction of GM (Wang et al., 2022). Moreover, the production of aromatic compounds during the HTC process, as evidenced by the FTIR analysis, does not appear to affect the growth of the seedlings. The statistical analysis derived from one-way ANOVA and Tukey's HSD test is shown in Figure 3.6 where each letter links samples that are found to be statistically similar ($p < 0.05$). The statistical test confirmed that the samples HC_GM_Ext_5% belong to the same group as the control. It may suggest that the substitution of peat with a 5% hydrochar produced by HTC of extracted grape marc does not affect the seed germination and seedling growth.

Table 3.5 - Main parameters calculated in germination tests for each sample.

| Sample	AGR [%]	CVG [%]	ARLP [cm]	CVR [%]	AHLP [cm]	CVH [%]	RI [%]	MLV [%]
Control	100	0	3.30	12.58	1.67	4.54	-	-
HC_GM_5%	96.66	5.77	2.19	15.92	1.74	5.47	66.26	63.67
HC_GM_25%	93.33	11.55	0.42	35.46	0.47	40.69	12.82	12.31
HC_GM_50%	0	0	0	0	0	0	0	0
HC_GM_Ext_5%	96.66	5.77	3.22	6.56	2.13	2.58	97.35	94.35
HC_GM_Ext_25%	96.66	5.77	0.89	49.78	0.70	36.30	27.20	26.74
HC_GM_Ext_50%	63.33	15.28	0	0	0.01	2.44	0	0
GM_5%	100	0	0.97	28.22	1.54	13.25	29.47	29.47
GM_25%	46.66	40.41	0.18	59.16	0.17	54.27	5.30	2.12
GM_50%	90	10.00	0	0	0.01	0.00	0	0
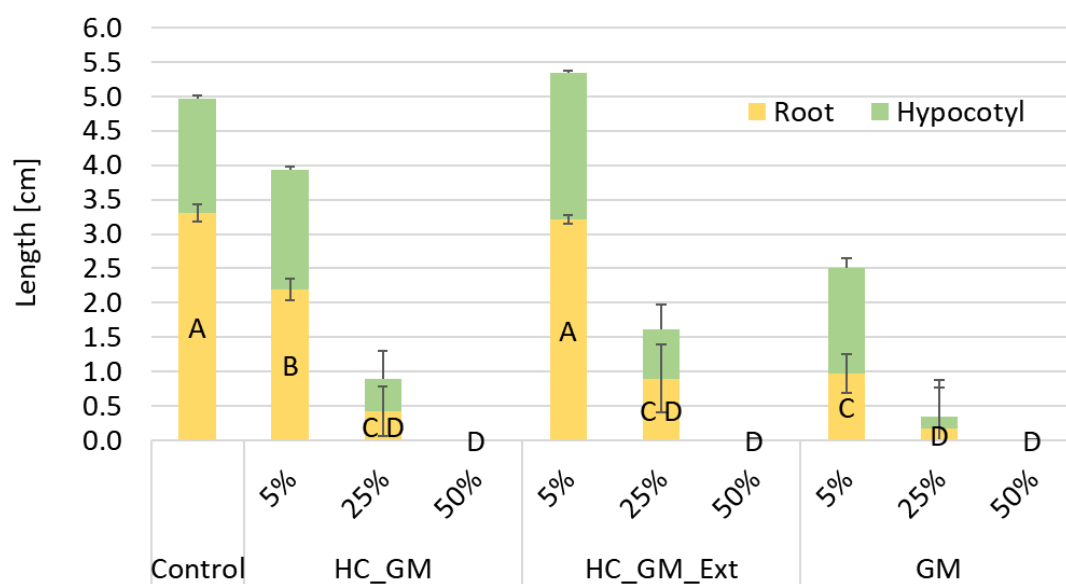
Figure 3.6 - Root and hypocotyl length of seedlings in germination tests and statistical results derived by Tukey's HSD test.

The HC produced from the extracted GM is characterized by a lower respirometric activity, as evidenced by the respirometric index value RA_4, calculated between the end of the lag phase and the end of the test, of 9.95 mgO$_2$/gTS, that is 33% of that associated to HC_GM_Ext (29.9 mgO$_2$/gTS). This feature could be explained by a possible removal of soluble and biodegradable organic compounds during the preliminary phase of extraction. The hypothesis seems to be confirmed by

what observed regarding the germination tests; the greater presence of soluble and biodegradable compounds in HC from non-extracted GM and the consequent higher consumption of oxygen could have determined a competition effect between microorganisms and seeds with a prevalence of the former.

3.4.3   Potential valorisation/management of PW

3.4.3.1   Biomethanisation Potential of PW

The results of the BMP tests performed on the PW samples are summarized in Figure 3.7 in terms of average cumulative biogas production over time. Both the samples show a very similar trend and, despite the possibility of the presence of organic toxic compounds in the process water, the observed production of methane seems to be fairly interesting. The specific production of methane accounted for 137 and 115 mlCH_4/gCOD for PW_GM and PW_GM_Ext, respectively. These results are comparable to those reported by other authors (M. Ahmed et al., 2021; Parmar & Ross, 2019) for PW generated from HTC applied to sewage digestate or agricultural waste. The average volumetric methane content in the produced biogas was always higher than 40% v/v. The modified Gompertz model matches the BMP experimental results very closely ($R^2 > 0.99$); the kinetic parameters are reported in Table 3.6. The lower values of maximum CH_4 production rate and Y_{CH4max} observed for PW_GM_Ext could be linked to the already mentioned possible removal of readily available organic compounds during the preliminary extraction treatment.
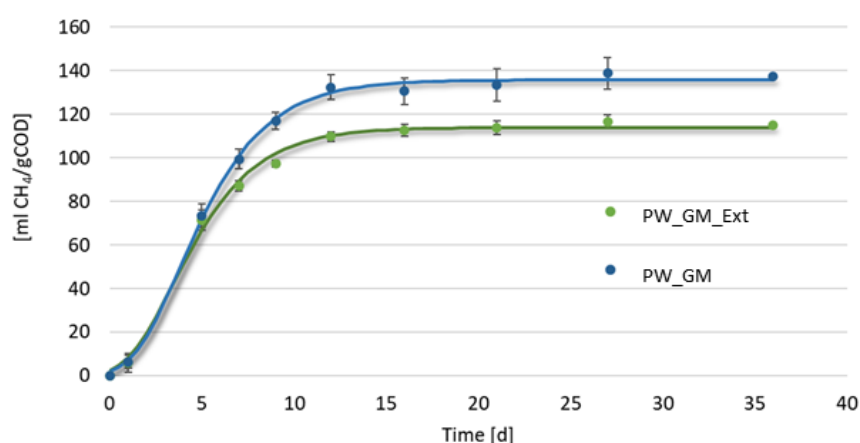

Figure 3.7 - Cumulative specific biomethane production from the HTC PW versus time (solid line indicates Gompertz-model curve).

Table 3.6 - Kinetic parameters calculated for the BMP tests.

Sample	$Y_{max}CH_4$ [ml CH_4 $gCOD_i^{-1}$]	R_{max} [ml CH_4 $gCOD_i^{-1}$ d^{-1}]	λ [d]	R^2 [-]
PW_GM	135.71	19.07	1.21	0.998
PW_GM_Ext	113.86	16.57	0.89	0.996

3.4.3.2 Assessment of the potential toxicity of PW in wastewater treatment plants

As autotrophic ammonium-oxidizing bacteria are characterized by slow growth rates and high sensitivity to inhibitors compared to heterotrophs, they can be conveniently employed as test organisms to assess the potential toxicity of liquid streams to be treated in wastewater treatment plants. Moreover, their toxicological responses to several chemicals correlate well to that of *vibrio fischeri* strain NRRL B11177 and methanogens (Ficara & Rozzi, 2001). The assessments performed in the present study showed potential acute toxicity of PW_GM and PW_GM_Ext at relatively low dosage (the IC50 values were 0.5 and 2.0 ml/L, respectively) (Figure 3.8).

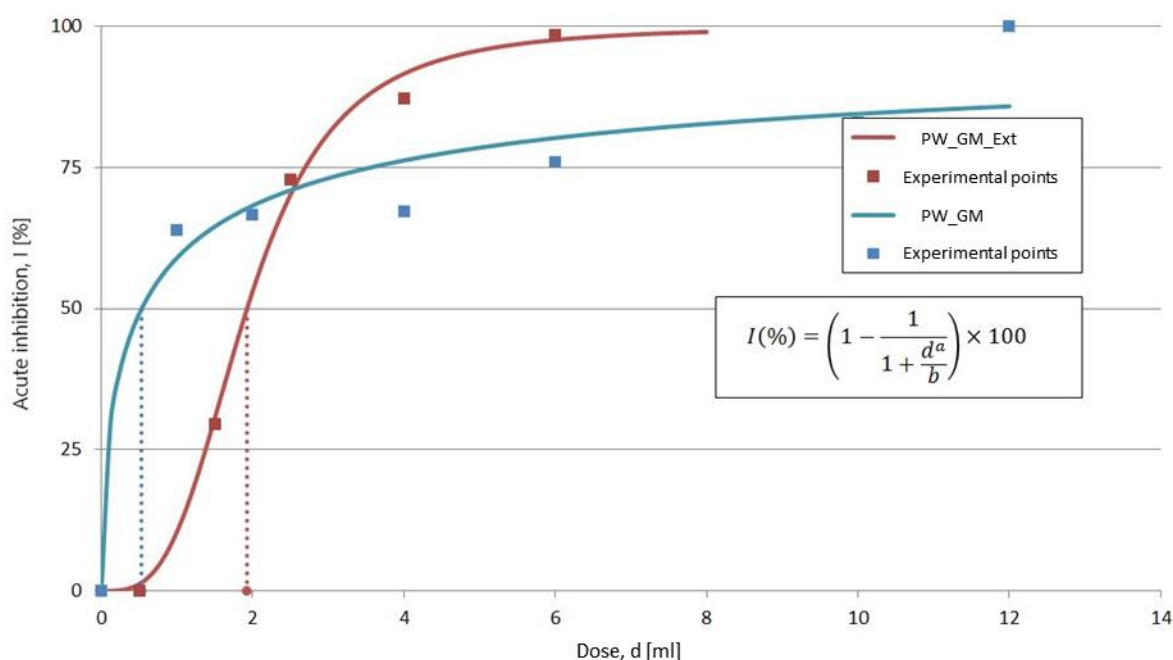$$I(\%) = \left(1 - \frac{1}{1 + \frac{d^a}{b}}\right) \times 100$$

Figure 3.8 - Dose-Response curves showing the acute inhibiting effects of PW_GM and PW_GM_Ext on unacclimated activated sludge. A sigmoid-function was used to interpolate the experimental data (PW_GM, a=0.58, b= 0.694, R^2= 0.944; PW_GM_Ext, a= 3.28, b= 8.547, R^2= 0.997).

Milia et al., (2016b) reported that phenolic compounds might severely inhibit unacclimated activated sludge even at low concentrations. Accordingly, the higher inhibiting effect of PW_GM was likely due to the expected higher concentration of phenols. As reported in previous studies,

liquid streams containing bio-recalcitrant compounds with high acute inhibiting effects may be successfully treated using advanced, low-cost, and efficient biological treatment technologies based on self-aggregated biomass such as aerobic granular sludge (Milia et al., 2016a), or well acclimated floc-shaped biomass (Milia et al., 2016b). In this sense, the high potential inhibiting effect observed in our study does not necessarily imply that aerobic biological treatment of PW_GM and PW_GM_Ext is not feasible, although particular attention should be paid to biomass selection and acclimation strategies.

3.5   Conclusions

Hydrothermal carbonization is one of the emerging and most promising technologies in the conversion of biomass and wet materials into added-value by-products. However, HTC mechanisms are still to be deeply understood and different feedstock can be differently affected by the process. Therefore, more research is needed to assess a suitable destination for HTC products and the real potentiality of the process.

In this work, the characterization of by-products derived from hydrothermal carbonization of grape marc was presented, and the possible use of HC as a fuel or peat substitute was discussed along with potential valorization or management options for PW, based on energy recovery or aerobic treatment, respectively.

The HC produced is characterized by a higher energy content compared with both the original feedstock and typical solid fuels, suggesting the feasibility of using HTC as a system for storing and exploiting the energy content of grape marc. The outcomes of the germination tests indicated that HC can be used as a soil amendment, partially replacing peat as a substrate for plant growth and contributing to drastically shortening the supply chain of soil improvers for countries, such as Mediterranean grape-producing ones, which do not have peat deposits. Furthermore, considering the global reduction of natural peatlands, the assessed potential for replacement of 5% obtained in this study is not negligible.

It was presented that, through the HTC process, over 90% of the output mass is PW in which many different compounds are dissolved. BMP tests showed that an energetic valorization thought biological process may be a feasible option. In contrast, PW showed toxic effects for aerobic microorganisms, and therefore the real feasibility of a traditional aerobic treatment must be carefully evaluated.

Interestingly, the potential for the implementation of HTC in an integrated context of waste biorefinery was addressed by applying the process also to grape marc previously subjected to polyphenol extraction and recovery treatment. The results obtained and the comparison with what was observed for the process applied to non-extracted GM, although in need of further investigation, seem to suggest that integration can have positive effects in terms of HC quality as soil improver due to the improved biostability and the reduced phytotoxicity.

In conclusion, hydrothermal carbonization applied to agricultural residues like grape marc may be a feasible and proper process for their valorization, producing an added-value material, the hydrochar, which can be used for agricultural purposes, partially replacing and saving the current natural substrates and acting as a carbon sink. Moreover, energy can be recovered from hydrochar and even from the process water, often considered a difficult-to-treat by-product and source of pollution.

The assessed ability to recover resources with high added value is crucial not only for the fight against climate change, but also for increasing the economic and environmental resilience of the agri-food sector, in turn supporting its overall sustainability.

Chapter 4

Valorisation of Spent Coffee Grounds through hydrothermal carbonization

In this Chapter, the experimental work on spent coffee grounds, together with their possible valorisation, is reported. In particular, experimental tests pointed to the possible use as solid fuel and as soil ameliorant are proposed. This work will be presented at the 3rd international HTC symposium to be held in Seoul, South Korea (2022).
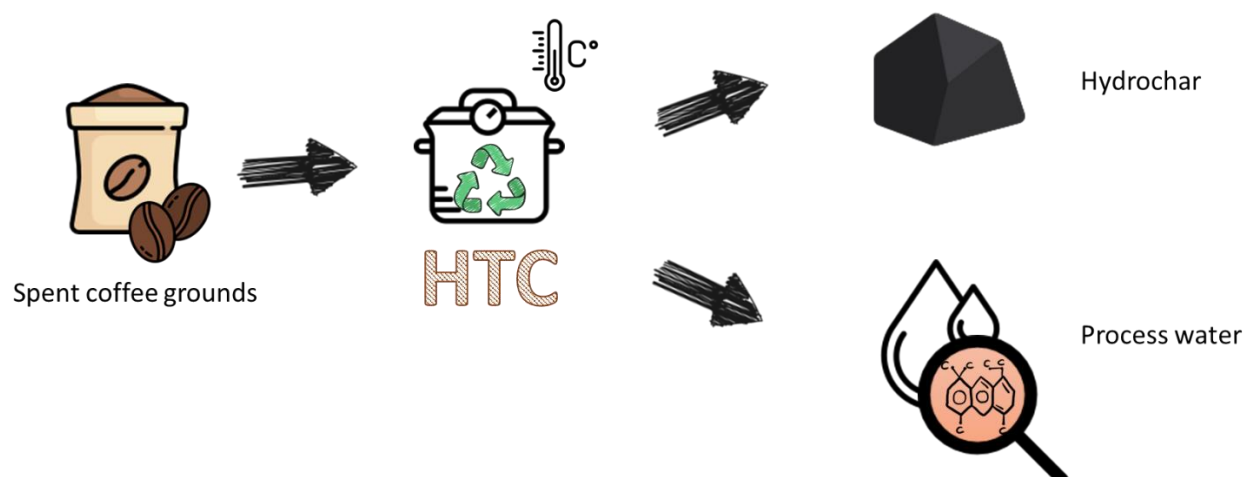
4.1 Abstract

Annual global coffee consumption, considered an integral part of the daily life of the world's population, has to date exceeded one billion kilograms. At present, the management and reuse of spent coffee grounds (SCG) involve substantial economic burdens and a significant environmental impact. Therefore, it is necessary to identify proper management systems that aim to fully satisfy the policies of circular economy and eco-sustainability. In this context, a possible option may be represented by the HTC process (hydrothermal carbonization). In this work, the feasibility of the application of HTC to SCG was studied. HTC tests were conducted at the temperature of 220 and 240 °C for 1 h. The hydrochars produced were characterised in terms of elemental analyses, FTIR, HHV, organic and nutrient content, and density in order to identify the better future use. In addition, germination tests were performed using hydrochar prepared at 220 °C in different post-treatment conditions (washed, dried and wet) in different mixtures with peat (concentrations of 5, 25, 50%) to check the phytotoxicity and the possibility to use it as soil ameliorant or peat substitute in plant growth. Finally, all the results were statistically validated. Moreover, the derived process water was physically and chemically characterised to find a final use or treatment. Biological degradability and toxicity (aerobic and anaerobic) were assessed with different tests (acute toxicity and BMP, reported in Chapter 8). The germination tests show the absence of phytotoxicity when 5% of hydrochar is mixed with peat.

4.2 Introduction

According to estimates by the International Coffee Organization (ICO), in the year between 2020 and 2021, global coffee consumption exceeded one billion kilograms with a compound annual growth rate of 1.8% (ICO - International Coffee Organization, 2021), configuring itself as one of the most demanded products in the world (McNutt & He, 2019). However, coffee consumption generates a substantial waste stream in the form of spent coffee grounds, the remaining part of ground coffee as a result of the beverage preparation process (McNutt & He, 2019). It is estimated that 650 kg of SCG are produced by preparing one ton of coffee, which leads to more than 6 million tons of SCG generated each year. The huge amount of SCG produced, considered as waste, is largely underused and underestimated as having no economic value (Afolabi et al., 2020).

Currently, there is no market demand for SCG, which generates disposal problems. Unlike other organic waste, most SCG is incinerated or landfilled, resulting in waste of resources and

environmental pollution (X. Zhang et al., 2020). Improper management of SCG involves significant risks of pollution, environmental contamination, and gas emissions (Afolabi et al., 2020). The potential release of toxic substances (e.g., caffeine, tannin, and phenols), the release of leachate, and greenhouse gas (GHG) emissions resulting from decomposition in landfills make SCG phytotoxic and dangerous for the environment (Afolabi et al., 2020).

To reduce inefficient landfilling, characterised by high economic costs and environmentally inconvenient, researchers tested alternative processes for treating this waste. In fact, after coffee production, spent coffee grounds are a valuable resource as they contain high amounts of sugars, oils, antioxidants, and other high-value compounds and constitute a potential energy source (McNutt & He, 2019).

As part of the circular economy and the biorefinery concept, in which renewable resources are converted into a range of low, medium, and high-value products, various scientific works have been published in order to valorise SCG to obtain materials with high added value. The research focused on the potential of using SCG for fermentation, for the production of biogas and biomaterials (e.g., bioplastics), in order to replace a small fraction of the current fossil raw materials (Massaya et al., 2019).

The objective of the present work was to evaluate the application of the HTC process to spent coffee grounds in order to use the hydrochar obtained as a soil improver or as a solid fuel. For this purpose, HTC tests were conducted under different operating conditions (220 and 240 °C for 1h), and the products obtained were characterised to evaluate the properties of interest. In particular, the evaluation of the possible use as a soil improver was conducted through the germination tests according to international standard protocols. The experimental methods, as well as the results obtained, are reported and deeply discussed.

4.2.1   Production and management of spent coffee grounds

The composition of SCG is highly variable and depends on a wide range of factors, such as the type of coffee and its growing conditions (McNutt & He, 2019). In fact, factors associated with harvest (climate, soil quality, harvest maturity, species, variety), conservation, roasting (temperature, time, etc.) and preparation method determine the characteristics and quantity of components present in SCG (Massaya et al., 2019). However, the common components are represented to a large extent by polysaccharides, in particular, cellulose and hemicellulose, which together make up about 50% of the dry mass of SCG (McNutt & He, 2019).

Coffee is composed of crude fibres (lignin, hemicellulose, cellulose, poly-oligo- and mono-saccharides), lipids (triacyl glycerides, fatty acids, and sterols), nitrogenous compounds (proteins, peptides, amino acids, melanoidins), and minerals. In addition, it contains small amounts of bioactive chemicals, i.e., alkaloids (caffeine and trigonelline), diterpenes (cafestol and kahweol), polyphenols (chlorogenic acids, tannins, tocopherols, and anthocyanins), responsible for the antioxidant, antimicrobial, and anti-carcinogenic properties of the coffee drink (Massaya et al., 2019).

Table 4.1 summarises the main components of green coffee, coffee after roasting, and the main products of the coffee production industry, i.e., coffee husk, pulp, silverskin, and spent coffee grounds. The data shown in Table 4.1 reports that SCG contain high amount of organic constituents such as hemicellulose, cellulose, and lignin, together with polyphenols and several others compounds. On the other hand, the inorganic fraction contains trace elements including potassium, magnesium, calcium, iron, and phosphorus.

Table 4.1 - Main components (as a percentage by dry weight) of green coffee, roasted coffee and by-products of coffee processing (modified from Massaya et al., 2019).

Components	Green coffee	Coffee pulp	Coffee husk	Silverskin	Roasted Coffee	SCG
Hemicellulose	3-10	2-66	4-10	4-22	n.a.	32-42
Cellulose	32-43	1-18	35-51	12-24	n.a.	7-13
Lignin	1-3	13-20	7-11	1-3	3	0-26
Lipids	8-18	2-5	0.5-6	0.3-4	10-16	2-24
Proteins	9-15	10-14	3-13	15-23	8-17	10-18
Ash	3-5	2-15	n.a.	5-8	4-6	1-2
Caffeine	1-3	0.5-3	0.5-2	0-1	1-3	0-0.4
Chlorogenic acid	1-12	1-6	2-3	3-4	2-9	1-3
Humidity	9-10	8-77	n.a.	5-7	1	50-60
Pectins	2	5.5-7.5	0.5-3	1	2	0
Total sugars	n.a.	14-15	48-68	7-17	n.a.	7-14
Total amino acids	7-11	n.a.	n.a.	n.a.	5-6	n.a.
Total dietary fiber	n.a.	58-64	18-30	56-63	47-50	21-59

n.a. = not available

According to the concept of biorefinery, SCG represent a lignocellulosic raw material, and the considerable quantities of bioactive chemicals present are suitable for recovery and valorisation in the food, pharmaceutical or chemical industries. The hemicellulose fraction is composed of monomers of mannose, galactose, and arabinose, and SCG also contain small amounts of sugar breakdown products, including 5-HMF (hydroxymethylfurfural), furfural, levulinic, and acetic acid (Massaya et al., 2019).

Biochemical, thermochemical, and chemical conversions of the primary products of spent coffee grounds have led to the isolation of important molecules (such as lactic acid) and the production of bioplastics, fuels and other high value-added materials, as shown in Figure 4.1.
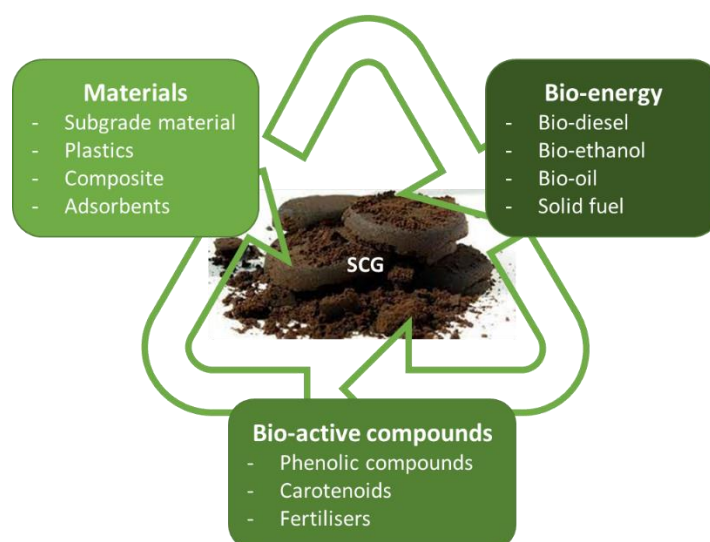

Figure 4.1 - Applications and by-products of spent coffee grounds (modified from McNutt and He, 2019).

The ability to operate without chemical additives or microbial cultures, the absence of gas emissions, the need for relatively moderate temperatures and processing times, and the overall efficiency of the process make HTC a sustainable option for the treatment of SCG. Due to its properties, the hydrochar produced can be applied in several fields, including bioenergy production (Afolabi et al., 2020).

In the literature, SCG used as feedstock in the HTC process made it possible to obtain a hydrochar with a carbon content of 60 - 84%, while the liquid resulting from the process can be exploited to obtain mono-oligosaccharides (60 minutes at 185 °C) (Cervera-Mata, Fernández-Arteaga, et al., 2021).

Crossley et al., (2020) studied the recovery of phosphorus (P) from process water using SCG in the HTC process in combination with nanofiltration and chemical precipitation in order to maximise the

total recovery of P. In fact, phosphorus, extracted mainly from phosphate rocks, is considered a non-renewable resource, since, according to estimates by the European Commission, existing reserves will only last for other 100 - 300 years.

Codignole Luz et al., (2018) studied the production of biomethane from the anaerobic co-digestion of SCG hydrochar, produced at different temperatures, with livestock wastewater showed a 32% higher energy conversion efficiency. Zhang et al., (2020) analysed the adsorption capacity of SCG hydrochar, in particular sulfonamides, bacteriostatic antibiotics frequently detected in the environment and causing environmental problems.

In the literature, the use of hydrochar as an organic soil ameliorant to improve the soil properties and promote the growth of edible plants has been studied, taking a further step towards the circular economy. It was proposed by Hernández-Soto et al. (2019) the use of hydrochar as a substitute for peat, verifying its practicability through germination tests. Hernández-Soto et al. (2019) reported the negative effect of SCG hydrochar on plant germination, due to the presence of phytotoxic compounds, and Bargmann et al., (2013) discovered inhibition on the germination of spring barley, closely related to some organic compounds adsorbed on hydrochar (Cervera-Mata, Lara, et al., 2021). Cervera-Mata et al. (2021) studied the use of hydrochar from SCG after washing, produced at two different temperatures (175 and 185 °C), as a soil improver for agricultural purposes, at concentrations of 1 and 2.5%, using Lactuca sativa. It turned out that the addition of hydrochar inhibits the growth of Lactuca sativa, but their role as biofortification agents was highlighted, enriching the plant in macro (Ca, Na, Mg) and microelements (Cu and Fe) thanks to its high content of polyphenols.

Research in this field is still evolving, and the HTC process on SCG is of great interest within the circular economy thanks to the products obtained, versatile, and with high added value (Cervera-Mata, Lara, et al., 2021). In this sense, this chapter aims to provide experimental data useful to contribute to the enrichment of the literature in the field of interest.

4.3   Materials and methods

SCG, used as feedstock in the hydrothermal carbonization tests, was collected at a coffee shop near the University of Cagliari facilities. The spent coffee grounds used for the preparation of the drink is of the grain type, branded Lavazza Top class. The SCG sample, taken in about 3 kg, was stored in an airtight container to preserve moisture at 4 °C to minimise microbial activity and, therefore, decomposition.

4.3.1   HTC processing

The HTC process took place into a stainless-steel pressurised reactor (BR-1000, Berghof), able to achieve temperatures up to 350 °C. An internal PTFE removable vessel with an inner volume of about 1.5 L facilitated the practical operations. The reactor was also equipped with an electrical heating jacket. In addition, the reactor head was equipped with valves for the extraction and/or injection of gas, for sampling during the process, control of the inside pressure generated, and a shaft for agitation. The reaction temperature was controlled by a thermocouple, connected to a probe immersed in the material, and connected to an external controller (BTC-3000, Berghof) that allowed monitoring and recording the temperature at any time during the test. The pressure generated was determined through an external pressure gauge connected to the controller. The desired temperature and the holding time were set through the controller, and the reactor was fully automated.

SCG were mixed with distilled water to obtain a mixture with 10% solid material (Total solid, TS, content of SCG = 42.15%). HTC tests were conducted 10 times at a temperature of 220 °C, to recover enough carbonized material for the subsequent characterisation and tests, and further 5 tests at 240 °C to evaluate the effect of two different temperatures on the characteristics of the product; all tests were conducted with a holding time of 1 h. After this period, the system was turned off, and the natural cooling phase was kept overnight. The nature of the material, the quantities, and the fine grain size did not require the use of the internal agitator since the turbulence generated by the heating was sufficient to make the process conditions homogeneous in each area of the reactor (Funke & Ziegler, 2010). At the end of cooling, the gas vent valve was slowly opened to allow the reactor to be opened safely.

A mass balance was performed on the input and output materials for each test. The hydrochar was separated from the process water using a filter press. The wet hydrochar was weighed, and a portion

was dried in oven at 105 °C to obtain the humidity content; the remaining HC was stored at 4 °C in plastic bags. HCs were labelled using a specific code indicating the feedstock (SCG), the temperature (220 or 240 °C) and the holding time (1h), e.g., SCG_240_1 is the HC produced from SCG at 240 °C for 1h. The recovered process water was vacuum filtered using a cellulose acetate filter (0.45 μm) and stored in plastic bottles at 4 °C. The solid materials (both feedstocks and HCs) were characterised. In order to determine the humidity and ash content, randomly sorted samples were heated up to 105 °C and 550 °C, respectively. The dried and combusted materials were weighed and compared with the initial weight. pH and electrical conductivity (EC) of SCG and HCs were measured using a multi-parameter probe (HI5521, Hanna Instruments).

4.3.2   HTC products characterisation

The dried hydrochar recovered from each HTC test was characterised by several analytical methods, such as density through a helium-pycnometer (AccuPyc II 1340), elemental analysis of carbon, hydrogen, nitrogen, and sulphur content using a CHN elemental analyser (CHN628, Leco) and CS analyser (SC632, Leco). The analysis of the calorific value of hydrochar and SCG was performed by a Mahler's calorimetric bomb (AC500, Leco), while the chemical surface analysis of spectroscopy FTIR was conducted by spectrophotometer (FT-IR6300A, Jasco) equipped with an ATR PRO ONE (diamond crystal) in the 4000-400 cm^{-1} spectral range, ris. 4.0 cm^{-1}, 50 scans.

The process water recovered from each HTC test was characterised in terms of pH and EC (HI5521, Hanna Instruments), total organic carbon (TOC) using a catalytic oxidation analyser (TOC-VCSN, Shimadzu), analysis of ion species by ion chromatography (ICS-90, Dionex), analysis of nitrogen compounds, total phenols and chemical oxygen demand (COD) by spectrophotometric methods (U-2000, Hitachi). Finally, the toxicity of PW on nitrifying bacteria was assessed using the method described by Ficara and Rozzi, (2001).

4.3.3   Valorisation and treatability tests

According to UNI EN 16086-2, standard germination tests on cress seeds were applied to both solid (SCG and SCG_220_1) and liquid materials (PW, SCG_220_1). Germination tests were carried out according to the contact method, while tests with PW according to the extraction method.

The tests with the contact method are based on the germination of 10 cress seeds per replicate placed in three squared Petri dishes (replicates, 10x10 cm) filled with a substrate (around 50 -60 g of humidified material). Sphagnum peat was used as reference material. This work was divided into

4 steps, and in each step, a different substrate was investigated. To reduce the possible phytotoxic compounds present in HC, two post-treatment were applied (washing and drying) to hydrochar. HC was post-treated with a washing phase where distilled water (10 times the solid mass) was used; the washing phase was repeated two times. A part of washed HC was stored wet, while the rest was dried at 105 °C. Both washed wet and washed dried HC were used in germination tests.

In Step 1, the substrates tested were washed and dried HC and peat mixtures in different concentrations (5, 25, and 50% HC). Same concentrations were used in Step 2 and Step 3, where the mixtures with washed dried HC and peat were fertilised using a liquid commercial fertiliser (Step 2), while washed wet hydrochar and peat were used as substrate in Step 3. In Step 4, SCG was used in mixture with peat (5, 25, 50, and 100% SCG); the mixtures were also used fertilised. Information on the structure of the germination tests is summarised in Table 4.2. For each step, water content of each mixture was corrected according to the fist test, as well as the pH using $CaCO_3$ followed by 24 h of stabilisation. The 10 seeds were sowed on the top of each Petri dish and a drop of water was added to each seed to assure the contact with the material. The dishes were closed, sealed with parafilm, and incubated with an angle of 70-80° (seeds upwards) in the dark at 25 °C for 72h. (pictures and further information are reported in Supplementary materials). After the incubation time, Petri dishes were opened, the germinated seeds were counted, and the seedlings roots were measured. According to the standard method and with the international scientific community, only the root of the seedlings was considered in the results; however, hypocotyl length was measured as well. Each mixture was characterised in terms of its moisture, ash, C, H, and N content, pH, and EC. In the tests conducted with the extraction method, PW from the HTC test ate 220 °C for 1h was considered as extracted of HC. These tests were used to assess the possibility of utilising PW in fertigation or determining the inhibition of seeds and plants growth. In these tests, Petri dishes were filled with perlite (< 2.5 mm) and covered with filter paper. Around 50 mL of the liquid samples were poured on the paper and 10 seeds were placed on the top of the dish. Three replicates (Petri dishes) were used. Distilled water was used as reference. After the dishes preparation, the procedure followed as described for the contact method. Tests were conducted with and without pH correction (phase 1 and phase 2, respectively) to be 5.5. PW, diluted PW (1:50) with distilled water, and liquid commercial fertiliser were used as liquid substrate.

Table 4.2 - Germination test details

	Step 1	Step 2	Step 3	Step 4
Substrate type	Washed dried hydrochar + peat	Washed dried hydrochar + fertilised peat	Washed wet hydrochar + peat	SCG and fertilised SCG
Control sample	100% Peat	100% Fertilized peat	100% Peat	100% Peat and 100% fertilized peat
% hydrochar	5% 25% 50%	5% 25% 50%	5% 25% 50%	-
% SCG	-	-	-	100%
Number of replicates (dishes)	3	3	3	3
Number of seeds per petri dish	10	10	10	10

Several parameters and indexes were calculated for each test, both on solids and liquids. Specifically, the germination rate GR for each petri dish, calculated with Equation 4.1.

$$GR\ [\%] = \frac{\text{number of germinated seeds}}{\text{total seeds [10]}} \cdot 100 \qquad (4.1)$$

The average germination rate AGR of the three replicates, calculated with Equation 4.2.

$$AGR\ [\%] = \frac{GR_1[\%] + GR_2[\%] + GR_3[\%]}{3} \qquad (4.2)$$

Where GR_1, GR_2, and GR_3 are the average germination rate for each replicate.

The coefficient of variation of the germination rate CVG, calculated with Equation 4.3.

$$CVG\ [\%] = \frac{\sqrt{\frac{\sum_{i=1}^{3}(GR_i\ [\%] - AGR[\%])^2}{2}}}{AGR\ [\%]} \cdot 100 \qquad (4.3)$$

The average length of the roots for each Petri dish (RLP) and the average length of the roots for the three replicates (ARLP), calculated with Equation 4.4.

$$\text{ARLP [cm]} = \frac{\text{RLP}_1[\text{cm}] + \text{RLP}_2[\text{cm}] + \text{RLP}_3[\text{cm}]}{3} \tag{4.4}$$

the coefficient of variation of the root length (CVR), calculated with Equation 4.5.

$$\text{CVR [\%]} = \frac{\sqrt{\frac{\sum_{i=1}^{3}(\text{RLP}_i[\text{cm}] - \text{ARLP}[\text{cm}])^2}{2}}}{\text{ARLP}[\text{cm}]} \cdot 100 \tag{4.5}$$

The root length index (RI), according to Equation 4.6, where RL is the average root length in each Petri dish and RL_C in the control sample.

$$\text{RI[\%]} = \frac{(\frac{\text{RL}_1}{\text{RL}_C} + \frac{\text{RL}_2}{\text{RL}_C} + \frac{\text{RL}_3}{\text{RL}_C})}{3} \times 100 \tag{4.6}$$

Finally, the Munoo-Liisa Vitality index (MLV), which compares the effect of germination and root length in each replicates and in the control sample, according to Equation 4.7.

$$\text{MLV [\%]} = \frac{(\text{GR}_{s1} \cdot \text{RL}_{s1}) + (\text{GR}_{s2} \cdot \text{RL}_{s2}) + (\text{GR}_{s3} \cdot \text{RL}_{s3})}{3 \cdot (\text{GR}_c \cdot \text{RL}_c)} \cdot 100 \tag{4.7}$$

Where GR_{s1}, GR_{s2}, and GR_{s3} are the germination rate of the three replicates and RL_{s1}, RL_{s2}, and RL_{s3} are the average length of the roots. GR_c and RL_c are the average germination rate and the average root length of the control sample, respectively. Tests are considered valid only if the control sample achieves 85% of AGR, at least.

4.4 Results and discussion

4.4.1 Characterization of HTC products

Table 4.3 reports the solid yield obtained in each test and the mass distribution of the output products. The comparison of the data shows that the solid yield in the tests conducted at a temperature of 240 °C is on average 51.94%, lower than that obtained in the tests conducted at 220 °C, equal to 58.80% (Figure 4.2). This is explainable given that higher temperatures result in a more effective decomposition of the material during the process due to the fragmentation and solubilisation of SCG macromolecules, resulting in a decrease in solid yield (Afolabi et al., 2020).

Table 4.3 - Operational parameters and average solid yield of HTC tests

Sample	Temperature [°C]	Solid yield [%]	Solid out [%]	Liquid out [%]	Gas out [%]
SCG_220_1	220	58.80 (0.43)	5.71 (0.04)	93.13 (0.08)	0.74 (0.10)
SCG_240_1	240	51.94 (0.84)	5.05 (0.08)	93.46 (0.13)	1.17 (0.06)

From the literature, it is clear that temperatures above 210 °C, such as those used in this study, are effective for a significant decomposition of the hemicellulose and lignin content of the SCG, resulting in considerable degradation of the cellulose in the conditions of the hydrothermal process (Afolabi et al., 2020). However, the mass distribution of the output products shows a similar percentage of PW for both temperature and a slightly higher amount of gas in tests performed at 240 °C with the subsequent reduction of solid.

Table 4.4 shows the elemental analysis results and the content of volatile matter (VM) and ash. The analyses were carried out both on the hydrochars from the individual tests (average value is reported) and on the mixtures carried out in view of the germination tests. S content was assessed lower than the detection limit (< 0.1%) and it is not reported. In Table 4.4, the abbreviation MIX indicates the material obtained by mixing the hydrochar produced by repetitions of the tests carried out under the same conditions, the letter W indicates the hydrochar produced by the same mixtures after washing. Also, the atomic ratios H/C, O/C and the C/N ratio of the analysed samples are given in Table 4.4. The volatile matter content of hydrochar produced at a temperature of 240 °C is slightly lower, probably due to the relatively lower organic matter content as a result of stronger HTC conditions.

The elemental analysis results indicate that the hydrothermal carbonization process involves changes in the elemental composition. In particular, there is an increase in the concentration of carbon in the solid. SCG reports a C content of 50.93%, while the hydrochar produced at 220 °C has an average C content of around 63%, while and the hydrochar produced at 240 °C is characterised by an average C content of around 66%. Washed hydrochar shows higher C content that probably indicates that inorganic substances and finer aggregates are eliminated during washing. The elemental composition of the analysed samples is represented in Figure 4.2.

Table 4.4 - Elemental percentage composition by weight on dry basis of C, H, N, ash, VM, O, and C/N, H/C, and O/C ratios of all analysed samples. The standard deviations of the mediated values are given in brackets.

| Sample	C [%]	H [%]	N [%]	Ash [%]	VM [%]	O [%]	C/N [-]	H/C [-]	O/C [-]
SCG	50.93 (0.15)	6.64 (0.33)	2.38 (0.02)	1.75 (0.34)	98.25 (0.34)	38.29	21.36 (0.19)	1.57	0.56
peat	45.21 (0.05)	5.55 (0.04)	1.09 (0.01)	1.51 (0.01)	98.49 (0.01)	46.65	41.62 (0.45)	1.47	0.77
SCG_220_1	63.58 (1.14)	6.97 (0.19)	2.59 (0.04)	0.69 (0.06)	99.31 (0.06)	26.18	24.57 (0.21)	1.32	0.31
SCG_220_1_MIX	62.97 (0.67)	6.65 (0.34)	2.58 (0.06)	0.73 (0.04)	99.27 (0.04)	27.07	24.41 (0.34)	1.27	0.32
SCG_240_1	66.11 (0.41)	6.73 (0.08)	2.98 (0.07)	0.79 (0.16)	99.21 (0.16)	23.39	22.23 (0.45)	1.22	0.27
SCG_220_1_MIX_W	67.66 (0.18)	7.16 (0.26)	2.68 (0.01)	0.27 (0.11)	99.73 (0.11)	22.22	25.25 (0.03)	1.27	0.25
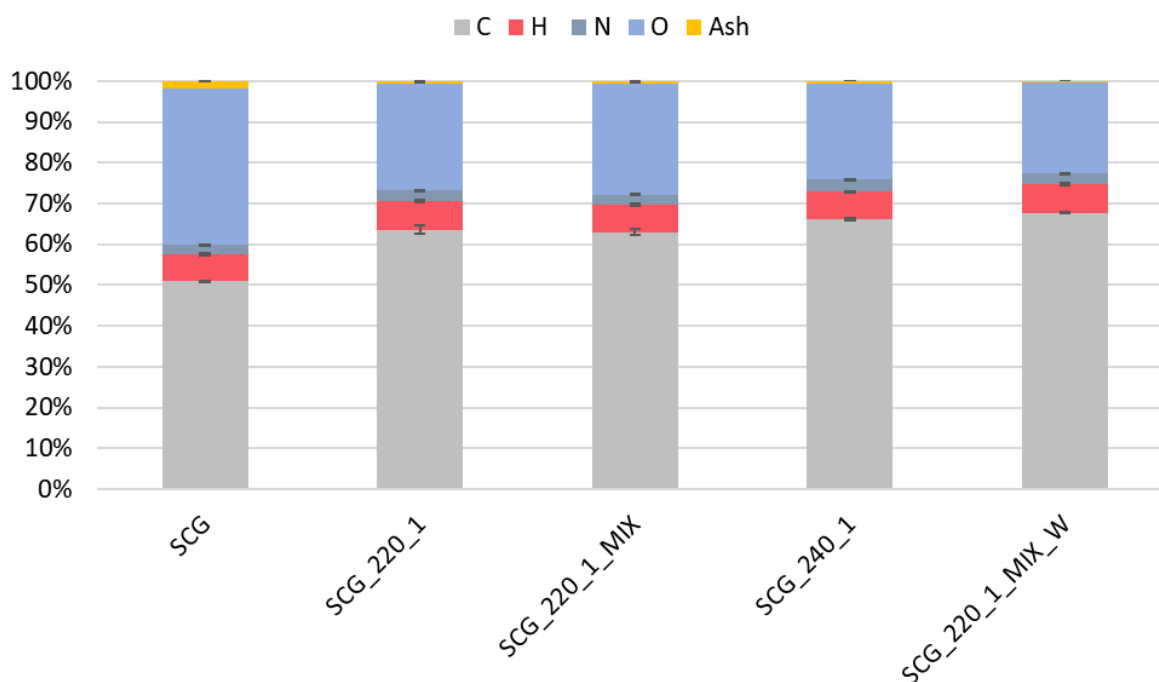
Figure 4.2 - Percentage composition by weight on a dry basis and standard deviation of C, H, N, O, and ash of SCG and relative HCs.

The oxygen content decreases as the carbon content in hydrochar increases. The H/C and O/C atomic ratios, estimated thanks to elemental analysis, were analysed using the Van Krevelen diagram, shown in Figure 4.3, which allows understanding the reaction paths associated with the HTC process (Afolabi et al., 2020). The Van Krevelen diagram shows the atomic ratios for the different materials being analysed. These ratios move from the upper right zone to the lower-left zone as a result of the hydrothermal carbonization process, highlighting an intensification of the degree of carbonization with the increase in the temperature of the HTC process. The diagram in Figure 4.3, provides evidence that the HTC process is predominantly governed by dehydration and decarboxylation reactions, as the H/C and O/C ratios have decreased significantly. These results suggest changes in the elemental compositions of hydrochar that favour energy applications as fuel (Afolabi et al., 2020). It is clearly visible that, by increasing the reaction temperature to 240 °C, the hydrochar produced move more in the lower-left region. In addition, the data at 240 °C demonstrate good repeatability.
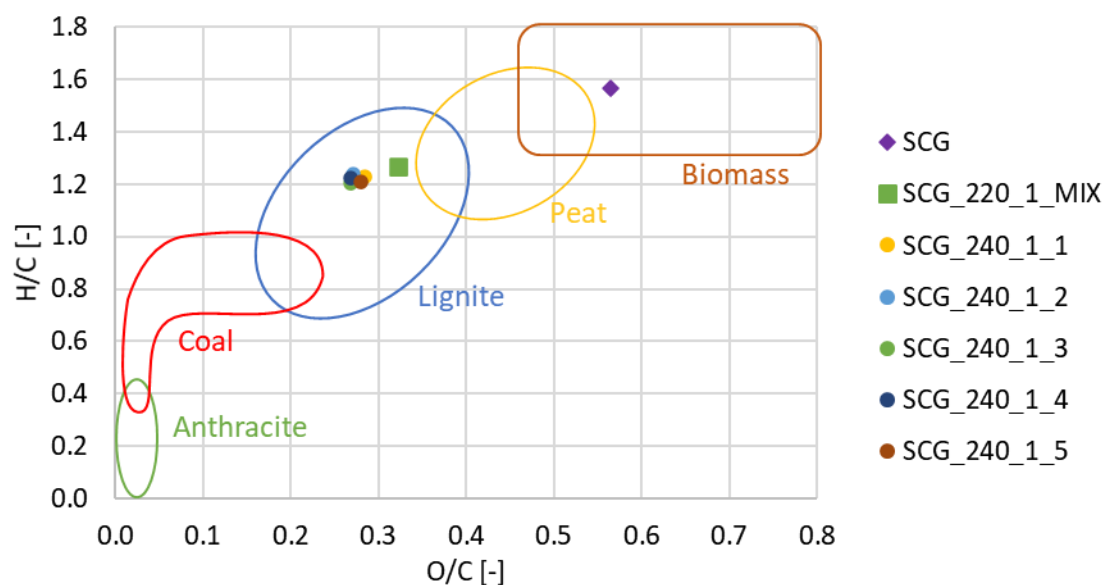
Figure 4.3 - Van Krevelen diagram with SCG, HC produced at 220 °C and the five HC repetitions produced at 240 °C.

The results of the calorimetric analysis, reported in Table 4.5, show an increase in the higher heating value (HHV) as the temperature of the HTC process increases. The HHV of hydrochar is an important feature for its possible use as a solid fuel. The effect of the HTC process on SCG is a significant increase in the HHV, up to values 42.6% higher than the feedstock. In addition, hydrochar HHV is higher compared to low-ranking fuels such as peat (17.1 MJ/kg), lignite (17.6-21.9 MJ/kg) and comparable to bituminous coal (30.2-31.0 MJ/kg) and anthracite (31.8-34.5 MJ/kg) as reported by Afolabi et al., (2020).

Table 4.5 - Average results and standard deviations in brackets of HHV analysis and % change in HHV and hydrochar density compared to SCG.

Sample	HHV [cal/g]	HHV [MJ/kg]	ΔHHV [%]	Density [t/m³]
SCG Card	5201.65 (2.45)	21.78 (0.01)	-	1.331 (0.001)
SCG_220_1_MIX	6934.55 (2.77)	29.03 (0.01)	+33.31	1.278 (0.001)
SCG_240_1	7418.79 (43.12)	31.06 (0.18)	+42.62	1.270 (0.001)
SCG_220_1_MIX_W	7070.49 (5.44)	29.60 (0.02)	+35.93	1.273 (0.001)

Figure 4.4 shows the HHV values from SCG and their hydrochars compared with reference values (Plaisant et al., 2012), of the HHV of different solid fuels. From the data analysis, it can be confirmed that the hydrochar from SCG may be used as a solid fuel for power generation or heating production. It should indeed be emphasised that the solid yield of the process involves a reduction in the initial mass of the SCG residue, the more relevant, the higher the temperature of the process. The reduction of the solid mass translates into an overall energy yield of the hydrochar similar to

feedstock. The chemical-physical characteristics of the materials produced by HTC are more appropriate for use as fuel than the feedstock.

Table 4.6 - Average results of HHV and elemental analysis of hydrochar compared with those of different fuels (partially modified from Plaisant et al. (2012).

Sample	HHV [MJ/kg]	C [%]	H [%]	N [%]	Ash [%]
SCG	21.78 (0.01)	50.93 (0.15)	6.64 (0.33)	2.38 (0.02)	1.75 (0.34)
SCG_220_1_MIX	29.03 (0.01)	62.97 (0.67)	6.65 (0.34)	2.58 (0.06)	0.73 (0.04)
SCG_240_1	31.06 (0.18)	66.11 (0.41)	6.73 (0.08)	2.98 (0.07)	0.79 (0.16)
SCG_220_1_MIX_W	29.60 (0.02)	62.97 (0.67)	6.65 (0.34)	2.58 (0.06)	0.27 (0.11)
*Sulcis coal (Sardinia)	22.95	66.49	6.18	1.41	11.45
*Usibelli coal (Alaska)	19.46	48.56	5.96	0.50	10.02
*South African coal	28.10	75.56	3.86	1.40	14.97
*Russian coal	29.39	81.55	1.64	0.79	12.62
*Wood chips (Sardinia)	18.76	49.95	6.14	0.11	0.37
*Wood pellets	18.45	79.51	11.18	0.32	0.42
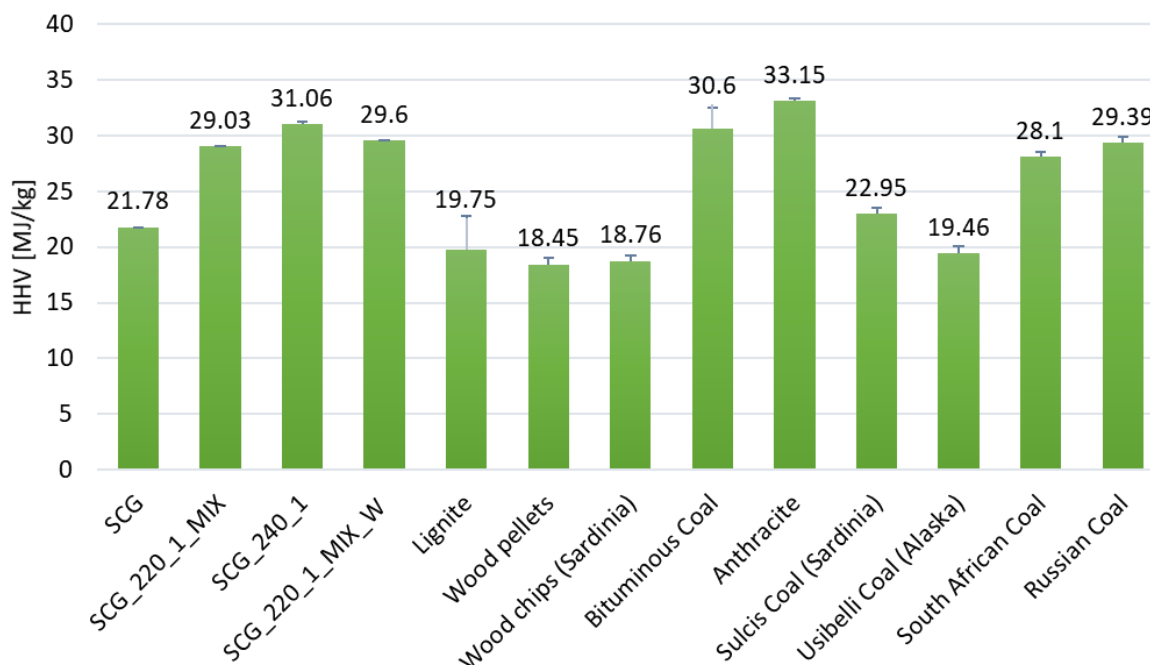
Figure 4.4 - Comparison of the average values of HHV of the samples analysed with other solid fuels (Plaisant et al., 2012).

FTIR analysis was used to identify the characteristic functional groups of the spectra of the materials under study and to highlight their surface chemical modification. Figure 4.5a shows the FTIR spectra

of hydrochars produced at the two different temperatures and SCG, while in Figure 4.5b the spectra of hydrochar produced at 220 °C before and after washing are compared; in both figures, it is possible to observe the modification in the chemical structure as a result of the HTC process. The zone between 3650-2500 cm^{-1} usually shows an absorption due to the υNH, υOH, and υC-H. The zone ranges from 2400 to 1900 cm^{-1} is intentionally corrected due to the peaks of CO_2 in air detected by the device. The zone between 1900 and 1500 cm^{-1} is the classic adsorption of alkynes and nitriles, with a prevalence of triple bonds. In wave numbers between 1800 and 1500 cm^{-1} there are absorptions due to double bonds, particularly by aromatic compounds with lower frequency (C=C). The zone between 1650 and 1300 cm^{-1} is characterised by peaks associated with nitro/nitroso-derivatives, aromatics, alkanes, and amides. Peaks between 1300 and 700 cm^{-1} can be related to simple bonds between atoms other than hydrogen (amines, esters, ethers). Instead, in the area with wavenumbers from 1000 cm^{-1} to 400 cm^{-1} there are absorptions associated with aromatic and halogen-derivatives (Nandiyanto et al., 2019). In general, the 1500-400 cm^{-1} zone is the fingerprint of each specific material. In Figures 4.5a-b, the fingerprint zone is different for each material, showing a modification in the chemical structure even though not very marked.
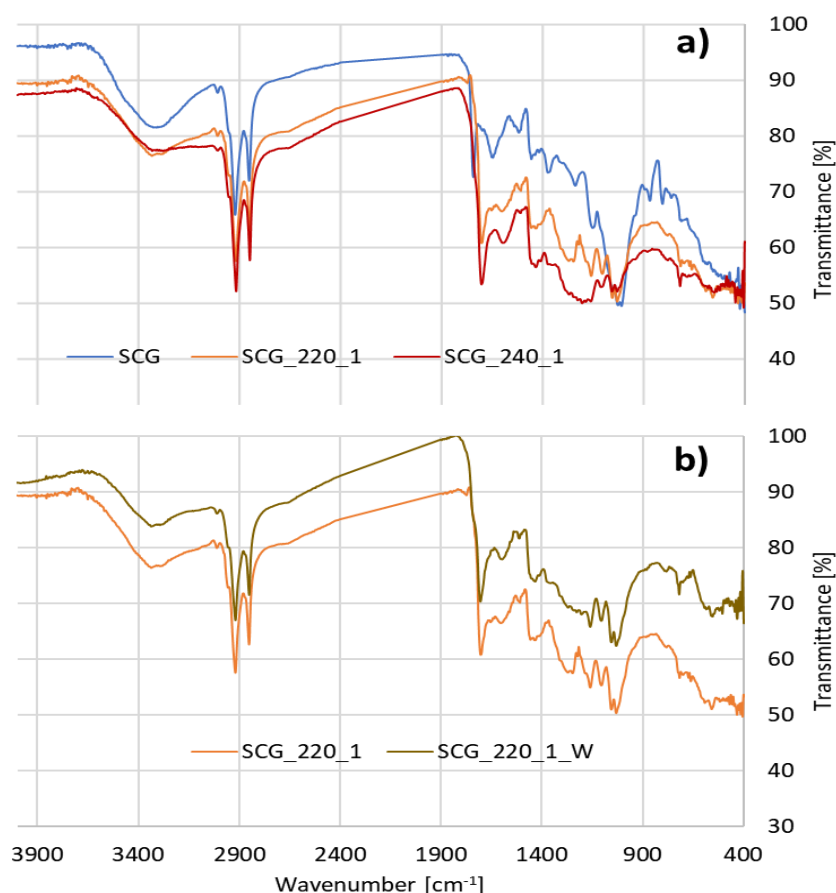

Figure 4.5 - FTIR spectra of a) SCG and hydrochars produced at 220 and 240 °C and b) HC at 220 °C and HC washed.

In Figure 4.5a, the two sharp peaks (2916 and 2848 cm^{-1}) showed in all the spectra are due to the stretching of CH bond, while the broad bend around 3300 cm^{-1} is associated with υOH, which decreased due to higher HTC temperature. The peak at 1733 cm^{-1}, related to υC=O, is shifted to the right in HC samples possibly due to the releasing of -OR group related to esters. υC-O-C can be seen at 1028 cm^{-1} which is reduced during HTC. The peak associated with δOH (1370 cm^{-1}) disappears in HC spectra. Peaks between 1560 and 1640 cm^{-1} are typically related to υC=C (Lazzari et al., 2018; Zuorro et al., 2014). Peaks typically related to unsaturated aromatic and aliphatic C=C bonds (1650-1598 cm^{-1}) and aromatic CH in bonds (719 cm^{-1}) increased in HC showing an overall major aromaticity of the carbonized system.

As highlighted in Figure 4.5b, the spectrum of washed HC (SCG_220_1_W) does not differ from SCG_220_1 except for the peak at 1244 cm^{-1} possibly related to C-O stretching of phenolic compounds (aromatic ester) that disappeared due to the washing.

The results of the TOC, TC (total carbon) and IC (inorganic carbon) of the process water of HTC tests are shown in Table 4.7, along with the pH and EC values.

Table 4.7 - Average TOC, pH and EC values of PW; standard deviations are shown in brackets.

Sample	pH [-]	EC [mS/cm]	TOC [g/L]	TC [g/L]	IC [g/L]
SCG	5.62 (0.26)	1.47 (0.02)	n.a.	n.a.	n.a.
SCG_220_1	4.03 (0.08)	3.74 (0.03)	10.02 (1.16)	10.30 (1.16)	0.28 (0.02)
SCG_240_1	4.19 (0.10)	3.65 (0.03)	10.16 (0.53)	10.47 (0.52)	0.31 (0.02)
SCG_220_1_MIX	n.a.	n.a.	10.85 (0.07)	11.14 (0.07)	0.29(0.00)

n.a. = not available

From the analysis of the results, it can be deduced that the process water contains a high amount of organic carbon, and, as the process temperature increases, there is a slight increase in the IC; this suggests that for temperatures above 200 °C, the carbon undergoes a gradual mineralisation (Langone & Basso, 2020). Also, SCG_220_1 was characterised in terms of N-NH$_3$ and COD, reporting concentrations of 641.5 mg/L and 46.6 g/L, respectively. The concentration of COD highlights the high content of organic matter present in PW samples.

From the analysis with the ion chromatography, the chromatograms for each process water were obtained (Figures 4.6a-b).
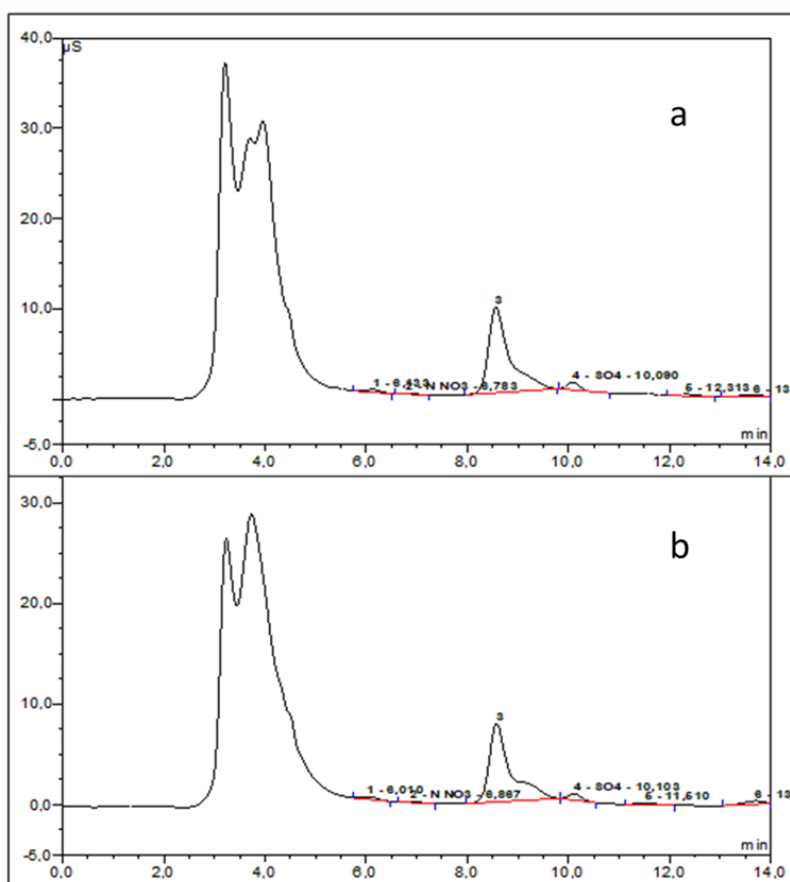
Figure 4.6 - Ion chromatograms of the PW of SCG_220_1 (a) and SCG_240_1 (b) tests.

Analysis with ion chromatography made it possible to investigate the presence and quantity of anions such as chlorides, nitrites, nitrates, and sulphates. In the chromatograms reported, the characteristic peaks of sulphates are rather evident, while the precise identification of the peak of chlorides (about 4 minutes on the x-axis) is of great difficulty, as an unknown anion species cover it; therefore, the quantification of chlorides by chromatograph was not possible. The average results of the ion species $N-NO_3^-$ and SO_4^{2-}, present in the samples of the PW produced by the HTC tests, are shown in Table 4.8.

Table 4.8 - Average results of the ion species $N-NO_3^-$ and SO_4^{2-}, with standard deviations reported in brackets.

Sample	$N-NO_3$ [mg/L]	SO_4 [mg/L]
SCG_220_1	5.04 (0.77)	20.36 (6.06)
SCG_240_1	4.13 (0.09)	20.39 (2.02)
SCG_220_1_MIX	3.99 (0.00)	26.16 (0.02)

The increase in temperature in HTC causes a decrease in ion analytes, possibly due to the degradation that molecules undergo at high temperatures. Starting from the results of the analysis

of the TC in the liquid and the percentage of C in the solid, a carbon mass balance was applied to define the distribution of the input C in the output HTC products. Considering the HTC input solid mass and the C% of SCG, the average C mass in input in the HTC tests was about 49.60 (0.02) gC. The distribution represented in Figure 4.7 shows that the carbon is mainly concentrated in the hydrochar. Comparing the two temperatures, as expected, tests conducted at 240 °C had a higher carbon content in the gas phase, while the TC in PW was maintained constant.
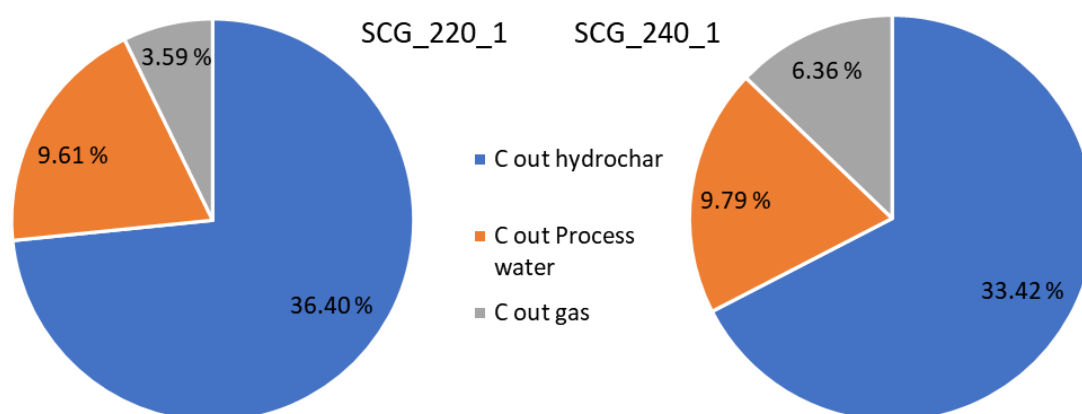
Figure 4.7 - Average output C distribution in the three phases from HTC tests at 220 and 240 °C.

4.4.2 Acute toxicity tests

Figure 4.8 shows the curves obtained from the acute toxicity tests on nitrifying bacteria showing the dosage of process water in the x-axis (ml/L) and acute inhibition (%). Nitrifying bacteria achieve inhibition of approximately 50% with a dosage of 8.03 ml/L of PW produced at 220 °C, and 3.41 mg/L of PW produced at 240 °C. These results demonstrate a significant acute toxic effect due to the PW, increasing as the process temperature increases. This result is relevant in assessing the final fate of the PW. However, an investigation in more detail on the speciation of carbon in the liquid phase is necessary in order to identify which of the organic compounds formed during the process are responsible for the toxic action and consequently appropriately direct the possible final treatment. Moreover, the tests were conducted on unacclimated bacteria and it evaluate the only acute inhibition. Therefore, different results may be achieved on an acclimated sludge making possible the aerobic treatment PW.
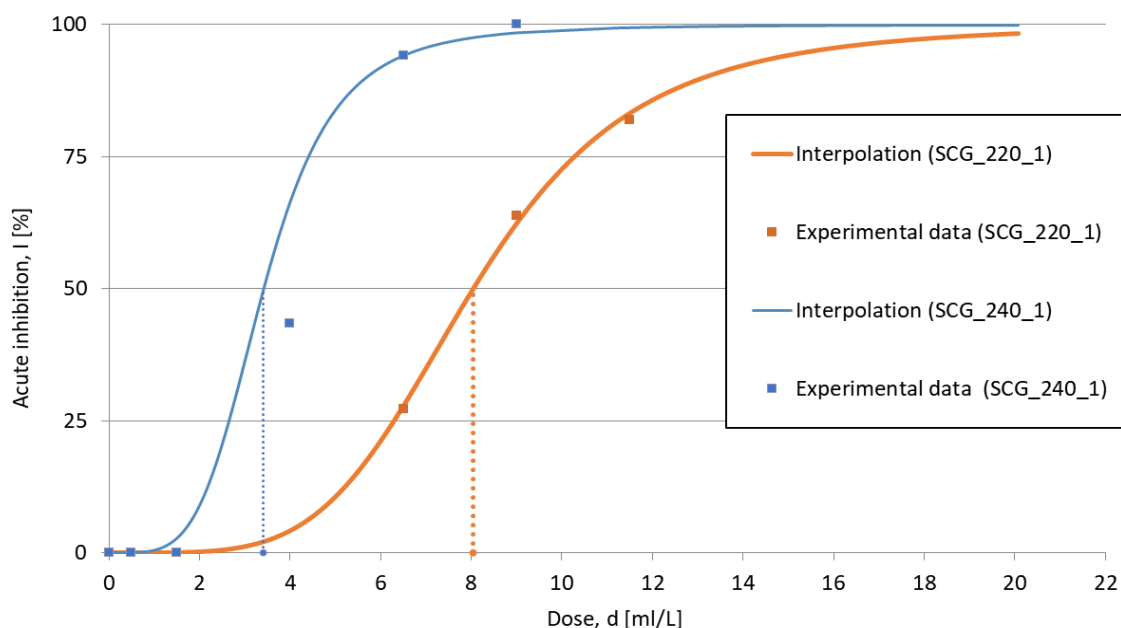
Figure 4.8 - Dose-inhibition curve of the toxicity tests conducted with process water produced at 220 and 240 °C on nitrifying bacteria.

4.4.3 Germination tests

The results of the germination test conducted in Step 1, Step 2, and Step 3 using washed dried, dried fertilised, and wet hydrochar and peat are shown in Figure 4.9 and reported in Table 4.9.

Expect the tests with 50% hydrochar (in all conditions) that achieved a 90% of AGR (86.67% for 5% washed dried and fertilised HC) and the sample with 5% washed dried and fertilised HC, all the samples achieved a 100% AGR.

The length of each root and each hypocotyl was manually measured. According to the data reported in Table 4.9 and considering the root length, the higher the concentration of HC in the samples, the higher the inhibition effect, as it is clear from the results of RI%. Taking into account the germination rate, even lower values can be seen in MLV%, confirming a phytotoxic effect with a higher concentration of HC. Overall, better results were achieved in the washed wet samples. Although, it should be considered that the concentration of HC (5, 25, and 50%) was considered in terms of weight of the material (wet or dried). Therefore, considering the overall amount of HC on dry basis, mixtures with wet HC contain less amount of HC because around 50% of the input mass was moisture. As a general consideration, negative effects can be related to HC even after post-treatments. However, samples with 5% HC achieved results comparable with the control, as confirmed by the statistical results reported in Figure 4.9, suggesting a feasible replacement of peat

with no, or minimised, adverse effects. Further results and discussion on germination tests and peat replacement can be found in Chapter 5.

Table 4.9 - Parameter for germination tests measured and calculated according to the UNI EN 16086-2:2012.

Substrate	Sample	AGR [%]	CVG [%]	ARLP [cm]	CVR [%]	Average hypocotyl [cm]	RI [%]	MLV [%]
	Peat	100.00	<0.01	5.49 (0.22)	5.03	2.17 (0.14)	-	-
Washed dried HC	Mix 5%	100.00	<0.01	5.42 (0.94)	20.90	2.25 (0.12)	98.72	70.77
	Mix 25%	100.00	<0.01	3.80 (1.78)	56.92	1.51 (0.94)	69.22	49.61
	Mix 50%	90.00	15.71	3.50 (0.35)	13.97	2.06 (0.09)	63.75	41.47
	Peat	100.00	<0.01	5.34 (0.18)	3.95	3.21 (0.18)	-	-
Washed dried and fertilised HC	Mix 5%	90.67	8.09	5.36 (0.20)	5.21	3.29 (0.08)	100.37	97.67
	Mix 25%	100.00	<0.01	4.18 (0.36)	10.92	2.38 (0.09)	78.28	76.80
	Mix 50%	86.67	15.38	2.31 (0.44)	22.23	1.65 (0.28)	43.26	40.79
	Peat	100.00	<0.01	6.27 (0.52)	2.29 (0.07)	9.96	-	-
Washed wet HC	Mix 5%	100.00	<0.01	6.13 (0.60)	1.83 (0.23)	12.73	97.77	89.95
	Mix 25%	100.00	<0.01	5.20 (0.35)	1.88 (0.16)	8.02	82.93	82.66
	Mix 50%	90.00	<0.01	4.01 (0.32)	1.90 (0.23)	10.90	63.96	62.13

Regarding the germination tests performed in Step 4 using SCG and SCG fertilised, no germinated seed was found in the samples, leading to an AGR of 0% and confirming the phytotoxic effect of SCG, already reported by other authors (Cervera-Mata, Lara, et al., 2021; Hernández-Soto et al., 2019).

Concerning tests conducted on process water using the extract method, both germination tests (Phase 1 and Phase 2) reported a germination rate of 0% in each Petri dish where the process water, diluted or not, was present, regardless of pH correction. The germination of cress seeds occurred only in the control sample. Therefore, process water has a phytotoxic effect, also evidenced by the

acute toxicity test results on nitrifying bacteria. A deeper discussion is provided in Chapter 5 where different PW in diverse dilutions were tested for fertigation purposes.

The statistical tests (One-way ANOVA and HSD Tukey's test) were applied to the results obtained in the germination tests in order to assess the significant differences between samples. ANOVA reported the presence of one sample at least statistically different ($p < 0.001$), rejecting the null hypothesis. Tukey's test was applied to verify statistical similarities or differences between each pair of samples. Results are reported in Figure 4.9 using the Compact Letter Display method. In the figure, samples linked by the same letters are not considered significantly different. An ad hoc statistical test was applied to each germination test, only considering the average roots length. Figure 4.9 shows that the samples with 5% peat replaced by the new materials report similar results to the controls, while higher amounts (25% and 50%) differ, negatively in this case having shorter roots. In addition, as post-treatments, fertilisation seems not to lead to any improvement to the root length, and, referring to the letters in Figure 4.9, drying after washing seems to remove some inhibiting compounds since the sample with 50% HC have shown similar results to 25% compared to the other two tests where 50% and 25% differ. It can be concluded that replacing 5% peat with washed HC (either wet, dried, and fertilised) is possible with no adverse effect on the root length and seed germination, as confirmed by AGR values in Table 4.9.
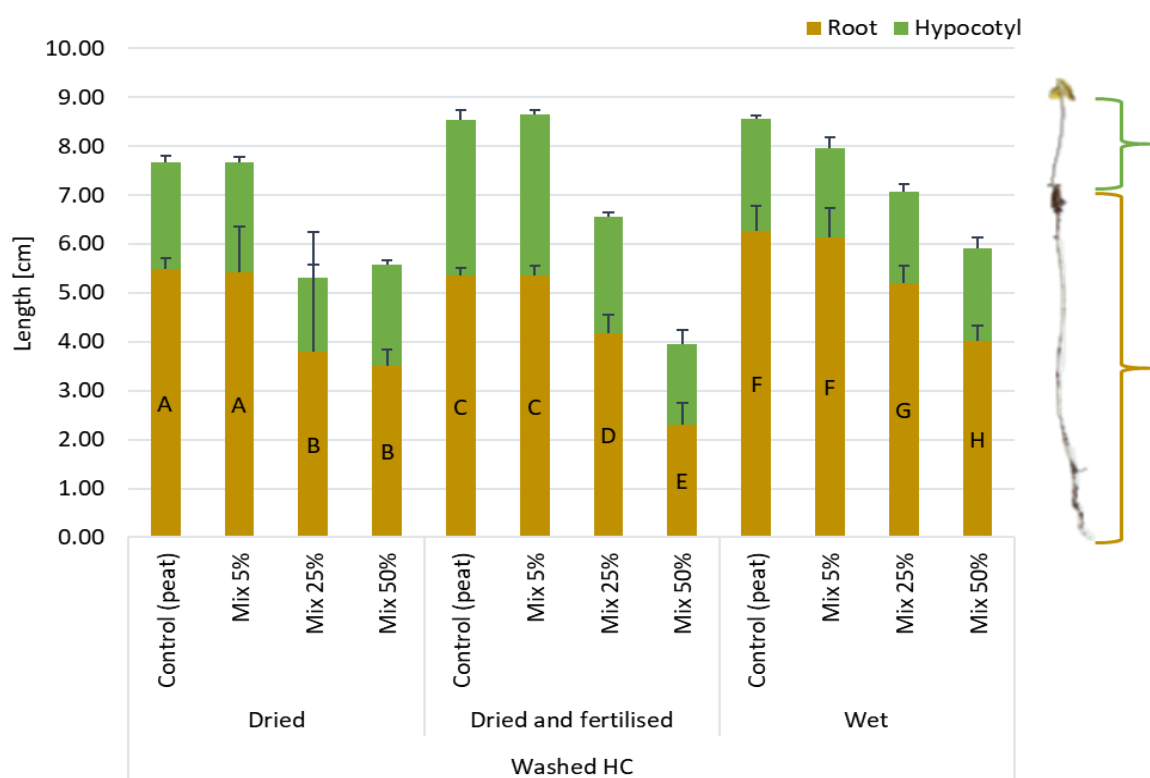

Figure 4.9 - Average root and hypocotyl length and standard deviations of germinated seeds in substrates with different ratios of washed hydrochar from SCG and peat.

4.5   Conclusions

Hydrothermal carbonization has proven to be a potential alternative approach for the valorisation of SCG that are produced in large quantities every year globally. The HTC process produced a hydrochar with different physicochemical characteristics than the feedstock. In addition, the increase in the temperature of the process has influenced the final quality of the product, with a decrease in solid yields and O/C and H/C ratios, due to dehydration and decarboxylation reactions, which intensifies the degree of carbonization, as highlighted by the Van Krevelen diagram. With regard to energy applications, the increase in energy content of the produced hydrochar justify its possible use as a potential fuel to replace natural resources for energy production.

As for possible applications as a soil improver, germination tests have shown that hydrochar can be used as a partial replacement for peat. The mixture of peat with 5 % hydrochar was found to be the best substrate among the tested ones, having results similar to control (peat). In contrast, substrates with 25 and 50% hydrochar have an inhibitory effect on plant growth. Although the 5% mixture does not entail significant improvements compared to peat, the possibility of using hydrochar even in partial replacement of 5% is of great importance in light of the criticality represented by the worldwide availability of natural peat deposits not too far from a near depletion. Therefore, a resource-saving of 5% can undoubtedly be significant. From these estimates, hydrochar used in small quantities turns out to be a good soil improver with results comparable to peat.

Further research developments in germination testing could consist of specific preconditioning configurations, such as the use of matrices other than peat (e.g., compost) to be mixed with hydrochar, and humidification and storage, for a predetermined number of days, of the material to be tested, in order to verify the degradation of phytotoxic compounds as a result of the growth of microorganisms. Precisely the concentration of toxic substances produced during hydrothermal carbonization, together with the extent of the microbial activity of the substrates, are parameters of fundamental importance to which due attention must be given in the research phase in order to control germination and to root development (Dalias et al., 2018).

In conclusion, the different applications of hydrochar will be a key point in the future in terms of reuse and valorisation of spent coffee grounds, and further research will be essential to reduce the environmental impact of this waste.

Chapter 5

Benefits and limitations of using hydrochars from organic residues as replacement for peat on growing media

This chapter reports the results of germination tests on hydrochar and PW from digestate, spent coffee ground, and grape marc before and after extraction in ethanol solution. The preliminary results of this work have been presented at the 5th CIGR International Conference 2021. A modified version of this chapter is under review at the open access journal Horticulturae. This work was conducted in collaboration with the biochar group at the Leibniz Institute for Agricultural Engineering and Bioeconomy e.V. (ATB), in Potsdam (Germany), under the supervision of Dr Judy Libra and Dr Jürgen Kern.
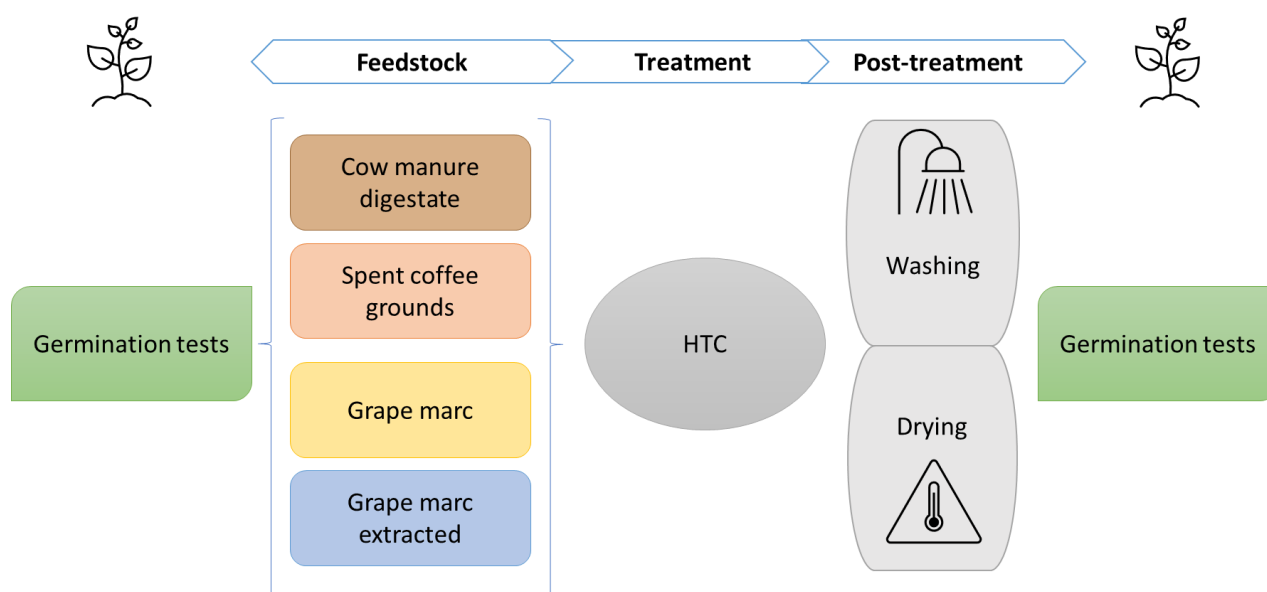
5.1 Abstract

In order to meet the rising demand for growing media in horticulture and the need to preserve natural peatlands, new technologies and feedstocks for the production of peat-substitutes are required. Hydrothermal conversion of the globally increasing amounts of organic residues into char materials, hydrochars (HC), with peat-like properties may produce such substitutes and, at the same time, reduce the environmental impacts of organic residue management. In this work, cress seed germination tests were used to assess hydrochars produced from digestate (D), spent coffee grounds (SGC), and grape marc (GM) as a component in growing media. In order to provide a design basis for a process chain to valorize these organic residues, the potential benefits of some pre- and post-treatments (extraction, washing and drying) to remove phytotoxic compounds associated with process waters (PW) retained on the hydrochars were also analysed in germination tests and an aqueous nitrification bioassay with process water. All the hydrochars achieved similar (D) or better germination results (SCG, GM) when compared to their feedstock. The results showed a potential of replacing at least 5% peat in growing media and mostly depends on the feedstock and the pre- or post-treatments applied. All hydrochars from SCG and GM showed severe inhibition above 5%, while seeds growing in all post-treated D-hydrochar mixtures (5 - 50%) produced >3 times longer roots compared to the peat control. Initial evaluation of the relatively robust and quick nitrification test on the process waters showed high sensitivity and good agreement with the inhibition trends found in the germination tests. It was a better predictor than the chemical lumped parameters (TOC, total phenols) for the presence of phytotoxic compounds in the hydrochars and process waters. Such tests can be helpful in developing and optimizing process combinations for the hydrothermal production of peat replacements.

5.2 Introduction

Annually, large amounts of growing media are produced to grow a wide variety of plants including vegetables, fruits, floriculture ornamentals, tree and shrub ornamentals and speciality plants. A very well-known substrate in growing media is peat, characterized by a porous structure able to provide an optimal amount of air and water to promote the germination of seeds as well as the healthy growth of plant roots (Méndez et al., 2017). However, natural peatlands play an important role for carbon sequestration and their exploitation is not sustainable (Barbier & Burgess, 2021; Glenk & Martin-Ortega, 2018). Therefore, new peat-reduced or even peat-free materials in growing media

are necessary (Prasad et al., 2019; Vasander et al., 2003). Many researchers have been investigating the feasibility of using renewable sources such as organic residues generated from agricultural and industrial activities as peat replacement. Among the different materials tested so far (pyrolyzed tomato plants, rice husks, and shrimp-derived chitin (Nocentini et al., 2021), date palm residues (Raja et al., 2021), pyrochar from wood (Steiner & Harttung, 2014), and pyrochar from green waste (Tian et al., 2012)), hydrothermal carbonized char seems to be particularly suitable since it possesses peat-like characteristics that make it a feasible candidate as an additive or even substitute for peat in growing media for horticulture (Dalias et al., 2018; Roehrdanz et al., 2019).

Hydrothermal carbonized char (hydrochar) can be produced from a variety of wet organic materials through the hydrothermal carbonization process (HTC) using water under subcritical conditions (Allen et al., 1996; Elliott et al., 1991). Besides the hydrochar, the HTC process produces a liquid phase (process water) and a small amount of gas. The solid phase shows similarities with materials like peat or lignite and often a high nutrient content that makes it feasible for use as soil improver (Álvarez et al., 2017; Puccini et al., 2018). In addition, several studies showed that solid products of thermal treatment positively impact the carbon balance of soil, working as a carbon sink in the concept of carbon farming (Bates, 2010; Schofield et al., 2019). The HTC-process water is generally enriched in nutrients and a wide range of soluble organic compounds, such as phenols, furfurals, organic acids, etc., resulting from the degradation of sugars, lignin, carbohydrates, etc. that occurs during the HTC process (Berge et al., 2011; Libra et al., 2011; Reza et al., 2016; Titirici et al., 2008). After HTC, the separated hydrochar can retain high amounts of this process water with a water content ranging from 50-85%, depending on the separation process. Thus, the wet hydrochar can hold high concentrations of organic and inorganic compounds, many of which may be phytotoxic (Bargmann et al., 2013; EN 16086-2:2012). Post-processing of chars is often necessary before soil application such as heating, leaching or washing, aging, pelletizing, composting (Dalias et al., 2018; Puccini et al., 2018; Thomas, 2021). In addition, environmentally sound applications for the process water (e.g. fertigation for nutrient recycling (Fregolente et al., 2019), biogas production (Wirth & Mumme, 2014) or treatment in wastewater systems (Ferrentino et al., 2021) are required.

The addition of each pre- and post-processing step increases capital and energy costs for production systems, therefore, rapid tests and indicators are needed that can be used to determine appropriate process conditions and steps in the search to produce materials for growing media. Various assessment indicators have been developed to characterize the quality of char materials, ranging from limit values for lumped and individual pollutants using standardized physio-chemical analyses

(EBC, 2021; IBI, 2015) to soil function characteristics such as carbon stability and ionic exchange capacity (Cross & Sohi, 2013) to estimates of ecotoxicity using bioassays (IBI, 2015; Oleszczuk et al., 2013). Bioassays can be especially useful in providing guidance for application rates to specific soil or crop types (Domene et al., 2015). Char materials can directly affect plant performance by decreasing seed germination and/or plant growth, or indirectly by influencing the soil structure and microbiome; especially the nitrification cycle is sensitive to the presence of nitrification inhibitors (J. Norton & Ouyang, 2019). The bioassay seed germination is often used as an early indicator of the effects of char quality on plant performance since successful it is an essential first step for plant growth and development (Olszyk et al., 2018; Rogovska et al., 2012). The germination of plant seeds is primarily based on the initiation of growth from the dormant, still largely undifferentiated embryo (Kozlowski, 1971; Makhaye et al., 2021; Mofokeng et al., 2021). It occurs if optimal conditions are provided, such as the presence of water and oxygen, a minimum temperature (Bierhuizen & Wagenvoort, 1974; Kozlowski, 1971) and, in the case of light germs, photoinduction. Various methods have been studied using a variety of seed types (lettuce, spring barley, cress, tomatoes, etc.) in homogenous mixtures (such as soil/hydrochar in pots (Bargmann et al., 2013), soil/pyrochar in shallow germination boxes, (Olszyk et al., 2018), on moist substrate wetted with an aqueous solution (water extract from feedstock and pyrochar on filter paper, (Rogovska et al., 2012); single compounds on cotton pads or HTC process water in sand, (Bargmann et al., 2013); HTC process water in agar medium, (Fregolente et al., 2019) or suspended on moist filter paper over the material to test for volatile compounds (Bargmann et al., 2013; Busch et al., 2012). In addition, various bioassays are available to measure inhibition of nitrifiers in soil (Kaur-Bhambra et al., 2021; J. M. Norton & Stark, 2011) and in water systems (Ficara & Rozzi, 2001; Pagga et al., 2006).

To date, specific regulations for using char for agricultural purposes in European countries are lacking. However, as the demand for growing media is increasing, EU regulations on fertilizers will be soon updated (July 2022) allowing the use of organic products derived from pyrolysis and gasification processes. This upcoming modification could boost the valorization of organic residues for soil applications. However, a wide variety of thermal conversion processes besides pyrolysis and gasification can produce potentially beneficial char materials (Gabhane et al., 2020). In this framework, more research is needed to assess the real benefits and limitations on the use of a variety of chars in growing media in order to widen the spectrum of appropriate feedstocks and production processes for char materials.

This study assesses the feasibility of using hydrothermally treated carbon-rich material derived from three common organic residues in Europe, manure digestate (D), spent coffee grounds (SCG) and grape marc (GM), as a peat substitute in plant growing media. Furthermore, in order to provide a basis for the design of a process chain to valorize these agro-industrial organic wastes, the potential benefit of some pre- (extraction of ethanol-water soluble compounds, such as phenols from GM) and post-treatments (washing and drying) to remove organic compounds from the hydrochars that may affect plant performance were also analysed. Standardized plant and bacteria-based bioassays were selected for their ease, sensitivity, and speed in assessing toxic effects on living organisms. Standard cress germination tests using peat were chosen as the most appropriate to determine inhibitory effects of the hydrochars and its associated process water on germination and subsequent root growth (EN 16086-2:2012). These germination results are compared to those from an aqueous bioassay using aerobic nitrifying bacteria with the process water to assess its potential to predict whether post-treatment is required for the hydrochar and process water.

5.3   Material and methods

5.3.1   Feedstocks and HTC by-products

In this study, three different feedstocks were treated via the hydrothermal carbonization (HTC) process, including: (1) separated solid digestate (D) from cow manure collected from a biogas plant (Dobbrikow, Brandenburg, Germany), (2) spent coffee grounds (SCG) collected from a local coffee shop at the University of Cagliari (Italy), and (3) grape marc (GM) from a winery in southern Sardinia (Italy). D and SCG feedstocks were used as they were collected without pre-treatment. Two types of GM feedstock were studied; GM without pre-treatment was compared to GM extracted in an ethanol solution (GM_Ext) to evaluate the effect of a pre-treatment to remove phenolic compounds from GM before HTC.

For the HTC tests, the solid content was set at 13% for D and 10% for SCG, GM and GM_Ext. Digestate was treated in an 18.9 L pressurized reactor (Parr, Model 4557) in the facilities of ATB – Leibniz Institute (Potsdam, Germany) at the temperature of 240 °C and a holding time of 1 h. The conversion of SCG, GM and GM_Ext was carried out in a 1.5 L reactor (Berghof, BR-1000) at the laboratory of the University of Cagliari (Cagliari, Italy), at the temperature of 220 °C for 1 h. For the HTC conversion in the 1.5 L reactor, three tests were conducted at the same process conditions to

ensure reproducibility and to recover enough carbonized material for the subsequent germination tests.

After each test, the gas formed was released, and the carbonized slurry was separated through a filter press into the solid (HC) and the liquid phase (PW). The process water was filtered at 0.45 μm and stored in plastic bottles at 4 °C for further characterization. Hydrochar from GM and GM_Ext were dried at 105 °C after separation from process water and stored in plastic bags (GM-HC-Dried, GM_Ext-HC-Dried). Hydrochar from D and SCG was washed two times with 30 °C water as post-treatment in order to reduce the amount of organic soluble compounds that may be toxic for plants. In each washing step, water was added to the hydrochar and stirred for 5 minutes, then it was separated into the two phases and the steps were repeated. In general, water mass three times the mass of solid was used to wash the hydrochar. Wet washed hydrochar from D and SCG was divided into two parts. One part was dried in oven at 105 °C and stored in plastic bags at room temperature (D-HC-WDried, SCG-HC-WDried), while the remaining part was stored wet in vacuumed bags at 4 °C (D-HC-WWet, SCG-HC-WWet).

5.3.2   Products characterization

Feedstock, hydrochars, and process water were physically and chemically characterized. In accordance with the ASTM D5373-16 and ASTM D7582-15, the content of C, H, N, S, O, and ash was evaluated to describe the composition of the material and the modifications that occurred during the HTC process. pH and electrical conductivity (EC) were measured according to EN 13037:2012 and EN 13038:2012, respectively. Moreover, total organic carbon (TOC), chemical oxygen demand (COD), total amount of phenols and concentration of acetic acid were estimated for the process water samples. TOC was evaluated through a TOC analyser (Shimadzu – TOC-VCSH) while COD was measured with the standard titration method after digestion of samples at 150 °C for 2h. Colorimetric determination of phenols was applied using Folin-Ciocalteu reagent with a UV-spectrophotometer (U-2000, Hitachi) and the absorbance of the samples was measured at 765 nm. Lastly, acetic acid concentrations were measured through GC-FID (7890B, Agilent Technologies). As described in Ficara & Rozzi, (2001), the acute toxicity of process water on ammonium-oxidizing bacteria in activated sludge was assessed using a pH-stat titration unit (ANITA, Ammonium NITrification Analyser). Increasing volumes of process water were added to 1L of unacclimated activated sludge (after 24h of aeration) and the corresponding inhibition was determined for each

dosage. Each test lasted a total of 4 hours. At the end of the test, the IC50 (the dose that inhibits 50% sludge activity) was estimated.

5.3.3 Germination tests

Different germination tests were carried out according to the European standard EN 16086-2:2012. Tests using the contact method for the solid substrates and the extraction method for the process water were performed.

5.3.3.1 Contact method for solid substrates

The germination tests were carried out on cress seeds (Lepidium sativum) using Sphagnum peat as reference material according to the standard. The tests with the solid substrates (feedstock, hydrochar) were performed at three different mixtures of peat and solid, 5%, 25%, and 50% (wt%, FM, fresh matter); 100% peat was used as a control. An overview of the samples tested, post-treatments used, and moisture content of the fresh mass is given in Table 5.1. The hydrochars from D and SCG were first washed, and tests were made with wet and dried hydrochar, while hydrochar from GM and GM_Ext was dried with no washing step.

After the preparation of the mixtures, the water content was adjusted with the fist tests to have a proper moisture content (60-70%wt). EC was checked to be < 80 mS/m and pH to be in the range 5.5 – 6.5. Samples with lower pH were adjusted by adding $CaCO_3$ and left to stabilize for 24h. Around 60 g of material was placed into squared Petri dishes to completely fill them and 10 seeds were sowed on the top of the Petri dishes with one drop of water for each. Petri dishes were closed, sealed with parafilm, and incubated in the dark at 25 °C for 72 h. Three replicate Petri dishes were used for each sample. After 72 h, the Petri dishes were opened, and the germination rate (GR) (the ratio of the number of germinated seeds in the sample to the number germinated in the control), and the length of the roots (RL) was determined for each sample. The average germination rate (AGR) and root length index (RI) for the three replicates were calculated according to Equations 5.1 and 5.2 below. In addition, the Munoo-Liisa vitality index (MLV) was calculated according to Equation 5.3.

$$\text{AGR[\%]} = \frac{\text{GR}_1[\%]\ \text{GR}_2[\%]\ \text{GR}_3[\%]}{3} \tag{5.1}$$

Where GR_1, GR_2, and GR_3 are the germination rates in each replicate.

$$RI[\%] = \frac{(\frac{RL_1}{RL_C} + \frac{RL_2}{RL_C} + \frac{RL_3}{RL_C})}{3} \times 100 \qquad (5.2)$$

Where RL_1, RL_2, and RL_3 are the average root length in each replicate while RL_C is the average root length in the control samples.

$$MLV[\%] = \frac{(GR_1 RL_1) + (GR_2 RL_2) + (GR_3 RL_3)}{3(GR_C RL_C)} \times 100 \qquad (5.3)$$

Where GR_C is the average germination rate in the control.

5.3.3.2   *Extraction method for liquid substrates*

To assess the possible exploitation of the HTC process water as soil fertilizer and to better understand inhibition effects caused by phytotoxic compounds, process water and process water diluted (1:2 and 1:10) from HTC tests on SCG, GM, and GM_Ext were used as liquid substrates in germination tests using the extraction method. Squared Petri dishes were filled with perlite and covered with filter paper (Whatman). Process water and diluted process water were poured on the filter, 10 seeds were placed on the top, and the Petri dishes were closed with parafilm. The same procedure for incubation and measuring used in the contact method was applied to the extraction method.

5.3.4   Statistical analyses

Results of root length were validated through statistical analyses (one-way ANOVA and Tukey's HSD test) using the JMP software by SAS to assess the significance of the obtained measurements.

Table 5.1 - Overview of samples tested

	Material/Code	Pre-/post-treatment	Water Content [% wt]	Mixing ratio between material and peat [% wt, FM]			
	Peat	none (used as it is)	74.42	-	-	-	100 (used as control)
Feedstocks	D	separated at biogas plant	70.87	5	25	50	100
	SCG	none (used as it is)	57.85	5	25	50	100
	GM	none (used as it is)	6.17	5	25	50	100
	GM_Ext	extraction in ethanol solution	7.40	n.t	n.t	n.t	n.t
Hydrochars	HC_D	washed after HTC	83.59	5	25	50	n.t
		washed and dried	0*	5	25	50	n.t
	HC_SCG	washed after HTC	70.54	5	25	50	n.t
		washed and dried	0*	5	25	50	n.t
	HC_GM	after HTC	66.4	n.t	n.t	n.t	n.t
		dried	0*	5	25	50	n.t
	HC_GM_Ext	after HTC	69.2	n.t	n.t	n.t	n.t
		dried	0*	5	25	50	n.t

	Materials	Pre-/post-treatment	TOC [g/L]	Dilution ratio (process water:distilled water) [% wt]			
Process water	PW_SCG	diluted with distilled water	10.85	0	10	50	100
	PW_GM	diluted with distilled water	9.21	0	10	50	100
	PW_GM_Ext	diluted with distilled water	8.17	0	10	50	100

*Samples were dried at 105°C for 24h; n.t. = not tested.

5.4   Results and discussion

5.4.1   Properties of selected substrates: feedstocks, hydrochar and process water

Results of the elemental characterization (C, H, N, O, S, and ash contents) of the materials used in this work, feedstocks, the produced hydrochars, and peat, are shown in Figure 5.1. The carbon content was higher in all hydrochars compared to their feedstocks and also peat as a result of the HTC treatment, while ash and oxygen content were generally reduced. Using the Van Krevelen diagram (Figure 5.2), where the materials are represented in terms of their atomic ratios of H/C and O/C, the degree of carbonization of the materials can be evaluated. Due to the higher loss of hydrogen and oxygen relative to carbon in the hydrothermal treatment, the values for hydrochar are lower than those of the feedstock, closer to the values for more condensed materials such as lignite and anthracite coals. The anaerobically digested cow manure already starts closer to peat and the D-HC produced at more severe HTC conditions (240 °C) has the lowest values, bringing it closer to the range commonly found for pyrochars. The other hydrochar occupy the lower region that is commonly referred to peat-lignite. This modification towards peat-like and lignite-like properties may be useful for soil application, especially in terms of seed germination, since the use of the original biomass may promote the proliferation of microorganisms which can be competitors of seeds in the germination phase (Harper & Lynch, 1980).

Hydrothermal treatment also shifted the C/N ratios in the solids. Although the range remained similar for the feedstocks and hydrochars, with values between 21 to 41, the effect was different depending on the feedstock. The C/N ratio decreased for digestate from 31 to 21, while this was reversed for SCG, GM, and GM_Ext (Table 5.2) This ratio is generally used to estimate the relative carbon and nitrogen availability for plants. When C/N ratio is too high (> 35), it results in microbial N-immobilization (Bengtsson et al., 2003). The lower C/N ratio, the faster nitrogen is released on soil for plant uptake (Brust, 2019; Watson et al., 2006). Most of the C/N ratios for the hydrochars lie close to the range optimal for plant growth (20-30) (Brust, 2019).
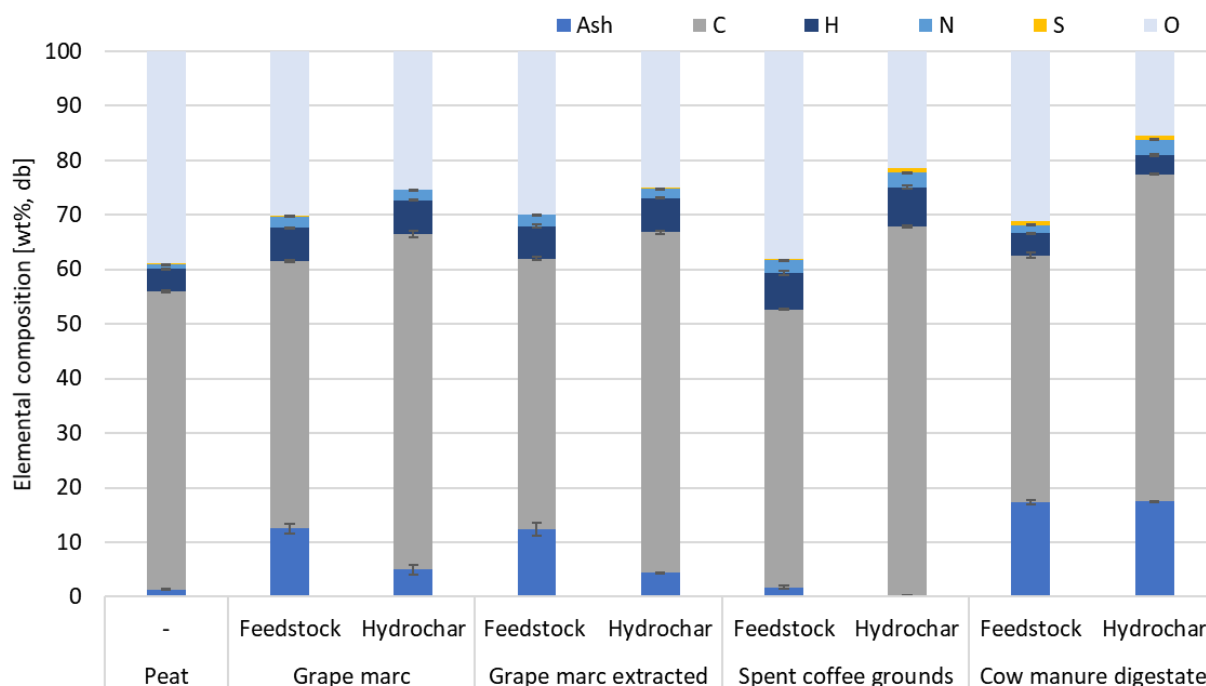
Figure 5.1 – Distribution of ash and macro-element content (wt%, db) in peat, HTC feedstock, and resulting hydrochars.
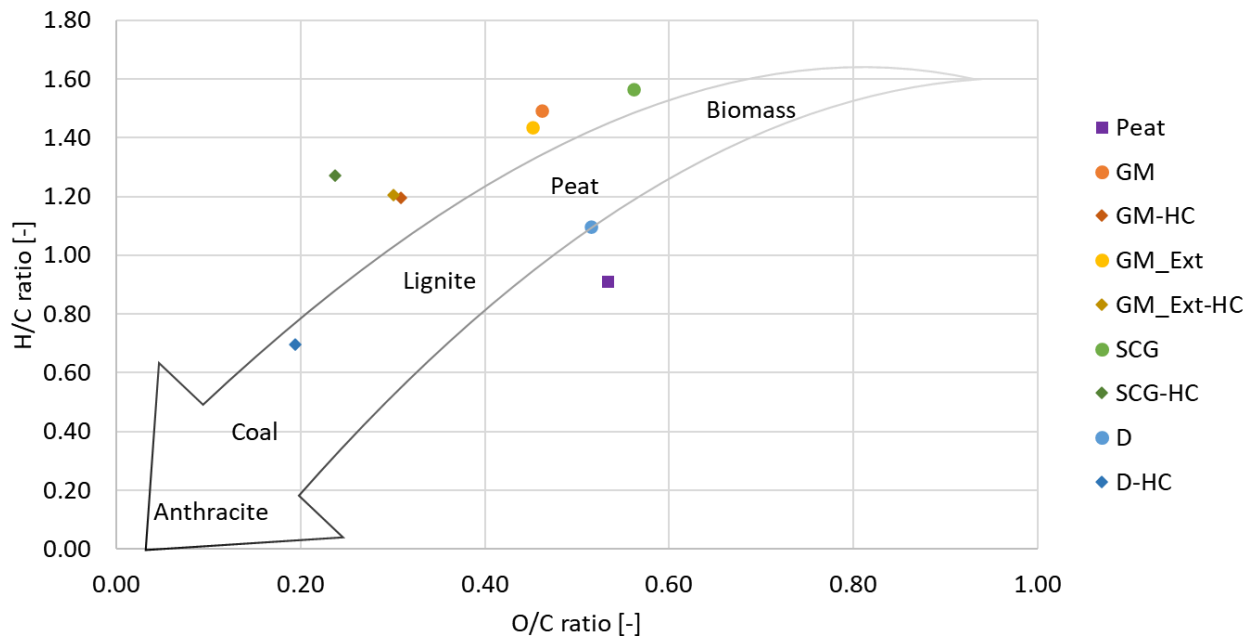

Figure 5.2 – Van Krevelen's diagram of atomic ratios H/C and O/C for the feedstocks and hydrochars with reference regions for typical organic materials.

Table 5.2 – C/N ratio of feedstocks and hydrochars.

Material	D	D-HC	SCG	SCG-HC	GM	GM-HC	GM_Ext	GM_Ext-HC
C/N [-]	31.47	20.90	21.36	25.25	23.56	33.30	23.75	37.18

The process water associated with the hydrochars from SCG, GM and GM_Ext were characterized by high TOC and COD, acidic pH, and high concentrations of acetic acid and total phenols (Table 5.3). The high amount of dissolved organic compounds is likely to be inhibitory to many microorganisms and plants. Many aqueous tests are available to study toxic effect on aerobic bacteria. In this study, a common test of the acute toxicity of process water on nitrifying bacteria was carried out as an indicator for the treatability of the process water in aerobic wastewater treatment plant and/or whether it is safe to use the process water on soils to recycle nutrients. In Table 5.3, the results of the acute toxicity are reported as the inhibiting dose for 50% of the microbial population in ml per L of nitrifying sludge (IC50). The lower the value for IC50 is, the higher the inhibitory effect. Of the three process waters, GM had the highest inhibitory effect, more than 14 times stronger than that of SCG.

Table 5.3 - Characterization of process water samples from the hydrothermal carbonization of the feedstocks.

PW samples	pH [-]	EC [mS/cm]	TOC [g/L]	COD [gO$_2$/L]	Total Ph [g/L]	Acetic acid [g/L]	IC50 [ml/L]
D	5.34	8.79	11.72	35.00	n.a.	2.36	n.a.
SCG	4.03	3.74	10.02 (±1.16)	29.58 (±0.48)	1.92 (±0.03)	2.01 (±0.04)	8.21
GM	4.37	12.53	10.20 (±0.02)	29.78 (±0.02)	1.32 (±0.02)	2.64 (±0.12)	0.58
GM_Ext	4.26	11.71	8.64 (±0.03)	26.47 (±0.05)	1.52 (±0.02)	2.87 (±0.15)	2.02

n.a. = not available

5.4.2   Effect of feedstocks and hydrochars on seed germination and root length

The effect of the different feedstock and hydrochar mixtures on the germination of cress seeds is shown in Figure 5.3. The average germination rate (AGR), which relates the average values from the individual samples to the 100% peat control, is used to compare the effects. For all three feedstocks, almost no seeds germinated in the Petri dishes filled with only feedstock. However, germination in mixtures with peat was successful, achieving AGRs of 100% for feedstock mixtures of D up to 50%. Feedstock mixtures for both SCG and GM already showed inhibitory effects at 25%. Most hydrochar

mixtures achieved high germination rates. AGR values were similar for D feedstock and hydrochar, while hydrothermal and post-treatment of SCG improved AGR, reaching 90% of the control germination rates for 50% SCG-hydrochar mixtures for both the wet and dried forms. Treatment of GM, however, did not improve germination at 50% mixtures of dried hydrochar from GM_Ext and GM, which were inhibited by 37% and 100%, respectively.
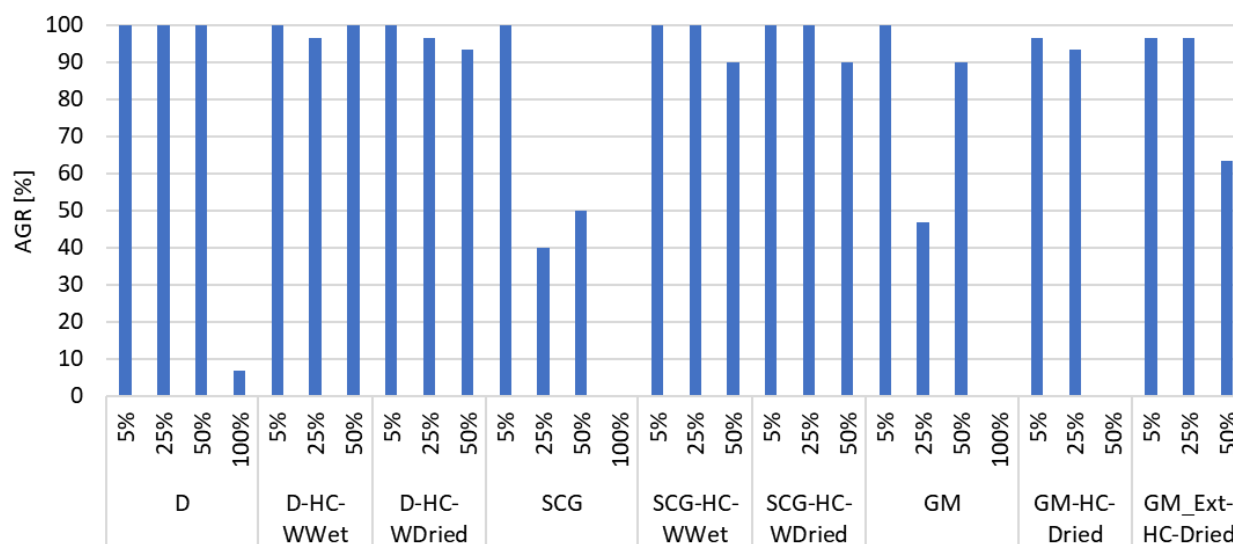

Figure 5.3 – Average germination rates (AGR) assessed for the different hydrochars and their related feedstocks. The results are expressed relative to the controls (100%).

The average root length of seedlings measured during the germination tests for the feedstocks and hydrochar mixtures are reported in Figures 5.4a-c. Statistical significance was evaluated using a one-way ANOVA and the Tukey's HSD test, in which samples connected by the same letters are not significantly different. Of the three feedstocks, only mixtures with D promoted root growth, with significantly longer roots in mixtures up to 50% compared to the control. All mixtures of SCG and GM significantly reduced RL, even at the 5% level, although the germination rates were not affected at this mixture. At 25 and 50%, almost no roots developed for SCG and GM, even though some seeds did germinate. In contrast, in Petri dishes with 100% of the three feedstocks both germination and root growth were almost totally inhibited. Similar inhibition by SCG has been reported by other authors (Cervera-Mata, Fernández-Arteaga, et al., 2021), which have attributed this phytotoxic effect to the presence of toxic organic compounds in SCG. Another possible inhibitory effect of the feedstock samples may be due to the mould that developed in those samples with low germination rates. Future tests should clarify whether germination was inhibited due to mould growth or

whether mould grew as a result of inhibited germination, e.g., by sterilizing the feedstock before germination tests.

The hydrothermal treatment of the feedstocks with post-treatment (washing and/or drying) reduced the inhibitory effects of all three feedstocks to varying degrees. For D, RLs similar to the control were achieved for all mixtures of the wet washed hydrochar according to Tukey´s HSD test (Figure 5.4a). In contrast, better RL results were obtained from the Petri dishes using dried washed hydrochar, especially in samples containing 25% and 50% hydrochar. This difference may be attributed to the removal of soluble (via washing) and volatile (via drying) organic compounds through the post-treatments. For SCG, the hydrothermal and post-treatment showed promising results, especially in low percentage mixtures (5 and 25%) (Figure 5.4b). In fact, all samples with peat replaced by 5% hydrochar achieved results similar to the control. However, higher amounts of hydrochar showed some inhibition in germination (50%) and in root growth (25 and 50%). No benefit was seen from the extra drying step. In contrast, almost all the mixtures of dried hydrochar from GM showed substantial inhibition even at low percentage (Figure 5.4c). Only the 5% mixture of ethanol extracted dried hydrochar (GM_Ext) had root lengths similar to the control. It is likely the presence of phytotoxic compounds, such as phenolic compounds or volatile fatty acids (VFAs, e.g. acetic acid) reduced the germination of seeds and the root growth (Bargmann et al., 2013; Busch et al., 2013; Kern et al., 2017).
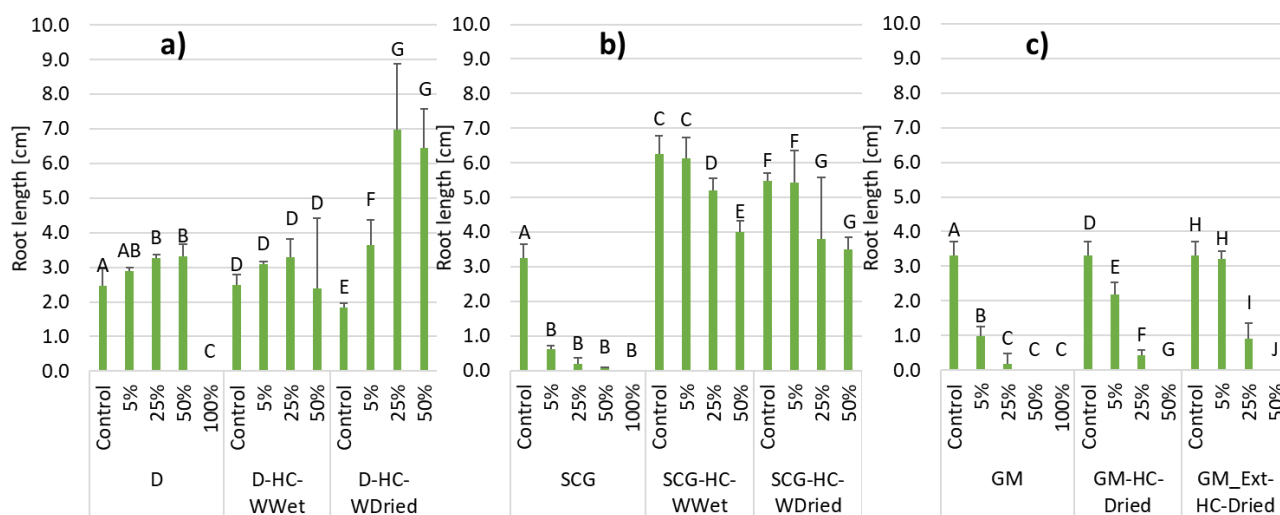
Figure 5.4 – Average root length of seedlings deriving from germination tests using a) D and the related wet and dried hydrochar, b) SCG and the related wet and dried hydrochar, c) and GM and the related dried hydrochar. Samples connected by the same letters are not significantly different.

The Munoo-Liisa vitality index (MLV), which takes into account both the average germination rate AGR and average root length of the cress seedlings compared to the control, was used to evaluate

the overall performance. The MLV and RI values for all feedstocks and hydrochar are shown in Figure 5.5. A reference line at 80% is also shown since some legislation (e.g., the Finnish Act on Fertilizer Products) has set this as a target value for MLV % in cress germination tests (Maunuksela et al., 2012). Although values below this target are presumed to indicate the presence of potential phytotoxic compounds in the substrate tested, Maunuksela et al., (2012) found that pig manure, a material conventionally used on soil, had MLV values lower than 80%, and suggested 60% be considered adequate for good product quality.

All the hydrochars in this study achieved better MLV results when compared to their feedstock. Post-treatments had positive effects on both germination and root growth, especially the application of both washing and drying. The D-feedstock and wet washed hydrochar mixtures had MLV values well above the target 80%, but the washed and dried D-hydrochar achieved much higher MLV, over 300% at mixtures of up to 50%. Although the MLV for SCG-feedstock and hydrochar mixtures were very much lower than those for D, the trends for the hydrochars were similar. Hydrothermal treatment of SCG with both washing and drying produced improved germination, increasing MLV from 16% for the 5% feedstock mixture to 50% and 65% and to 40% and 60% for the 25% and 50% hydrochar-mixtures (wet and dried), respectively. In contrast, only the 5% mixture of hydrochar from GM and GM_Ext achieved similar germination results. Although the pre-treated GM with ethanol extraction produced a carbonized material that showed improved results in comparison with hydrochar produced without pre-treatment, these improvements were effective only when low percentages of hydrochar were used in the growth substrate.
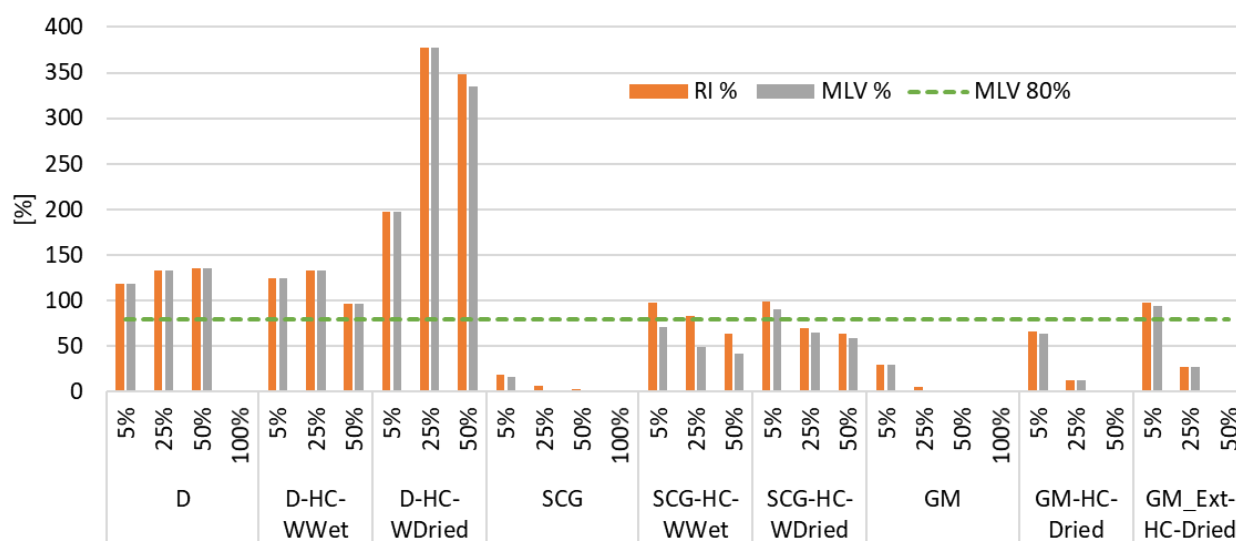
Figure 5.5 – Values of root length index (RI), and Munoo-Liisa vitality index (MLV) calculated for each sample in germination tests with the contact method. The results are expressed relative to the controls (100%).

5.4.3   Effect of process water on seed germination

Germination tests using the extraction method were carried out with the process waters from the hydrothermal treatment of the three feedstocks (SCG, GM, and GM_Ext) that caused the highest inhibition in the peat-replacement tests discussed previously. Such tests with process water may be helpful to answer questions on whether post-treatment of the hydrochars is advisable before application as a soil amendment or growth media and/or on how to treat the process water.

The AGR shown in Figure 5.6a indicate that all samples of process water from the three feedstocks inhibited germination to some extent. The process water from GM_Ext had the least effect, with AGR ranging from 90% (10% dilution) to 40% (undiluted). No germination was seen for undiluted SCG and GM process water. The effect of the process water was much stronger on the root length (Figure 5.6b). The root length was decreased in all samples, ranging from almost no growth with undiluted process water to 45 - 55% shorter roots for the 10% dilution.
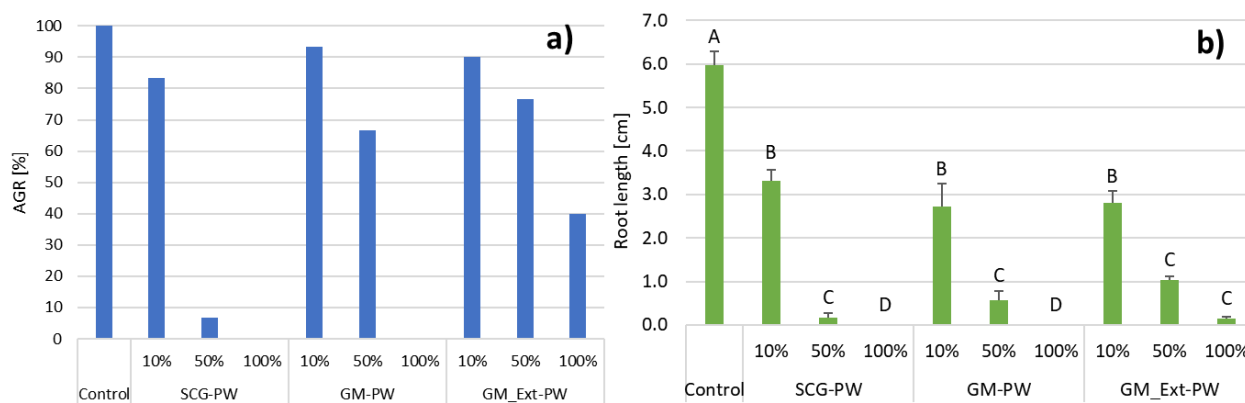
Figure 5.6 – Germination test results using process water for a) average germination rate, b) average root length. Samples connected by the same letters are not significantly different.

High inhibition was seen for all 3 process waters, with MLV decreasing at higher concentrations of process water (Figure 5.7). The MLV of all samples remained well below the target value of 80%, only reaching 47% for the 10% SCG-process water dilution. The inhibition is likely due to the high amount of organic compounds dissolved in the process water (Table 5.3). Process water typically contain high concentrations of many small molecular organic compounds that may be inhibitory to germination, such as furan and phenolic compounds, aldehydes as well as VFAs and other organic acids (Libra et al., 2011; Titirici et al., 2008; Bargmann et al., 2013). The high TOC and COD concentrations (8.64 - 10.2 gTOC/L; 26.47 - 29.78 gCOD/L) of the process water means that even at a 10% dilution, the seeds are exposed to the equivalent of a high-strength wastewater. This consideration is supported by different authors (Bargmann et al., 2013; G. Wang, 2022) who found similar inhibition of germination and seedling growth from process water. Bargmann et al., (2013) identified some specific compounds (guaiacol, levulinic acid, and glycolic acid) that inhibited cress seed germination and three others (acetic acid, glycolaldehyde dimer and catechol) that negatively impacted growth. They also found that they could use the differences between the dissolved organic carbon content in their process water from 5 feedstocks to predict germination-inhibiting effects. In Figure 5.7, however, it can be seen that the small differences between the TOC or acetic acid values in the process water from the three feedstocks do not correspond to the differences in MLV. An additional lumped parameter, total phenols (Total Ph), was also measured in the process water (Figure 5.7), but the values do not follow the trend found in the germination tests. The highest Total Ph concentration was measured for SCG, but SCG has highest MLV at the 10% process water dilution. It is interesting to note that the pre-treatment for GM_Ext, where mainly polyphenolic compounds were extracted from the feedstock with ethanol, did not reduce the Total Ph measured in the

108

process water compared to GM. Nonetheless, the process water from the GM_Ext showed less inhibition on the seed germination and root growth than GM-PW. Thus, Total Ph does not seem suitable as an indirect indicator of inhibition for these feedstock process waters.
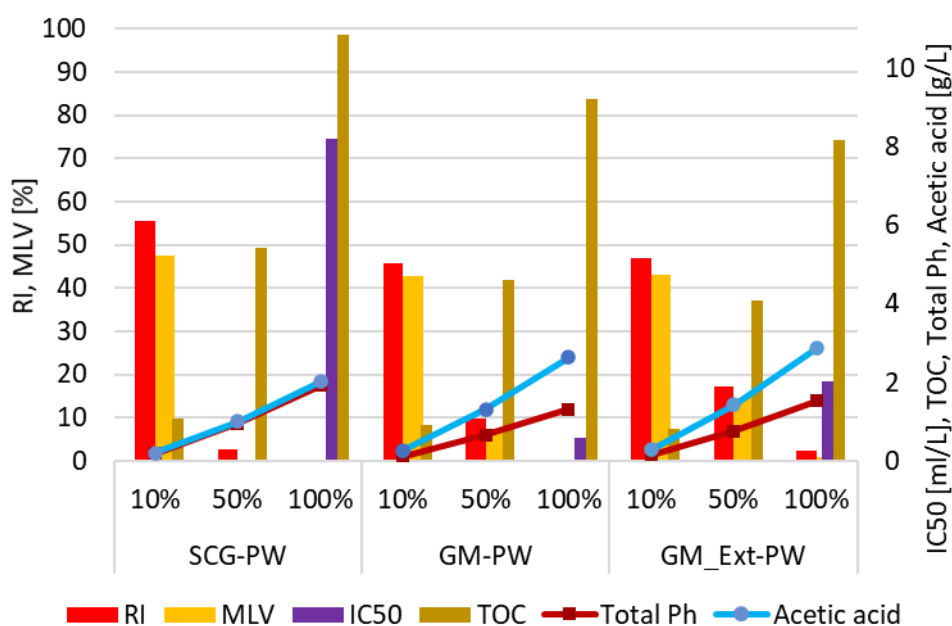

Figure 5.7 – Acetic acid, Total Ph, IC50, and TOC and Root length index (RI), and Munoo-Liisa Vitality index (MLV) in germination tests using process water.

The trend in the inhibitory effects seen with the MLV values is better matched by the results of the bioassay using aerobic nitrifying bacteria. The feedstock process water with the lowest MLV and IC50 (which indicates the highest inhibition) is GM, while SCG has the highest values for MLV and IC50. Nitrifying bacteria are essential in the nitrogen cycle (Schmidt & Belser, 2015), converting ammonia to nitrates in soil and in wastewater treatment plants. Inhibitors for these bacteria can be purposely added to fertilizers to minimize N losses and improve N use efficiency in agricultural ecosystems (Papadopoulou et al., 2020) or stringently avoided to ensure nitrogen removal in wastewater systems (Ficara & Rozzi, 2001; Pagga et al., 2006). The results here show that this aqueous bioassay with ammonium-oxidizing bacteria is very sensitive to inhibitors that affect nitrification as well as germination. The most highly diluted samples in this study, 10% process water, are still more than twelve times more concentrated than the measured IC50 value for SCG, and for GM almost 180 times more concentrated. In Figure 5.8, the germination results for both the solid and liquid products from the HTC of GM and GM_Ext are compared to the IC50 measured for the process water. The MLV for the hydrochar and process water both show less inhibition from the pre-treated GM than from GM and this corresponds well with the IC50 values. Comparing the two

tests, acute toxicity test on nitrifying bacteria is faster than germination tests, considering the time used by the former for the material preparation, incubation (72 h), and the roots measurement. On the other hand, tests on nitrifying bacteria requires 24 h of aeration for the activated sludge preparation and only 4 hours to obtain the results. In addition, this kind of test considerably reduces the evaluation effort as the only task required is to dose a certain amount of sample about every 20 minutes.
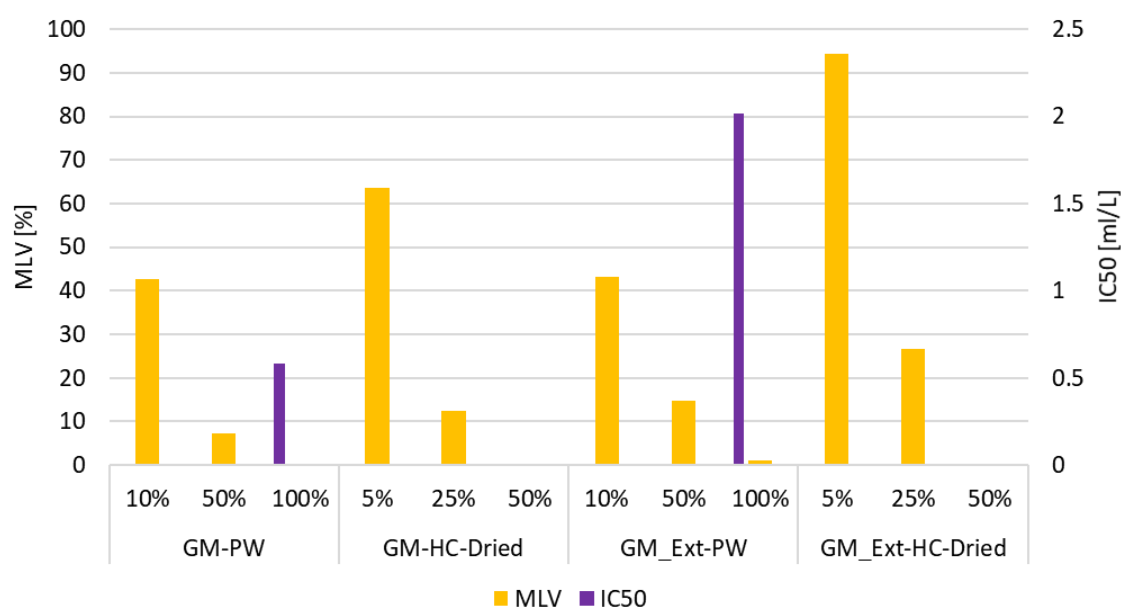

Figure 5.8 - Comparison between MLV for hydrochar and process water for GM and GM_Ext and the IC50 for process water.

5.5   Conclusions

Germination tests on hydrochars from D, SCG, and GM showed that they may be considered as a substitute for peat in growing media. However, the quantity of peat that can be substituted varies according with the feedstock type and the pre-treatments or post-treatments applied. Both the washed and dried washed hydrochar from D achieved MLV higher than the target value of 80%, but the addition of the drying step significantly improved root length compared to 100% peat in mixtures up to 50% D-HC. Likewise, the MLV values for hydrochar from SCG improved when both post-treatments were applied, reaching 80% in mixtures up to 25% SCG-HC. Hydrochar from GM with only the drying step showed high inhibition only reaching 64% in the 5% mixture, however, with pre-treatment, GM_Ext-HC reached almost 100% of the control values at 5% mixture. The potential of replacing at least 5% of peat in growing media for horticulture can make a substantial contribution in reducing the global use of natural peatlands. The inhibition that affected samples

containing a high amount of hydrochar from SCG and GM may be due to the formation of phytotoxic compounds during the HTC process and retention of process water on the hydrochar. Pretreatment of the feedstock (GM extraction) and post-treatments of the hydrochars (washing and drying) have positive effects on germination. Initial evaluation of the relatively robust and quick nitrification bioassay on the process waters showed high sensitivity and good agreement with the inhibition trends found in cress germination tests. It was a better predictor than the chemical lumped parameters (TOC, total phenols) for the presence of phytotoxic compounds in the hydrochars and process waters. Such tests can be helpful in developing and optimizing process combinations for the hydrothermal production of peat replacements.

Chapter 6

Cigarette butts: a valuable raw material? A preliminary evaluation of their potential recovery as a solid fuel

This chapter gives a contribution to the general knowledge of the HTC process and on its applicability to synthetic organic residues, helping to recognise the goodness of the technical solution proposed. Specifically, the treatment of a residue that can have harmful effects on the health of people and the environment, such as the cigarettes butts, is presented here. The results of this work will be presented at the 3rd international HTC symposium (2022) in Seoul, South Korea.
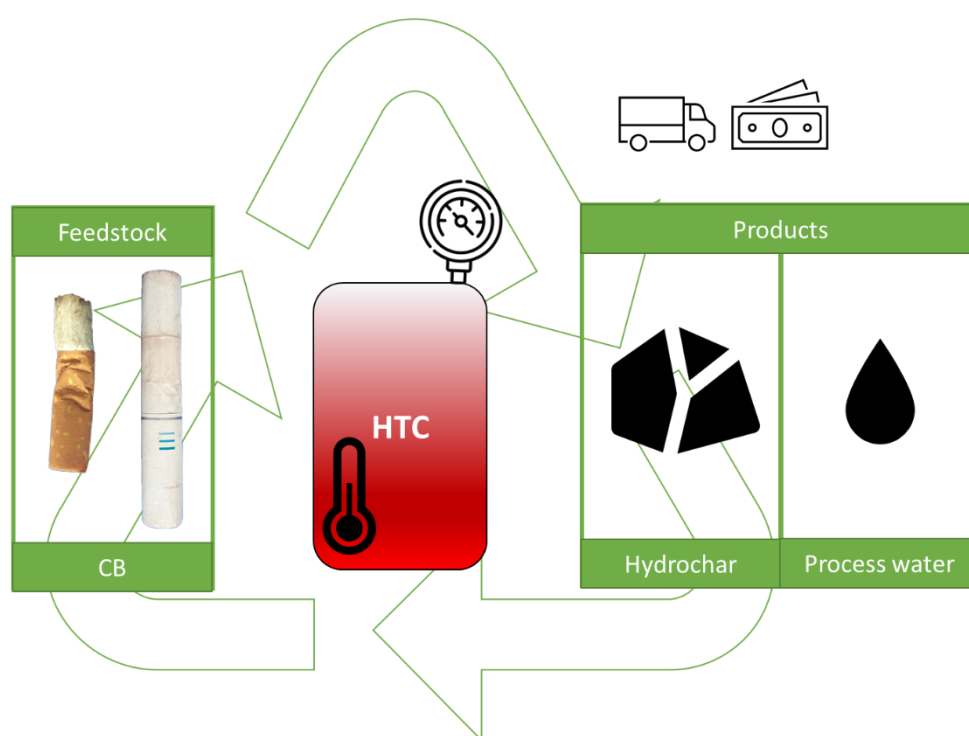
6.1 Abstract

Globally about 5.6 trillion cigarettes are smoked every year, and estimates show an expected increase of up to 9 trillion in 2025. Furthermore, alternative tobacco products such as HEETS sticks (a heat-not-burn cigarette) for IQOS are also growing in popularity. Each cigarette leaves behind a waste residue, the cigarette butt, mainly made up of paper, unburnt tobacco, and filtration material. Since a high number of smokers do not dispose of cigarette butts properly, they may become sources of environmental pollution. Based on an abandonment rate of 75%, 54 billion butts per year (about 9750 tons) are, therefore, dispersed into the environment. In this work, the conversion of cigarette residues by the process of hydrothermal carbonization was investigated at the temperature of 220 and 240 °C at 1 h. HTC process was used to treat the common cigarette butts as well as the more recent HEETS butts. In addition, further tests at 240 °C for 1 h were performed on the mix of common cigarettes and HEETS butts to simulate a combined collection. The produced solid material was characterised to establish its physical-chemical properties and to hypothesise feasible uses. A characterisation campaign was also applied to the process water, aiming at assessing its treatment and/or valorisation. Results show a great increase in carbon and energy content and a decrease in ash content, making the produced hydrochar suitable for energy recovery. Moreover, the reduction in volume and mass obtained contribute to saving transport costs.

6.2 Introduction

Globally, in the last two decades, attention to environmental protection and pollution-related issues has considerably grown, even considering specific forms of contamination deriving by particular categories of residue too long neglected. Among them, cigarette butts are characterised by a considerable difficulty of management linked both to widespread production and improper management (Chapman, 2006; d'Heni Teixeira et al., 2017; Harris, 2011).

Globally, the consumption of smoked tobacco products (such as cigarettes and cigars) is still an actual issue that involves over 1 billion smokers of all ages (Rahman et al., 2020; Torkashvand et al., 2020), generating every year trillions of butts (Marah & Novotny, 2011; Torkashvand et al., 2020). In general, a cigarette is a single-use and short-life product. In fact, smoking a cigarette takes about 5-10 min and produces ash, smoke (several compounds, which may be toxic, and particulate matter, PM), and the solid residue, the butt which mainly consists of unburnt tobacco, paper, and filter (Poppendieck et al., 2016; Wu et al., 1997). Cigarette butts (CBs) are considered the icon of the litter

as it is easy to find a cigarette butt walking on the street. Unfortunately, although this kind of waste is highly toxic due to its nature, many people have the nasty habit of using the street, beaches, and park as their personal ashtray, leaving their butts on the ground after they have finished smoking. Due to their small size, cigarette butts can be found everywhere and can be carried by wind or rainwater to the main water bodies (Rahman et al., 2020). These waste are considered environmentally hazardous due to the large number of dangerous chemicals such as heavy metals, PAHs, nicotine, and several others formed during the combustion (Beutel et al., 2021; Kurmus & Mohajerani, 2020; Marah & Novotny, 2011; Torkashvand et al., 2020). In addition, the filter, which is the main component of CB, is made of non-biodegradable materials (e.g., cellulose acetate) (Belzagui et al., 2021; Harris, 2011), which can make it persistent in the environment for a long time (Belzagui et al., 2021; Freire Lima et al., 2021). Other issues not directly connected to the release of toxic chemicals are the ingestion by animals and fire risk caused by those who abandon cigarettes light (Torkashvand et al., 2020).

Due to all the harmful and dangerous features of cigarettes, manufacturers of major brands have launched new products that do not require combustion. An example is the heat-not-burn tobacco products (HnB), where tobacco sticks are heated with an electronically controlled heating device without combustion (Simonavicius et al., 2019). It is an alternative to traditional smoking and is based on a process of heating tobacco up to 350 °C. Although they do not generate smoke (and, therefore, PM), they still produce a butt residue (CBH), which leads to the same issue as the classical cigarette butts. Due to the widespread dispersion, collecting this particular residue is challenging and costly (Torkashvand et al., 2020). This is highlighted by the fact that there are no specific valorisation strategies to handle it. To date, landfill disposal and combustion with other waste are the main management systems used for CB. This work aims to propose a feasible treatment for the safe management and valorisation of cigarette butts (CB and CBH). Hydrothermal carbonization (HTC) is used to convert CB and CBH into a valuable solid material to recover energy and save costs related to their management, especially given the mass reduction occurred in HTC process, which save transport costs. Moreover, disinfection of the materials is assured by the process temperature, as well as the release in solution and the destruction of several compounds, which make the solid new material safer to handle. The treatability of the derived process water and their valorisation were also tested.

The experimental activity was planned and developed as a first approach to the treatment for the valorisation of cigarette butts. In particular, it was intended to produce a material potentially

suitable as solid fuel. Different HTC tests were performed at different temperatures (220 - 240°C) and different process durations (1 and 3 hours) to assess the influence of temperature and holding time on the final quality/quantity of the products. The materials tested and those obtained under different operating conditions were subjected to characterisation of chemical and physical properties consistent with the above hypotheses of reuse.

6.3   Materials and methods

6.3.1   Cigarettes butts and HTC process

The HTC tests were conducted on industrial cigarettes butts (CB) without any differentiation of brand, the residues of cigarettes HEETS (CBH, Philip Morris S.A, Switzerland), usable with a recent HnB technology called IQOS (I Quit Ordinary Smoking), and a mix of the two types of cigarettes butts mixed in equal parts (1:1 by weight).

This choice is motivated by the fact that these materials have a greater homogeneity in their composition and a large amount of information provided by their manufacturers compared to other smoked tobacco products (e.g., roll-your-own cigarettes - produced by hand from shredded tobacco, cigars, bidis, kreteks). Materials are shown in Figure 6.1. Both CB and CBH are multi-material based. In detail, CB are composed of paper, tobacco (unburnt), and a filter (cellulose acetate), while CBH are made of paper, tobacco and two kinds of filter, a porous filter similar to that one present in CB (cellulose acetate) and a polymer-film filter made of bioplastic (PLA, polylactic acid). Moreover, both CB and CBH contain various additives to slow or accelerate the combustion or give special flavours.

Both CB and CBH were collected in specific bins outside the facilities of the University of Cagliari to obtain a representative sample. The collected materials were stored in airtight containers (Fig.4.3) and left in precautionary quarantine for 48 hours in order to avoid any hygienic-sanitary risk. The two samples were sieved (1.18 mm,) to remove a significant proportion of residual ash; a significant amount of each sample was weighed and heated up to 105 °C in oven until a constant weight was achieved to assess the moisture content. Dried samples were heated up to 550 °C in muffle to calculate the ash content.

The HTC tests were carried out into 1L stainless-steel pressurised reactor (Berghof BR-1000). The reactor was equipped with an external heating jacket, a head equipped with a thermocouple and output valves for gas and liquid sampling, a pressure gauge with safety system, and a shaft together

with the agitator motor; the water-tightness of the system is guaranteed by a gasket that interposes between the head and the reactor body. The latter is connected to a controller with which it is possible to interact, monitoring and recording the conditions evolutions inside the reactor.

Since the material had low humidity, distilled water was added to achieve a solid-to-liquid ratio of 10. HTC tests were conducted at 220 and 240 °C with a holding time of 1 h. Moreover, additional tests were conducted at 220 °C for 1h on the mix (CBM) and 220 °C for 3 h for only CB. All the tests were conducted three times. When the temperature was kept for the decided holding time, the system was turned off and left to cool overnight.

Before opening the reactor, the gas was released, and the carbonized material was separated through a filter-press into the solid and liquid phase. To obtain a reliable mass balance, the materials used were weighted in each step. Hydrochar was vacuumed stored in plastic bags, while process water was filtered (0.45 μm) and stored in plastic bottles at 4 °C. A randomly sorted portion of HC was dried at 105 °C and burnt at 550 °C to assess the water and the ash content, respectively. Samples were labelled with an alphanumeric code reporting the information about the feedstock, the temperature and the time applied (e.g., the sample of industrial cigarette butts treated at 240 °C for 1h was labelled as CB_240_1). Table 6.1 summarises the operational parameters for the different tests and the code assigned to each derived sample.

Table 6.1 – Summary of operational conditions applied in each test and the corresponding code.

Feedstock	Temperature [°C]	Holding time [h]	Code
	220	3	CB_220_3
CB	220	1	CB_220_1
	240	1	CB_240_1
CBH	220	1	CBH_220_1
	240	1	CBH_240_1
CBM	240	1	CBM_240_1

Figure 6.1 – Industrial cigarette butts (a) and HEETS cigarette butts for IQOS (b).

6.3.2   Feedstock and HTC products characterisation

The characterisation of solid materials (feedstocks and HC) included the determination of the concentrations of carbon, hydrogen, and nitrogen through a CHN analyser (CHN628, LECO), higher heating values (HHV) through an Isoiperbolic Calorimeter (LECO®, AC500). Moreover, ATR-FTIR (Attenuated Total Reflection - Infrared Spectroscopy in Fourier Transform) was used to chemically identify the materials produced by the HTC process (FT-IR6300A, JASCO), in the 4000-400 cm^{-1} spectral range, ris. 4.0 cm^{-1}, 50 scans, and ATR module equipped with diamond crystal. Lastly, the determination of the density of the materials was performed through a helium-pycnometer (AccuPyc II 1340).

Process water characterisation included the measurement of pH and electrical conductivity (EC) and pH using a multi-parameter probe (Hanna HI-5521). Total organic carbon (TOC) in PW was evaluated using a TOC analyser (TOC-VCSN, Shimadzu Corporation), while the concentration of specific anions (chlorides, sulphates, nitrates) was made by ion chromatography (ICS-90, Dionex). A deeper characterisation is presented in Chapter 8.

6.4   Results and discussion

The preliminary characterisation involved the process feedstock, i.e., the butts of industrial cigarettes, identified by the initials CB and those of HEETS cigarettes for IQOS, indicated by the abbreviation and CBH. The two types of butts have been divided respectively into paper, filters, and unburnt tobacco, and paper, polymer filters, acetate filters, and unburnt tobacco. The average mass

distribution of the components of both materials is illustrated in the pie charts in Figure 6.2 (total CB weight = 1.63 g; total CBH weight = 3.5 g).

Figure 6.2 – Average composition by weight of CB and CBH.

Table 6.2 shows the characterisation results for each component of the two samples in terms of elemental percentage composition (C, H, N, S, and O) and determination of ash and volatile solids. The table also reports the average values relating to the whole samples reconstructed, taking into account the weight ratios of the various components.

Table 6.2 – Elemental composition of the two types of butts and of the respective fractions of which they are made.

Sample	Component	C [%]	H [%]	N [%]	S [%]	O [%]	Ash [%]
CB	Paper	31.20 (0.43)	4.87 (0.12)	0.35 (0.01)	< 0.1	45.80	17.80 (0.36)
	Tobacco	38.90 (0.70)	5.25 (0.09)	2.79 (0.03)	0.55	45.70	7.38 (1.17)
	Acetate filter	45.50 (0.19)	5.44 (0.03)	0.35 (0.02)	<0.1	46.80	1.91 (2.21)
	CB	37.7	5.14	0.76	0.01	46.90	10.30
CBH	Paper	30.60 (0.56)	4.40 (0.47)	0.27 (0.08)	< 0.1	52.70	12.00 (0.50)
	Tobacco	42.00 (0.48)	5.40 (0.08)	2.12 (0.13)	0.52	40.50	10.12 (1.21)
	Polymer filter	46.90 (0.28)	5.34 (0.07)	0.11 (0.04)	< 0.1	47.30	0.27 (0.05)
	Acetate filter	44.90 (0.05)	5.48 (0.03)	0.21 (0.04)	< 0.1	48.00	1.33 (0.39)
	CBH	42.00	5.20	0.80	< 0.1	46.20	5.70

Sulphur detection limit = 0.1%

Table 6.3 shows the results obtained for measurement of pH and electrical conductivity of the various and PW obtained.

Table 6.3 – Summary of liquid yield (%), pH and electrical conductivity.

Sample	Process water [%]	pH [-]	Electrical conductivity [mS/cm]
CB_220_3	105.45 (0.07)	3.90 (0.06)	10.53 (0.24)
CB_220_1	105.17 (0.12)	3.83 (0.05)	8.66 (0.58)
CB_240_1	105.23 (0.35)	3.99 (0.07)	8.29 (0.44)
CBH_220_1	106.70 (0.35)	3.27 (0.01)	6.79 (0.07)
CBH_240_1	105.97 (1.25)	3.28 (0.05)	6.41 (0.53)
CBM_240_1	104.77 (0.67)	3.48 (0.01)	6.66 (0.40)

The table shows an increase in terms of liquid yield, interpretable either as a production of water, linked to the different reactions typical of the HTC treatment (in particular dehydration), or as a variation in terms of density of the process water, related to the feedstock and the compounds formed during HTC in PW. The EC increased from 4.03 mS/cm to over 8 mS/cm for CB treated at 1h and over 10 mS/cm at 3h, and from 2.33 mS/cm to over 6 for CBH. The pH values are between 3 and 4, as expected, given the typically acidic nature of the products of this treatment compared to the initial pH of CB and CBH of 6.44 and 6.75, respectively. It is not possible to deduce significant effects due to the different process conditions.

Table 6.4 shows the analysis data by ion chromatography, providing the averages and standard deviations of the tests characterized by the same operating parameters (feedstock, temperature, and holding time).

Table 6.4 – Summary of mean and standard deviations of the results obtained with ion chromatography analysis.

Sample	Chlorides [mg/L]	Nitrates [mg/L]	Sulphates [mg/L]
CB_220_3	119.9 (9.1)	31.8 (9.6)	323.6 (61.1)
CB_220_1	118.2 (22.2)	34.5 (1.0)	319.1 (47.1)
CB_240_1	132.0 (33.1)	29.8 (5.3)	292.0 (64.3)
CBH_220_1	140.6 (20.7)	14.9 (3.1)	279.0 (8.9)
CBH_240_1	90.8 (30.5)	5.9 (1.7)	212.0 (70.2)
CBM_240_1	92.2 (4.3)	18.4 (1.5)	287.0 (11.3)

The results show considerable variability, particularly regarding chlorides; however, the concentrations do not seem to be directly due to the temperature and duration used during the

tests. In terms of nitrates and sulphates, the concentrations are higher for the PW corresponding to the CB; also, an increase in temperature corresponds to lower concentrations for both samples. The holding time does not seem to affect these ions behaviour significantly. As far as the CBM test is concerned, all the values fall on average between those of the PW of CB and CBH. Table 6.5 shows the results (average values and standard deviations) of total carbon, total inorganic carbon, and total organic carbon measured for each test.

Table 6.5 – Average results of the PW TOC meter analyses, for tests with the same operating parameters.

Sample	TC [g/L]	IC [g/L]	TOC [g/L]
CB_220_3	24.91 (0.35)	0.01 (0.00)	24.90
CB_220_1	24.33 (2.24)	0.89 (0.04)	23.45
CB_240_1	22.37 (3.38)	0.99 (0.05)	21.38
CBH_220_1	30.83 (1.46)	0.88 (0.03)	29.95
CBH_240_1	27.04 (5.27)	0.91 (0.01)	26.14
CBM_240_1	22.72 (2.38)	0.74 (0.09)	21.99

From the results, it can be seen that the highest values are relative to the samples obtained from the HEETS for IQOS. For both CB and CBH, an increase in temperature corresponds to decreased carbon concentrations, while holding time does not significantly affect the data.

Regarding the characterisation of the solid phase, in terms of solid yield, the values for industrial cigarette butts are higher than those obtained with CBH. At shorter residence times, there is an increase, albeit minimal, in the solid yield for both ICH and CBH, unlike what happens with an increase in temperature, which corresponds to lower solid yields. The histogram in Figure 6.3 reports the average composition of the samples in terms of C, H, N, S, O, and ash. The data show considerable increases in the percentage of carbon in hydrochar compared to the feedstock, which reports values of 37.7% and 42.0% for CB and CBH, respectively. Hydrogen and nitrogen have also slightly increased, while oxygen has decreased considerably. This behaviour is in line with what is expected from HTC treatment (Funke & Ziegler, 2010; Libra et al., 2011). Also, the increase in temperature seems to correspond to a higher concentration of output carbon. To better understand the changes in the elementary composition, in Figure 6.3, a graphical comparison is proposed.
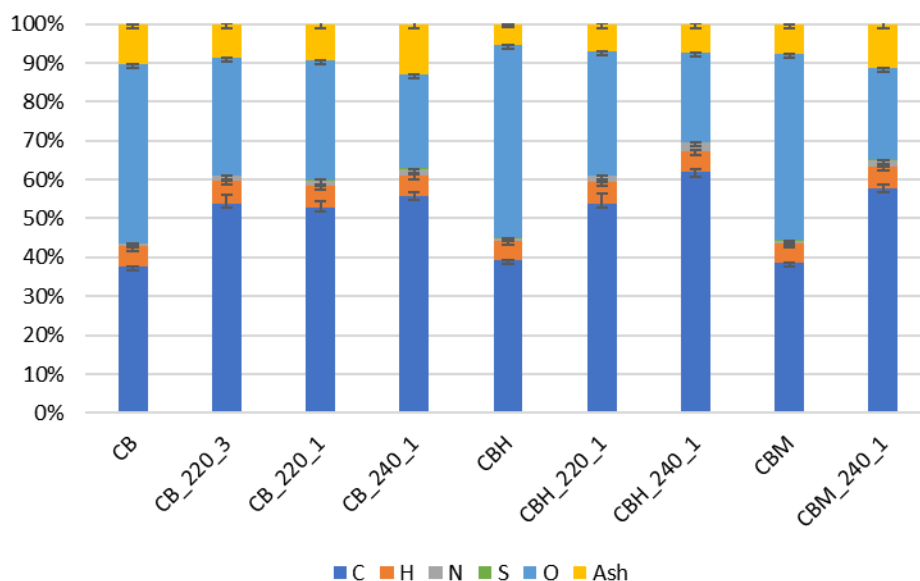
Figure 6.3 – Histogram of the average composition of the input materials and the respective HC obtained under different operating conditions.

In order to examine the degree of carbonization of products obtained through the HTC treatment, the atomic ratios H/C and O/C have been calculated for each sample and reported in Van Krevelen's diagram (Figure 6.4), which allows describing the changes in the carbonization grade of the HTC products compared to the feedstocks (Kim et al., 2003). The results obtained show a substantial decrease in both ratios.
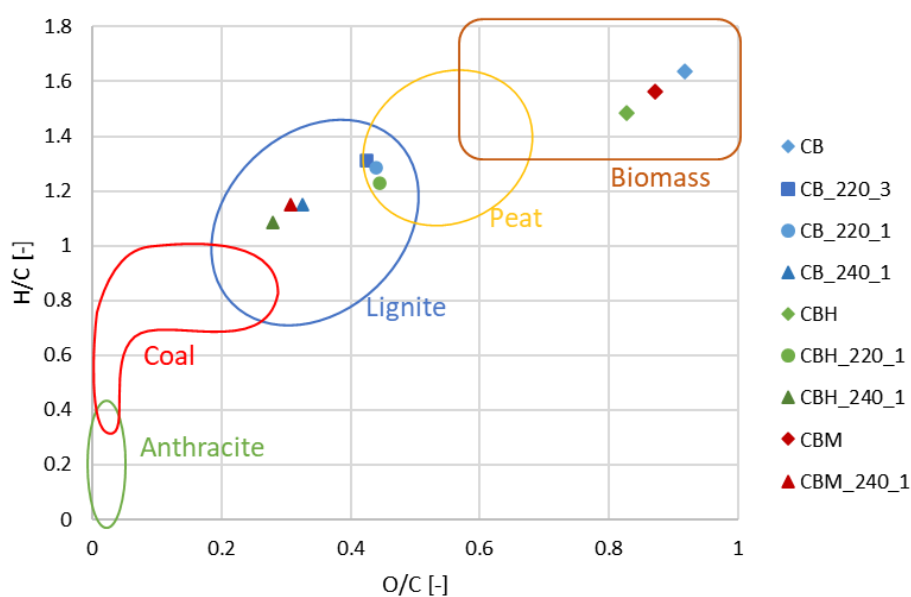
Figure 6.4 – Van Krevelen's diagram referring to feedstocks and to HCs produced under different operating conditions.

The point cloud follows the typical trend dictated by the dehydration reaction. An increase in temperature corresponds to an improvement in the characteristics of the final product; in fact, the tests conducted at 240 °C produce a material falling within the lignite area while the tests conducted at 220 °C produce a material with characteristics more attributable to peat. The holding time seems not to have a clear influence, as evidenced by the results related to the samples CB_220_1 and CB_220_3. In addition, CBM showed similar characteristics to both CB and CBH.

Figure 6.5 represents the density comparison between the input materials and the corresponding hydrochar.
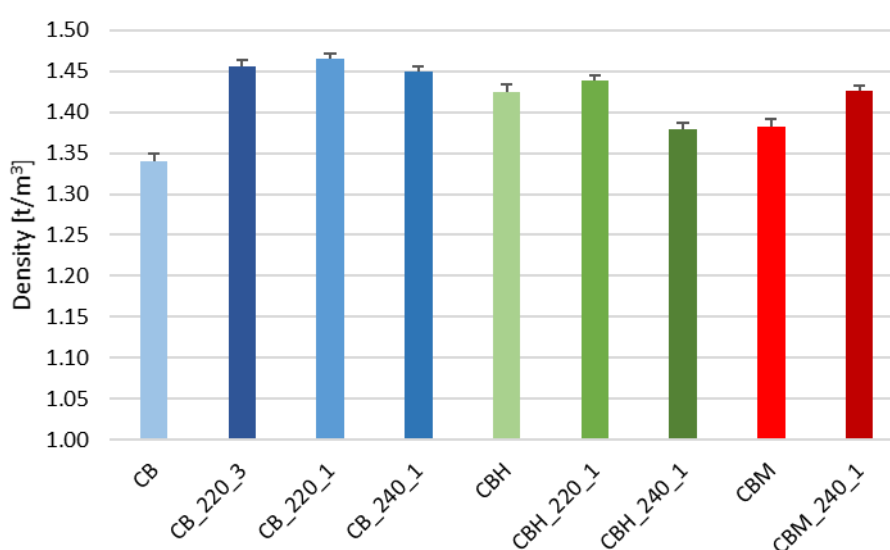
Figure 6.5 – Comparison of the density values of the feedstocks and their respective HCs under the different operating parameters.

The results obtained showed increases in the density of HTC's products compared to the feedstock, especially for samples from CB and CBM. The increase in temperature would seem to determine a decrease in density, as well as the holding time, even if the high variability of the data does not allow for highlighting significant variations. Concerning the HCs obtained from CBH samples, the graph shows a general decrease in density values at higher temperature.

In Figure 6.6, the FTIR spectra of the components of CB and hydrochars formed at 220°C and 240°C for 1h are showed, while in Figure 6.7 the spectra of the CBH components and derived HCs produced in 1h at 220 and 240 °C are represented. In HCs from CB, the typical broad band associated with υOH (around 3300 cm^{-1}) and the sharp two peaks (2916 and 2848 cm^{-1}) associated with υCH are recognisable, which both appears in spectra of paper and tobacco; in addition, some contributions of CH vibrations (δ/ρ) are present in the range 1400 – 1300 cm^{-1}. In contrast, the sharp peak at 1733

cm^{-1} (υC=O), 1211 cm^{-1} (υCO), and 1364 cm^{-1} in the spectrum of the filter as acetyl groups (Belzagui et al., 2021), related to ester, disappears in the HCs spectra, while a peak at 1683 cm^{-1}, possibly due to the C=C stretching, appears. The sharp peak attributed to C-O stretching at 1027 is still present in HC, but less sharp. The δNH is evidenced at 1600 cm^{-1} in both HCs coming from the tobacco spectrum. Overall, the two HCs spectra reports the same shape with no relevant modification due to the HTC conditions. Likewise, the sample treated for 3 h (CB_220_3) reported an overlapping spectrum to the other samples (spectrum reported in Supplementary materials).
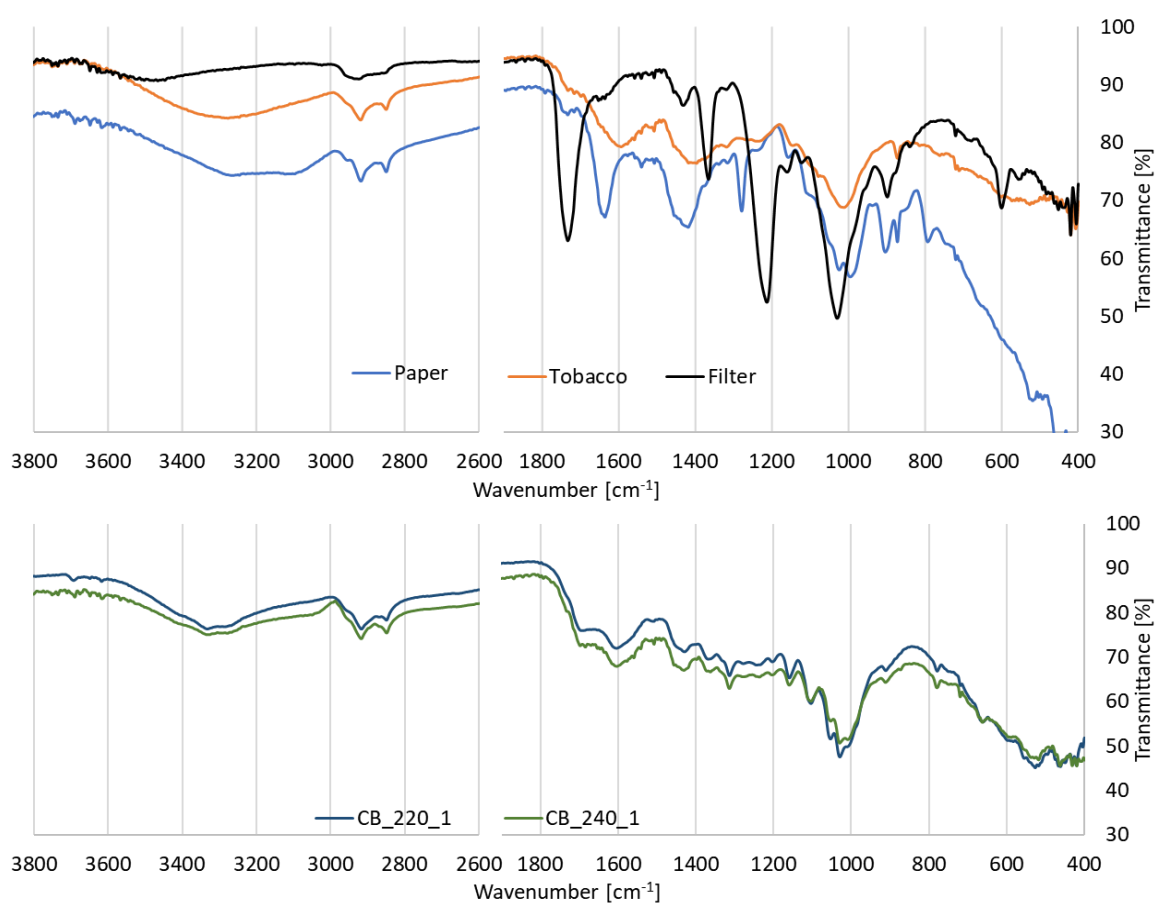
Figure 6.6 – FTIR spectra of CB components and hydrochars produced at 220 and 240 °C for 1h.
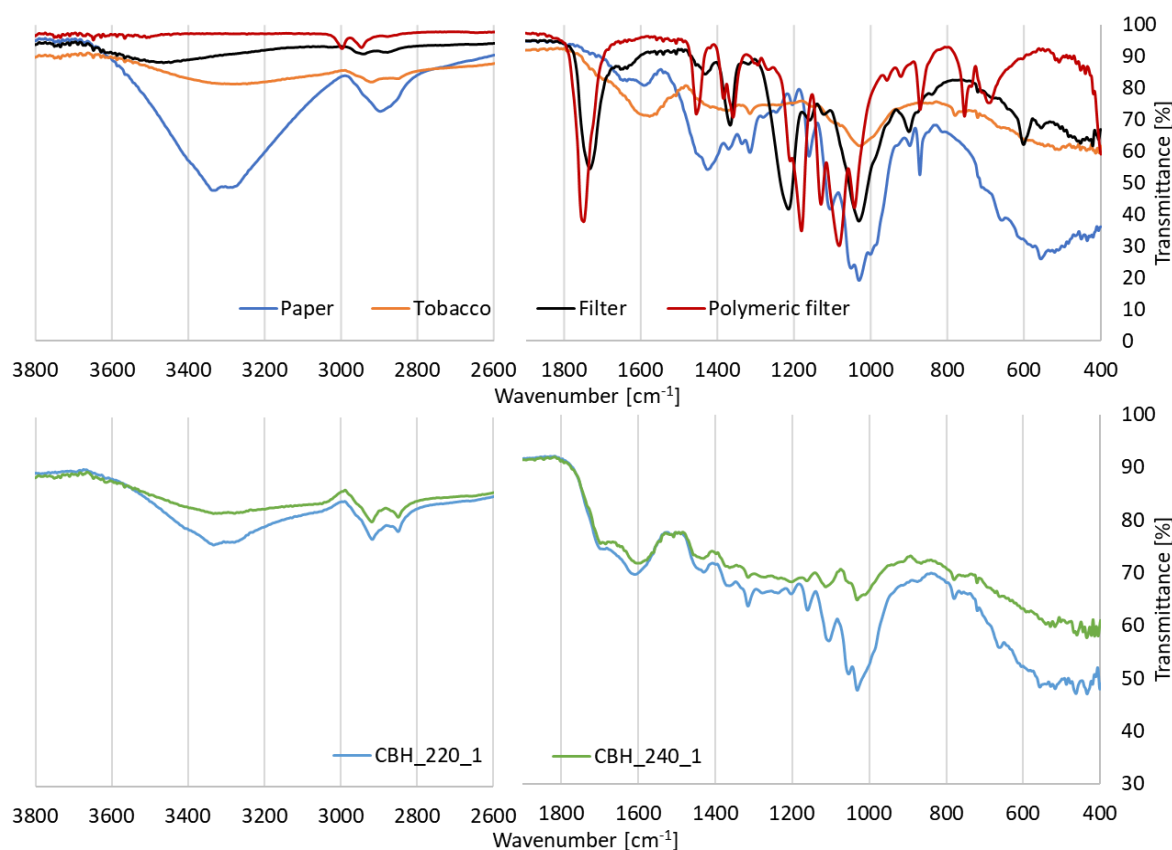
Figure 6.7 – FTIR spectra of CBH components and hydrochars produced at 220 and 240 °C for 1h.

Despite the presence of an additional material (polymeric filter) in CBH, that added new chemical components, the spectra of the HCs from CBH seem to report similar results of HCs from CB. CBH_240_1 shows the presence of all the peaks reported in the peak of CBH_220_1, but with a less intensity. Moreover, the HC deriving from the mix of CB and CBH (CBM) presented a spectrum totally similar to CB and CBH. These results could give important indications for the process set-up, more specifically in terms of operating conditions. By increasing temperature and holding time, the produced hydrochar did not relevantly change neither its composition nor its surface chemical characteristics, as shown by FTIR spectra. Therefore, there is no need to apply more energy-intensive conditions. A low temperature (220 °C or even less) may be sufficient to obtain similar materials and, therefore, recover/save more energy.

Figure 6.8 represents the comparison between the values of higher calorific value related to the two feedstocks and the respective HC under the different operating conditions; the evaluation is important for the possibility of using HC for energy recovery as solid fuel.
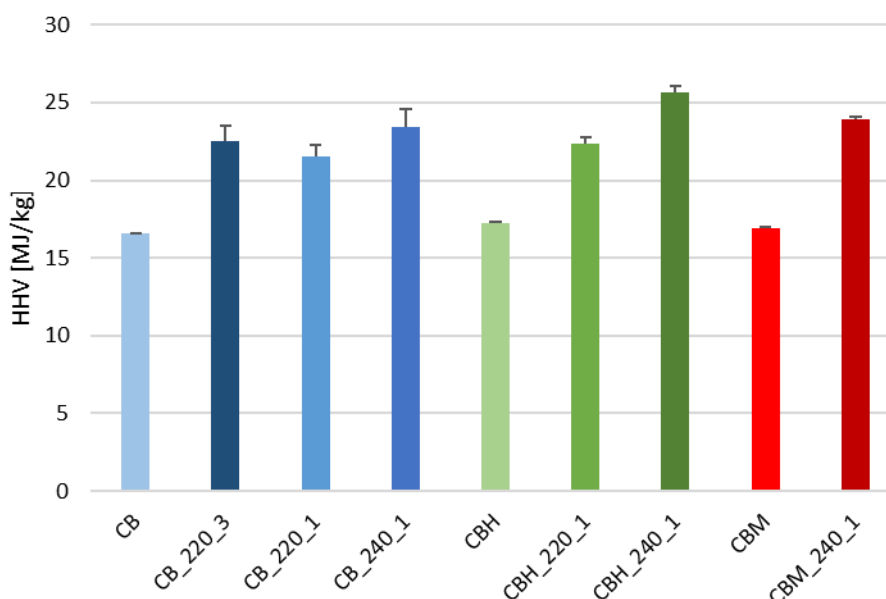
Figure 6.8 – HHV comparison between feedstocks and related HCs under the different operating conditions.

The graph shows a relevant increase in HHV for all types of HC, with good results also for the sample obtained from the mix of butts; this could suggest not only their intended use as fuels but would release from the need to differentiate the different kinds of butts.

6.5   Conclusions

The cigarette butt sums up some of the worst features which can be found in waste, i.e., futility and dangerousness of consumption. Its widespread production and consumption, the presence of toxic substances, the frequent abandonment, that is often uncontrollable and cause of risks for the environment, the difficulty in separate collection or removal from the environment, as a result of abandonment, and in valorisation due to the heterogeneous composition are only a few of the issues related to cigarette butts.

The most obvious solution is to stop cigarette production or be educated smokers; however, 10% of the global population smokes and has an addiction caused by tobacco products. The disappearance of old and rooted habits and customs is challenging to eradicate. The experience of recent years has shown that in several countries, the reduction in the number of smokers caused by the enactment of prohibitions and awareness-raising campaigns has been followed by a new increase, especially among the youngest (Torkashvand et al., 2020). The adoption of new smoking methods such as electronic cigarettes has yet to pass many health and other important requirements. Therefore, butts will continue to be an environmental problem for a long time.

This work aimed to investigate the application of the hydrothermal carbonization process as a technical solution in the treatment of cigarette butts that allows limiting the risks for the environment and health and, at the same time, to valorise this waste.

The activity carried out was consistent with these intentions, having provided interesting results in view of a conversion of butts into a solid fuel.

A step toward the circular economy approach would be to recycle the acetate from the filters to produce containers and the production of hydrochar from cigarette butts and its use as a soil improver in tobacco cultivation by the same companies that grow tobacco.

In all HCs there was an increase in carbon concentration and a substantial decrease in H/C and O/C ratios. Moreover, the higher heating values of HCs were higher than the respective feedstocks. In these terms, there is an improvement in the characteristics of the final product, in light of the objectives of butts valorisation as solid fuel.

Density analyses, especially for CB and its HCs, also provided good results. In fact, an increase in density results in a reduction in volumes, both for the transport phase and in the case that the waste continues to be managed as non-recyclable waste and, therefore, partly landfilled, with a reduction in transport/disposal costs.

In conclusion, the preliminary results obtained during the experimental work are encouraging to state that HTC can be considered for a beneficial valorisation of cigarette butts. It is necessary to continue the investigation to shed light in particular on the nature of the newly formed organic compounds (e.g., aromatics) and their effect in the environment, on the need to provide for a treatment of the process water (results and discussion in Chapter 8), and on the combustion behaviour of hydrochars.

Chapter 7

Valorization of PPE waste produced during COVID-19 pandemic through Hydrothermal Carbonization (HTC): a preliminary study

This chapter is the result of the preliminary study conducted on the HTC of personal protective equipment (PPE) such as masks and gloves deriving by the ongoing COVID19 pandemic, suggesting HTC as a suitable treatment for their safe handling and sustainable management. This work was realised in collaboration with the Biochar research group at the Leibniz Institute – ATB led by Dr Judy Libra in Potsdam (Germany) and Dr Kyoung Ro (USDA-ARS, Florence, SC - USA). In this chapter, the only results on masks are presented (pictures of gloves and related hydrochars can be found in Supplementary materials). A modified version of this work is under submission to international journal.
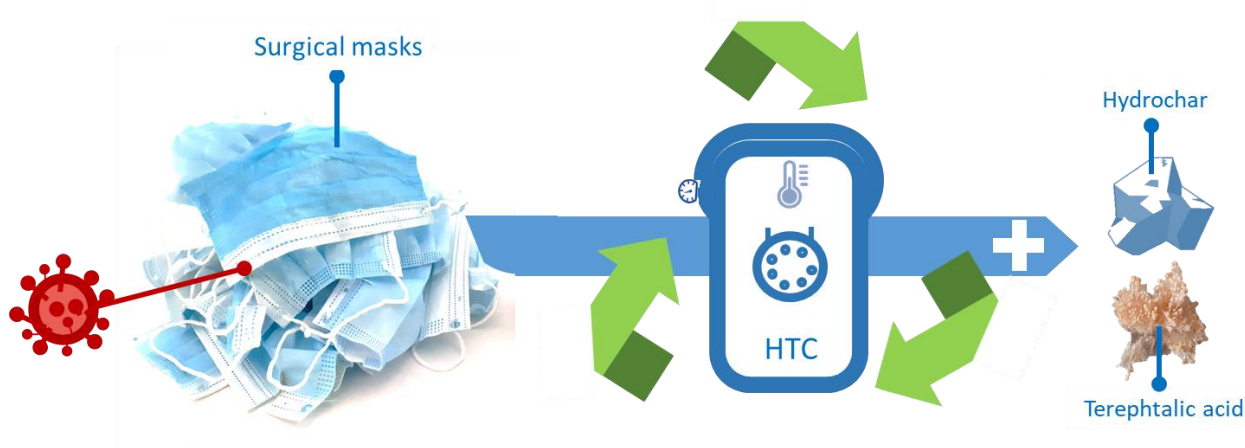
7.1   Abstract

Recently, the need to limit the spread of Covid-19 pandemic has required several measures of prevention and control among which is the use of face disposable masks. The sudden increase in waste mask production, together with the risk related to handling a potentially infectious material, entails challenging solutions for its correct management and disposal. In a circular economy context, a sustainable approach must be pursued with the aim of converting used masks and, more generally, plastic waste into useful end products. This works aims at a preliminary evaluation of hydrothermal carbonization as a potential method of surgical masks valorization through its conversion into a carbon enriched material, to be used, for instance, as solid fuel. HTC tests were carried out at T=220°C and a holding time of 3 hours, using acetic acid as catalyst, and the produced hydrochar was characterized in terms of mass and energy yield, elemental analysis, HHV, and physical-chemical and superficial properties by means of TGA, SEM, FTIR, and BET analyses. Under the applied conditions, masks formed a melt reduced in mass and volume. The produced hydrochar was characterized by carbon content and HHV higher than the original masks. When the experiment was carried out with acetic acid, a new crystal phase was produced, that was identified as terephthalic acid. The obtained results indicate that surgical masks, made of non-renewable and non-biodegradable polymers, could be treated through hydrothermal carbonization for achieving not only sanitization but also to produce a solid fuel or a raw material for terephthalic acid production, a precursor in surgical mask production.

7.2   Introduction

Since December 2019, the COVID-19 pandemic has significantly impacted various aspects of daily life. The rapid growth in infection in many countries has led to the introduction of numerous rules and restrictions aimed at protecting human health and life. Since transmission and spreading of the COVID-19 virus are mainly due to the droplets of saliva released by an infected person when coughs or sneezes (World Health Organization and the United Nations Children's Fund (UNICEF), 2020), it became essential to prevent the infections through the use of personal protective equipment (PPE), such as masks, surgical gloves, face shields, goggles, and gowns (Dharmaraj et al., 2021; Liang et al., 2021). Especially, face masks have become the first prevention measure used to fight the virus spreading worldwide and are, nowadays, everyday items, as well as phones, clothes, accessories, etc. (Yousef et al., 2021). Based on the filtration capacity and the sealing ability towards stopping

respiratory droplets to move through or around the device, different types of masks are available in the market. The Filtered Face Piece FFP2 type is a high-efficiency mask in terms of protection, wearability, and ease of breathing, specifically aimed at protecting the wearer. It is generally made of 5 layers of polypropylene (PP) and polyethylene (PE), an ear strap made of polyamide and a nose wire (generally steel made). However, due to the lower economic cost, the most widespread masks are the surgical type (3-ply type) characterized by good filtration capacity, hypoallergenic feature, cheaper price, and lower breathing resistance, mainly aimed at protecting other people from a potential transmission by the mask wearer (Crespo et al., 2021; Prata et al., 2020). They consist of three non-woven fabric layers mainly composed of polypropylene. Other plastic materials such as polystyrene, polycarbonate, polyethylene, or polyester are also applied to increase mask density. Wearing face masks has been demonstrated as a very effective and easy to implement system to cut down transmission routes, but their single-use nature results in the generation of massive amount of waste. Current estimation on the average use of disposable face masks by the global population indicates the need of 1097 billion masks per year, which corresponds to 8388 thousand tonnes of produced waste masks requiring proper management (Patrício Silva et al., 2021). The system applied so far to potentially infectious waste is incineration, mainly aimed at killing pathogens or, for areas not equipped with incineration plants, disposal in sanitary landfill after steaming and boiling at a high temperature (Dharmaraj et al., 2021; Fang et al., 2018). However, this amounts to a linear approach that is not anymore compatible with the sustainability and circular economy principles, aimed at combining the prevention of impacts with the recovery of high-value resources. At a global level, the progressive depletion of resources in a context of increasing demand requires identifying new approaches for waste valorization as a potential resource. This is particularly pertinent in the current COVID-19 pandemic where health and safety concerns pose new challenges in both resources supply and waste management. Therefore, a generalized, robust and flexible energy and resource recycling process able to deal with very large amounts of waste masks and more generally of polymer waste needs to be developed.

Plastics in general and specifically polypropylene, which represents 30% of the overall plastic production, are at present widely used and have become the primary support of the modern lifestyle due to their low cost of production and a wide range of relevant properties such as low density, durability and corrosion resistance. Plastic waste management is a major challenge to be faced due to the huge amounts produced together with its low degradability, which causes serious environmental problems. Plastic waste contains various polymers with low-density and high-density

materials such as polyethylene (PE), polypropylene (PP), polyethylene terephthalate (PET), polyvinyl chloride (PVC), polystyrene (PS), polycarbonate (PC) and more. A characteristic feature among them is a high content of volatile matter, high viscosity at low melting points and high energy density due to very low moisture and ash content. Several studies have been investigating the application of thermochemical treatments such as liquefaction or gasification at higher temperatures to convert plastic waste into fuels (e.g., gas and oil) with higher calorific values or carbon-enriched material (Brillard et al., 2021; Duangchan & Samart, 2008; Lee et al., 2022; Ro et al., 2014). Recently, the possibility to produce added value carbonaceous material by applying hydrothermal carbonization to plastic waste is gaining interest (Adolfsson et al., 2018). HTC is a thermochemical conversion process that can be used to obtain energy or new materials from organic matrices in presence of water under subcritical conditions. This technology aims to produce a carbon-rich product, called hydrochar, which allows for material and energy recovery through the use as solid fuel, adsorbent, soil amendment, pathogen removal and medical applications (Ducey et al., 2017). To date, HTC has been extensively applied on bio-based products, which, due to their high organic content and intrinsic humidity, possess optimal characteristics for the execution of the process, (Funke & Ziegler, 2010; Libra et al., 2011), while few studies have been carried out on synthetic polymers (Adolfsson et al., 2018; Shen, 2020). The process flexibility towards several organic matrices that can be used as feedstock, the possibility to guarantee the destruction of the genetic material (Ducey et al., 2017) and consequently the disinfection of the waste as well as the potential adoption in decentralized utilities make it worthy to consider it for the management of waste masks.

With these premises, this work focuses on the feasibility to turn single-use masks into added-value products through hydrothermal carbonization. The HTC process has been carried out in both catalyzed (through the addition of acetic acid) and non-catalyzed conditions, at a temperature of 220 °C and a duration of 3 hours. The final products have been characterized in terms of mass and energy yield, elemental analysis, HHV, and physical-chemical and superficial properties by means of TGA, SEM, FTIR and BET analyses.

To the best of our knowledge, the HTC process has never been applied so far to PPE; consequently, this work aims to provide a first and preliminary contribution in exploring the potential role of HTC on the suitable management of waste masks.

7.3 Materials and methods

Used 3-ply masks (Figure 7.1) were collected and sterilized in a bath of sodium hypochlorite (0.5%V/V) for safe handling. After a few days, masks were energetically washed with distilled water and dried in air. Subsequently, the metal parts that were designed to conform to the shape of the nose were removed. HTC tests were carried out on masks with a L/S (liquid-to-solid) ratio of 10 L/kg, at a temperature of 220 °C and a holding time of 3 hours. Experiments were carried out on the masks as a whole, considering both PPE layers and ropes. As a liquid medium, both distilled water and a distilled water solution containing 5%V/V of acetic acid glacial were used. All the tests were conducted in triplicate.

Figure 7.1 - Used mask collected for HTC tests

HTC process took place in a 1L stainless-steel pressurized and thermostated reactor (Berghof GmbH), according to the pre-set operating parameters. After making sure that the solid material was completely immersed in the medium, the reactor was sealed through the use of a PTFE gasket. Then, the system was heated from ambient temperature to 220 °C and held at this value for the desired holding time of 3 hours for each test. After the test, the electric heater was turned off, and the whole device was cooled to the room temperature spontaneously. As soon as the test apparatus reached room temperature, the exhaust valve was opened, and the process gas was removed. The liquid-solid material formed in the tests was subjected to further operations in order to separate the solid phase, i.e., the hydrochar, from the process water. The solid fraction was, at first, manually separated from the liquid using lab tong, and what could not be separated manually was filtered

using a pump and a cellulose nitrate filter with a pore size of 0.45 µm. The collected solids were thoroughly dried in a ventilated oven at 105 °C and then stored in plastic bags, while the liquid phase was collected in plastic bottles and stored at 4 °C for further characterization. HTC products were labelled with M and MA, depending on the acid absence or presence, respectively.

Process water and solid products deriving from HTC tests were chemically and physically characterized, which included analyses of macro-elements (C, H, N) and ash content, thermal analyses (TGA/DSC), density, and higher heating value (HHV). In addition, Fourier-transform infrared spectroscopy (FTIR), scanning electron microscope (SEM), and Brunauer–Emmett–Teller (BET) method, as a basis for the measurement of the specific surface area, were applied to the solid fraction. For the liquid phase, pH, electrical conductivity (EC), density, total carbon (TC), inorganic carbon (IC) and total organic carbon (TOC) were measured. Ultimate analysis for carbon, hydrogen, and nitrogen content was performed using a CHN analyzer (LECO 628). Oxygen concentration was determined by difference.

Thermal analysis was carried out by thermogravimetric analyzer together with differential scanning calorimeter (PerkinElmer STA 6000), estimating volatile matter, ash content, and fixed carbon according to the TGA results. The higher heating value was estimated with a calorimetric bomb (LECO AC500). H/C (hydrogen/carbon) and O/C (oxygen/carbon) atomic ratios of hydrochar and raw material were also determined. XRD analysis was carried out with a PXRD Diffractometer (Panalytical Xpert Pro), while Fourier-transform infrared spectroscopy (FTIR) with a Jasco FT-IR6300A spectrometer equipped with an ATR PRO ONE (diamond crystal) in the 4000-400 cm^{-1} spectral range (ris. 4.0 cm^{-1}, 50 scans). Finally, SEM analysis was carried out using a scanning electron microscope (SEM Ultra Plus, Carl Zeiss Microscopy GmbH, Germany). Gas sorption measurements were performed using the Autosorb iQ MP from Quantachrome Instruments. The nitrogen sorption measurements were performed at 77 K. The Brunauer–Emmett–Teller (BET) specific surface area was calculated from the adsorption data in the p/p0 range 0.05–0.17. Total pore volume was calculated at p/p0=0.875, while mean pore diameter was determined by applying both the density functional theory (DFT) model (assuming N_2 as the adsorptive gas, cylindrical pores, and a silica-based surface) on the isotherm adsorption branch, and the Barrett–Joyner–Halenda (BJH) model to the isotherm desorption branch.

The mass yield of solids during the HTC process was evaluated by carefully weighting the dried samples and subsequently performing mass and energy balances, according to Equation 7.1.

$$Mass\ Yield = \frac{Mass\ of\ hydrochar}{Mass\ of\ raw\ sample} \cdot 100\% \tag{7.1}$$

The energy yield was calculated based on the mass yield and the relationship between the higher heating value of the hydrochar and the higher heating value of the raw sample, according to Equation 7.2.

$$Energy\ Yield = Mass\ Yield \cdot \frac{HHV\ of\ hydrochar}{HHV\ of\ raw\ sample} \cdot 100\% \tag{7.2}$$

The analysis of the liquid fraction involved pH and electrical conductivity measurements with a benchtop meter (model HI 5521-01, Hanna Instruments S.R.L.), which was precisely calibrated before each reading. Total and inorganic carbon content, as well as TOC, were determined using a total organic carbon analyzer (TOC-V$_{CSN}$, Shimadzu Corporation).

7.4   Results and discussion

The hydrochars obtained during the tests conducted on masks without and with acetic acid are illustrated in Figures 7.2a-b, respectively. Under the applied conditions, a melt was formed, having a very different physical appearance from the source material. Besides, the hydrochars produced during the test with acetic acid (Figure 7.2b) possessed very different macroscopic characteristics from those produced without acid (Figure 7.2a), indicating that acetic acid could have acted as a catalyst during the HTC reactions and consequently led to more severe transformations of the original materials. M hydrochars were compact porous solids, whilst in MA hydrochars (Figure 7.2b), two different solid phases can be recognized: a porous solid and a crystal phase (as detailed in Figure 7.2c).

The solid mass yields were 92.13 and 96.95% for M and MA, respectively, which are fairly high values compared with those assessed for hydrochars deriving from biogenic materials (Libra et al., 2011). Results of elemental and ash analyses on masks and on the different materials produced after HTC are resumed in Table 7.1 and depicted in Figure 7.3. It can be highlighted that hydrothermal carbonization determined an increase in carbon and hydrogen content and a consequent decrease in oxygen concentration. The highest increase in carbon and hydrogen content was assessed for MA (8,14 and 10,73%, respectively). The ash content after HTC was reduced to very small percentages

compared to the original masks. The highest decrease in ash content was assessed for M (- 89,06 %).
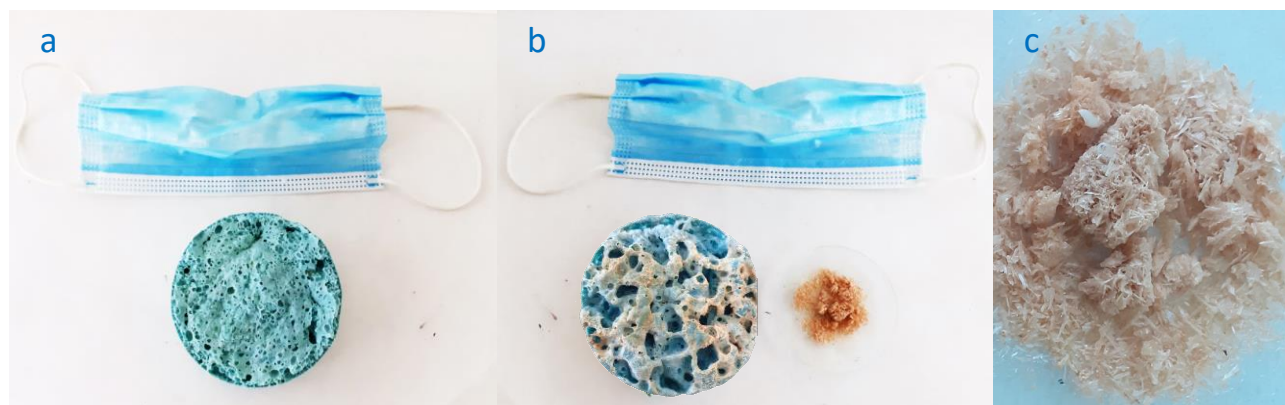
Figure 7.2 - Surgical mask and produced hydrochars: a) M, b) MA, and c) detail of MA crystals.

The assessed elemental changes after HTC, in particular a higher percentage of carbon and a lower percentage of oxygen, may be the result of dehydration and decarboxylation processes that typically occur during hydrothermal conversion treatments resulting in a hydrogen and oxygen removal from the solid matrix, in the form of H_2O and CO_2. The above-mentioned transformations can be visually described by the Van Krevelen diagram, in which the molar ratios of H/C and O/C of the feedstock and the HTC products are represented (Figure 7.4). In this diagram, the intensity of the carbonization process is shown by the distance at which the carbonization products are placed with respect to the source materials. Typically, during HTC experiments carried out on biomass, as the carbonization intensity increases, the H/C and O/C molar ratios of the hydrochars move from upper right to lower left (Poerschmann et al., 2014). In the case of masks, it seems that only the atomic ratio O/C is reduced, while the H/C is kept constant. However, both the original materials and HTC products are placed in the diagram in the typical fuel zone.

Table 7.1 - Elemental composition and ash content (%dry basis) along with atomic ratios H/C and O/C of the samples

Sample	Ash [%]	C [%]	H [%]	N [%]	O [%]	H/C [-]	O/C [-]
Masks	1.92 (0.04)	76.21 (0.89)	12.02 (0.53)	2.08 (0.20)	7.77 (1.22)	1.892	0.077
M	0.21 (0.02)	82.99 (1.14)	13.22 (0.35)	0.17 (0.03)	3.41 (1.47)	1.911	0.031
MA	0.59 (0.04)	82.41 (0.09)	13.31 (0.19)	0.17 (0.04)	3.68 (0.26)	1.938	0.032
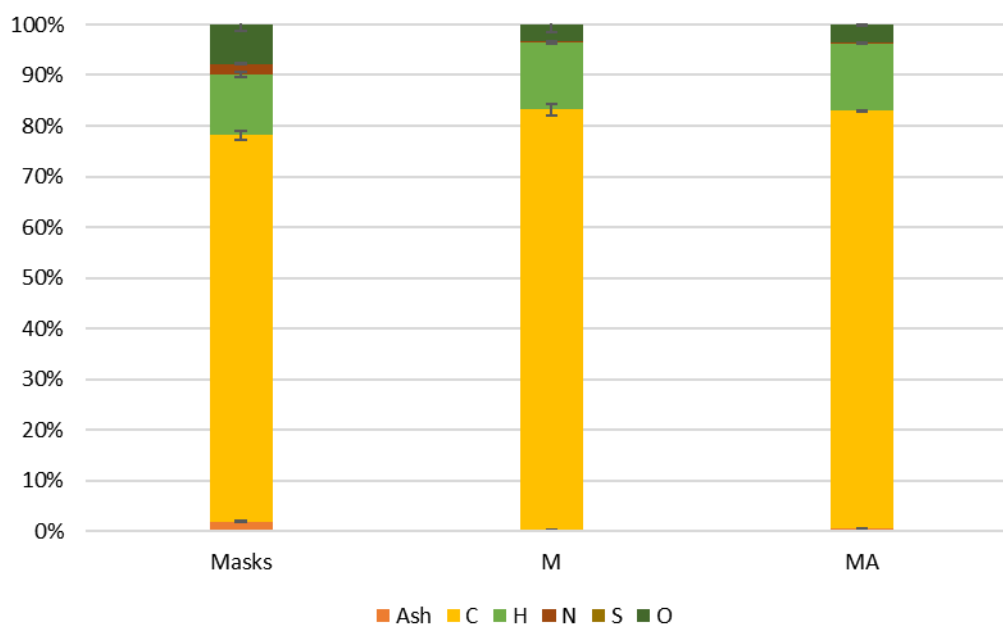
Figure 7.3 – HTC solid products and raw material composition – percentage values
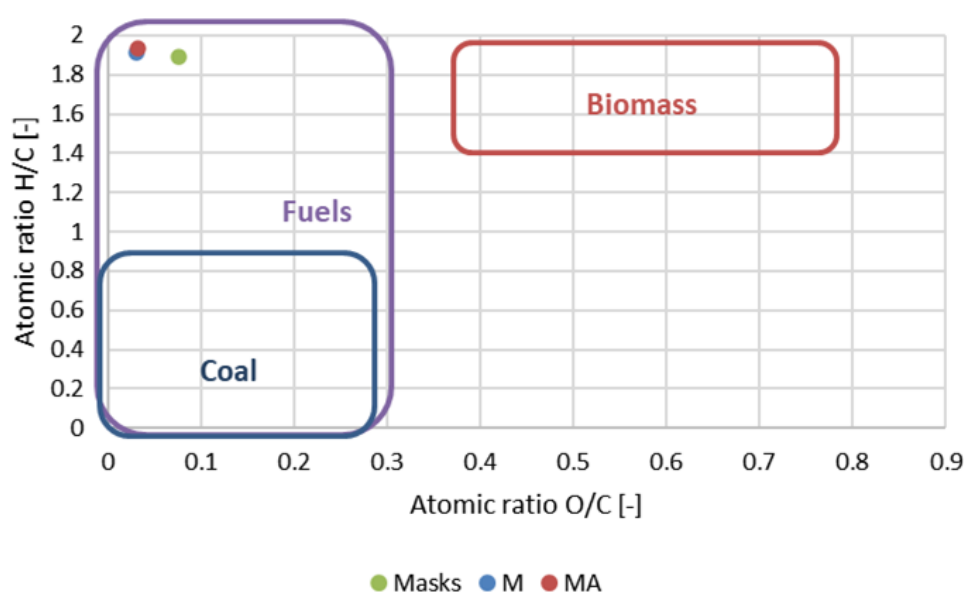
Figure 7.4 – Van Krevelen diagram for masks and HTC products

The HHV values assessed for masks and for the produced hydrochars are summarized in Table 7.2 and graphically illustrated in Figure 7.5. The heat of combustion possessed by masks is similar to that of diesel (44.80 MJ/kg) and Anthracite (32.50 MJ/kg), respectively (Linstrom, 1997). After HTC treatment, HHV increased by approximately 5% (5.03 and 5.13 % for M and MA, respectively). This is an interesting result in view of hydrochar valorization for energy recovery purposes. However, it should be noted that the energy yields obtainable with the combustion of the produced hydrochars

are similar to those from the original materials, due to the partial reduction of the mass during the HTC process (see Table 7.2, third column). In any case, although the measurement of the energy density on volumetric basis has not been the subject of this experimental work, it should also be noted that the HTC process typically produces a consistent volume reduction and thus a relevant increase in this parameter, which is again a positive aspect when assessing the feasibility of HTC process. In fact, the higher the energy density of the fuel, the more energy may be stored or transported for the same amount of volume.

Table 7.2 Energy properties of HTC products and raw materials – average values (n=3)

Sample	Average HHV [MJ/kg]	Energy yield [-]
Masks	43.12 (0.51)	-
M	45.29 (0.21)	0.97
MA	45.33 (0.17)	1.01
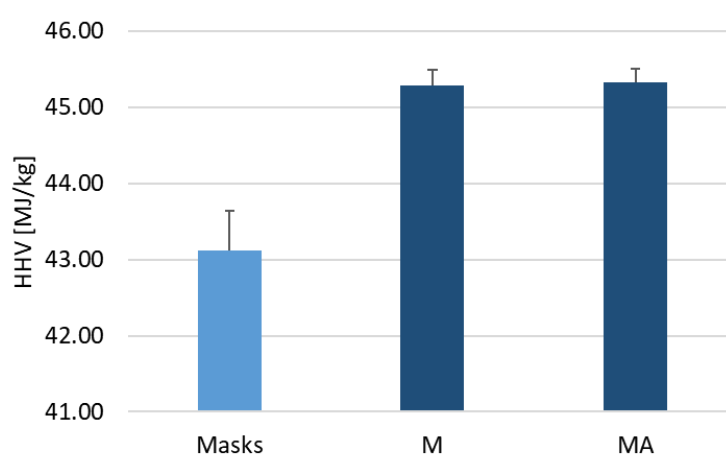
Figure 7.5 – Higher heating values of HTC products and raw material

With the aim of highlighting the transformations that occurred during the HTC process, the source materials and the produced hydrochars were subjected to additional analyses such as TGA, XRD, FTIR, SEM and BET.

Figure 7.6 illustrates the results from TGA carried out on masks and on the solid product obtained during HTC. All the results indicate that during the process, the chemical composition of masks was altered, originating new products that were not simply enriched in the carbon content or altered in terms of ash and oxygen content. For instance, by comparing the thermal decomposition curves of mask and that of M and MA hydrochars, different decomposition temperatures can be evidenced, which indicate that original polymers were altered and converted into new carbon materials.
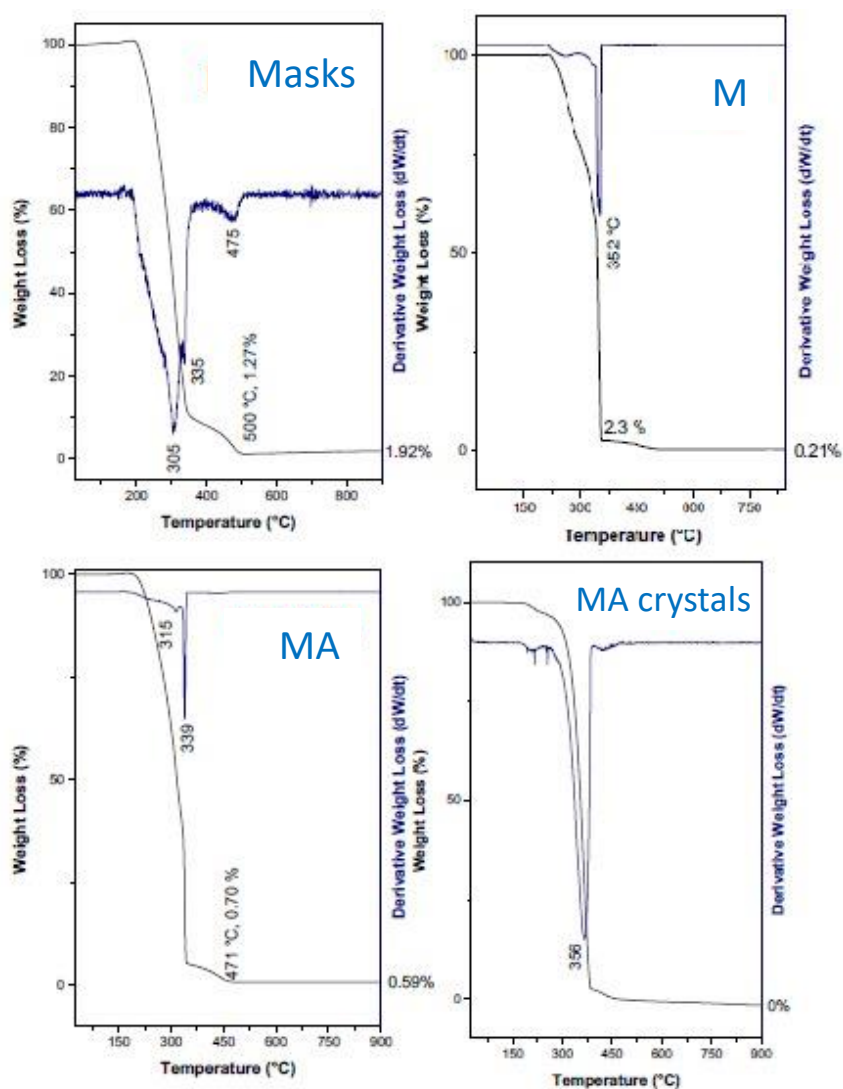
Figure 7.6 Thermogravimetric curves of surgical masks and their HTC products

XRD analysis was particularly useful in detecting the nature of crystals formed during MA test. In Figure 7.7, a comparison of the XRD patterns of M, MA, and crystals produced during MA test is represented. The MA spectrum indicates the presence of two different compounds: polypropylene and terephthalic acid. The spectrum of crystals obtained during MA test almost completely overlap with terephthalic acid spectrum. Based on these results, it can be deduced that the presence of acetic acid allowed a more radical transformation of the material and the production of a new compound that is the precursor of polyethylene or polypropylene in the manufacturing process of the masks (van Leeuwen, 2003; Zhou et al., 2006).
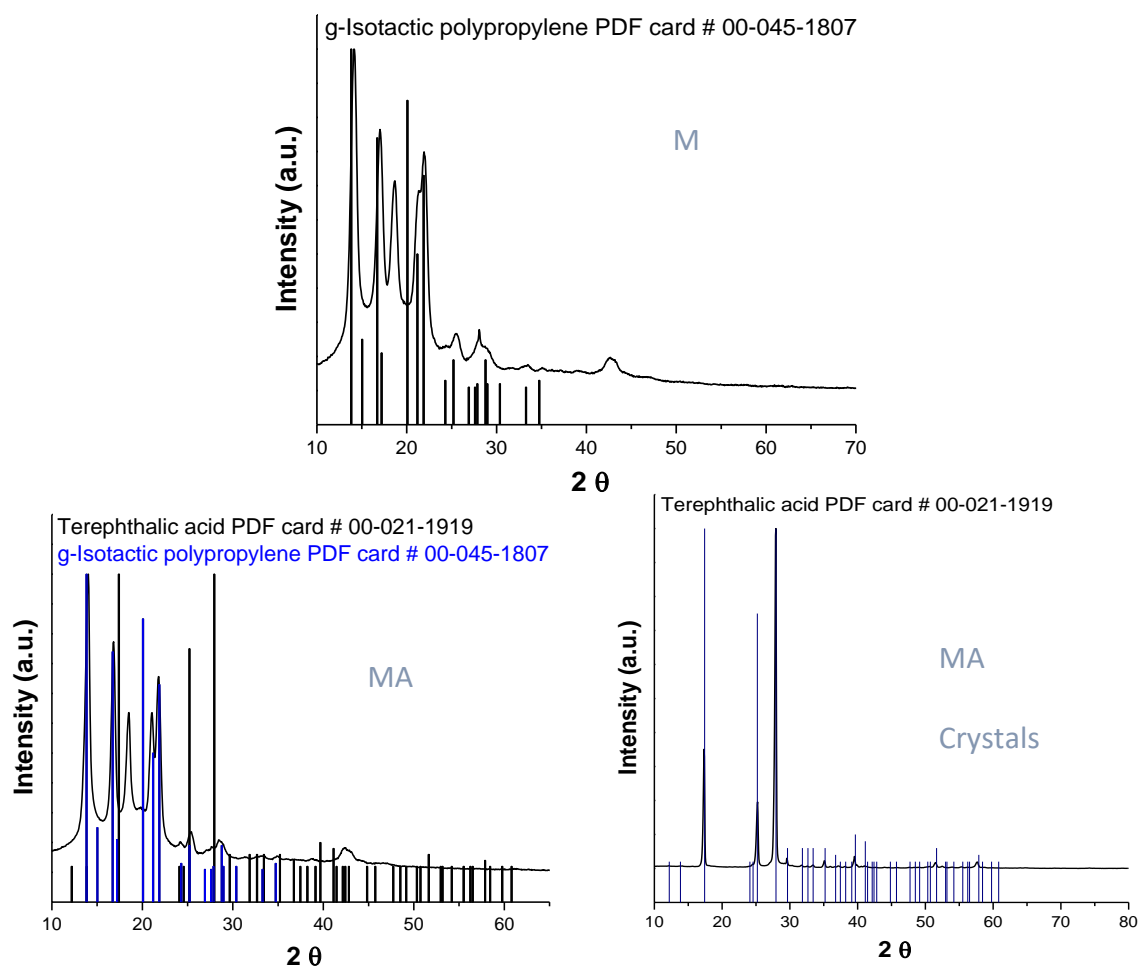
Figure 7.7 – XRD spectrum of M and MA hydrochar and crystals produced during MA HTC test

Figures 7.8 and 7.9 illustrate the results of FTIR analyses on masks and their HTC products. The area between 1800 and 2400 cm^{-1} is not considered because it is influenced by background noise. More specifically, Figure 7.8 shows a comparison between masks and polypropylene (PP), indicating a good similarity between the two spectra. In Figure 7.9, a comparison is made between masks and the M and MA hydrochars. As a result of HTC, the spectrum of the source material is partially modified since new peaks are formed, and some others disappear. In detail, the broad bend at around 3400 cm^{-1}, generally associated with OH stretching, is reduced in the spectra of HCs and in PP. The peaks related to CH groups vibrations are present in all spectra as sharp peaks (around 2951-2853 cm^{-1}, 1457 and 1375 cm^{-1}, and 999, 971, and 841 cm^{-1}) (Krylova & Dukštienė, 2013), while the peak associable to C=O at 1736 cm^{-1} is evident in the mask and PP spectra while in HC spectra disappears and a new peak on the right (1682 cm^{-1}), possibly related to C=C, appears. Finally, the peak at 1165 cm^{-1} may be related to C-O (Stuart, 2004).
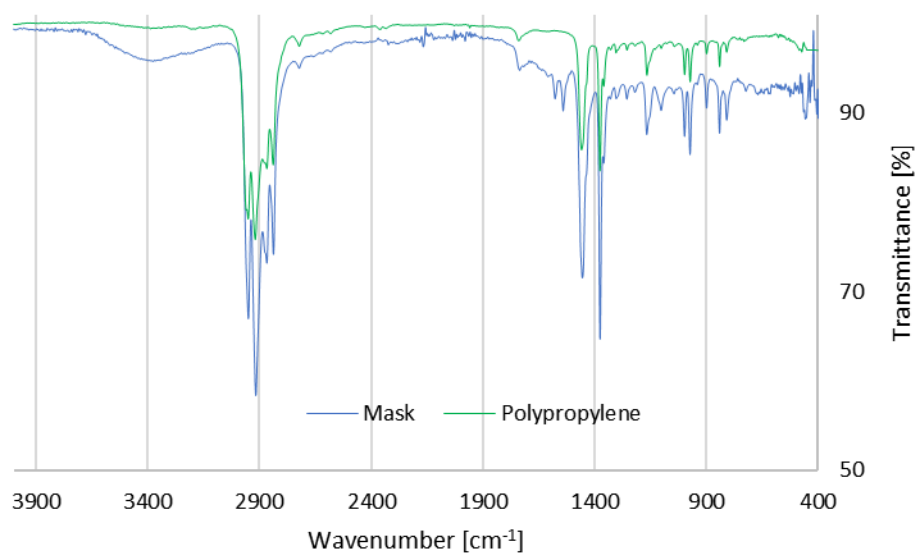
Figure 7.8 – FTIR spectra of surgical mask and co-polymer propylene-ethylene
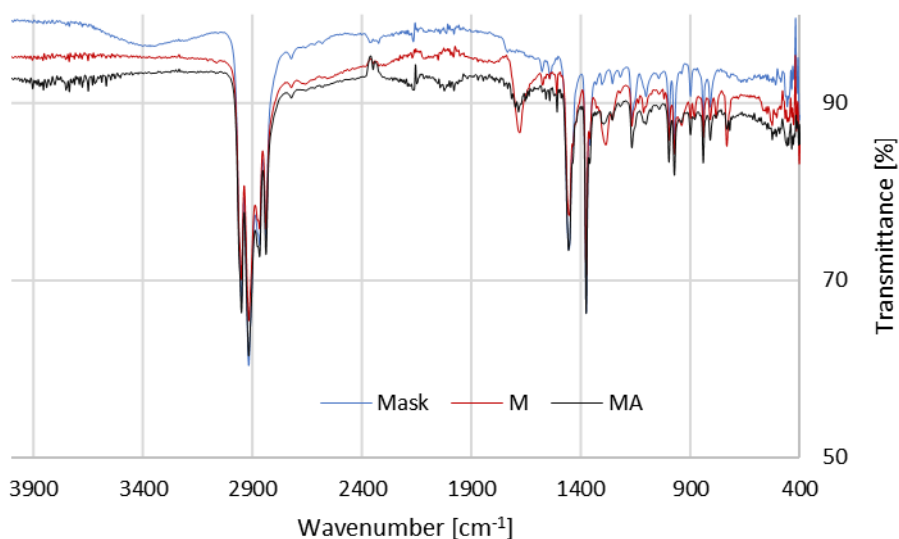
Figure 7.9 – FTIR spectra of surgical mask and HTC solid products

SEM analysis evidenced a radical transformation of the physical structure of masks following the HTC process. The fibers of non-woven fabric recognizable in masks (Figure 7.10a) were destroyed during the process, both in the absence and presence of acetic acid (Figure 7.10b and 7.10c). Figure 7.10d shows crystals of terephthalic acid formed in presence of acetic acid.

The specific surface area and the pore size distribution of the produced hydrochars were finally determined through the BET method. M and MA hydrochar were characterized by a superficial area of 37.7 and 24.5 m^2/g and a micro-mesoporous volume of 0.03 and 0.02 cm^3/g, respectively. Overall, the chemical structure of surgical masks was significantly changed.
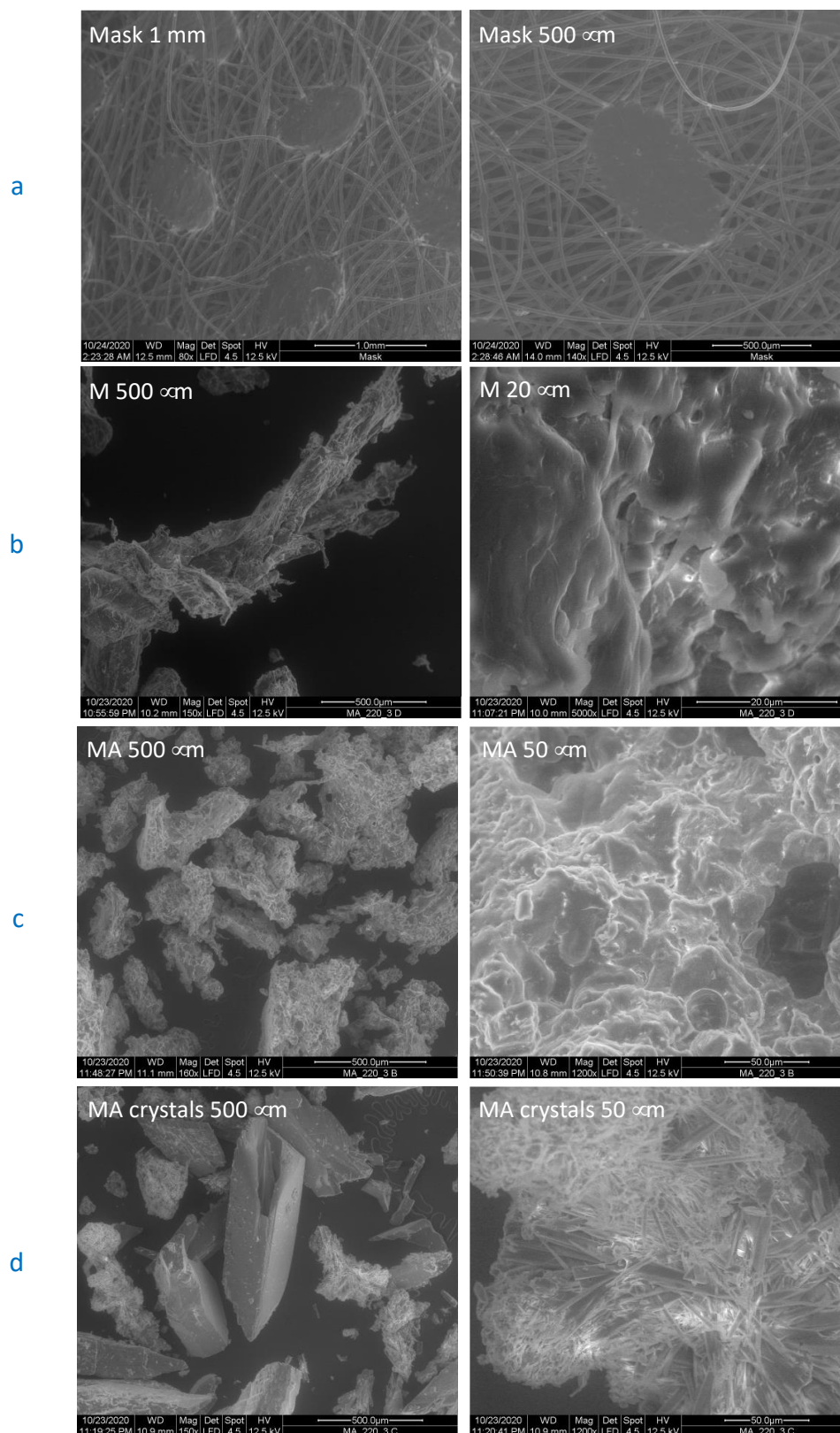
Figure 7.10 – SEM imaging of a) surgical mask and HTC solid product: b) M hydrochar, c) MA hydrochar and d) MA crystals.

Finally, Table 7.3 resumes the results of analyses performed on the liquid phase obtained after HTC tests. The final pH was lower after HTC test carried out in presence of acetic acid. TOC values were strongly influenced by the addition of acetic acid. A quantity of 5% corresponds to an initial TOC in the liquid phase of 20 g/L. The obtained TOC after HTC test indicate that acetic acid favoured the dissolution of the organic compound from the solid matrices.

Table 7.3 – Liquid phase characterization – pH, electrical conductivity and carbon content in the process water

Sample	pH	Electrical Conductivity [mS/cm]	TOC [g/L]	TC [g/L]	IC [g/L]
M	3.82	0.51	2.65	2.67	0.02
MA	2.70	1.28	26.59	26.75	0.17

7.5 Conclusions

Hydrothermal carbonization of waste materials has great potential to become an environmentally friendly conversion process to produce a wide range of products. HTC has several advantageous properties compared to other hydrothermal conversion technologies which make it interesting for decentralized applications and for waste streams with poor fuel characteristics such as low calorific value, high moisture content and heterogeneity. Moreover, hydrothermal carbonization working conditions ensure full disinfection, which is very useful when this process is carried out on residues potentially contaminated by viruses or pathogens. While biogenic waste is at present largely investigated, HTC of plastic waste for hydrochar production is still in the early stages of development and therefore there are many aspects requiring additional research.

This work has been aimed at preliminary assessing the feasibility of HTC as a treatment or pre-treatment system for disposable face masks, capable of enhancing this type of residue and guaranteeing their safe management. This objective represents a step toward the implementation of a modern approach to waste management, especially in terms of sustainability but also in line with the cardinal principle of proximity. In fact, HTC could associate wide technical-economic flexibility of application with delocalization of the treatment, allowing for effective action of recovery of materials.

To the best of our knowledge, this experimental work represents the first attempt to apply HTC process to surgical masks.

The conducted experiments showed that masks can be transformed into new products possessing very different characteristics in terms of both physical appearance and chemical structure and

composition, especially when acetic acid was used as a catalyst. The produced hydrochar is enriched in carbon content and possess a higher HHV, which are positive aspects in carbon sequestration and for reducing GHG emissions. When the experiments on mask were carried out with acetic acid, a crystal phase was produced, that was identified as terephthalic acid. These characteristics suggest the potential use of hydrochars as fuel or as a raw material for terephthalic acid production, a precursor in surgical mask production.

Further investigations are needed to assess the influence of operating conditions on the quality of the final products and on the potential uses of the produced hydrochar, as well as the eventual co-treatment of organic waste of different origins, therefore envisaging wider applications that include several categories of synthetic waste currently considered problematic (for example waste from the recycling phases of plastic packaging), but also plastic waste and biomass whose co-treatment based on pyrolysis gave already promising results.

Chapter 8

Process waters characterisation for their valorisation and suitable treatment

In this chapter, the results of the characterisation campaign carried out on the process water from HTC tests on the different feedstocks, partially presented in the previous chapters, are compared and discussed. This chapter aims to investigate the liquid HTC product to propose feasible enhancement/treatment options such as extraction of chemicals, using on soil (fertigation), energy production (anaerobic digestion via BMP tests), and aerobic treatment.

Fertigation   Biomethane   Chemicals   Traeatment
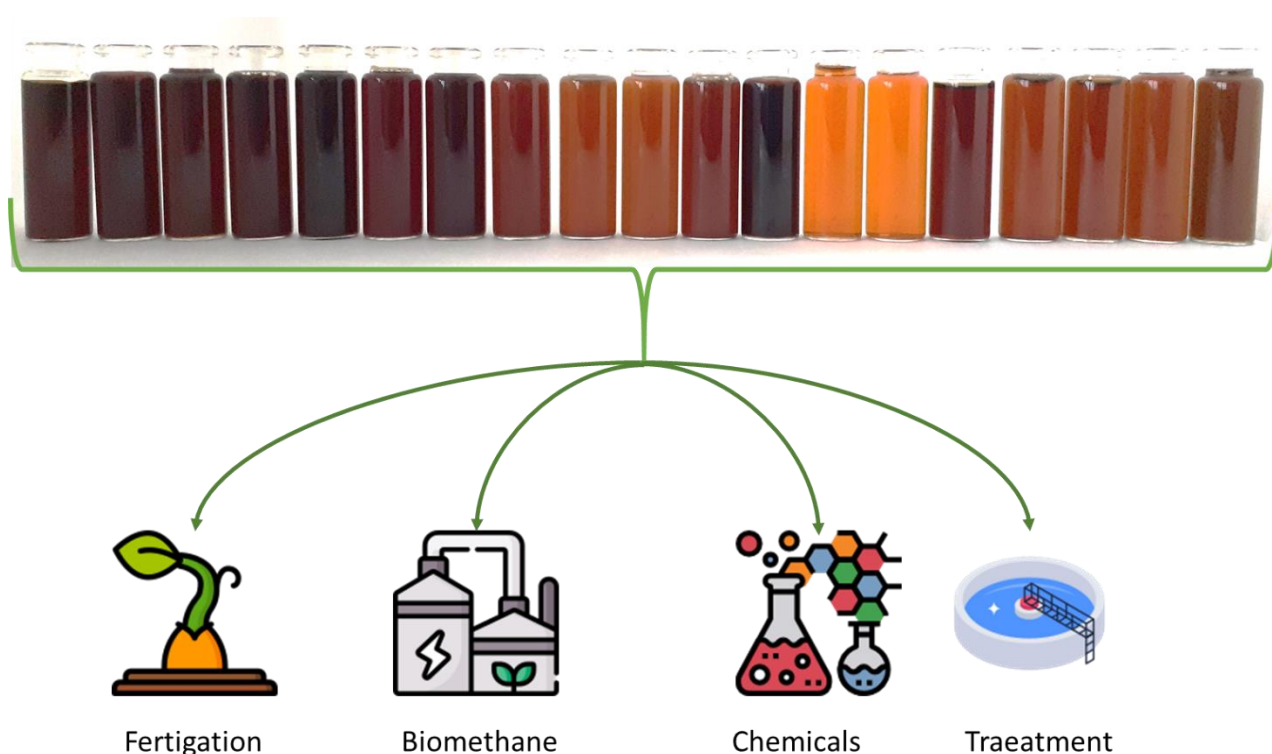
8.1   Abstract

To date, scientific works focused on the solid hydrothermal carbonization product, often not considering the liquid by-product. However, due to its nature and the high organic load, it is raising interest increasingly. Around 90% of the total output mass from HTC treatment is process water, and it possibly can cause environmental issues when improperly handled. In this work, process waters from several HTC treatments were considered. PWs were characterised and tested for different applications. Nutrient content was established, and germination tests were conducted to assess their feasibility in fertigation. In addition, acute toxicity tests were carried out on nitrifying bacteria to investigate their aerobic treatability, and biomethane potential tests were performed to exploit their energetic content. Germination tests and acute toxicity tests result in high inhibition tests on living organisms (seeds/seedlings and aerobic bacteria), justified by the high content of organic compounds such as phenols (up to 2g/L) or acetic acid (2-30 g/L). In contrast, tests on anaerobic sludge showed no relevant inhibition, producing almost up to 200 mlCH$_4$/gCOD and suggesting anaerobic treatment as a suitable option for process water. The phosphorus contents do not indicate a convenient recovery; however, potassium concentrations were found relatively high in all samples suggesting a possible recovery process. In general, tests confirmed the need for process water to be treated.

8.2   Introduction

Hydrothermal carbonization is a wet process used to convert organic residues into a carbonaceous material (hydrochar) with high added value. In recent years, the interest in this technology has considerably grown thanks to some aspects that characterise it and are particularly advantageous in waste management and valorisation issues. The possibility of operating in the presence of water, for example, allows avoiding drying treatments, expensive from an energy point of view, which are, instead, strictly necessary in other types of thermochemical processes. This technology is also very flexible, as it can operate on different types of organic matrices and may be integrated with other treatment processes.

The process takes place under controlled conditions of temperature and pressure. The water is kept in subcritical conditions and acts both as a solvent and catalyst, promoting a series of reactions such as hydrolysis, condensation, decarboxylation, and dehydration. The amount of water used in the process is usually very high, up to 90% of the total input mass, involving process water (PW) production that must be carefully considered for its correct management and enhancement.

So far, most of the research has focused on the properties of the resulting solid product and its different possible valorisation options (Maniscalco et al., 2020; Tasca et al., 2019). On the other hand, studies concerning process water are currently less numerous. To develop the HTC process on an industrial scale, it is necessary to identify adequate technologies for the disposal and recovery of this by-product. The characteristics of the process water could suggest both the reuse within the same HTC process (recirculation) and an external valorisation for the recovery of additional materials and/or energy.

Among the few studies available, Langone and Basso (2020) research has been oriented to the characterisation of process water to obtain chemicals, fuels, energy, as well as other valuable products for the local economy. The study published by Owsianiak et al. (2016), conducted through a Life Cycle Assessment (LCA), showed that there are still significant uncertainties both about the composition of process water and its potential exploitation.

In this context, the objective of this work was to characterise the process waters deriving from the hydrothermal carbonization of various feedstocks: spent coffee grounds, hemp, hemp digestate, digestate from agro-industrial residues, cigarette butts and HEETS butts, and grape marc, for their valorisation or treatment. In this regard, the possibility of recovery of nutrients and chemicals such as phosphorus, potassium, and VFA (e.g., acetic acid) was evaluated. Germination tests were also conducted to evaluate the potential use of PW as fertiliser (results showed in Chapter 5) and biochemical methane potential (BMP) tests to verify the feasibility of energy generation. Finally, acute toxicity tests were carried out to assess the suitability of the process water for aerobic biological treatment.

8.2.1   Process water background

During the HTC process, reactions on solid feedstocks result in mass transfer in the liquid phase. The composition of the process water depends on the incoming feedstock and the operating conditions of the HTC process, mainly temperature, holding time, and solid-to-liquid ratio (S/L). The PW management must be evaluated according to its quality; therefore, a proper characterisation is necessary. In general, process waters contain high concentrations of organic matter as indicated by the values of soluble COD (Chemical Oxygen Demand), TOC (Total Organic Carbon), BOD_5 (Biochemical Oxygen Demand), and the relative richness of nutrients (N, P, K). Suspended solids in PW was found to be between 25%wt and 55%wt in the case of anaerobically digested and dehydrated sewage sludge (ADSS) by He et al. (2015) and 17%wt and 30%wt in the treatment of

agro-industrial digestate by Ekpo et al. (2016), passing from 170 to 250 °C. In contrast, Mäkelä et al. (2018) reported that the suspended solids in process water tends to decrease at higher reaction temperature in the treatment of wastewater from pulp and board production, showing the different properties due to the feedstock.

The pH of HTC process water from wet feedstock is usually around 4.5 or lower, except in ADSS treatment, where the pH is generally alkaline, mainly due to the digestate high buffering capacity (Berge et al., 2011). In addition, Aragón-Briceño et al. (2017) showed that the pH of the PWs obtained by HTC of ADSS can be affected by the S/L, increasing with higher solid load, and the temperature of the HTC process due to the presence of several substances such as nitrogen-derived compounds, and volatile fatty acids (VFAs), generated during hydrothermal treatment (Langone & Basso, 2020; Qiao et al., 2011). Higher pH values (9.15 and 8.08) were reported by Aragón-Briceño et al. (2017)at lower HTC temperatures (160 °C and 250 °C).

Typically, the process water is dark (yellowish to dark brownish). In the treatment of urban sewage sludge, Xu and Jiang (2017) proposed to use the PW colour as an index to predict the amount of dissolved organic compounds and to evaluate the purification of PW. They, as well as He et al. (2015), observed that, raising the temperature from 180 to 300 °C, PW becomes lighter (yellowish) from dark (brown), while the TOC content decreases.

As reported by several authors (Berge et al., 2011; Libra et al., 2011), several organic compounds are formed in the PW as a result of the degradation of the feedstock. According to Berge et al. (2011), up to 30% of the initial carbon present in the input material can be dissolved in PW. For example, Oliveira et al. (2013) found the 17% of the input carbon in PW from agro-industrial digestate. Process water is generally characterised by high TOC values (Stemann et al., 2013). Oliveira et al. (2013), analysing process water from agro-industrial digestate and in combination with other biomass (e.g., corn silage and poultry manure), found TOC values in the range of 13 – 26 g/L. VFAs concentrations in PW also increases with temperature and solid load. Aragón-Briceño et al. (2017) reported total VFA concentrations of 191, 406, and 715 mgCOD/L for treatments at 160 °C, 220 °C, and 250 °C, respectively, and 909 to 4606 mgCOD/L increasing the solid load from 2.5 to 30%. As a hydrolysis product, acetic acid is the main constituent of VFAs produced in the treatments, which finds a wide range of applications in industry and biochemistry if recovered (Berge et al., 2011). In addition, the HTC releases proteins and carbohydrates into the PW; however, the release is higher at lower temperature (160 °C) and decrease at 240 °C, as observed in the treatment of anaerobic granular sludge (AGS) and municipal ADSS by Yu et al. (2018, 2017). Also, PWs are often

characterised by a relatively high content of nutrients, such as nitrogen, potassium, and phosphorus (Langone & Basso, 2020), and their presence and concentration depend on the initial composition of the feedstock and the process conditions (Alhnidi et al., 2020). Depending on the feedstock, different temperatures influence the distribution of nitrogen in by-products. In digestate, around 60% of input N is released in PW and the rest (40%) remained in the solid phase (He et al., 2013). Some studies showed that the release of N in PW increases significantly by increasing the HTC process temperature (Kruse et al., 2016; Yu et al., 2018), which is essential when the hydrochar is used as a fuel, as NOx emissions are reduced. In contrast, the majority of phosphorus (up to 60-70%) is retained in the hydrochar (C. I. Aragón-Briceño et al., 2020). As reported by Shi et al. (2014), minimal amounts of P, Ca, Fe, Al, and Mn are released into the PW, while most of them accumulated in the hydrochar, with higher effect with temperature. Solubilisation into PW and immobilisation in the hydrochar also depend on the process conditions and on the type of feedstock (Ekpo et al., 2016). Heavy metals are mostly concentrated in hydrochar, even though a small quantities can be detected in PW, representing a potential environmental problem (Huang & Yuan, 2016; Langone & Basso, 2020). Zhai et al. (2016) pointed out that pH plays a significant role in the distribution of heavy metals. Alkaline and acidic condition showed opposite effect. In general, alkaline environment tends to stabilised heavy metals in hydrochar, as supported by He et al. (2015) in their study on the addition of CaO in HTC. Shi et al. (2013) showed that the presence of heavy metals in PW is also influenced by temperature; the higher the temperature, the higher the concentration of heavy metals. Moreover, the strong presence of potentially toxic organic compounds in PW is released from the solid feedstock or formed during HTC, e.g., 5-hydroxymethylfurfural (HMF), phenol, cresol, and catechol (Langone & Basso, 2020) may cause environmental and health problems. However, it can be seen as a resource as well, considering the high commercial value of these kind of chemicals.

8.3   Materials and methods

8.3.1   Process water production

The PWs used in this work derive from HTC tests performed on several feedstocks, including:
- spent coffee grounds, Lavazza Top class brand;
- hemp and hemp digestate;
- digestate from agro-industrial residues;
- HEETS cigarettes butts for IQOS;
- cigarette butts;
- Cannonau grape marc, and the residue grape marc after ethanol-solution extraction.

As stated in the previous chapters, the HTC tests were conducted in a pressurised reactor (1.5 L) equipped with a heating jacket and a controller. After each test, the carbonized material was separated into the solid and the liquid phase through a filter press. The process water was vacuum-filtered at 0.45 μm and stored at 4 °C in plastic bottles. Each HTC test was performed three times, and the PW of the replicates were mixed to obtain a composite sample. Table 8.1 reports the HTC tests conditions, the feedstocks and the code of each sample used in this work.

Table 8.1 - Summary of HTC tests: feedstocks, operating conditions, and derived samples.

Feedstock	Temperature [°C]	Holding time [h]	Sample code
Spent coffee grounds	220	1	SCG_220_1
	240	1	SCG_240_1
Hemp	180	1	H_180_1
	180	3	H_180_3
	200	1	H_200_1
	220	1	H_220_1
Hemp digestate	180	1	D_180_1
	180	3	D_180_3
	180	6	D_180_6
	200	1	D_200_1
	200	3	D_200_3
	200	6	D_200_6
	220	1	D_220_1
Digestate from agro-industrial residues	220	1	DMIX_220_1
HEETS cigarette butts	220	1	CBH_220_1
	240	1	CBH_240_1
Cigarettes butts	220	1	CB_220_1
	240	1	CB_240_1
Cigarettes and HEETS butts	240	1	CBM_240_1
Grape marc	220	1	GM_220_1
Grape marc extracted	220	1	GM_Ext_220_1

8.3.2 Process water characterisation and valorisation

The characterisation of PW included several measurements such as density, pH and electrical conductivity (EC), total organic carbon (TOC) and chemical oxygen demand (COD) content, anions concentration such as chlorides, nitrates, nitrates, and sulphates presence, volatile fatty acids, macronutrients (P, K, and Ca), organic compounds (e.g., total phenols), and metals (i.e., Fe, Al, As, Zn, Pb, Cd, and Cu). In addition, tests conducted on nitrifying bacteria were used to assess the toxicity of the PWs to define their feasible treatability in traditional wastewater treatment plants.

Also, the energy content of the PW was assessed through biochemical methane potential (BMP) tests to verify their feasibility as a substrate for anaerobic digestion (AD) to be converted in biogas. Density was evaluated using a standard glass float gauge densitometer, pH and EC were measured using a benchtop meter (HI5521, Hanna Instruments), while TOC through TOC a catalytic oxidation analyser (TOC-VCSN, Shimadzu Corporation). COD was measured by titration using Mohr's salt and ferroin as indicator after complete oxidation with potassium dichromate in sulfuric acid and the addition of silver sulphate as a catalyst and mercuric sulphate to remove chlorides interference at 150 °C for 2 h).

Anionic species were investigated with ion chromatograph (ICS-90, Dionex), and nutrients and metals content were evaluated through an ICP-OES (Optima 7000, Perkin Elmer). VFAs were measured using a GC-FID (7890B, Agilent Technology) after acidification (pH < 2), while the total phenols concentrations were assessed spectroscopically (U-2000, Hitachi) using the Folin-Ciocalteu assay; results were expressed as mg of phenol per L by using phenol calibration curve.

8.3.3   Acute toxicity test

Acute toxicity test is used to assess the suitability of PW for aerobic biological treatment. The test measures the effect of increasing doses of the investigated substance on the activity of nitrifying bacteria responsible for the oxidation of ammoniacal nitrogen ($N-NH_3$) to nitrous nitrogen ($N-NO_2^-$). The inhibition of this biomass, as nitrifying bacteria are the most sensitive, can be cautiously considered representative of the toxic effect that the biomass present in the entire activated sludge process of a traditional plant can suffer. The method involves the initial measurement of the nitrifying activity of an active sludge sample (test suspension, 1 L) in the presence of ammonium ion as a substrate (blank test); subsequently, increasing doses of the test substance (with a modified pH equal to the sludge pH) are added to the sludge at sufficiently close regular intervals so as not to allow the biomass to be adapted to the substance. Inhibition is calculated as a decrease in the sludge activity as a result of the addition of the substance, compared to the activity measured in the blank test. The measurement of nitrifying activity is based on the stoichiometric relationship between ammonium oxidation by nitrifying bacteria and the production of acidity. As described by Ficara and Rozzi (2001), the test was carried out inside a glass reactor (2 L) equipped with constant aeration, agitation, and a pH-stat titration unit (ANITA, Ammonium NITrification Analyser) which allows recording the flow rate of alkaline titrating solution necessary to maintain the pH at equilibrium

conditions. In this way, it was possible to calculate the corresponding oxidation rate of ammoniacal nitrogen.

8.3.4 BMP tests

BMP tests were conducted to verify whether PWs could be exploited for energy production, integrating the HTC process with AD and fully embracing the concept of circular economy. Three replicates were prepared mixing PW samples with methanogenic sludge in dark-brown glass bottles (120 ml) to obtain a food-to-microorganisms ratio (F/M) set at 0.5 gCODsubstrate/gCODbiomass, considered optimal by Chynoweth et al. (1993). In addition, three replicates only containing methanogenic sludge were used as reference. To ensure anaerobic conditions, oxygen was removed purging with nitrogen, the bottles were sealed, and incubated, keeping them in agitation, at 39 °C for 30 days. Around every 3 days, the produced gas was measured using a water-displacement method using a volume column and analised with GC-FID (7890B, Agilent Technology) to obtain the composition in terms of CO_2 and CH_4.

8.4 Results and Discussion

8.4.1 Characterisation of process water

A deep characterisation of PW is essential for its valorisation and/or treatment. Table 8.2 shows the average liquid yields (output liquid mass compared to the input liquid mass) for each sample after HTC, pH, electrical conductivity (EC), total organic carbon (TOC) and chemical oxygen demand (COD); the standard deviations are shown in brackets. The liquid yield behaves oppositely to the solid one; it increases both as the process temperature increases (with the same holding time) and as the holding time increases (with the same process temperature). Such high liquid yields (above 100%) are caused by the solubilisation of solid matter, as evidenced by TOC, COD, and EC values. Indeed, the density of the PW increased from 1.00 (density of distilled water) up to 1.03 g/cm^3, confirming the results. The pH of the process water is around 4 or lower, except in digestate samples, which, given its high buffering capacity and its high initial pH (8.8), has an alkaline pH. In general, the pH decreases during the HTC process as shown by several authors (C. Aragón-Briceño et al., 2017). As shown in Figure 8.1, a correlation cannot be found between variation in operating parameters and change in pH since there are no large variations in pH between one test and another. This consideration is also valid for electrical conductivity. EC turns out to be higher in process water from

digestate, with a maximum of 31.51 mS/cm in agro-industrial digestate, which indicates a high amount of ions in the solution.

Table 8.2 - Liquid yields of each HTC test, pH, EC, TOC and COD of each process water sample.

Sample code	Liquid yield [%]	pH	EC [mS/cm]	TOC [g/L]	COD [g/L]
SCG_220_1	103.15 (0.09)	3.86	4.33	11.31 (0.00)	29.85 (0.50)
SCG_240_1	103.54 (0.15)	4.09	4.19	10.73 (0.07)	27.36 (0.00)
H_180_1	101.20 (0.88)	3.69	9.03	12.31 (0.18)	29.85 (0.50)
H_180_3	102.15 (0.63)	3.66	9.94	10.16 (0.06)	26.12 (0.35)
H_200_1	102.65 (2.50)	3.55	8.95	11.31 (0.13)	27.11 (0.35)
H_220_1	104.93 (1.67)	3.53	8.33	9.32 (0.08)	23.05 (0.76)
D_180_1	97.36 (5.38)	7.62	26.35	9.36 (0.06)	24.21 (0.76)
D_180_3	99.90 (1.42)	7.55	26.82	9.24 (0.07)	23.71 (0.57)
D_180_6	101.29 (1.56)	7.42	27.23	8.99 (0.11)	23.13 (0.35)
D_200_1	100.48 (0.65)	7.91	26.50	6.95 (0.08)	19.24 (0.76)
D_200_3	101.58 (0.17)	7.81	26.69	7.89 (0.02)	21.06 (0.29)
D_200_6	102.86 (0.19)	7.38	27.93	7.15 (0.03)	19.90 (0.70)
D_220_1	101.95 (0.68)	7.34	28.67	8.80 (0.13)	23.38 (0.70)
DMIX_220_1	98.92 (5.70)	7.41	31.51	10.87 (0.02)	28.19 (0.76)
CBH_220_1	106.70 (0.33)	3.15	6.63	32.68 (0.12)	73.63 (1.41)
CBH_240_1	105.95 (1.27)	3.17	7.30	29.68 (0.39)	68.16 (2.11)
CB_220_1	105.20 (0.13)	3.76	9.36	21.51 (0.31)	62.69 (1.99)
CB_240_1	105.25 (0.38)	3.88	10.20	20.30 (0.02)	50.75 (1.41)
CBM_240_1	104.79 (0.69)	3.38	7.43	21.10 (0.13)	51.24 (0.70)
GM_220_1	101.58 (0.39)	4.45	12.88	10.14 (0.15)	29.85 (0.00)
GM_Ext_220_1	101.61 (0.15)	4.34	11.82	8.79 (0.05)	26.87 (1.41)
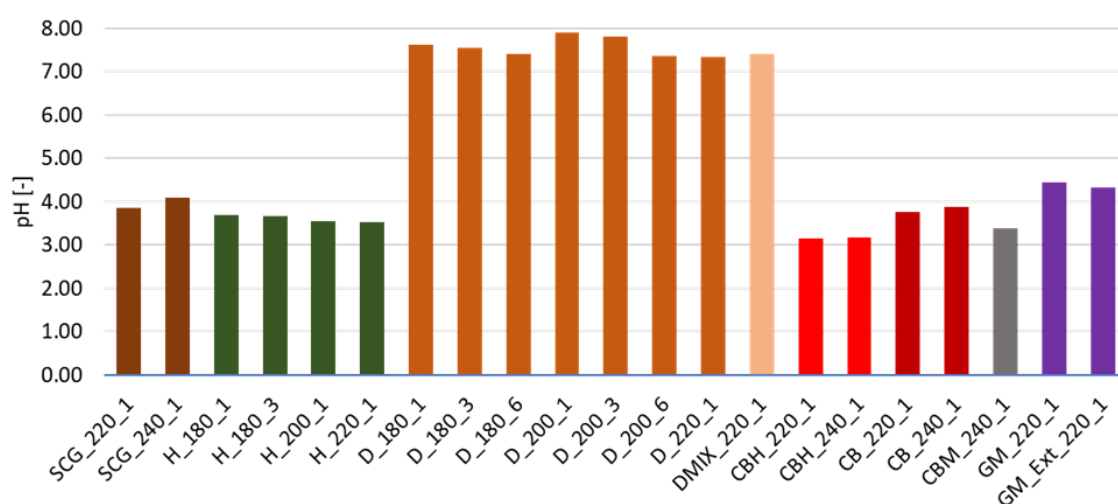
Figure 8.1 – pH of PW deriving from the different HTC tests

Relatively high values of TOC between 7 and 33 g/L were found. The highest values were reported in process water resulting from the treatment of the two types of cigarettes. From Figure 8.2, TOC tends to decrease with the effect of temperature and time. As expected, the COD is always greater than the TOC and shows a similar trend. The results are consistent with the values reported in literature (Berge et al., 2011).
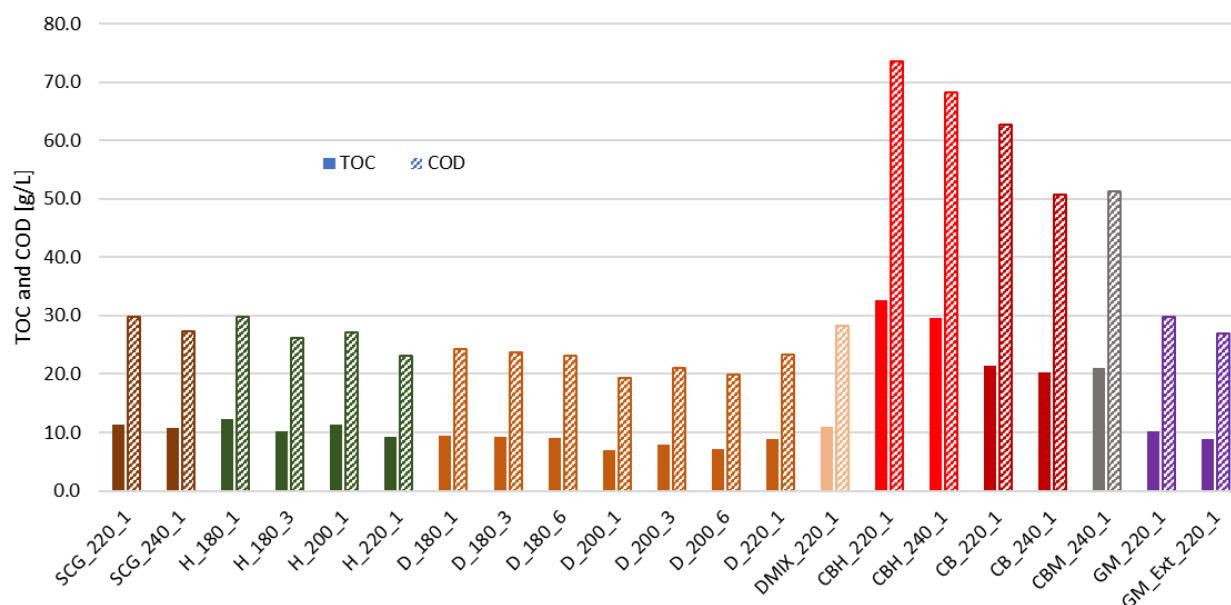
Figure 8.2 – TOC and COD values of the PW samples

Through the analysis with ion chromatography, it was possible to investigate the presence and quantity of anions such as chlorides, nitrites, nitrates, and sulphates. The results are shown in Table 8.3. Due to their solubility, large concentrations of chlorides can be noted in almost all process waters, except in the case of the two types of cigarettes in which the lowest values are detected. In PWs from the treatment of SCG, it was not possible to identify the peak related to chlorides in the chromatogram, as it was covered by an unknown anion species. Also, nitrites are absent in all samples, while nitrates are present in lower concentrations than other detected anions. As for sulphates, their values are very similar for all feedstocks, with the lowest values for hemp and SCG. Compared with the Italian limits for discharge into surface water in Table 8.4, the values reported so far determine the PWs to be treated before being discharged as wastewater; only the concentrations of sulphates remain below the limit.

Table 8.3 - Concentration of chlorides, nitrates, and sulphates in process water.

Sample code	Cl⁻ [mg/L]	N-NO₃ [mg/L]	SO₄ [mg/L]
SCG_220_1	n.a.	5.04	20.36
SCG_240_1	n.a.	4.06	19.08
H_180_1	1029.95	137.93	44.69
H_180_3	1179.00	110.87	53.47
H_200_1	962.74	115.06	46.25
H_220_1	1048.68	133.92	31.23
D_180_1	2970.71	4.88	n.d.
D_180_3	5206.68	50.87	172.37
D_180_6	4374.97	47.61	174.88
D_200_1	4342.33	n.d.	n.d.
D_200_3	4756.48	53.04	325.11
D_200_6	4769.17	40.44	178.53
D_220_1	3970.50	n.d.	171.34
DMIX_220_1	3566.98	120.49	335.73
CBH_220_1	140.62	14.97	278.83
CBH_240_1	90.81	5.96	211.67
CB_220_1	118.24	34.48	319.15
CB_240_1	132.04	29.84	291.90
CBM_240_1	92.19	18.39	286.67
GM_220_1	883.67	15.41	302.30
GM_Ext_220_1	866.24	45.92	359.63

n.a. = not available; n.d.=not detected

Table 8.4 - Limit values for discharge into surface waters and municipal sewage treatment plants according to the Italian Legislative Decree no. 152 of 11/05/99.

Parameters	U.M.	Discharge into surface waters	Discharge into sewage treatment plant
pH	[-]	5.5-9.5	5.5-9.5
COD	[mg/L]	160	500
Chlorides	[mg/L]	1200	1200
Nitrates	[mg/L]	20	30
Sulphates	[mg/L]	1000	1000
Total phosphorus	[mg/L]	10	10
Total phenols	[mg/L]	0.5	1
Aluminium	[mg/L]	1	2
Arsenic	[mg/L]	0.5	0.5
Cadmium	[mg/L]	0.02	0.02
Iron	[mg/L]	2	4
Lead	[mg/L]	0.2	0.3
Copper	[mg/L]	0.1	0.4
Zinc	[mg/L]	0.5	1

Through the ICP-OES analysis, the concentrations of macronutrients (P, K, Ca), iron (Fe), and aluminium (Al) in the process water were measured (Table 8.5). The objective was to understand if these elements could be recovered from the process water and, secondly, to characterise the liquid phase for the subsequent bio-gasification tests; phosphorus, in particular, is a fundamental element for the growth of microorganisms while metals are inhibiting. P, K, and Ca were detected in all the PW samples, while Fe and Al were only found in PWs resulting from the treatment of the two types of cigarettes butts (CB and CBH).

Figure 8.3 shows that P concentration is relatively higher in process water from both types of GM, SCG, and DMIX, compared to the other feedstocks. D_200_6 is the only sample that, with 9.6 mg/L, complies with the regulatory discharge limit of 10 mg/L in Table 8.4. In general, lower values can be found at higher process temperatures. As for potassium, high concentrations are reported in the case of process water from digestate and grape marc (Figure 8.3); PWs from digestate showed the largest quantities reaching 7 g/L.

Table 8.5 - Concentration of P, K, Ca, Fe, and Al in PW samples.

Sample	P [mg/L]	K [mg/L]	Ca [mg/L]	Fe [mg/L]	Al [mg/L]
SCG_220_1	150.5	836.2	93.3	n.d.	n.d.
SCG_240_1	92.7	645.7	35.4	n.d.	n.d.
H_180_1	33.2	1768.0	351.5	n.d.	n.d.
H_180_3	46.7	2019.0	326.8	n.d.	n.d.
H_200_1	40.6	1805.0	323.1	n.d.	n.d.
H_220_1	16.5	1599.0	397.1	n.d.	n.d.
D_180_1	32.4	5741.0	194.7	n.d.	n.d.
D_180_3	42.6	6474.0	244.1	n.d.	n.d.
D_180_6	36.1	6259.0	173.9	n.d.	n.d.
D_200_1	17.4	4759.0	54.8	n.d.	n.d.
D_200_3	19.3	5718.0	212.5	n.d.	n.d.
D_200_6	9.6	6920.0	415.0	n.d.	n.d.
D_220_1	33.4	6688.8	409.6	n.d.	n.d.
DMIX_220_1	112.8	7124.0	7.2	n.d.	n.d.
CBH_220_1	67.7	1127.0	2678.0	31.5	770.5
CBH_240_1	53.9	948.6	2831.3	31.5	844.8
CB_220_1	34.2	1390.0	2024.0	16.3	3.0
CB_240_1	27.8	1531.0	1775.0	4.6	2.0
CBM_240_1	45.6	1122.0	1940.0	37.0	80.7
GM_220_1	204.3	4132.0	n.d.	n.d.	n.d.
GM_Ext_220_1	229.0	3853.0	n.d.	n.d.	n.d.

n.d. = not detected
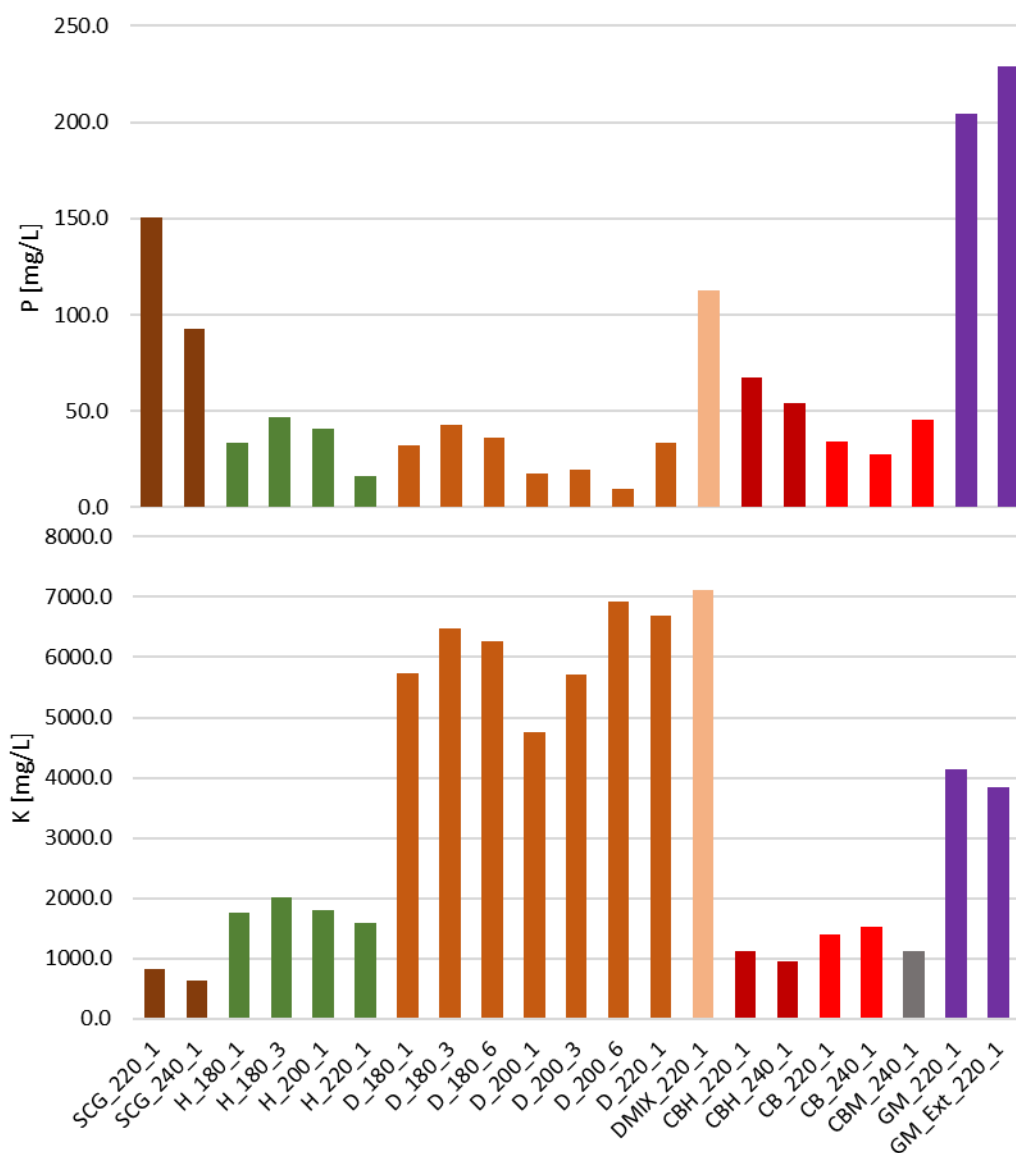
Figure 8.3 – Phosphorus and potassium concentrations in PWs.

Comparing the results with literature data (Belete et al., 2019, 2021), it is highlighted that the phosphorus content in the process water is relatively low to be extracted and recovered, which may not be convenient; in contrast, the path of recovery K is still a feasible option. The potassium present in the liquid phase, deriving from the two types of digestate and grape marc, could be extracted and used for the production of fertilisers based on NPK or as a basic element for the synthesis of a large number of compounds that find practical application in different industrial fields, as reported by Crossley et al. (2020), e.g., in chemical industry as potassium hydroxide used to produce liquid soap or detergents or in pharmaceuticals or as potassium chloride for the production of medical drops and saline solutions. As for phosphorus, the values are much lower and it would be necessary to carry out a cost-benefit analysis to evaluate the actual convenience of a possible extraction process keeping in mind that even a small amount recovered can be seen as an excellent opportunity both

because the natural deposits of this element are slowly depleting and to reduce the climate impacts due to the production of nitrogen fertilisers (Hämäläinen et al., 2021).

In PW derived from cigarettes butts and grape marc, concentrations of the specific metals were investigated (arsenic, zinc, lead, cadmium, and copper). Results are reported in Table 8.6.

Table 8.6 - Concentration of As, Zn, Pb, Cd, and Cu in the process waters of cigarettes butts and grape marc.

Sample code	As [mg/L]	Zn [mg/L]	Pb [mg/L]	Cd [mg/L]	Cu [mg/L]
CBH_220_1	1.04	2.78	n.d.	0.20	0.15
CBH_240_1	1.00	2.71	n.d.	0.20	0.11
CB_220_1	0.11	3.33	0.09	0.20	0.10
CB_240_1	n.d.	3.07	0.07	0.21	0.10
CBM_240_1	0.03	2.23	0.05	0.20	0.11
GM_220_1	n.d.	1.16	0.10	0.17	0.12
GM_Ext_220_1	n.d.	1.60	0.10	0.17	0.11

n.d. = not detected

Elements such as Zn and Cd are present in concentrations that exceed the limit for discharge into the municipal sewage treatment plant (Table 8.4) in all the samples analysed, while As is present in excessive quantities only in the case of PWs from CBH.

VFAs such acetic acid (HAc), propionic (HPr), isobutyric (HIBu), butyric (HBu), isovaleric (HIVal), valeric (HVal), isocaproic (HICap), caproic (HCap), and heptanoic (HEpt) deriving from GC measurements are reported in Table 8.7; valeric acid (HVal)was absent in all PW samples and, therefore, is not reported.

From the data, the most present acid is acetic acid. Reported values were similar to literature data (Wirth et al., 2015; Yu et al., 2018). In process water from sewage sludge treatment, the study by Wirth et al. (2015) reported concentrations of 2.06 g/L of acetic acid and 0.12 g/L and 0.03 g/L of propionic and butyric acid, respectively. As can also be seen from Figure 8.4, concentrations of acetic acid were found higher than the literature data treating agro-industrial digestate, hemp (at 180 °C), and grape marc; in PWs from CH and CBH, the concentrations of acetic acid stand out among all, reaching 30 g/L in CB_240_1. It may be due to the degradation of the filter, mainly composed of cellulose acetate. The high concentrations of acetic acid are promising for the next phase of bio-gasification, as it is the starting substrate in acetoclastic methanogenesis for methane formation.

Table 8.7 - Concentration of VFAs in PW samples.

Sample code	HAc [mg/L]	HPr [mg/L]	HIBu [mg/L]	HBu [mg/L]	HIVal [mg/L]	HICap [mg/L]	HCap [mg/L]	HEpt [mg/L]
SCG_220_1	2075.7	448.4	n.d.	n.d.	350.1	483.2	277.9	682.6
SCG_240_1	1818.1	456.6	135.4	182.1	340.3	493.6	555.2	665
H_180_1	5875.2	321.6	378.8	344.3	266.5	414.5	452.5	543.5
H_180_3	4521.3	335.5	421.1	307.1	247.2	401.4	439.9	n.d.
H_200_1	2797.9	346.3	277.6	292.8	252.1	389.6	445	265.5
H_220_1	1153.9	369.1	280	290.2	252.5	388	438.8	n.d.
D_180_1	2129	416.3	n.d.	181.1	321.6	248.4	563.1	n.d.
D_180_3	1098.9	400.3	281.2	n.d.	321.3	501.3	561.2	n.d.
D_180_6	1100.6	n.d.	n.d.	n.d.	318.8	n.d.	n.d.	n.d.
D_200_1	1867.8	191.3	136.1	178.9	163.6	499.5	566.1	329.8
D_200_3	1027	427.6	n.d.	n.d.	318.6	240.9	577.6	n.d.
D_200_6	1874.7	476.9	n.d.	n.d.	333.3	n.d.	565.5	n.d.
D_220_1	2376	526.5	n.d.	n.d.	337.9	n.d.	588.5	n.d.
DMIX_220_1	3410.4	1213.5	391.5	389.1	354.2	489.4	589.6	386.3
CBH_220_1	13780	391.7	286.9	377	322.3	480.5	n.d.	335.2
CBH_240_1	12119	415.6	n.d.	398.5	326.1	242.9	275.4	701.7
CB_220_1	28249	426	131.7	364.7	319.3	495.1	552.7	665.3
CB_240_1	30434	501.3	267.7	371.5	329.2	486.6	564	335
CBM_240_1	19589	429.4	n.d.	379.1	330.1	483.8	278	337.2
GM_220_1	2670.8	425.1	152.3	201	353	528.8	580.1	703
GM_Ext_220_1	2892.1	413.4	276.3	n.d.	326.1	536.1	571.2	n.d.

n.d. = not detected
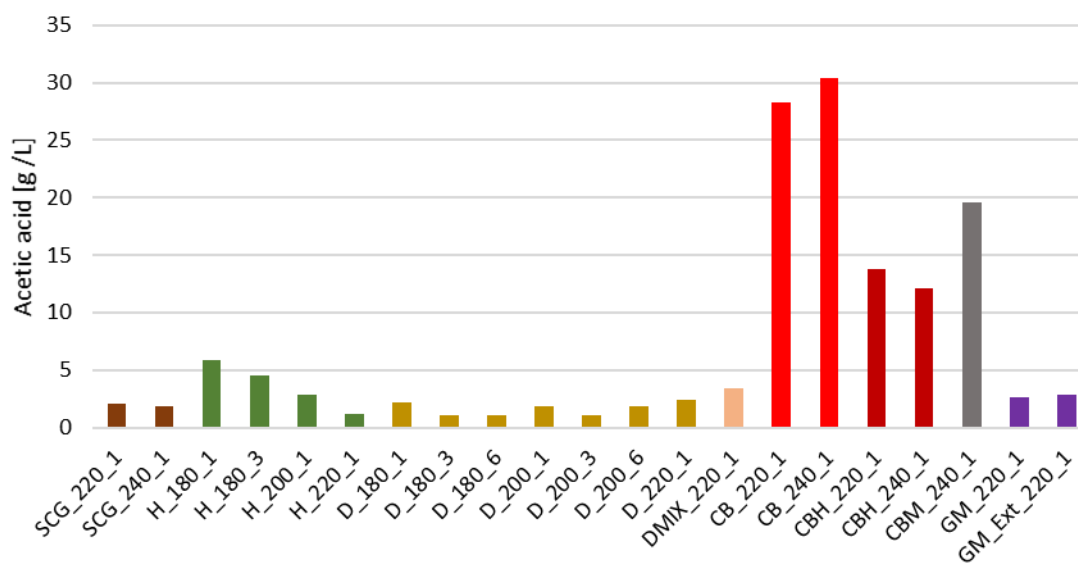
Figure 8.4 – Acetic acid concentration in PW samples

To propose the possible treatment and safely handle the PW, the quantification of total phenols, considered a common and potentially toxic category of compounds produced during HTC, was measured (Table 8.8). All samples reported high concentrations with increasing trend with temperature and decreasing with holding time.

Table 8.8 - Concentration of total phenols.

Sample code	Total phenols [mg/L]	Sample code	Total phenols [mg/L]	Sample code	Total phenols [mg/L]
SCG_220_1	1867.6	D_180_1	1565.3	CBH_220_1	1535.3
SCG_240_1	2334.5	D_180_3	1435.4	CBH_240_1	1775.1
H_180_1	1476.0	D_180_6	1445.4	CB_220_1	2184.7
H_180_3	1627.8	D_200_1	1825.0	CB_240_1	2354.5
H_200_1	1907.6	D_200_3	1835.0	CBM_240_1	1914.9
H_220_1	2083.4	D_200_6	1405.4	GM_220_1	1475.3
DMIX_220_1	3163.7	D_220_1	2014.8	GM_Ext_220_1	1275.5

8.4.2 Aerobic treatment feasibility of PW

Figures 8.5 and 8.6 show the results of acute toxicity tests obtained for PW from HTC of SCG and hemp. The curves show the trend of acute inhibition (%) as a function of the dosage of the process water (ml/L).

In samples from SCG, nitrifying bacteria achieve 50% inhibition with a dosage of 8.03 ml/L of process water at 220 °C and 3.41 ml/L with process water at 240 °C. The increase in HTC process temperature leads to an increase in the toxicity of the process water, therefore, an increase in toxic/inhibiting compounds.
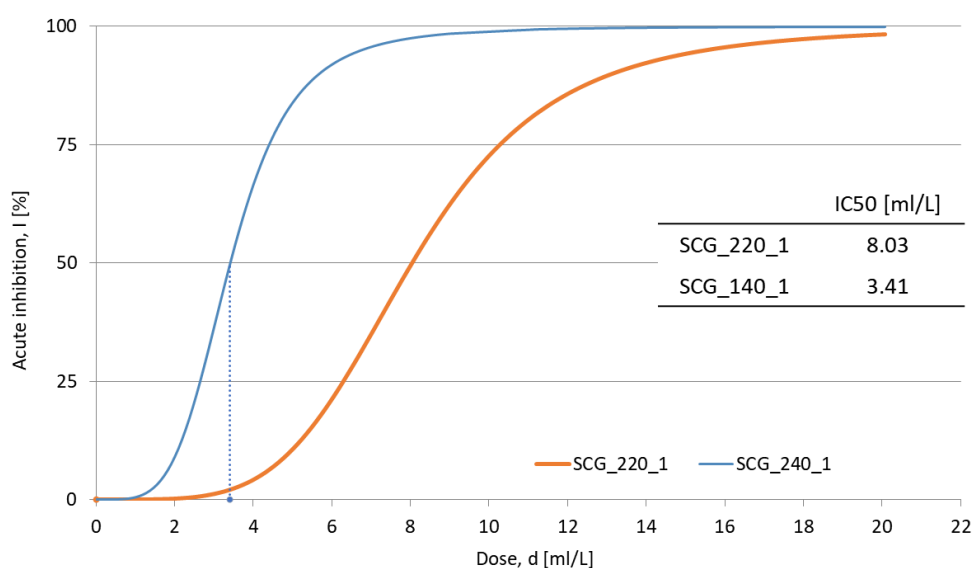
Figure 8.5 - Dose-inhibition curves of the toxicity test on process water derived from SCG.

Likewise, in samples from hemp (Figure 8.6), the toxicity increases as the temperature of the process increase. There are no major differences between the process waters from the H_180_1 tests and H_200_1, while the sample produced at 220 °C shows increased toxicity.
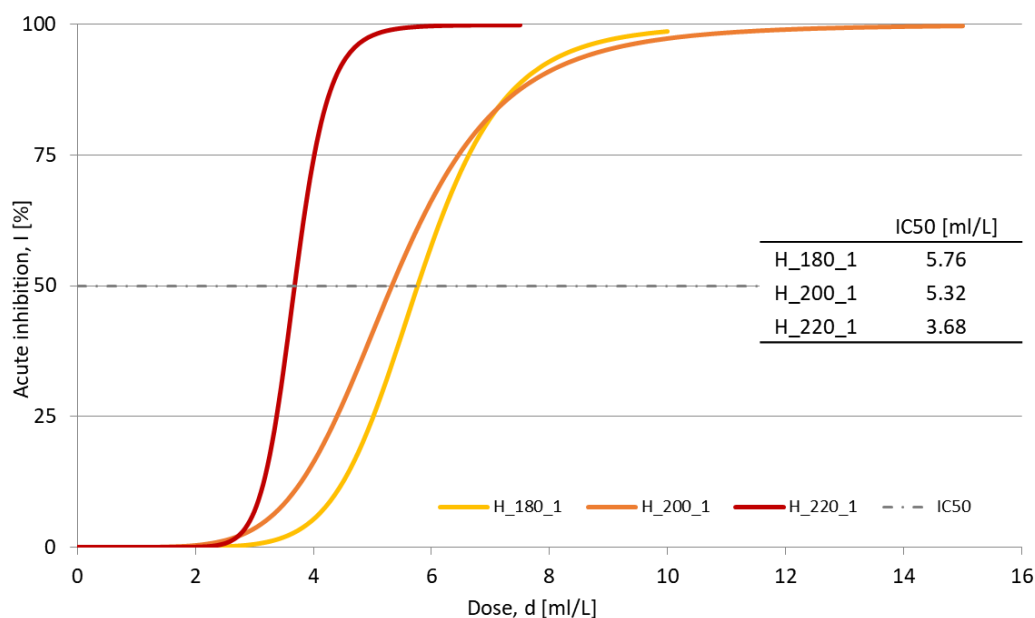
Figure 8.6 – Dose-inhibition curves of the toxicity test on process water derived from hemp.

Figure 8.7 shows the inhibiting concentration values as a function of the HTC process conditions in the case of hemp digestate. At constant process temperature, toxicity increases as the holding time increases (from 1 to 3 h) and then decreases to 6 h. The lowest toxicity is achieved in the case of the D_180_6; this could be caused by a relatively low temperature (180 °C) and a high residence time (6 h) that could remove certain toxic compounds in other cases present. With a constant holding time of 1h, the toxicity decreases with increasing process temperature (from 180 to 200 °C) and then increases to 220 °C.
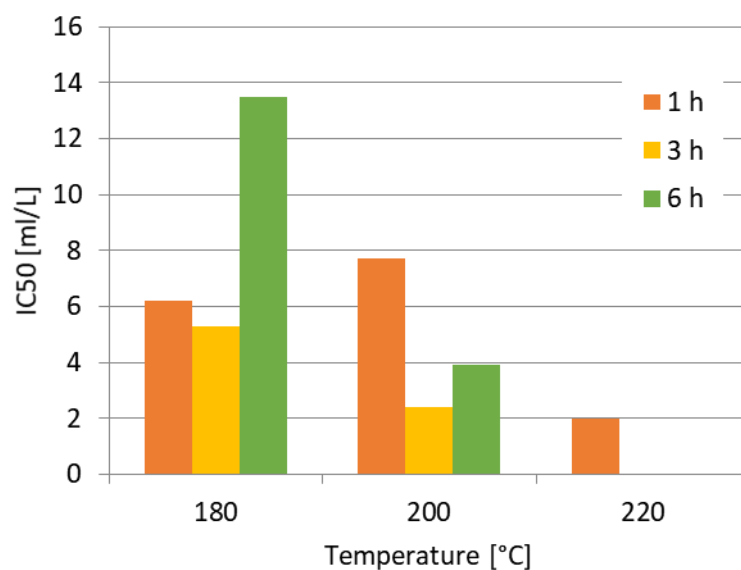
Figure 8.7 – IC 50 values of PW from hemp at the different process conditions.

In Figure 8.8, inhibiting concentrations are shown for PW of the two types of cigarettes butts (CB and CBH). Process water from the treatment CBH is more toxic than CB, with the opposite behaviour to the concentrations of phenols, higher in the case of CB (Table 8.8). This consideration leads to thinking that other toxic compounds are present in the waters to determine such high toxicity.
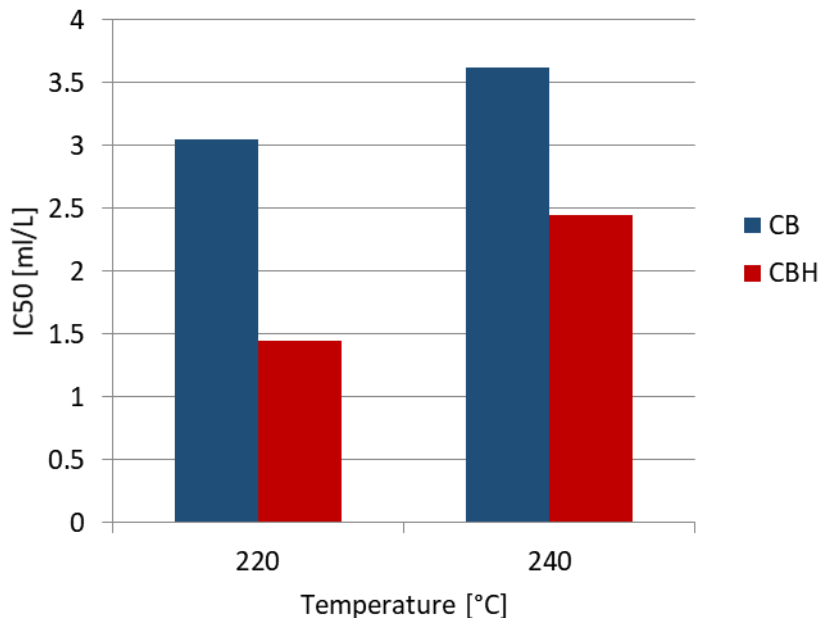
Figure 8.8 - Inhibiting concentrations (IC50) of process waters from the treatment of CB and CBH as a function of the process temperature with a constant residence time of 1 h.

Analysing the dose-inhibition curves of process water from GM and GM_Ext (Figure 8.9), it is noted that nitrifying bacteria achieve inhibition of 50% with a dosage of only 0.53 ml/L in PW from GM and 1.9 ml/L in GM_Ext. The process water of the grape marc is the most toxic of the process waters

analysed. The results demonstrate a toxic effect, almost immediate, and then settle around 65% up to a dosage of 6 ml/L; with 12 ml/L, the inhibition is total. The inhibiting effect related to GM_Ext is presented at higher dosages, but the interpolated curve is narrower with a toxic effect that increases with a higher slope; this turns into a complete inhibition of bacteria for a dosage equal to 6 ml/L, about the half compared to the previous case.

In Figure 8.10, where the total phenols concentration is compared with the IC50 values, for SCG, hemp, and GM, an increase in the concentration of total phenols corresponds to an increase in toxicity (decrease the inhibiting concentration). This cannot be stated for the other feedstocks (hemp digestate and the two types of cigarettes butts), implying that the organic phenolic compounds (or their concentrations) contained in PW may be different for each feedstock and may affect the activated sludge in diverse ways.
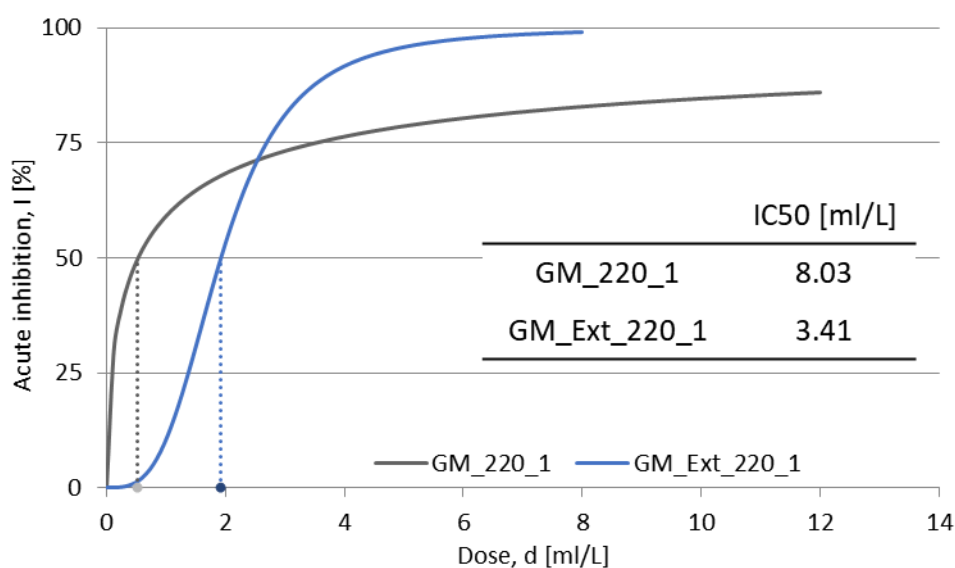
Figure 8.9 - Dose-inhibition curves of the toxicity test on process water derived from SCG.
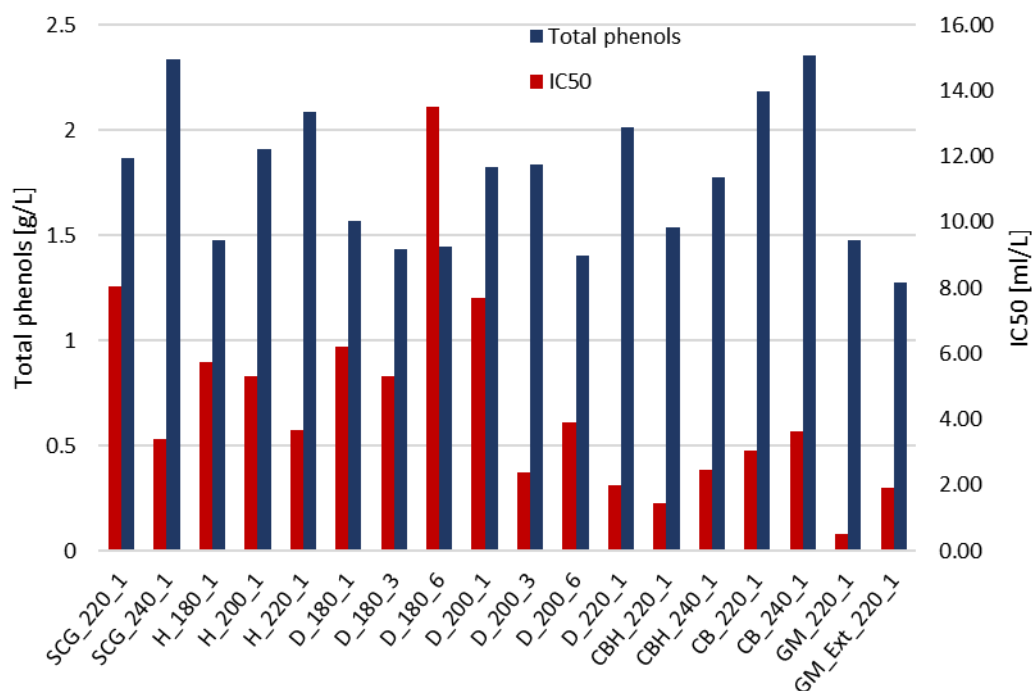
Figure 8.10 Total phenols concentration in PW and IC50 values of each PW sample.

These former considerations suggest that there could be a correlation between the presence of phenols and the toxic effect on aerobic bacteria in some feedstocks. It should be noted that the pre-treatment (extraction) of the GM led to the formation of process water with a lower and less toxic concentration of phenols. In general, however, the results demonstrate a significant toxic effect by all PW samples.

What has been achieved suggests some points of reflection on the final fate of the process waters. There was a potential criticality concerning activated sludge biological processes in which a nitrification phase is present. Based on the available information, the speciation of carbon in the liquid phase has been studied in more detail to identify which organic compounds are the main responsible for the toxic effect and direct the final treatment. Unfortunately, as shown in Figure 8.11, it is not possible to associate a big part of the organic carbon present in the solution with specific compounds from the available analyses. Percentages between 20 and 80% of organic carbon are unidentified ('Other' in Figure 8.11). This unknown component could be represented by other organic acids, furan acids and still unknown compounds. However, the concentrations of volatile fatty acids are very high, so a promising treatment alternative can be anaerobic digestion which offers a possibility of energy recovery. In addition, the digested liquid could be easily treated at an urban wastewater treatment plant (Tasca et al., 2019). Acetic acid accounts for about 5-20% of total organic carbon, reaching 50-60% in the PWs of CB. In addition, the development of the bacterial

population should be favoured by the discrete concentrations of nutrients that may make, in addition, these waters suitable for agricultural applications.
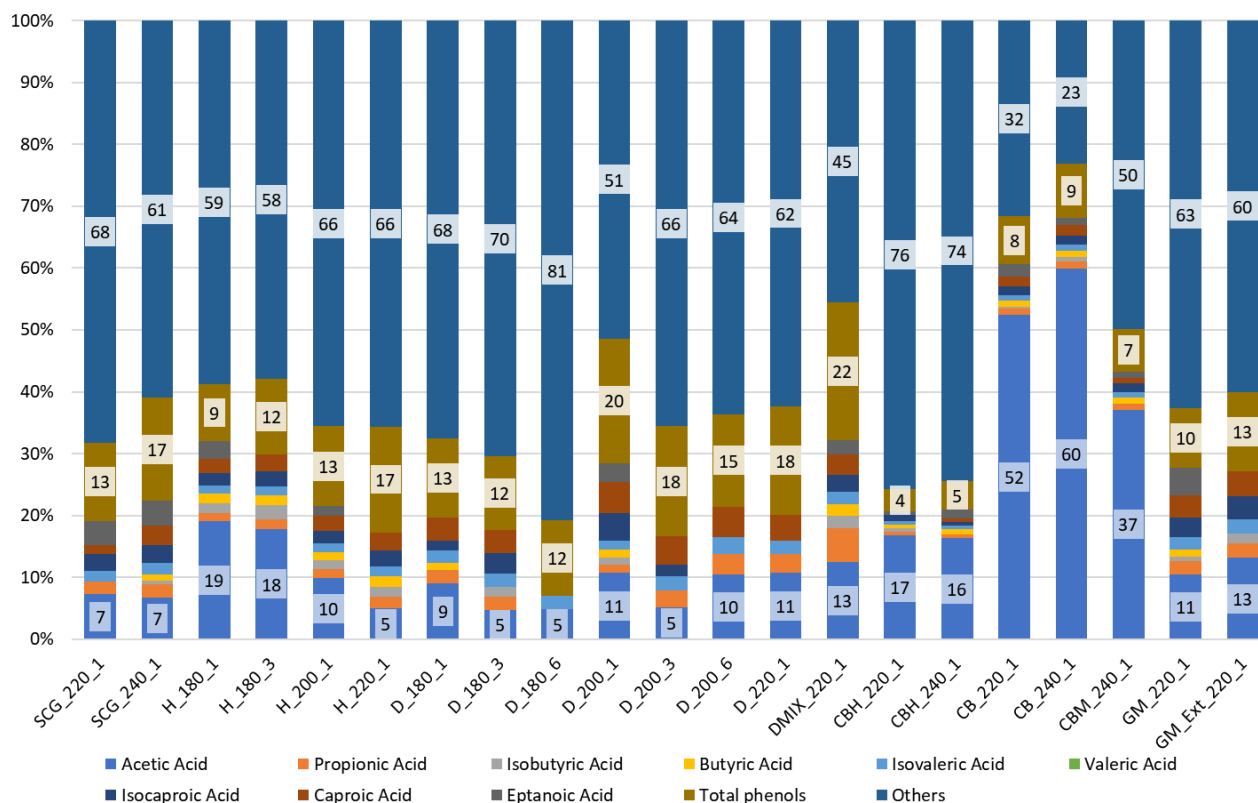
Figure 8.11 – Organic carbon distribution in PW samples

8.4.3   Energetic valorisation of PW

Table 8.9 shows the main physical-chemical characteristics of the inoculum (methanogenic sludge) used in BMP tests.

Table 8.9 - Values of total solids, volatile solids, ash, and COD for inoculum.

	TS [%]	**VS [%TS]**	**Ash [%TS]**	**COD [g/L]**
methanogenic sludge	2.13 (0.22)	51.97 (1.52)	48.03 (1.52)	20.90 (1.00)

During the incubation, the bio-gasification potential for process water was assessed. Table 8.10 shows the specific cumulated production of methane during the testing period (28 days), expressed as the ratio between the volume expressed as ml of the produced methane and the initial COD content of the PW. The data have been cleaned of possible methane produced by the inoculum (blank production reported in Supplementary materials).

Table 8.10 - Specific cumulative methane production in PW samples.

Days	5	8	13	16	20	28
Sample Code			[ml CH$_4$/gCOD]			
SCG_220_1	27.09	42.72	56.18	59.51	60.25	61.83
SCG_240_1	29.00	41.39	49.04	52.74	53.08	55.22
H_180_1	38.38	80.06	96.96	99.98	100.72	101.45
H_180_3	28.92	57.52	77.25	78.32	79.07	81.88
H_200_1	29.16	66.95	75.01	80.74	82.39	82.39
H_220_1	25.41	69.19	83.73	89.05	89.65	91.06
D_180_1	60.34	66.31	72.19	73.51	74.40	75.81
D_180_3	64.13	76.24	81.78	82.64	82.64	82.64
D_180_6	65.22	80.32	86.46	87.28	87.49	88.01
D_200_1	45.57	55.59	61.47	63.42	63.55	63.55
D_200_3	41.00	48.14	55.82	57.08	57.84	59.22
D_200_6	29.10	37.71	41.03	41.15	41.15	41.15
D_220_1	25.88	31.95	43.33	47.70	48.89	50.97
CBH_220_1	96.00	155.67	186.41	189.96	189.96	189.96
CBH_240_1	72.28	120.54	147.44	153.16	155.31	157.63
CB_220_1	75.68	98.39	105.23	105.23	105.23	105.23
CB_240_1	103.58	112.54	122.23	123.81	124.94	126.60
GM_220_1	73.47	108.14	132.41	132.41	133.22	138.73
GM_Ext_220_1	71.43	92.27	110.47	112.60	113.57	116.51

Subsequently, the percentage of methanisation of process water compared to the theoretical conversion (stoichiometrically, from 1 g of removed COD, a maximum of 350 ml CH$_4$ can be obtained) was evaluated (Figure 8.12).
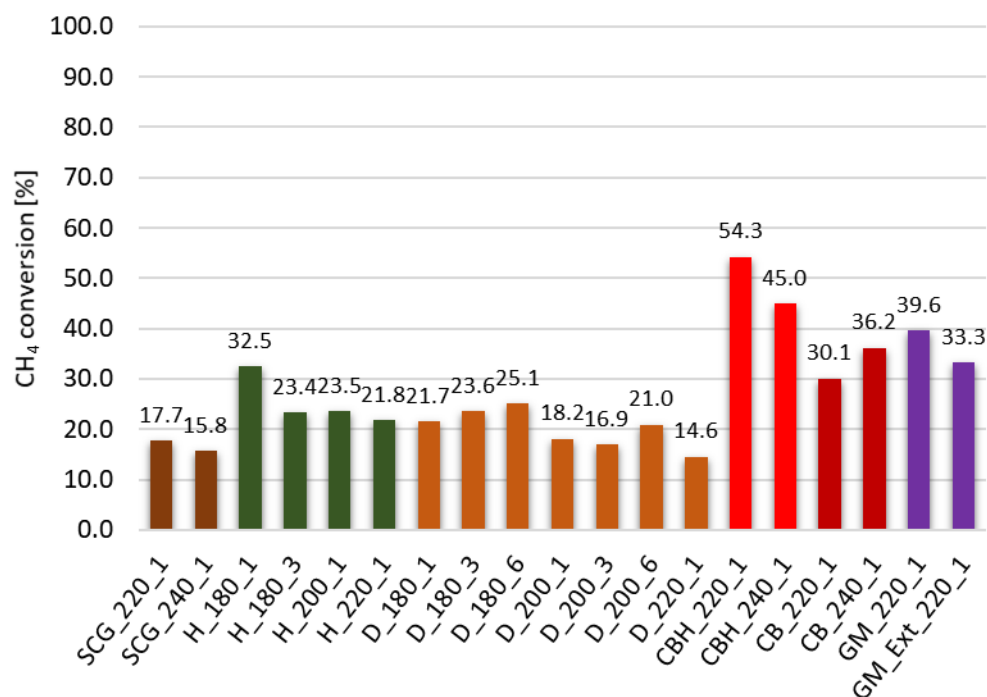
Figure 8.12 – Conversion percentage of COD in PW in methane compared to the theoretical conversion.

The PWs of SCG, hemp, and hemp digestate exhibit the lowest methanisation rates; H_180_1 shows the highest production among the process waters of these three feedstocks. The production from PW of SCG is reduced comparing PW at 220 °C to PW at 240 °C; this also applies to PW of CBH, where the greatest methane production was shown. On the other hand, methane production from PW of CB increases with the process temperature and could be due to a higher content of both VFA and phenols in the substrate CB_240_1. The process water of the grape marc shows a good methane production; the lowest value was achieved for GM_Ext. It is interesting to analyse the trend of the specific production of cumulated methane of the two feedstocks that had the greatest production of CH$_4$ (CBH_220_1 and CBH_240_1). The curves are reported in Figure 8.13. The curves related to the methane production of the other samples are reported in Supplementary materials.
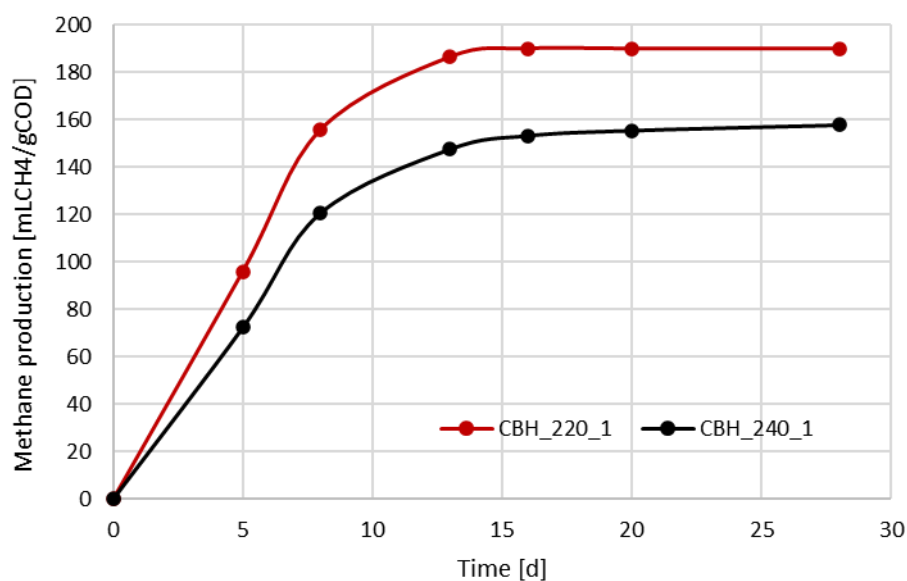
Figure 8.13 – Cumulative and specific production of methane over time for CBH samples.

Analysing the graph, both PWs show a high methane production during the first eight days of experimentation; the curve CBH_220_1 shows a greater slope. From the eighth day onwards, the two curves become practically parallel. On the fifteenth day, the CBH_220_1 curve reaches a methane production of 189.96 mlCH$_4$/gCOD, which keeps constant until the end of the test, while the CBH_240_1 curve continues to grow until the end of the trial slightly.

8.5   Conclusions

This study aimed to contribute to the sustainable management of process water deriving from HTC through the characterisation of liquid residues from the treatment of different types of organic feedstocks and the application of experimental tests aimed at studying their potential use in fertigation (Chapter 5), the production of methane achievable through anaerobic digestion, treatment through aerobic biological processes.

The characterisation activities highlight how process waters are rich in organic and inorganic compounds, representing potentially valuable chemicals or environmental threats. The comparative analysis between the different process waters showed a non-negligible variation in the physical and chemical characteristics as a function of the treated feedstocks and the operating parameters of the HTC process (e.g., density and pH). This variability influences the valorisation options pursued and may represent a limit in applying this process at an industrial scale, as already stated by Langone and Basso (2020).

The process waters analysed reported relatively low phosphorus concentrations. PW from the treatment of grape marc, spent coffee grounds, and digestate from agro-industrial residues holds higher phosphorus concentrations than those produced from cigarettes, hemp, and hemp digestate. Noted the low availability of this element on the European continent, extraction from process water could be an interesting option but should be evaluated based on a cost-benefit analysis. As for potassium, the process waters of hemp digestate, digestate from agro-industrial residues, and grape marc showed relatively high concentrations. In this case, the path of recovery is, therefore, more viable. Another valuable compound is represented by acetic acid, of which the process waters of the two types of cigarettes butts (CB and CBH) are particularly enriched and for which it could, consequently, hypothesise an extraction and recovery treatment.

In general, the measured concentrations for carbon, phosphorus, potassium, and calcium make the PWs suitable for agricultural application, particularly in fertigation. However, as presented in Chapter 5, the presence of organic compounds (e.g., acetic acid and phenols) could inhibit plant development. The results in Chapter 5 showed that the diluted process water delayed the germination process but did not inhibit it completely. So, if applied in specific quantities, process water could provide the nutrients needed for the development of plants.

The data showed that process water contains concentrations above the Italian wastewater discharge limits of several substances (e.g., heavy metals, phenols, chloride, P), hence, the need for their treatment. The acute toxicity tests demonstrate a significant toxic effect on nitrifying bacteria by all process water, making them unsuitable for biological treatment in which there is a nitrification phase. However, as already stated, a phase of acclimatisation of the biomass will likely make the treatment possible; therefore, a more in-depth analysis is necessary. Anaerobic digestion could be a valid alternative. The data obtained during the bio-methanation tests indicate that the process water resulting from the HTC process of the two types of cigarettes butts and grape marc can lead to the highest specific production of methane, ranging from 100 to 190 mlCH$_4$/gCOD. In these cases, anaerobic digestion could energetically support the HTC process, creating a positive energy balance (Langone & Basso, 2020). In addition, the digested liquid residue could be easily treated at a wastewater treatment plant (Tasca et al., 2019).

In conclusion, the work carried out has contributed to the knowledge of the HTC liquid treatment residue characteristics and has allowed highlighting possible valorisation options in terms of materials and energy recovery. However, it should be noted that there are still uncertainties about the composition and the actual viability of the valorisation options identified, which highlight the

need for further studies concerning the effects of process variables on the final products obtained and on the possible integration of the HTC process with other treatments and valorisation technologies.

Conclusions

In this work the hydrothermal carbonization process was applied to different organic materials such as hemp, grape marc, spent coffee grounds, AD digestate from hemp, from cow manure, and from agricultural residues, cigarette butts, surgical masks and gloves. The HTC input materials and the resulting products were physically and chemically characterised to be tested for different applications such as energy production by combustion or biological treatment (AD), as soil ameliorant, as peat substitute in growing media or fertigation, or to be biologically treated in aerobic wastewater treatment plant.

Compared to the feedstocks, hydrochars showed for all the tested materials strong physical and chemical modification as evidenced by the FTIR spectra and by the elemental composition (an increase in carbon content and a reduced content of ash). According to the increased HHV, hydrochar may be used as solid fuel, which, considering the initial humidity of feedstock and the necessary drying pre-treatment, entails a higher energy recovery compared to the feedstock, as reported in Figure S.30 (in Supplementary materials) where the energy balances proposed for the energetic valorisation of GM show that the integration of HTC with more common processes (AD and combustion) is convenient. Following HTC, all the tested materials showed a reduced volume and, despite the low solid yield, an increased density. In some cases (CB and CBH) a volume reduction of over 70% was attained (please refer to Table S.11, where the changes in the density of the materials are reported, and to Figure S.22, where the output volume of HC is compared to the volume of 1 t of feedstock entering the process). This fact can be translated into a saving of transport and storage costs. Moreover, due to the higher dewaterability, proved during the experimental activity, less energy can be used to remove humidity. The physical properties of the HTC materials make them feasible to be pelletised in order to save space in transport or have a safer handling; for instance, when added on soil, pellets may be a desirable option, compared to powdery material, for the issues related to its dispersion.

The possibility to use hydrochar as peat substitute in growing media for seed germination was tested for cow manure digestate, spent coffee grounds, and grape marc, showing that low amount of HC can partially substitute peat with similar or even better results. However, the addition of higher amount, especially SCG and GM, showed high inhibition. Pre- and post-treatments tested (extraction, drying, washing) seem to have positive effect on seed germination and plant growth, removing some phytotoxic compounds. However, since these steps can be expensive, further tests

should be carried out to understand which compounds cause inhibition, how to remove them or whether it is possible to destroy or avoid producing them by adequately setting the HTC process parameters.

Particular materials, such as plastic materials (masks), may not be strongly converted at the low HTC temperatures; nevertheless, as reported in Chapter 7, HTC agglomerate the plastic material reducing the volume and saving transport costs, with little chemical modifications. Moreover, the HTC conditions assure the disinfection for safe handling, eliminating the biological and possibly infective matter. As demonstrated by FTIR spectra, the resulting material does not differ from the initial masks; therefore, masks can be recycled, and the plastic constituent can be re-inserted in the productive cycle. The addition of acetic acid as catalyst in the treatment of masks results in the formation of crystals which are demonstrated to be terephthalic acid, basic molecule of several plastic polymers (e.g., polyethylene terephthalate, polypropylene, etc.).

Process water is the main HTC product in mass; however, the current research is mainly focused on hydrochar. PW should be properly treated, since as shown in Chapter 8, it contains many different compounds which can become an environmental problem when improperly managed. In this work, the potential valorisation of PW was tested through characterising the liquid. The high amount of nutrient in PW may suggest the use in fertigation; however, the germination tests showed in Chapter 5 reported inhibition effect due to the compounds formed during HTC and dissolved in PW. Moreover, the aerobic treatability was tested through the bioassay on nitrifying bacteria. Despite the assessed acute inhibition, aerobic treatment may be still a feasible option after an acclimation phase.

The high amount of VFAs may make PW a suitable substrate for AD to produce biogas and, therefore, energy. Results demonstrate that AD may be a good enhancement option. Moreover, VFA, acetic acid in particular, can be recovered and used for different applications considering its high commercial value. Depending on the type of feedstock, a wide range of compounds is formed in PW during HTC causing difficulties in characterisation and handling.

In conclusion, this work demonstrated that hydrothermal carbonization is a suitable process for the treatment of a wide range of organic materials. Depending on the feedstock, the resulting products may have different properties and characteristics which make them feasible for diverse applications. In general, all the feedstock tested may be used as solid fuel with several advantages, such as higher energy content, reduced volume, possible reduced emission during combustion, ease of dewatering, etc. The use on soil is promising when low amount of hydrochar is used, whilst high

amount exerts phytotoxic effect. However, pre- or post-treatments may be applied to reduce phytotoxic compounds. Process water may be biologically treated: anaerobically, to produce biogas and remove some organic compounds (e.g., VFA) and aerobically, but an acclimatation phase may be necessary.

HTC proved to be a promising process in the biorefinery concept, especially when integrated with other processes (AD, aerobic degradation, etc.). Materials and energy can be recovered by HTC and re-introduced in the productive cycle and in the market, promoting the circular economy and the zero-waste concept.

References

Adolfsson, K. H., Lin, C., & Hakkarainen, M. (2018). Microwave Assisted Hydrothermal

Carbonization and Solid State Postmodification of Carbonized Polypropylene. *ACS*

Sustainable Chemistry & Engineering, *6*(8), 11105–11114.

https://doi.org/10.1021/acssuschemeng.8b02580

Afolabi, O. O. D., Sohail, M., & Cheng, Y.-L. (2020). Optimisation and characterisation of hydrochar

production from spent coffee grounds by hydrothermal carbonisation. *Renewable Energy*,

147, 1380–1391. https://doi.org/10.1016/j.renene.2019.09.098

Ahmed, A., Abu Bakar, M. S., Azad, A. K., Sukri, R. S., & Phusunti, N. (2018). Intermediate pyrolysis

of Acacia cincinnata and Acacia holosericea species for bio-oil and biochar production.

Energy Conversion and Management, *176*, 393–408.

https://doi.org/10.1016/j.enconman.2018.09.041

Ahmed, M., Andreottola, G., Elagroudy, S., Negm, M. S., & Fiori, L. (2021). Coupling hydrothermal

carbonization and anaerobic digestion for sewage digestate management: Influence of

hydrothermal treatment time on dewaterability and bio-methane production. *Journal of*

Environmental Management, *281*, 111910.

https://doi.org/10.1016/j.jenvman.2020.111910

Akarsu, K., Duman, G., Yilmazer, A., Keskin, T., Azbar, N., & Yanik, J. (2019). Sustainable valorization

of food wastes into solid fuel by hydrothermal carbonization. *Bioresource Technology*, *292*,

121959. https://doi.org/10.1016/j.biortech.2019.121959

Alhnidi, M.-J., Wüst, D., Funke, A., Hang, L., & Kruse, A. (2020). Fate of Nitrogen, Phosphate, and

Potassium during Hydrothermal Carbonization and the Potential for Nutrient Recovery.

ACS Sustainable Chemistry & Engineering, *8*(41), 15507–15516.

https://doi.org/10.1021/acssuschemeng.0c04229

Alibardi, L., Astrup, T. F., Asunis, F., Clarke, W. P., De Gioannis, G., Dessì, P., Lens, P. N. L.,
Lavagnolo, M. C., Lombardi, L., Muntoni, A., Pivato, A., Polettini, A., Pomi, R., Rossi, A.,
Spagni, A., & Spiga, D. (2020). Organic waste biorefineries: Looking towards
implementation. *Waste Management*, *114*, 274–286.
https://doi.org/10.1016/j.wasman.2020.07.010

Allen, S. G., Kam, L. C., Zemann, A. J., & Antal, M. J. (1996). Fractionation of Sugar Cane with Hot,
Compressed, Liquid Water. *Industrial & Engineering Chemistry Research*, *35*(8), 2709–2715.
https://doi.org/10.1021/ie950594s

Álvarez, M. L., Gascó, G., Plaza, C., Paz-Ferreiro, J., & Méndez, A. (2017). Hydrochars from Biosolids
and Urban Wastes as Substitute Materials for Peat. *Land Degradation & Development*,
28(7), 2268–2276. https://doi.org/10.1002/ldr.2756

Ambaye, T. G., Vaccari, M., van Hullebusch, E. D., Amrane, A., & Rtimi, S. (2021). Mechanisms and
adsorption capacities of biochar for the removal of organic and inorganic pollutants from
industrial wastewater. *International Journal of Environmental Science and Technology*,
18(10), 3273–3294. https://doi.org/10.1007/s13762-020-03060-w

Ansorge, O. (2009). *Biogenic amines and grapes: Effect of microbes and fining agents*. 6.

Aragón-Briceño, C. I., Grasham, O., Ross, A. B., Dupont, V., & Camargo-Valero, M. A. (2020).
Hydrothermal carbonization of sewage digestate at wastewater treatment works:
Influence of solid loading on characteristics of hydrochar, process water and plant
energetics. *Renewable Energy*, *157*, 959–973.
https://doi.org/10.1016/j.renene.2020.05.021

Aragón-Briceño, C., Ross, A. B., & Camargo-Valero, M. A. (2017). Evaluation and comparison of
product yields and bio-methane potential in sewage digestate following hydrothermal

treatment. *Applied Energy*, *208*, 1357–1369.

https://doi.org/10.1016/j.apenergy.2017.09.019

Arauzo, P. J., Atienza-Martínez, M., Ábrego, J., Olszewski, M. P., Cao, Z., & Kruse, A. (2020).

Combustion Characteristics of Hydrochar and Pyrochar Derived from Digested Sewage

Sludge. *Energies*, *13*(16), 4164. https://doi.org/10.3390/en13164164

Asquer, C., Melis, E., Scano, E. A., & Carboni, G. (2019). Opportunities for Green Energy through

Emerging Crops: Biogas Valorization of Cannabis sativa L. Residues. *Climate*, *7*(12), 142.

https://doi.org/10.3390/cli7120142

Asunis, F., De Gioannis, G., Isipato, M., Muntoni, A., Polettini, A., Pomi, R., Rossi, A., & Spiga, D.

(2019). Control of fermentation duration and pH to orient biochemicals and biofuels

production from cheese whey. *Bioresource Technology*, *289*, 121722.

https://doi.org/10.1016/j.biortech.2019.121722

Barbier, E. B., & Burgess, J. C. (2021). *Economics of Peatlands Conservation, Restoration and*

Sustainable Management (p. 53). United Nations Environment Programme.

Bargmann, I., Rillig, M. C., Buss, W., Kruse, A., & Kuecke, M. (2013). Hydrochar and Biochar Effects

on Germination of Spring Barley. *Journal of Agronomy and Crop Science*, *199*(5), 360–373.

https://doi.org/10.1111/jac.12024

Bargmann, I., Rillig, M. C., Kruse, A., Greef, J.-M., & Kücke, M. (2014). Effects of hydrochar

application on the dynamics of soluble nitrogen in soils and on plant availability. *Journal of*

Plant Nutrition and Soil Science, *177*(1), 48–58. https://doi.org/10.1002/jpln.201300069

Bartlett, A. I., Hadden, R. M., & Bisby, L. A. (2019). A Review of Factors Affecting the Burning

Behaviour of Wood for Application to Tall Timber Construction. *Fire Technology*, *55*(1), 1–

49. https://doi.org/10.1007/s10694-018-0787-y

Basso, D., Patuzzi, F., Castello, D., Baratieri, M., Rada, E. C., Weiss-Hortala, E., & Fiori, L. (2016). Agro-industrial waste to solid biofuel through hydrothermal carbonization. *Waste Management*, *47*, 114–121. https://doi.org/10.1016/j.wasman.2015.05.013

Bates, A. K. (2010). *The biochar solution: Carbon farming and climate change*. New Society Publishers.

Becker, G. C., Wüst, D., Köhler, H., Lautenbach, A., & Kruse, A. (2019). Novel approach of phosphate-reclamation as struvite from sewage sludge by utilising hydrothermal carbonization. *Journal of Environmental Management*, *238*, 119–125. https://doi.org/10.1016/j.jenvman.2019.02.121

Belete, Y. Z., Leu, S., Boussiba, S., Zorin, B., Posten, C., Thomsen, L., Wang, S., Gross, A., & Bernstein, R. (2019). Characterization and utilization of hydrothermal carbonization aqueous phase as nutrient source for microalgal growth. *Bioresource Technology*, *290*, 121758. https://doi.org/10.1016/j.biortech.2019.121758

Belete, Y. Z., Mau, V., Yahav Spitzer, R., Posmanik, R., Jassby, D., Iddya, A., Kassem, N., Tester, J. W., & Gross, A. (2021). Hydrothermal carbonization of anaerobic digestate and manure from a dairy farm on energy recovery and the fate of nutrients. *Bioresource Technology*, *333*, 125164. https://doi.org/10.1016/j.biortech.2021.125164

Belzagui, F., Buscio, V., Gutiérrez-Bouzán, C., & Vilaseca, M. (2021). Cigarette butts as a microfiber source with a microplastic level of concern. *Science of The Total Environment*, *762*, 144165. https://doi.org/10.1016/j.scitotenv.2020.144165

Bengtsson, G., Bengtson, P., & Månsson, K. F. (2003). Gross nitrogen mineralization-, immobilization-, and nitrification rates as a function of soil C/N ratio and microbial activity. *Soil Biology and Biochemistry*, *35*(1), 143–154. https://doi.org/10.1016/S0038-0717(02)00248-1

Berge, N. D., Ro, K. S., Mao, J., Flora, J. R. V., Chappell, M. A., & Bae, S. (2011). Hydrothermal

Carbonization of Municipal Waste Streams. *Environmental Science & Technology*, *45*(13),

5696–5703. https://doi.org/10.1021/es2004528

Beutel, M. W., Harmon, T. C., Novotny, T. E., Mock, J., Gilmore, M. E., Hart, S. C., Traina, S.,

Duttagupta, S., Brooks, A., Jerde, C. L., Hoh, E., Van De Werfhorst, L. C., Butsic, V.,

Wartenberg, A. C., & Holden, P. A. (2021). A Review of Environmental Pollution from the

Use and Disposal of Cigarettes and Electronic Cigarettes: Contaminants, Sources, and

Impacts. *Sustainability*, *13*(23), 12994. https://doi.org/10.3390/su132312994

Bierhuizen, J. F., & Wagenvoort, W. A. (1974). Some aspects of seed germination in vegetables. 1.

The determination and application of heat sums and minimum temperature for

germination. *Scientia Horticulturae*, *2*(3), 213–219. https://doi.org/10.1016/0304-

4238(74)90029-6

Biller, P., Ross, A. B., Skill, S. C., Lea-Langton, A., Balasundaram, B., Hall, C., Riley, R., & Llewellyn, C.

A. (2012). Nutrient recycling of aqueous phase for microalgae cultivation from the

hydrothermal liquefaction process. *Algal Research*, *1*(1), 70–76.

https://doi.org/10.1016/j.algal.2012.02.002

Binner, E., Böhm, K., & Lechner, P. (2012). Large scale study on measurement of respiration

activity (AT4) by Sapromat and OxiTop. *Waste Management*, *32*(10), 1752–1759.

https://doi.org/10.1016/j.wasman.2012.05.024

Boulanger, A., Pinet, E., Bouix, M., Bouchez, T., & Mansour, A. A. (2012). Effect of inoculum to

substrate ratio (I/S) on municipal solid waste anaerobic degradation kinetics and potential.

Waste Management, *32*(12), 2258–2265. https://doi.org/10.1016/j.wasman.2012.07.024

Bridgwater, A. (2000). Fast pyrolysis processes for biomass. *Renewable and Sustainable Energy*

Reviews, *4*(1), 1–73. https://doi.org/10.1016/S1364-0321(99)00007-6

Brillard, A., Kehrli, D., Douguet, O., Gautier, K., Tschamber, V., Bueno, M.-A., & Brilhac, J.-F. (2021). Pyrolysis and combustion of community masks: Thermogravimetric analyses, characterizations, gaseous emissions, and kinetic modeling. *Fuel*, *306*, 121644. https://doi.org/10.1016/j.fuel.2021.121644

Brust, G. E. (2019). Management Strategies for Organic Vegetable Fertility. In *Safety and Practice for Organic Food* (pp. 193–212). Elsevier. https://doi.org/10.1016/B978-0-12-812060-6.00009-X

Busch, D., Kammann, C., Grünhage, L., & Müller, C. (2012). Simple Biotoxicity Tests for Evaluation of Carbonaceous Soil Additives: Establishment and Reproducibility of Four Test Procedures. *Journal of Environmental Quality*, *41*(4), 1023–1032. https://doi.org/10.2134/jeq2011.0122

Busch, D., Stark, A., Kammann, C. I., & Glaser, B. (2013). Genotoxic and phytotoxic risk assessment of fresh and treated hydrochar from hydrothermal carbonization compared to biochar from pyrolysis. *Ecotoxicology and Environmental Safety*, *97*, 59–66. https://doi.org/10.1016/j.ecoenv.2013.07.003

Cai, J., Li, B., Chen, C., Wang, J., Zhao, M., & Zhang, K. (2016). Hydrothermal carbonization of tobacco stalk for fuel application. *Bioresource Technology*, *220*, 305–311. https://doi.org/10.1016/j.biortech.2016.08.098

Cao, Z., Hülsemann, B., Wüst, D., Illi, L., Oechsner, H., & Kruse, A. (2020). Valorization of maize silage digestate from two-stage anaerobic digestion by hydrothermal carbonization. *Energy Conversion and Management*, *222*, 113218. https://doi.org/10.1016/j.enconman.2020.113218

Cao, Z., Jung, D., Olszewski, M. P., Arauzo, P. J., & Kruse, A. (2019). Hydrothermal carbonization of biogas digestate: Effect of digestate origin and process conditions. *Waste Management*, *100*, 138–150. https://doi.org/10.1016/j.wasman.2019.09.009

Casazza, A. A., Aliakbarian, B., Lagazzo, A., Garbarino, G., Carnasciali, M. M., Perego, P., & Busca, G. (2016). Pyrolysis of grape marc before and after the recovery of polyphenol fraction. *Fuel Processing Technology*, *153*, 121–128. https://doi.org/10.1016/j.fuproc.2016.07.014

Celletti, S., Lanz, M., Bergamo, A., Benedetti, V., Basso, D., Baratieri, M., Cesco, S., & Mimmo, T. (2021). Evaluating the Aqueous Phase From Hydrothermal Carbonization of Cow Manure Digestate as Possible Fertilizer Solution for Plant Growth. *Frontiers in Plant Science*, *12*, 687434. https://doi.org/10.3389/fpls.2021.687434

Cervera-Mata, A., Fernández-Arteaga, A., Navarro-Alarcón, M., Hinojosa, D., Pastoriza, S., Delgado, G., & Rufián-Henares, J. Á. (2021). Spent coffee grounds as a source of smart biochelates to increase Fe and Zn levels in lettuces. *Journal of Cleaner Production*, *328*, 129548. https://doi.org/10.1016/j.jclepro.2021.129548

Cervera-Mata, A., Lara, L., Fernández-Arteaga, A., Ángel Rufián-Henares, J., & Delgado, G. (2021). Washed hydrochar from spent coffee grounds: A second generation of coffee residues. Evaluation as organic amendment. *Waste Management*, *120*, 322–329. https://doi.org/10.1016/j.wasman.2020.11.041

Chapman, S. (2006). Butt clean up campaigns: Wolves in sheep's clothing? *Tobacco Control*, *15*(4), 273–273. https://doi.org/10.1136/tc.2006.017590

Chynoweth, D. P., Turick, C. E., Owens, J. M., Jerger, D. E., & Peck, M. W. (1993). Biochemical methane potential of biomass and waste feedstocks. *Biomass and Bioenergy*, *5*(1), 95–111. https://doi.org/10.1016/0961-9534(93)90010-2

Codignole Luz, F., Volpe, M., Fiori, L., Manni, A., Cordiner, S., Mulone, V., & Rocco, V. (2018). Spent coffee enhanced biomethane potential via an integrated hydrothermal carbonization-anaerobic digestion process. *Bioresource Technology*, *256*, 102–109. https://doi.org/10.1016/j.biortech.2018.02.021

Crespo, C., Ibarz, G., Sáenz, C., Gonzalez, P., & Roche, S. (2021). Study of Recycling Potential of

FFP2 Face Masks and Characterization of the Plastic Mix-Material Obtained. A Way of

Reducing Waste in Times of Covid-19. *Waste and Biomass Valorization*, *12*(12), 6423–6432.

https://doi.org/10.1007/s12649-021-01476-0

Crippa, M., Solazzo, E., Guizzardi, D., Monforti-Ferrario, F., Tubiello, F. N., & Leip, A. (2021). Food

systems are responsible for a third of global anthropogenic GHG emissions. *Nature Food*,

2(3), 198–209. https://doi.org/10.1038/s43016-021-00225-9

Cross, A., & Sohi, S. P. (2013). A method for screening the relative long-term stability of biochar.

GCB Bioenergy, *5*(2), 215–220. https://doi.org/10.1111/gcbb.12035

Crossley, O. P., Thorpe, R. B., Peus, D., & Lee, J. (2020). Phosphorus recovery from process waste

water made by the hydrothermal carbonisation of spent coffee grounds. *Bioresource*

Technology, *301*, 122664. https://doi.org/10.1016/j.biortech.2019.122664

Dalias, P., Prasad, M., Mumme, J., Kern, J., Stylianou, M., & Christou, A. (2018). Low-cost post-

treatments improve the efficacy of hydrochar as peat replacement in growing media.

Journal of Environmental Chemical Engineering, *6*(5), 6647–6652.

https://doi.org/10.1016/j.jece.2018.10.042

Danso-Boateng, E. (2015). *Biomass hydrothermal carbonisation for sustainable engineering*

[\copyright Eric Danso-Boateng]. https://dspace.lboro.ac.uk/dspace-

jspui/handle/2134/19043

de Jager, M., Röhrdanz, M., & Giani, L. (2020). The influence of hydrochar from biogas digestate on

soil improvement and plant growth aspects. *Biochar*, *2*(2), 177–194.

https://doi.org/10.1007/s42773-020-00054-2

Demirbaş, A. (2001). Carbonization ranking of selected biomass for charcoal, liquid and gaseous

products. *Energy Conversion and Management*, *42*(10), 1229–1238.

https://doi.org/10.1016/S0196-8904(00)00110-2

Dharmaraj, S., Ashokkumar, V., Pandiyan, R., Halimatul Munawaroh, H. S., Chew, K. W., Chen, W.-

H., & Ngamcharussrivichai, C. (2021). Pyrolysis: An effective technique for degradation of

COVID-19 medical wastes. *Chemosphere*, *275*, 130092.

https://doi.org/10.1016/j.chemosphere.2021.130092

d'Heni Teixeira, M. B., Duarte, M. A. B., Raposo Garcez, L., Camargo Rubim, J., Hofmann Gatti, T., &

Suarez, P. A. Z. (2017). Process development for cigarette butts recycling into cellulose

pulp. *Waste Management*, *60*, 140–150. https://doi.org/10.1016/j.wasman.2016.10.013

Dimitriadis, A., & Bezergianni, S. (2017). Hydrothermal liquefaction of various biomass and waste

feedstocks for biocrude production: A state of the art review. *Renewable and Sustainable

Energy Reviews*, *68*, 113–125. https://doi.org/10.1016/j.rser.2016.09.120

Ding, L., Wang, Z., Li, Y., Du, Y., Liu, H., & Guo, Y. (2012). A novel hydrochar and nickel composite

for the electrochemical supercapacitor electrode material. *Materials Letters*, *74*, 111–114.

https://doi.org/10.1016/j.matlet.2012.01.070

Domene, X., Hanley, K., Enders, A., & Lehmann, J. (2015). Short-term mesofauna responses to soil

additions of corn stover biochar and the role of microbial biomass. *Applied Soil Ecology*,

89(Supplement C), 10–17. https://doi.org/10.1016/j.apsoil.2014.12.005

Duangchan, A., & Samart, C. (2008). Tertiary recycling of PVC-containing plastic waste by

copyrolysis with cattle manure. *Waste Management*, *28*(11), 2415–2421.

https://doi.org/10.1016/j.wasman.2007.12.010

Ducey, T. F., Collins, J. C., Ro, K. S., Woodbury, B. L., & Griffin, D. D. (2017). Hydrothermal

carbonization of livestock mortality for the reduction of pathogens and microbially-derived

DNA. *Frontiers of Environmental Science & Engineering*, *11*(3), 9.

https://doi.org/10.1007/s11783-017-0930-x

EBC. (2021). *European Biochar Certificate—Guidelines for a Sustainable Production of Biochar*.

European Biochar Foundation (EBC), Arbaz, Switzerland; Version 9.5E of 1st August 2021.

http://european-biochar.org

Ekpo, U., Ross, A. B., Camargo-Valero, M. A., & Williams, P. T. (2016). A comparison of product

yields and inorganic content in process streams following thermal hydrolysis and

hydrothermal processing of microalgae, manure and digestate. *Bioresource Technology*,

200, 951–960. https://doi.org/10.1016/j.biortech.2015.11.018

Elliott, D. C., Beckman, D., Bridgwater, A. V., Diebold, J. P., Gevert, S. B., & Solantausta, Y. (1991).

Developments in direct thermochemical liquefaction of biomass: 1983-1990. *Energy &*

Fuels, *5*(3), 399–410. https://doi.org/10.1021/ef00027a008

Erdogan, E., Atila, B., Mumme, J., Reza, M. T., Toptas, A., Elibol, M., & Yanik, J. (2015).

Characterization of products from hydrothermal carbonization of orange pomace including

anaerobic digestibility of process liquor. *Bioresource Technology*, *196*, 35–42.

https://doi.org/10.1016/j.biortech.2015.06.115

European Commission. (2001). *Working Document on the Biological Treatment of Biowaste*.

http://www.cre.ie/docs/EU_BiowasteDirective_workingdocument_2nddraft.pdf

Fan, M., Dai, D., & Huang, B. (2012). Fourier Transform Infrared Spectroscopy for Natural Fibres. In

S. Salih (Ed.), *Fourier Transform—Materials Analysis*. InTech.

https://doi.org/10.5772/35482

Fang, J., Zhan, L., Ok, Y. S., & Gao, B. (2018). Minireview of potential applications of hydrochar

derived from hydrothermal carbonization of biomass. *Journal of Industrial and Engineering*

Chemistry, *57*, 15–21. https://doi.org/10.1016/j.jiec.2017.08.026

Ferreira, A. F. (2017). Biorefinery Concept. In M. Rabaçal, A. F. Ferreira, C. A. M. Silva, & M. Costa (Eds.), *Biorefineries* (Vol. 57, pp. 1–20). Springer International Publishing. https://doi.org/10.1007/978-3-319-48288-0_1

Ferrentino, R., Merzari, F., Grigolini, E., Fiori, L., & Andreottola, G. (2021). Hydrothermal carbonization liquor as external carbon supplement to improve biological denitrification in wastewater treatment. *Journal of Water Process Engineering*, *44*, 102360. https://doi.org/10.1016/j.jwpe.2021.102360

Ficara, E., & Rozzi, A. (2001). PH-Stat Titration to Assess Nitrification Inhibition. *Journal of Environmental Engineering*, *127*(8), 698–704. https://doi.org/10.1061/(ASCE)0733-9372(2001)127:8(698)

Fitzer, E., Kochling, K.-H., Boehm, H. P., & Marsh, H. (1995). Recommended terminology for the description of carbon as a solid (IUPAC Recommendations 1995). *Pure and Applied Chemistry*, *67*(3), 473–506. https://doi.org/10.1351/pac199567030473

Fregolente, L. G., Miguel, T. B. A. R., de Castro Miguel, E., de Almeida Melo, C., Moreira, A. B., Ferreira, O. P., & Bisinoti, M. C. (2019). Toxicity evaluation of process water from hydrothermal carbonization of sugarcane industry by-products. *Environmental Science and Pollution Research*, *26*(27), 27579–27589. https://doi.org/10.1007/s11356-018-1771-2

Freire Lima, C., Amaral dos Santos Pinto, M., Brasil Choueri, R., Buruaem Moreira, L., & Braga Castro, Í. (2021). Occurrence, characterization, partition, and toxicity of cigarette butts in a highly urbanized coastal area. *Waste Management*, *131*, 10–19. https://doi.org/10.1016/j.wasman.2021.05.029

Fryda, L., Visser, R., & Schmidt, J. (2018). Biochar replaces peat in horticulture: Environmental impact assessment of combined biochar & bioenergy production. *Detritus*, *Volume 05-March 2019*(0), 1. https://doi.org/10.31025/2611-4135/2019.13778

Funke, A., & Ziegler, F. (2010). Hydrothermal carbonization of biomass: A summary and discussion of chemical mechanisms for process engineering. *Biofuels, Bioproducts and Biorefining*, *4*(2), 160–177. https://doi.org/10.1002/bbb.198

Gabhane, J. W., Bhange, V. P., Patil, P. D., Bankar, S. T., & Kumar, S. (2020). Recent trends in biochar production methods and its application as a soil health conditioner: A review. *SN Applied Sciences*, *2*(7), 1307. https://doi.org/10.1007/s42452-020-3121-5

Gao, Y., Wang, X., Wang, J., Li, X., Cheng, J., Yang, H., & Chen, H. (2013). Effect of residence time on chemical and structural properties of hydrochar obtained by hydrothermal carbonization of water hyacinth. *Energy*, *58*, 376–383. https://doi.org/10.1016/j.energy.2013.06.023

Gilbert, N. (2012). One-third of our greenhouse gas emissions come from agriculture. *Nature*, nature.2012.11708. https://doi.org/10.1038/nature.2012.11708

Glenk, K., & Martin-Ortega, J. (2018). The economics of peatland restoration. *Journal of Environmental Economics and Policy*, *7*(4), 345–362. https://doi.org/10.1080/21606544.2018.1434562

Hämäläinen, A., Kokko, M., Kinnunen, V., Hilli, T., & Rintala, J. (2021). Hydrothermal carbonisation of mechanically dewatered digested sewage sludge—Energy and nutrient recovery in centralised biogas plant. *Water Research*, *201*, 117284. https://doi.org/10.1016/j.watres.2021.117284

Harper, S. H. T., & Lynch, J. M. (1980). MICROBIAL EFFECTS ON THE GERMINATION AND SEEDLING GROWTH OF BARLEY. *New Phytologist*, *84*(3), 473–481. https://doi.org/10.1111/j.1469-8137.1980.tb04554.x

Harris, B. (2011). The intractable cigarette "filter problem." *Tobacco Control*, *20*(Supplement 1), i10–i16. https://doi.org/10.1136/tc.2010.040113

He, C., Giannis, A., & Wang, J.-Y. (2013). Conversion of sewage sludge to clean solid fuel using

hydrothermal carbonization: Hydrochar fuel characteristics and combustion behavior.

Applied Energy, *111*, 257–266. https://doi.org/10.1016/j.apenergy.2013.04.084

He, C., Wang, K., Giannis, A., Yang, Y., & Wang, J.-Y. (2015). Products evolution during

hydrothermal conversion of dewatered sewage sludge in sub- and near-critical water:

Effects of reaction conditions and calcium oxide additive. *International Journal of Hydrogen*

Energy, *40*(17), 5776–5787. https://doi.org/10.1016/j.ijhydene.2015.03.006

Hernández-Soto, M. C., Hernández-Latorre, M., Oliver-Tomas, B., Ponce, E., & Renz, M. (2019).

Transformation of Organic Household Leftovers into a Peat Substitute. *Journal of Visualized*

Experiments, *149*, 59569. https://doi.org/10.3791/59569

Hitzl, M., Corma, A., Pomares, F., & Renz, M. (2015). The hydrothermal carbonization (HTC) plant

as a decentral biorefinery for wet biomass. *Catalysis Today*, *257*, 154–159.

https://doi.org/10.1016/j.cattod.2014.09.024

Huang, H., & Yuan, X. (2016). The migration and transformation behaviors of heavy metals during

the hydrothermal treatment of sewage sludge. *Bioresource Technology*, *200*, 991–998.

https://doi.org/10.1016/j.biortech.2015.10.099

IBI. (2015). *Standardized Product Definition and Product Testing Guidelines for Biochar That Is Used*

in Soil. International Biochar Initiative; Version 2.1. https://biochar-

international.org/characterizationstandard/

ICO - International Coffee Organization. (2021). *Coffee Market Report—November 2021*.

https://www.ico.org/documents/cy2021-22/cmr-1121-e.pdf

Ischia, G., & Fiori, L. (2020). Hydrothermal Carbonization of Organic Waste and Biomass: A Review

on Process, Reactor, and Plant Modeling. *Waste and Biomass Valorization*.

https://doi.org/10.1007/s12649-020-01255-3

IUPAC. (1997). *Compendium of Chemical Terminology, 2nd ed. (The "Gold Book"). Compiled by A. D. McNaught and A. Wilkinson.* Blackwell Scientific Publications, Oxford.

Jung, D., & Kruse, A. (2017). Evaluation of Arrhenius-type overall kinetic equations for hydrothermal carbonization. *Journal of Analytical and Applied Pyrolysis*, *127*, 286–291. https://doi.org/10.1016/j.jaap.2017.07.023

Kabadayi Catalkopru, A., Kantarli, I. C., & Yanik, J. (2017). Effects of spent liquor recirculation in hydrothermal carbonization. *Bioresource Technology*, *226*, 89–93. https://doi.org/10.1016/j.biortech.2016.12.015

Kambo, H. S., & Dutta, A. (2015). A comparative review of biochar and hydrochar in terms of production, physico-chemical properties and applications. *Renewable and Sustainable Energy Reviews*, *45*, 359–378. https://doi.org/10.1016/j.rser.2015.01.050

Kambo, H. S., Minaret, J., & Dutta, A. (2018). Process Water from the Hydrothermal Carbonization of Biomass: A Waste or a Valuable Product? *Waste and Biomass Valorization*, *9*(7), 1181–1189. https://doi.org/10.1007/s12649-017-9914-0

Karl, K., & Tubiello, F. N. (2021). *Methods for estimating greenhouse gas emissions from food systems*. FAO. https://doi.org/10.4060/cb7028en

Kaur-Bhambra, J., Wardak, D. L. R., Prosser, J. I., & Gubry-Rangin, C. (2021). Revisiting plant biological nitrification inhibition efficiency using multiple archaeal and bacterial ammonia-oxidising cultures. *Biology and Fertility of Soils*. https://doi.org/10.1007/s00374-020-01533-1

Kebelmann, K., Hornung, A., Karsten, U., & Griffiths, G. (2013). Intermediate pyrolysis and product identification by TGA and Py-GC/MS of green microalgae and their extracted protein and lipid components. *Biomass and Bioenergy*, *49*, 38–48. https://doi.org/10.1016/j.biombioe.2012.12.006

Kern, J., Tammeorg, P., Shanskiy, M., Sakrabani, R., Knicker, H., Kammann, C., Tuhkanen, E.-M.,

   Smidt, G., Prasad, M., Tiilikkala, K., Sohi, S., Gascó, G., Steiner, C., & Glaser, B. (2017).

   SYNERGISTIC USE OF PEAT AND CHARRED MATERIAL IN GROWING MEDIA – AN OPTION TO

   REDUCE THE PRESSURE ON PEATLANDS? *Journal of Environmental Engineering and*

   Landscape Management, *25*(2), 160–174.

   https://doi.org/10.3846/16486897.2017.1284665

Kim, S., Kramer, R. W., & Hatcher, P. G. (2003). Graphical Method for Analysis of Ultrahigh-

   Resolution Broadband Mass Spectra of Natural Organic Matter, the Van Krevelen Diagram.

   Analytical Chemistry, *75*(20), 5336–5344. https://doi.org/10.1021/ac034415p

Kodymová, J., Heviánková, S., Kyncl, M., & Rusín, J. (2021). *Testing the Impact of the Waste*

   Product from Biogas Plants on Plant Germination and Initial Root Growth. 7.

Koottatep, T., Fakkaew, K., Tajai, N., Pradeep, S. V., & Polprasert, C. (2016). Sludge stabilization

   and energy recovery by hydrothermal carbonization process. *Renewable Energy*, *99*, 978–

   985. https://doi.org/10.1016/j.renene.2016.07.068

Kozlowski, T. T. (1971). Seed Germination and Seedling Development. In *Seed Germination,*

   Ontogeny, and Shoot Growth (pp. 41–93). Elsevier. https://doi.org/10.1016/B978-0-12-

   424201-2.50008-0

Kruse, A., Funke, A., & Titirici, M.-M. (2013). Hydrothermal conversion of biomass to fuels and

   energetic materials. *Current Opinion in Chemical Biology*, *17*(3), 515–521.

Kruse, A., Koch, F., Stelzl, K., Wüst, D., & Zeller, M. (2016). Fate of nitrogen during hydrothermal

   carbonization. *Energy & Fuels*, *30*(10), 8037–8042.

Krylova, V., & Dukštienė, N. (2013). Synthesis and Characterization of Ag2S Layers Formed on

   Polypropylene. *Journal of Chemistry*, *2013*, 1–11. https://doi.org/10.1155/2013/987879

Kumar, A., Jones, D., & Hanna, M. (2009). Thermochemical Biomass Gasification: A Review of the Current Status of the Technology. *Energies*, *2*(3), 556–581. https://doi.org/10.3390/en20300556

Kumar, M., Olajire Oyedun, A., & Kumar, A. (2018). A review on the current status of various hydrothermal technologies on biomass feedstock. *Renewable and Sustainable Energy Reviews*, *81*, 1742–1770. https://doi.org/10.1016/j.rser.2017.05.270

Kurmus, H., & Mohajerani, A. (2020). The toxicity and valorization options of cigarette butts. *Waste Management*, *104*, 104–118. https://doi.org/10.1016/j.wasman.2020.01.011

Langone, M., & Basso, D. (2020). Process Waters from Hydrothermal Carbonization of Sludge: Characteristics and Possible Valorization Pathways. *International Journal of Environmental Research and Public Health*, *17*(18), 6618. https://doi.org/10.3390/ijerph17186618

Lazzari, E., Schena, T., Marcelo, M. C. A., Primaz, C. T., Silva, A. N., Ferrão, M. F., Bjerk, T., & Caramão, E. B. (2018). Classification of biomass through their pyrolytic bio-oil composition using FTIR and PCA analysis. *Industrial Crops and Products*, *111*, 856–864. https://doi.org/10.1016/j.indcrop.2017.11.005

Lee, G., Eui Lee, M., Kim, S.-S., Joh, H.-I., & Lee, S. (2022). Efficient upcycling of polypropylene-based waste disposable masks into hard carbons for anodes in sodium ion batteries. *Journal of Industrial and Engineering Chemistry*, *105*, 268–277. https://doi.org/10.1016/j.jiec.2021.09.026

Lehmann, J., & Joseph, S. (2009). Biochar for Environmental Management—An Introduction. In J. Lehmann & S. Joseph (Eds.), *Biochar for Environemental Management: Science and Technology* (pp. 1–12). Earthscan. http://www.biochar-international.org/projects/book

Liang, Y., Song, Q., Wu, N., Li, J., Zhong, Y., & Zeng, W. (2021). Repercussions of COVID-19 pandemic on solid waste generation and management strategies. *Frontiers of*

Environmental Science & Engineering, *15*(6), 115. https://doi.org/10.1007/s11783-021-1407-5

Libra, J. A., Ro, K. S., Kammann, C., Funke, A., Berge, N. D., Neubauer, Y., Titirici, M.-M., Fühner, C., Bens, O., Kern, J., & Emmerich, K.-H. (2011). Hydrothermal carbonization of biomass residuals: A comparative review of the chemistry, processes and applications of wet and dry pyrolysis. *Biofuels*, *2*(1), 71–106. https://doi.org/10.4155/bfs.10.81

Linstrom, P. (1997). *NIST Chemistry WebBook, NIST Standard Reference Database 69* [Data set]. National Institute of Standards and Technology. https://doi.org/10.18434/T4D303

López Barreiro, D., Prins, W., Ronsse, F., & Brilman, W. (2013). Hydrothermal liquefaction (HTL) of microalgae for biofuel production: State of the art review and future prospects. *Biomass and Bioenergy*, *53*, 113–127. https://doi.org/10.1016/j.biombioe.2012.12.029

Lucian, M., Volpe, M., Gao, L., Piro, G., Goldfarb, J. L., & Fiori, L. (2018). Impact of hydrothermal carbonization conditions on the formation of hydrochars and secondary chars from the organic fraction of municipal solid waste. *Fuel*, *233*, 257–268. https://doi.org/10.1016/j.fuel.2018.06.060

Mäkelä, M., Benavente, V., & Fullana, A. (2016). Hydrothermal carbonization of industrial mixed sludge from a pulp and paper mill. *Bioresource Technology*, *200*, 444–450. https://doi.org/10.1016/j.biortech.2015.10.062

Mäkelä, M., Forsberg, J., Söderberg, C., Larsson, S. H., & Dahl, O. (2018). Process water properties from hydrothermal carbonization of chemical sludge from a pulp and board mill. *Bioresource Technology*, *263*, 654–659. https://doi.org/10.1016/j.biortech.2018.05.044

Makhaye, G., Mofokeng, M. M., Tesfay, S., Aremu, A. O., Van Staden, J., & Amoo, S. O. (2021). Influence of plant biostimulant application on seed germination. In *Biostimulants for Crops*

from Seed Germination to Plant Development (pp. 109–135). Elsevier.

https://doi.org/10.1016/B978-0-12-823048-0.00014-9

Maniscalco, M. P., Volpe, M., & Messineo, A. (2020). Hydrothermal Carbonization as a Valuable

Tool for Energy and Environmental Applications: A Review. *Energies*, *13*(16), 4098.

https://doi.org/10.3390/en13164098

Marah, M., & Novotny, T. E. (2011). Geographic patterns of cigarette butt waste in the urban

environment. *Tobacco Control*, *20*(Supplement 1), i42–i44.

https://doi.org/10.1136/tc.2010.042424

Marin-Batista, J. D., Mohedano, A. F., Rodríguez, J. J., & de la Rubia, M. A. (2020). Energy and

phosphorous recovery through hydrothermal carbonization of digested sewage sludge.

Waste Management, *105*, 566–574. https://doi.org/10.1016/j.wasman.2020.03.004

Masoumi, S., Borugadda, V. B., Nanda, S., & Dalai, A. K. (2021). Hydrochar: A Review on Its

Production Technologies and Applications. *Catalysts*, *11*(8), 939.

https://doi.org/10.3390/catal11080939

Massaya, J., Prates Pereira, A., Mills-Lamptey, B., Benjamin, J., & Chuck, C. J. (2019).

Conceptualization of a spent coffee grounds biorefinery: A review of existing valorisation

approaches. *Food and Bioproducts Processing*, *118*, 149–166.

https://doi.org/10.1016/j.fbp.2019.08.010

Maunuksela, L., Herranen, M., & Torniainen, M. (2012). Quality Assessment of Biogas Plant End

Products by Plant Bioassays. *International Journal of Environmental Science and

Development*, 305–310. https://doi.org/10.7763/IJESD.2012.V3.236

McNutt, J., & He, Q. (Sophia). (2019). Spent coffee grounds: A review on current utilization. *Journal

of Industrial and Engineering Chemistry*, *71*, 78–88.

https://doi.org/10.1016/j.jiec.2018.11.054

Méndez, A., Cárdenas-Aguiar, E., Paz-Ferreiro, J., Plaza, C., & Gascó, G. (2017). The effect of sewage sludge biochar on peat-based growing media. *Biological Agriculture & Horticulture*, *33*(1), 40–51. https://doi.org/10.1080/01448765.2016.1185645

Merzari, F., Goldfarb, J., Andreottola, G., Mimmo, T., Volpe, M., & Fiori, L. (2020). Hydrothermal Carbonization as a Strategy for Sewage Sludge Management: Influence of Process Withdrawal Point on Hydrochar Properties. *Energies*, *13*(11), 2890. https://doi.org/10.3390/en13112890

Milia, S., Malloci, E., & Carucci, A. (2016a). Aerobic granulation with petrochemical wastewater in a sequencing batch reactor under different operating conditions. *Desalination and Water Treatment*, 1–10. https://doi.org/10.1080/19443994.2016.1191778

Milia, S., Porcu, R., Rossetti, S., & Carucci, A. (2016b). Performance and Characteristics of Aerobic Granular Sludge Degrading 2,4,6-Trichlorophenol at Different Volumetric Organic Loading Rates: Water. *CLEAN - Soil, Air, Water*, *44*(6), 615–623. https://doi.org/10.1002/clen.201500127

Mofokeng, M. M., Araya, H. T., Araya, N. A., Makgato, M. J., Mokgehle, S. N., Masemola, M. C., Mudau, F. N., du Plooy, C. P., & Amoo, S. O. (2021). Integrating biostimulants in agrosystem to promote soil health and plant growth. In *Biostimulants for Crops from Seed Germination to Plant Development* (pp. 87–108). Elsevier. https://doi.org/10.1016/B978-0-12-823048-0.00004-6

Mohan, D., Pittman, C. U., & Steele, P. H. (2006). Pyrolysis of Wood/Biomass for Bio-oil: A Critical Review. *Energy & Fuels*, *20*(3), 848–889. https://doi.org/10.1021/ef0502397

Muhlack, R. A., Potumarthi, R., & Jeffery, D. W. (2018). Sustainable wineries through waste valorisation: A review of grape marc utilisation for value-added products. *Waste Management*, *72*, 99–118. https://doi.org/10.1016/j.wasman.2017.11.011

Muntoni, A. (2019). Waste biorefineries: Opportunities and perspectives. *Detritus*, *Volume 05-March 2019*(0), 1. https://doi.org/10.31025/2611-4135/2019.13791

Nandiyanto, A. B. D., Oktiani, R., & Ragadhita, R. (2019). How to Read and Interpret FTIR Spectroscope of Organic Material. *Indonesian Journal of Science and Technology*, *4*(1), 97. https://doi.org/10.17509/ijost.v4i1.15806

Niinipuu, M., Latham, K. G., Boily, J.-F., Bergknut, M., & Jansson, S. (2020). The impact of hydrothermal carbonization on the surface functionalities of wet waste materials for water treatment applications. *Environmental Science and Pollution Research*, *27*(19), 24369–24379. https://doi.org/10.1007/s11356-020-08591-w

Ning, X., Teng, H., Wang, G., Zhang, J., Zhang, N., Huang, C., & Wang, C. (2020). Physiochemical, structural and combustion properties of hydrochar obtained by hydrothermal carbonization of waste polyvinyl chloride. *Fuel*, *270*, 117526. https://doi.org/10.1016/j.fuel.2020.117526

Nizamuddin, S., Baloch, H. A., Griffin, G. J., Mubarak, N. M., Bhutto, A. W., Abro, R., Mazari, S. A., & Ali, B. S. (2017). An overview of effect of process parameters on hydrothermal carbonization of biomass. *Renewable and Sustainable Energy Reviews*, *73*, 1289–1299. https://doi.org/10.1016/j.rser.2016.12.122

Nocentini, M., Panettieri, M., García de Castro Barragán, J. M., Mastrolonardo, G., & Knicker, H. (2021). Recycling pyrolyzed organic waste from plant nurseries, rice production and shrimp industry as peat substitute in potting substrates. *Journal of Environmental Management*, *277*, 111436. https://doi.org/10.1016/j.jenvman.2020.111436

Norton, J. M., & Stark, J. M. (2011). Chapter Fifteen—Regulation and Measurement of Nitrification in Terrestrial Systems. In M. G. Klotz (Ed.), *Methods in Enzymology* (Vol. 486, pp. 343–368). Academic Press. https://doi.org/10.1016/B978-0-12-381294-0.00015-8

Norton, J., & Ouyang, Y. (2019). Controls and Adaptive Management of Nitrification in Agricultural Soils. *Frontiers in Microbiology*, *10*, 1931. https://doi.org/10.3389/fmicb.2019.01931

OIV - International Organisation of Vine and Wine Intergovernmental Organisation. (2021). *Statistical Report on World Vitiviniculture*. https://www.oiv.int/public/medias/7909/oiv-state-of-the-world-vitivinicultural-sector-in-2020.pdf

Okolie, J. A., Rana, R., Nanda, S., Dalai, A. K., & Kozinski, J. A. (2019). Supercritical water gasification of biomass: A state-of-the-art review of process parameters, reaction mechanisms and catalysis. *Sustainable Energy & Fuels*, *3*(3), 578–598. https://doi.org/10.1039/C8SE00565F

Oleszczuk, P., Jośko, I., & Kuśmierz, M. (2013). Biochar properties regarding to contaminants content and ecotoxicological assessment. *Journal of Hazardous Materials*, *260*, 375–382. https://doi.org/10.1016/j.jhazmat.2013.05.044

Oliveira, I., Blöhse, D., & Ramke, H.-G. (2013). Hydrothermal carbonization of agricultural residues. *Bioresource Technology*, *142*, 138–146. https://doi.org/10.1016/j.biortech.2013.04.125

Olszyk, D. M., Shiroyama, T., Novak, J. M., & Johnson, M. G. (2018). A Rapid-Test for Screening Biochar Effects on Seed Germination. *Communications in Soil Science and Plant Analysis*, *49*(16), 2025–2041. https://doi.org/10.1080/00103624.2018.1495726

Onay, O., & Kockar, O. M. (2003). Slow, fast and flash pyrolysis of rapeseed. *Renewable Energy*, *28*(15), 2417–2433. https://doi.org/10.1016/S0960-1481(03)00137-X

Owsianiak, M., Ryberg, M. W., Renz, M., Hitzl, M., & Hauschild, M. Z. (2016). Environmental Performance of Hydrothermal Carbonization of Four Wet Biomass Waste Streams at Industry-Relevant Scales. *ACS Sustainable Chemistry & Engineering*, *4*(12), 6783–6791. https://doi.org/10.1021/acssuschemeng.6b01732

Pagés-Díaz, J., Cerda Alvarado, A. O., Montalvo, S., Diaz-Robles, L., & Curio, C. H. (2020). Anaerobic

bio-methane potential of the liquors from hydrothermal carbonization of different

lignocellulose biomasses. *Renewable Energy*, *157*, 182–189.

https://doi.org/10.1016/j.renene.2020.05.025

Pagga, U., Bachner, J., & Strotmann, U. (2006). Inhibition of nitrification in laboratory tests and

model wastewater treatment plants. *Chemosphere*, *65*(1), 1–8.

https://doi.org/10.1016/j.chemosphere.2006.03.021

Papadopoulou, E. S., Bachtsevani, E., Lampronikou, E., Adamou, E., Katsaouni, A., Vasileiadis, S.,

Thion, C., Menkissoglu-Spiroudi, U., Nicol, G. W., & Karpouzas, D. G. (2020). Comparison of

Novel and Established Nitrification Inhibitors Relevant to Agriculture on Soil Ammonia- and

Nitrite-Oxidizing Isolates. *Frontiers in Microbiology*, *11*, 581283.

https://doi.org/10.3389/fmicb.2020.581283

Parmar, K. R., & Ross, A. B. (2019). Integration of Hydrothermal Carbonisation with Anaerobic

Digestion; Opportunities for Valorisation of Digestate. *Energies*, *12*(9), 1586.

https://doi.org/10.3390/en12091586

Patrício Silva, A. L., Prata, J. C., Duarte, A. C., Barcelò, D., & Rocha-Santos, T. (2021). An urgent call

to think globally and act locally on landfill disposable plastics under and after covid-19

pandemic: Pollution prevention and technological (Bio) remediation solutions. *Chemical

Engineering Journal*, *426*, 131201. https://doi.org/10.1016/j.cej.2021.131201

Pecchi, M., & Baratieri, M. (2019). Coupling anaerobic digestion with gasification, pyrolysis or

hydrothermal carbonization: A review. *Renewable and Sustainable Energy Reviews*, *105*,

462–475. https://doi.org/10.1016/j.rser.2019.02.003

Perra, M., Lozano-Sánchez, J., Leyva-Jiménez, F.-J., Segura-Carretero, A., Pedraz, J. L., Bacchetta,

G., Muntoni, A., De Gioannis, G., Manca, M. L., & Manconi, M. (2021). Extraction of the

antioxidant phytocomplex from wine-making by-products and sustainable loading in

phospholipid vesicles specifically tailored for skin protection. *Biomedicine &*

Pharmacotherapy, *142*, 111959. https://doi.org/10.1016/j.biopha.2021.111959

Pinelo, M., Arnous, A., & Meyer, A. S. (2006). Upgrading of grape skins: Significance of plant cell-

wall structural components and extraction techniques for phenol release. *Trends in Food*

Science & Technology, *17*(11), 579–590. https://doi.org/10.1016/j.tifs.2006.05.003

Plaisant, A., Orsini, A., & Cara, R. (2012). *Caratterizzazione sistemi di campionamento e analisi a*

supporto delle attività di impianto. 49.

Poerschmann, J., Weiner, B., Wedwitschka, H., Baskyr, I., Koehler, R., & Kopinke, F.-D. (2014).

Characterization of biocoals and dissolved organic matter phases obtained upon

hydrothermal carbonization of brewer's spent grain. *Bioresource Technology*, *164*, 162–

169. https://doi.org/10.1016/j.biortech.2014.04.052

Poppendieck, D. G., Khurshid, S. S., & Emmerich, S. J. (2016). *Measuring Airborne Emissions from*

Cigarette Butts: Literature Review and Experimental Plan (NIST IR 8147; p. NIST IR 8147).

National Institute of Standards and Technology. https://doi.org/10.6028/NIST.IR.8147

Prasad, M., Chrysargyris, A., McDaniel, N., Kavanagh, A., Gruda, N. S., & Tzortzakis, N. (2019). Plant

Nutrient Availability and pH of Biochars and Their Fractions, with the Possible Use as a

Component in a Growing Media. *Agronomy*, *10*(1), 10.

https://doi.org/10.3390/agronomy10010010

Prata, J. C., Silva, A. L. P., Walker, T. R., Duarte, A. C., & Rocha-Santos, T. (2020). COVID-19

Pandemic Repercussions on the Use and Management of Plastics. *Environmental Science &*

Technology, *54*(13), 7760–7765. https://doi.org/10.1021/acs.est.0c02178

Puccini, M., Ceccarini, L., Antichi, D., Seggiani, M., Tavarini, S., Hernandez Latorre, M., & Vitolo, S.

(2018). Hydrothermal Carbonization of Municipal Woody and Herbaceous Prunings:

Hydrochar Valorisation as Soil Amendment and Growth Medium for Horticulture.

   Sustainability, *10*(3), 846. https://doi.org/10.3390/su10030846

Qiao, W., Yan, X., Ye, J., Sun, Y., Wang, W., & Zhang, Z. (2011). Evaluation of biogas production

   from different biomass wastes with/without hydrothermal pretreatment. *Renewable*

   Energy, *36*(12), 3313–3318. https://doi.org/10.1016/j.renene.2011.05.002

Rahman, M. T., Mohajerani, A., & Giustozzi, F. (2020). Possible Recycling of Cigarette Butts as Fiber

   Modifier in Bitumen for Asphalt Concrete. *Materials*, *13*(3), 734.

   https://doi.org/10.3390/ma13030734

Raja, A. M., Khalaf, N. H., & Alkubaisy, S. A. (2021). Utilization of Date Palm Waste Compost as

   Substitute For Peat Moss. *IOP Conference Series: Earth and Environmental Science*, *904*(1),

   012041. https://doi.org/10.1088/1755-1315/904/1/012041

Rajesh Banu, J., Preethi, Kavitha, S., Tyagi, V. K., Gunasekaran, M., Karthikeyan, O. P., & Kumar, G.

   (2021). Lignocellulosic biomass based biorefinery: A successful platform towards circular

   bioeconomy. *Fuel*, *302*, 121086. https://doi.org/10.1016/j.fuel.2021.121086

Ramke, H. G., Blohse, D., Lehmann, H., & Fettig, J. (2009, October 5). Hydrothermal carbonization

   of organic waste. *Twelfth International Waste Management and Landfill Symposium*.

   http://www.sardiniasymposium.it/sardinia2009/programme/programme.php

Reza, M. T., Freitas, A., Yang, X., & Coronella, C. J. (2016). Wet Air Oxidation of Hydrothermal

   Carbonization (HTC) Process Liquid. *ACS Sustainable Chemistry & Engineering*, *4*(6), 3250–

   3254. https://doi.org/10.1021/acssuschemeng.6b00292

Rezaee, M., Gitipour, S., & Sarrafzadeh, M.-H. (2020). Different Pathways to Integrate Anaerobic

   Digestion and Thermochemical Processes: Moving Toward the Circular Economy Concept.

   Environmental Energy and Economic Research, *4*(1).

   https://doi.org/10.22097/eeer.2019.189193.1090

Ro, K. S., Cantrell, K. B., & Hunt, P. G. (2010). High-Temperature Pyrolysis of Blended Animal

Manures for Producing Renewable Energy and Value-Added Biochar. *Industrial &*

Engineering Chemistry Research, *49*(20), 10125–10131.

https://doi.org/10.1021/ie101155m

Ro, K. S., Hunt, P. G., Jackson, M. A., Compton, D. L., Yates, S. R., Cantrell, K., & Chang, S. (2014).

Co-pyrolysis of swine manure with agricultural plastic waste: Laboratory-scale study. *Waste*

Management, *34*(8), 1520–1528. https://doi.org/10.1016/j.wasman.2014.04.001

Roehrdanz, M., Greve, T., de Jager, M., Buchwald, R., & Wark, M. (2019). Co-composted hydrochar

substrates as growing media for horticultural crops. *Scientia Horticulturae*, *252*, 96–103.

https://doi.org/10.1016/j.scienta.2019.03.055

Rogovska, N., Laird, D., Cruse, R. M., Trabue, S., & Heaton, E. (2012). Germination Tests for

Assessing Biochar Quality. *Journal of Environmental Quality*, *41*(4), 1014–1022.

https://doi.org/10.2134/jeq2011.0103

Román, S., Libra, J., Berge, N., Sabio, E., Ro, K., Li, L., Ledesma, B., Álvarez, A., & Bae, S. (2018).

Hydrothermal Carbonization: Modeling, Final Properties Design and Applications: A

Review. *Energies*, *11*(1), 216. https://doi.org/10.3390/en11010216

Ruyter, H. P. (1982). Coalification model. *Fuel*, *61*(12), 1182–1187. https://doi.org/10.1016/0016-

2361(82)90017-5

Sánchez Arias, V., Fernández, F. J., Rodríguez, L., & Villaseñor, J. (2012). Respiration indices and

stability measurements of compost through electrolytic respirometry. *Journal of*

Environmental Management, *95*, S134–S138.

https://doi.org/10.1016/j.jenvman.2010.10.053

Saqib, N. U., Baroutian, S., & Sarmah, A. K. (2018). Physicochemical, structural and combustion characterization of food waste hydrochar obtained by hydrothermal carbonization. *Bioresource Technology*, *266*, 357–363. https://doi.org/10.1016/j.biortech.2018.06.112

Schievano, A., Berenguer, R., Goglio, A., Bocchi, S., Marzorati, S., Rago, L., Louro, R. O., Paquete, C. M., & Esteve-Núñez, A. (2019). Electroactive Biochar for Large-Scale Environmental Applications of Microbial Electrochemistry. *ACS Sustainable Chemistry & Engineering*, *7*(22), 18198–18212. https://doi.org/10.1021/acssuschemeng.9b04229

Schmidt, E. L., & Belser, L. W. (2015). Nitrifying Bacteria. In A. L. Page (Ed.), *Agronomy Monographs* (pp. 1027–1042). American Society of Agronomy, Soil Science Society of America. https://doi.org/10.2134/agronmonogr9.2.2ed.c48

Schofield, H. K., Pettitt, T. R., Tappin, A. D., Rollinson, G. K., & Fitzsimons, M. F. (2019). Biochar incorporation increased nitrogen and carbon retention in a waste-derived soil. *Science of The Total Environment*, *690*, 1228–1236. https://doi.org/10.1016/j.scitotenv.2019.07.116

Sharma, H. B., Panigrahi, S., & Dubey, B. K. (2019). Hydrothermal carbonization of yard waste for solid bio-fuel production: Study on combustion kinetic, energy properties, grindability and flowability of hydrochar. *Waste Management*, *91*, 108–119. https://doi.org/10.1016/j.wasman.2019.04.056

Sheets, J. P., Yang, L., Ge, X., Wang, Z., & Li, Y. (2015). Beyond land application: Emerging technologies for the treatment and reuse of anaerobically digested agricultural and food waste. *Waste Management*, *44*, 94–115. https://doi.org/10.1016/j.wasman.2015.07.037

Shen, Y. (2020). A review on hydrothermal carbonization of biomass and plastic wastes to energy products. *Biomass and Bioenergy*, *134*, 105479. https://doi.org/10.1016/j.biombioe.2020.105479

Shi, W., Feng, C., Huang, W., Lei, Z., & Zhang, Z. (2014). Study on interaction between phosphorus and cadmium in sewage sludge during hydrothermal treatment by adding hydroxyapatite. *Bioresource Technology*, *159*, 176–181. https://doi.org/10.1016/j.biortech.2014.02.108

Shi, W., Liu, C., Ding, D., Lei, Z., Yang, Y., Feng, C., & Zhang, Z. (2013). Immobilization of heavy metals in sewage sludge by using subcritical water technology. *Bioresource Technology*, *137*, 18–24. https://doi.org/10.1016/j.biortech.2013.03.106

Simonavicius, E., McNeill, A., Shahab, L., & Brose, L. S. (2019). Heat-not-burn tobacco products: A systematic literature review. *Tobacco Control*, *28*(5), 582–594. https://doi.org/10.1136/tobaccocontrol-2018-054419

Smith, A. M., & Ross, A. B. (2016). Production of bio-coal, bio-methane and fertilizer from seaweed via hydrothermal carbonisation. *Algal Research*, *16*, 1–11. https://doi.org/10.1016/j.algal.2016.02.026

Song, W., & Guo, M. (2012). Quality variations of poultry litter biochar generated at different pyrolysis temperatures. *Journal of Analytical and Applied Pyrolysis*, *94*, 138–145. https://doi.org/10.1016/j.jaap.2011.11.018

Steiner, C., & Harttung, T. (2014). Biochar as a growing media additive and peat substitute. *Solid Earth*, *5*(2), 995–999. https://doi.org/10.5194/se-5-995-2014

Stemann, J., Putschew, A., & Ziegler, F. (2013). Hydrothermal carbonization: Process water characterization and effects of water recirculation. *Bioresource Technology*, *143*, 139–146. https://doi.org/10.1016/j.biortech.2013.05.098

Stökle, K., Hülsemann, B., Steinbach, D., Cao, Z., Oechsner, H., & Kruse, A. (2021). A biorefinery concept using forced chicory roots for the production of biogas, hydrochar, and platform chemicals. *Biomass Conversion and Biorefinery*, *11*(5), 1453–1463. https://doi.org/10.1007/s13399-019-00527-w

Stuart, B. (2004). *Infrared spectroscopy: Fundamentals and applications*. J. Wiley.

Tang, K., Struik, P. C., Yin, X., Thouminot, C., Bjelková, M., Stramkale, V., & Amaducci, S. (2016). Comparing hemp (Cannabis sativa L.) cultivars for dual-purpose production under contrasting environments. *Industrial Crops and Products*, *87*, 33–44. https://doi.org/10.1016/j.indcrop.2016.04.026

Tasca, A. L., Puccini, M., Gori, R., Corsi, I., Galletti, A. M. R., & Vitolo, S. (2019). Hydrothermal carbonization of sewage sludge: A critical analysis of process severity, hydrochar properties and environmental implications. *Waste Management*, *93*, 1–13. https://doi.org/10.1016/j.wasman.2019.05.027

Thomas, S. C. (2021). Post-processing of biochars to enhance plant growth responses: A review and meta-analysis. *Biochar*, *3*(4), 437–455. https://doi.org/10.1007/s42773-021-00115-0

Tian, Y., Sun, X., Li, S., Wang, H., Wang, L., Cao, J., & Zhang, L. (2012). Biochar made from green waste as peat substitute in growth media for Calathea rotundifola cv. Fasciata. *Scientia Horticulturae*, *143*, 15–18. https://doi.org/10.1016/j.scienta.2012.05.018

Titirici, M.-M., Antonietti, M., & Baccile, N. (2008). Hydrothermal carbon from biomass: A comparison of the local structure from poly- to monosaccharides and pentoses/hexoses. *Green Chemistry*, *10*(11), 1204. https://doi.org/10.1039/b807009a

Torkashvand, J., Farzadkia, M., Sobhi, H. R., & Esrafili, A. (2020). Littered cigarette butt as a well-known hazardous waste: A comprehensive systematic review. *Journal of Hazardous Materials*, *383*, 121242. https://doi.org/10.1016/j.jhazmat.2019.121242

Tran, K.-Q. (2016). Fast hydrothermal liquefaction for production of chemicals and biofuels from wet biomass – The need to develop a plug-flow reactor. *Bioresource Technology*, *213*, 327–332. https://doi.org/10.1016/j.biortech.2016.04.002

van Leeuwen, P. W. N. M. (2003). Catalysis, Homogeneous. In *Encyclopedia of Physical Science and Technology* (pp. 457–490). Elsevier. https://doi.org/10.1016/B0-12-227410-5/00085-5

Vasander, H., Tuittila, E.-S., Lode, E., Lundin, L., Ilomets, M., Sallantaus, T., Heikkilä, R., Pitkänen, M.-L., & Laine, J. (2003). [No title found]. *Wetlands Ecology and Management*, *11*(1/2), 51–63. https://doi.org/10.1023/A:1022061622602

Volpe, M., Goldfarb, J. L., & Fiori, L. (2018). Hydrothermal carbonization of Opuntia ficus-indica cladodes: Role of process parameters on hydrochar properties. *Bioresource Technology*, *247*, 310–318. https://doi.org/10.1016/j.biortech.2017.09.072

Wang, G. (2022). Key factors affecting seed germination in phytotoxicity tests during sheep manure composting with carbon additives. *Journal of Hazardous Materials*, 12.

Wang, G., Yang, Y., Kong, Y., Ma, R., Yuan, J., & Li, G. (2022). Key factors affecting seed germination in phytotoxicity tests during sheep manure composting with carbon additives. *Journal of Hazardous Materials*, *421*, 126809. https://doi.org/10.1016/j.jhazmat.2021.126809

Wang, T., Zhai, Y., Zhu, Y., Li, C., & Zeng, G. (2018). A review of the hydrothermal carbonization of biomass waste for hydrochar formation: Process conditions, fundamentals, and physicochemical properties. *Renewable and Sustainable Energy Reviews*, *90*, 223–247. https://doi.org/10.1016/j.rser.2018.03.071

Watson, C. A., Atkinson, D., Gosling, P., Jackson, L. R., & Rayns, F. W. (2006). Managing soil fertility in organic farming systems. *Soil Use and Management*, *18*, 239–247. https://doi.org/10.1111/j.1475-2743.2002.tb00265.x

Wirth, B., & Mumme, J. (2014). Anaerobic Digestion of Waste Water from Hydrothermal Carbonization of Corn Silage. *Applied Bioenergy*, *1*(1). https://doi.org/10.2478/apbi-2013-0001

Wirth, B., Reza, T., & Mumme, J. (2015). Influence of digestion temperature and organic loading rate on the continuous anaerobic treatment of process liquor from hydrothermal carbonization of sewage sludge. *Bioresource Technology*, *198*, 215–222. https://doi.org/10.1016/j.biortech.2015.09.022

World Health Organization and the United Nations Children's Fund (UNICEF). (2020). *Water, sanitation, hygiene, and waste management for the COVID-19 virus: Interim guidance*. World Health Organization. https://apps.who.int/iris/handle/10665/331846

Wu, D., Landsberger, S., & Larson, S. M. (1997). Determination of the elemental distribution in cigarette components and smoke by instrumental neutron activation analysis. *Journal of Radioanalytical and Nuclear Chemistry*, *217*(1), 77–82. https://doi.org/10.1007/BF02055352

Xiao, L.-P., Shi, Z.-J., Xu, F., & Sun, R.-C. (2012). Hydrothermal carbonization of lignocellulosic biomass. *Bioresource Technology*, *118*, 619–623. https://doi.org/10.1016/j.biortech.2012.05.060

Xu, S., Wang, C., Duan, Y., & Wong, J. W.-C. (2020). Impact of pyrochar and hydrochar derived from digestate on the co-digestion of sewage sludge and swine manure. *Bioresource Technology*, *314*, 123730. https://doi.org/10.1016/j.biortech.2020.123730

Xu, X., & Jiang, E. (2017). Treatment of urban sludge by hydrothermal carbonization. *Bioresource Technology*, *238*, 182–187. https://doi.org/10.1016/j.biortech.2017.03.174

Yao, C., Wu, P., Pan, Y., Lu, H., Chi, L., Meng, Y., Cao, X., Xue, S., & Yang, X. (2016). Evaluation of the integrated hydrothermal carbonization-algal cultivation process for enhanced nitrogen utilization in Arthrospira platensis production. *Bioresource Technology*, *216*, 381–390. https://doi.org/10.1016/j.biortech.2016.05.110

Yousef, S., Eimontas, J., Striūgas, N., & Abdelnaby, M. A. (2021). Pyrolysis kinetic behaviour and TG-FTIR-GC–MS analysis of Coronavirus Face Masks. *Journal of Analytical and Applied Pyrolysis*, *156*, 105118. https://doi.org/10.1016/j.jaap.2021.105118

Yu, Y., Lei, Z., Yang, X., Yang, X., Huang, W., Shimizu, K., & Zhang, Z. (2018). Hydrothermal carbonization of anaerobic granular sludge: Effect of process temperature on nutrients availability and energy gain from produced hydrochar. *Applied Energy*, *229*, 88–95. https://doi.org/10.1016/j.apenergy.2018.07.088

Yu, Y., Lei, Z., Yuan, T., Jiang, Y., Chen, N., Feng, C., Shimizu, K., & Zhang, Z. (2017). Simultaneous phosphorus and nitrogen recovery from anaerobically digested sludge using a hybrid system coupling hydrothermal pretreatment with {MAP} precipitation. *Bioresource Technology*, *243*, 634–640. https://doi.org/10.1016/j.biortech.2017.06.178

Zhai, Y., Liu, X., Zhu, Y., Peng, C., Wang, T., Zhu, L., Li, C., & Zeng, G. (2016). Hydrothermal carbonization of sewage sludge: The effect of feed-water pH on fate and risk of heavy metals in hydrochars. *Bioresource Technology*, *218*, 183–188. https://doi.org/10.1016/j.biortech.2016.06.085

Zhang, D., Wang, F., Shen, X., Yi, W., Li, Z., Li, Y., & Tian, C. (2018). Comparison study on fuel properties of hydrochars produced from corn stalk and corn stalk digestate. *Energy*, *165*, 527–536. https://doi.org/10.1016/j.energy.2018.09.174

Zhang, X., Zhang, Y., Ngo, H. H., Guo, W., Wen, H., Zhang, D., Li, C., & Qi, L. (2020). Characterization and sulfonamide antibiotics adsorption capacity of spent coffee grounds based biochar and hydrochar. *Science of The Total Environment*, *716*, 137015. https://doi.org/10.1016/j.scitotenv.2020.137015

Zhang, Y., Jiang, Q., Xie, W., Wang, Y., & Kang, J. (2019). Effects of temperature, time and acidity of hydrothermal carbonization on the hydrochar properties and nitrogen recovery from corn

stover. *Biomass and Bioenergy*, *122*, 175–182.

https://doi.org/10.1016/j.biombioe.2019.01.035

Zhao, K., Li, Y., Zhou, Y., Guo, W., Jiang, H., & Xu, Q. (2018). Characterization of hydrothermal

carbonization products (hydrochars and spent liquor) and their biomethane production

performance. *Bioresource Technology*, *267*, 9–16.

https://doi.org/10.1016/j.biortech.2018.07.006

Zhou, J.-H., Shen, G.-Z., Zhu, J., & Yuan, W.-K. (2006). Terephthalic Acid Hydropurification over

Pd/C Catalyst. In *Studies in Surface Science and Catalysis* (Vol. 159, pp. 293–296). Elsevier.

https://doi.org/10.1016/S0167-2991(06)81591-0

Żuk-Gołaszewska, K., & Gołaszewski, J. (2018). Cannabis sativa L. – Cultivation and Quality of Raw

Material. *Journal of Elementology*, 14. https://doi.org/10.5601/jelem.2017.22.3.1500

Zuorro, A., Lavecchia, R., & Natali, S. (2014). Magnetically modified agro-industrial wastes as

efficient and easily recoverable adsorbents for water treatment. *Chemical Engineering*

Transactions, *38*, 349–354. https://doi.org/10.3303/CET1438059

Supplementary materials

In this section all the pictures of the operational procedure and samples, both solid and liquid, and additional data are collected.

S.1.   Methods

S.1.1.   Experimental set-up

Figure S.1 – High-pressure reactor (Berghof).

Figure S.2 – PTFE vessel and stainless-steel vessel.
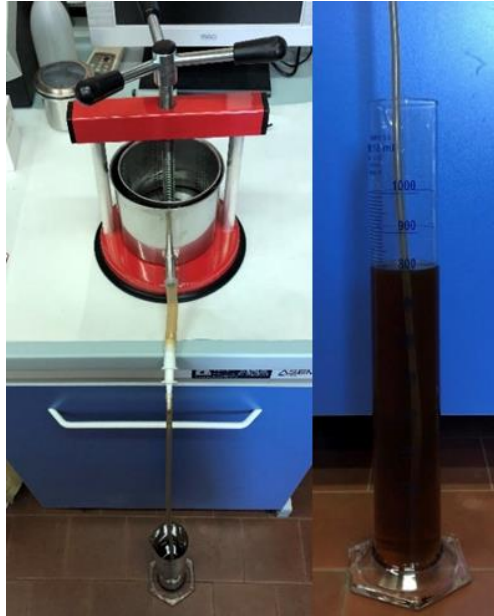
Figure S.3. Filter press and separation of PW from HC.

Figure S.4 – Wet hydrochar (from SCG) after separation through filter press.

Figure S.5 – Vacuum filtration of PW and PW filtered.

Figure S.6 – Solid residues (solid suspended) on acetate filter (0.45 µm) after PW filtration.

S.1.2. Acute toxicity tests
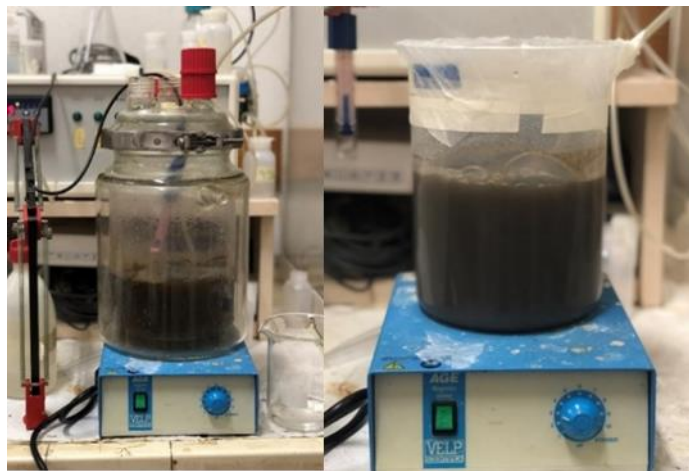
Figure S.7 – Batch reactor and biosensor for acute toxicity tests and activacted sludge.

S.1.3. Germination tests

Figure S.8 – Sphagnum Peat after sieving (< 10 mm).

Figure S.9 – Fist method for the water content determination for the mixture preparation in germination tests.

Figure S.10 – Mixture of HC (SCG) and peat for germination tests.

Figure S.11 – Washing phase for HC_220_1 with distilled water.

Figure S.12 – Washed wet hydrochar (SCG_220_1).

a) b) c)
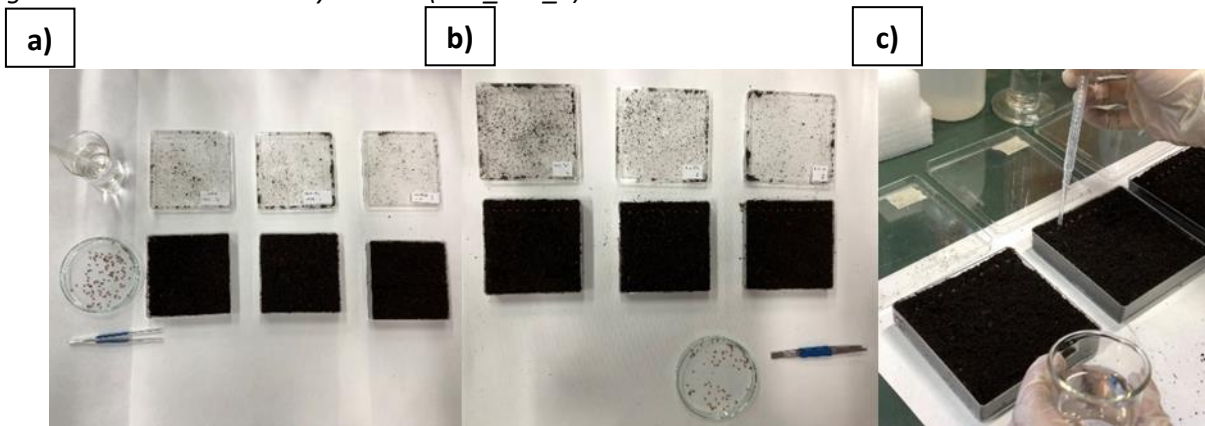
Figure S.13. a) Petri dishes filled with the mixtures, b) placing of seeds, and c) water drops adding upon each seed.
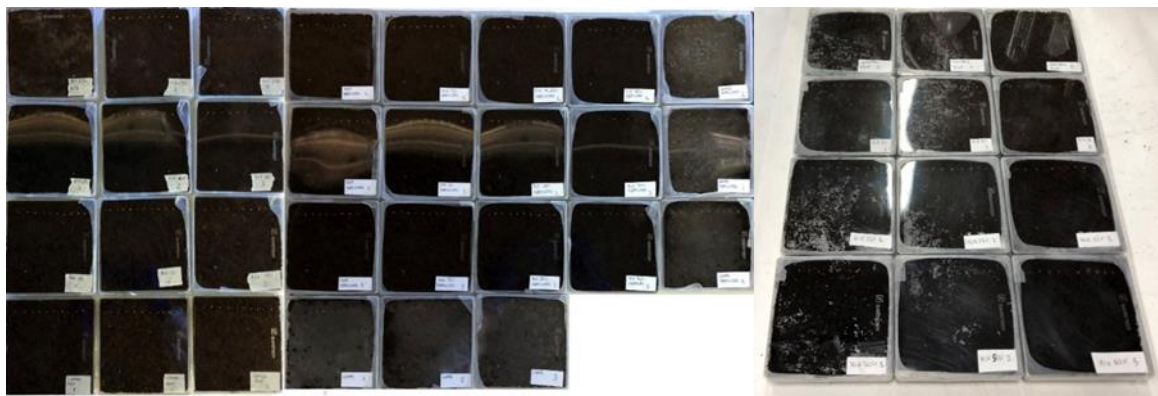
Figure S.14. Petri dishes before incubation containing different mixtures.
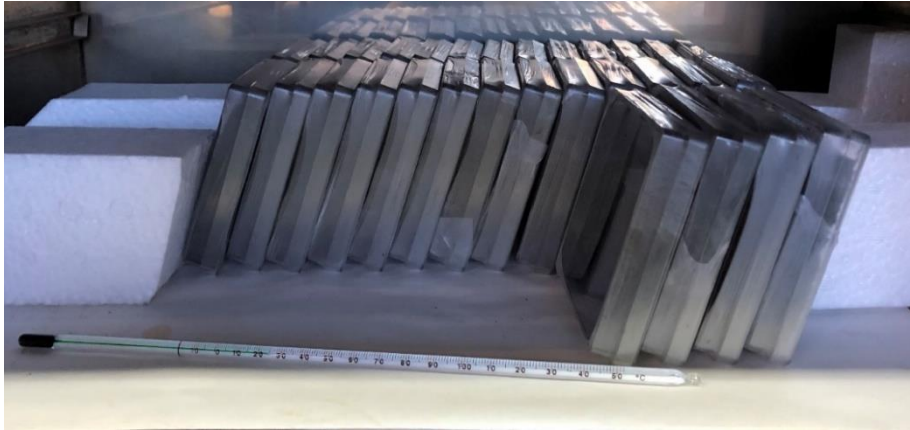
Figure S.15 – Petri dishes placed in oven at 25 °C for incubation with an agle of 70-80°.
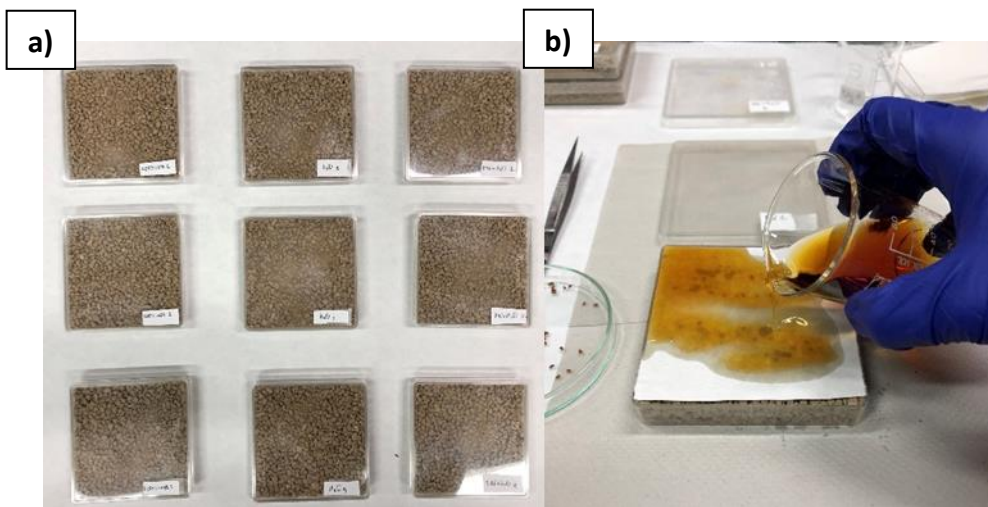
Figure S.16 – a) Petri dishes filled with perlite/pomice and b) preparation of germination tets with PW.

Figure S.17 – Crees seeds placed on the filter paper wet with PW, ready for incubation.
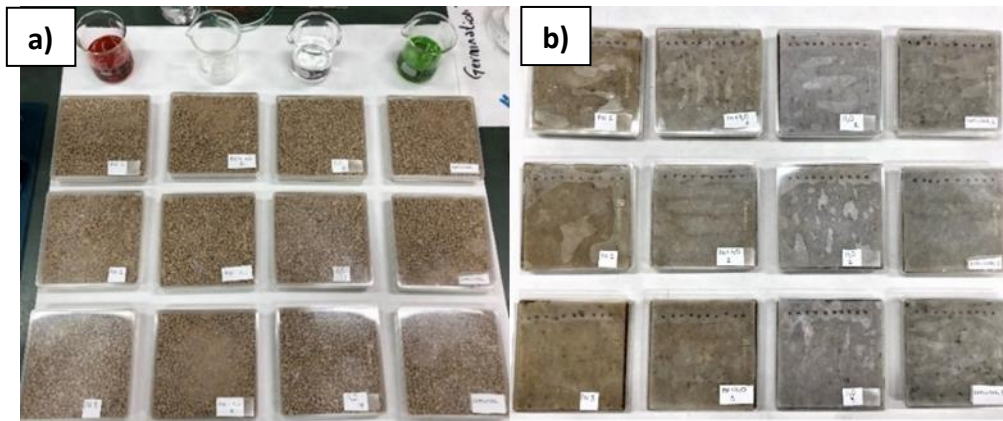
Figure S.18 – a) Materials used in germination tests with extracted liquids and b) Petri dishes after preparation.
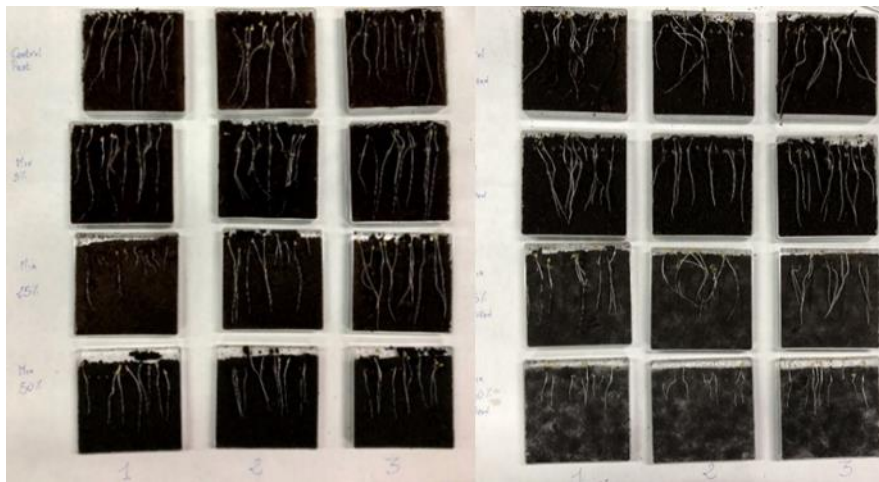
Figure S.19 - Result of germination tests conducted using HC from SCG and peat in different ratio.

Figure S.20 – Measuring seedlings and root length.

S.1.4. BMP tests

Figure S.21 – BMP tests: a) samples preparation, b) incubation, and c) biogas measurement.

S.2.   Materials

S.2.1.   Hemp digestate

Table S.1 – Pictures of hemp digestate and hydrochars produced at the different process conditions.

	Hemp digestate - D		
Feedstock			
	180 °C	**200 °C**	**220 °C**
1 h			
3 h			
6 h			
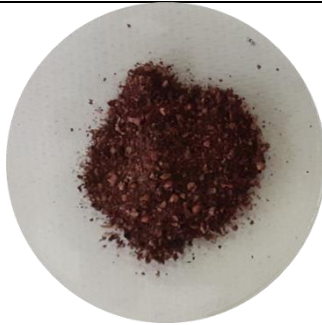
S.2.2.   Hemp

Table S.2 – Pictures of hemp and hydrochars produced at the different process conditions.

	Hemp - H		
Feedstock			
	180 °C	**200 °C**	**220 °C**
1 h			
3 h			

S.2.3. Grape marc

Table S.3 – Pictures of grape marc and grape marc extracted and hydrochars produced at 220 °C for 1h.

	Grape marc - GM	**Grape marc extracted – GM_Ext**
Feedstock		
	220 °C	
1 h		

S.2.4. Spent coffee grounds

Table S.4 – Pictures of spent coffee grounds and hydrochars produced at the different process conditions.

	Spent coffee grounds - SCG	
Feedstock		
	220 °C	**240 °C**
1 h		

S.2.5. Digestate from agro-industrial residues

Table S.5 – Pictures of digestate from agro-industrial residues and hydrochars produced at 220 °C for 1h.

Digestate from agro-industrial residues - DMIX

Feedstock

220 °C

1 h

S.2.6. Cigarettes butts

Table S.6 – Pictures of cigarette butts and hydrochars produced at the different process conditions.

Cigarette butts - CB	

Feedstock

220 °C	240 °C

1 h

3 h

Table S.7 – Pictures of HEETS cigarette butts and hydrochars produced at the different process conditions.

	Cigarette butts - CBH	
Feedstock		
	220 °C	**240 °C**
1 h		

Table S.8 – Pictures of the mix of cigarette butts and HEETS cigarette butts and hydrochars produced at 240 °C for 1h.

	Cigarette butts - CBM
Feedstock	
	240 °C
1 h	

S.2.7.   Covid19 waste – masks and gloves

Table S.9 – Pictures of surgical face masks and hydrochars produced at the different process conditions.

Masks - M

Feedstock	

220 °C

	Without acetic acid	**With acetic acid**
3 h		

Table S.10 – Pictures of latex gloves and hydrochars produced at the different process conditions.

Gloves

Feedstock

220 °C

Without acetic acid	With acetic acid

3 h

S.3. Additional data

S.3.1. Solid density

Table S.11 – Average solid yield of each HTC test and density (ρ) of the solid materials measured by helium-pycnometer (AccuPyc II 1340).

Samples	Solid yield [%]	ρ [g/cm^3]
SCG	-	1.331 (0.010)
SCG_220_1	58.79 (0.36)	1.278 (0.004)
SCG_240_1	51.94 (0.84)	1.270 (0.001)
Hemp	-	1.516 (0.002)
H_180_1	79.68 (1.55)	1.525 (0.004)
H_200_1	67.37 (3.80)	1.518 (0.003)
H_220_1	61.72 (4.35)	1.480 (0.002)
Hemp digestate	-	1.554 (0.002)
D_180_1	96.47 (0.68)	1.520 (0.002)
D_180_3	88.69 (0.70)	1.515 (0.001)
D_180_6	85.69 (0.64)	1.517 (0.001)
D_200_1	88.45 (1.43)	1.533 (0.004)
D_200_3	78.10 (1.05)	1.528 (0.002)
D_200_6	73.51 (0.85)	1.523 (0.001)
D_220_1	72.83 (1.08)	1.495 (0.002)
CBH	-	1.424 (0.002)
CBH_220_1	26.85 (0.53)	1.439 (0.001)
CBH_240_1	22.04 (1.19)	1.379 (0.001)
CB	-	1.340 (0.007)
CB_220_1	39.57 (0.98)	1.465 (0.002)
CB_240_1	31.96 (2.19)	1.449 (0.003)
CBM	-	1.382 (0.002)
CBM_220_1	28.03 (1.18)	1.425 (0.001)
GM	-	1.410 (0.001)
GM_220_1	59.63 (0.52)	1.344 (0.002)
GM_Ext	-	1.419 (0.002)
GM_Ext_220_1	62.28 (0.69)	1.347 (0.003)
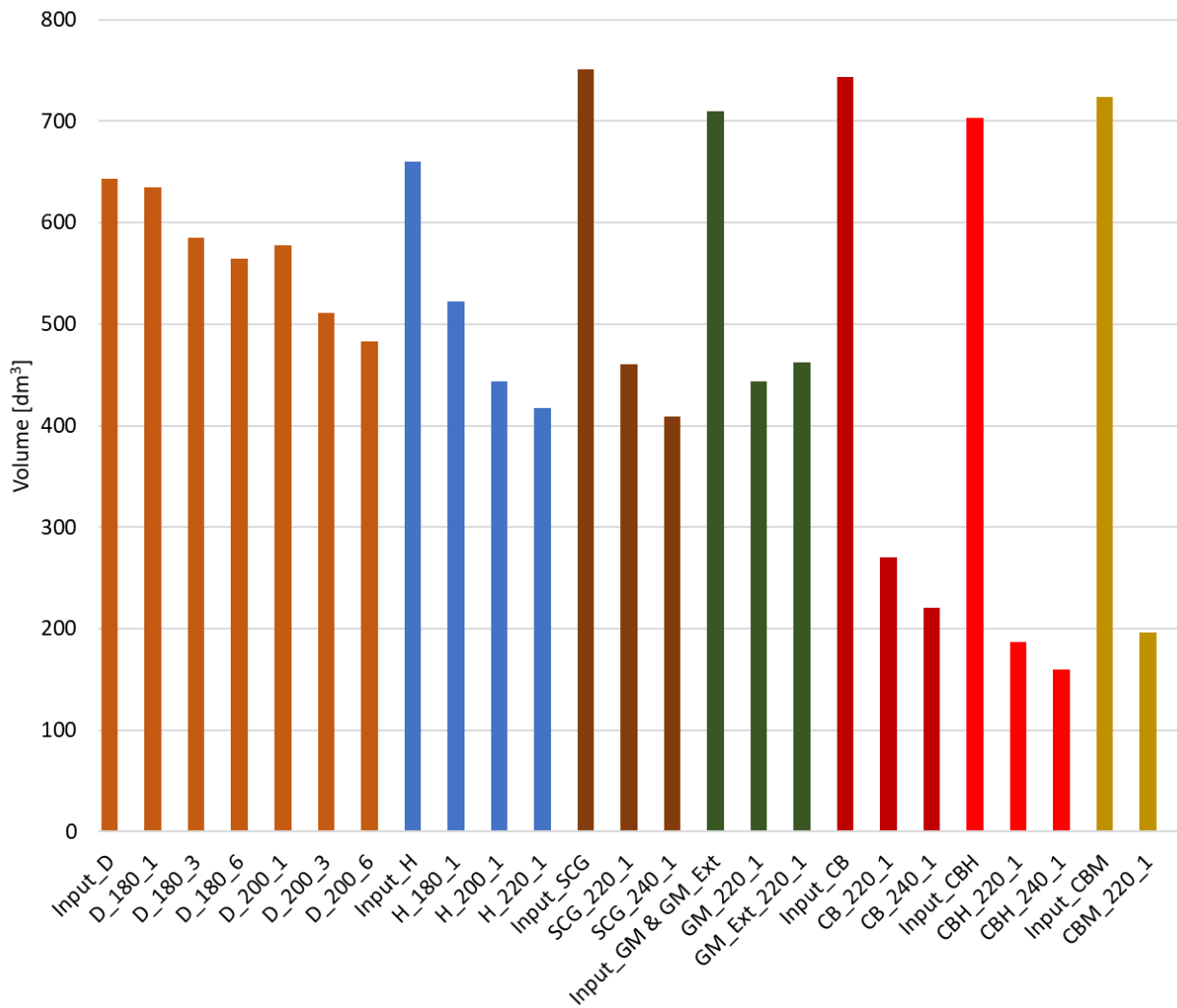
Figure S.22 – Input volume of each feedstock and related output volume according to the different HTC conditions considering the density of each material, the solid yield for each HTC tests, and the input HTC mass of 1 ton.
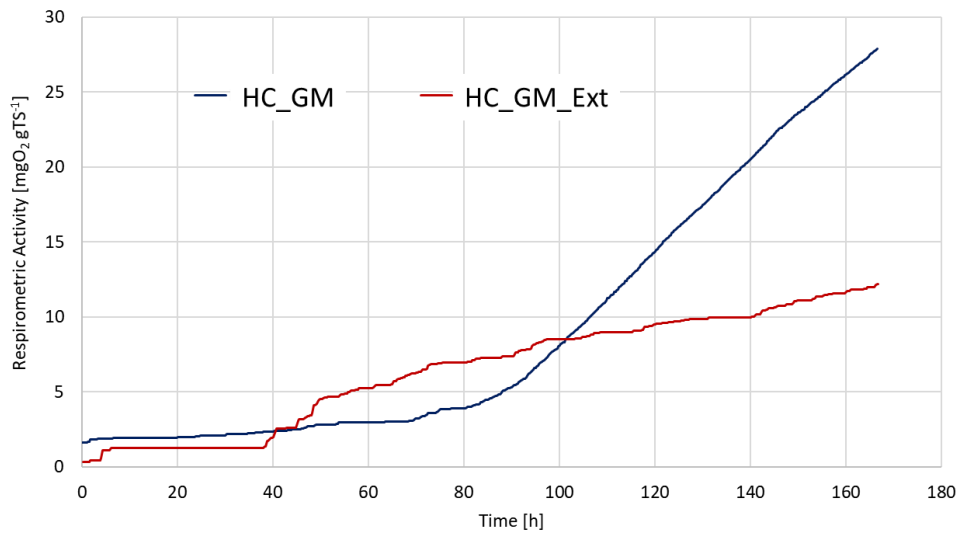
S.3.2. Respirometric activity

Figure S.23 – Respirometric activity index (RA) via SAPROMAT of HC_GM and HC_GM_Ext.
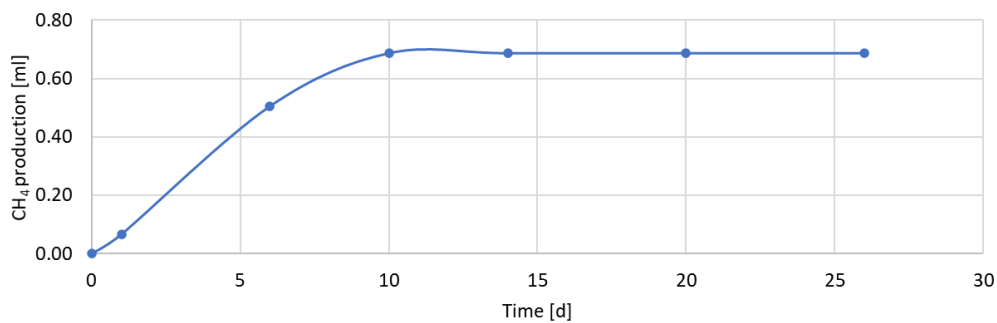
S.3.3. BMP tests

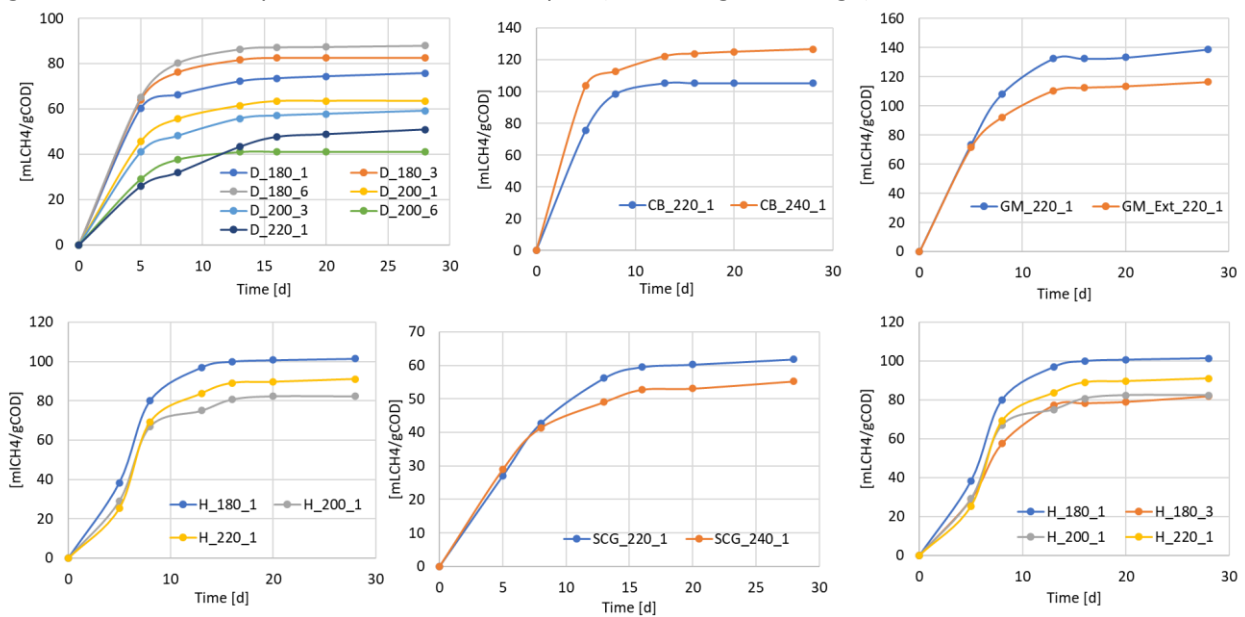*Figure S.24 – Methane production in blank samples (methanogenic sludge).*

Figure S.25 – Specific methane production from BMP test with different PWs.

S.3.4.   FTIR spectra
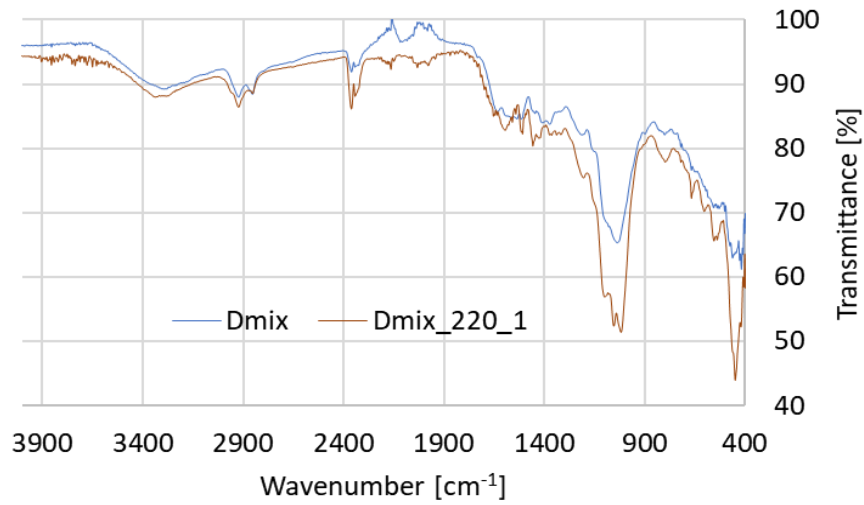
Figure S.26 – FTIR spectra of digestate from agricultural residues and hydrochar produced at 220 °C for 1h.
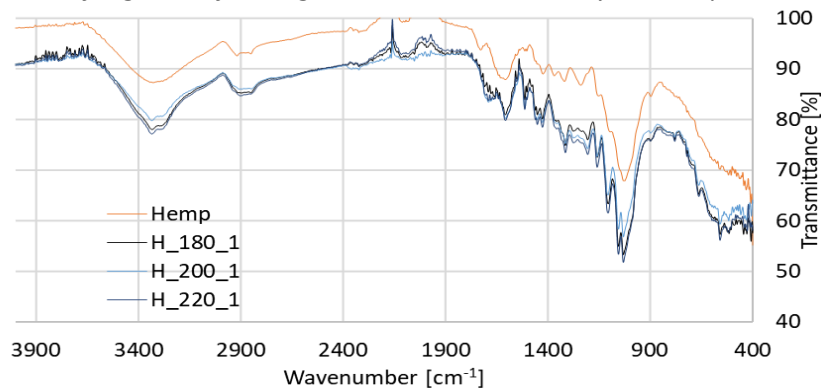

Figure S.27 – FTIR spectra of hemp and related hydrochars.
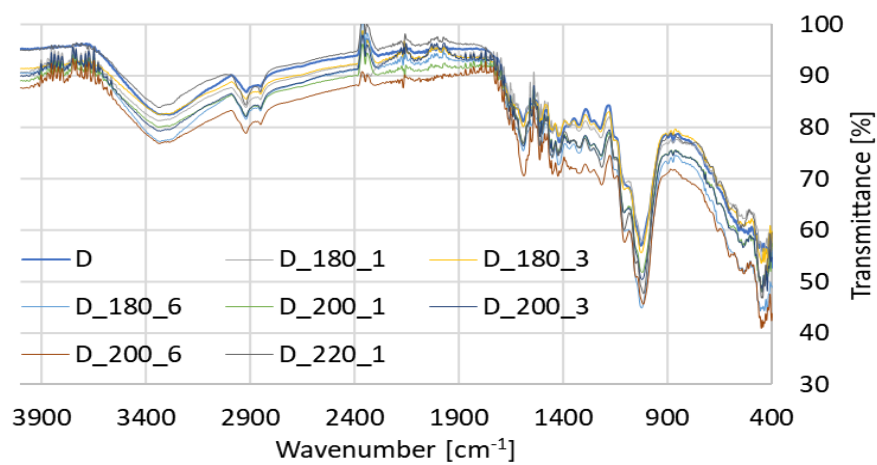

Figure S.28 – FTIR spectra of hemp digestate and related hydrochars.
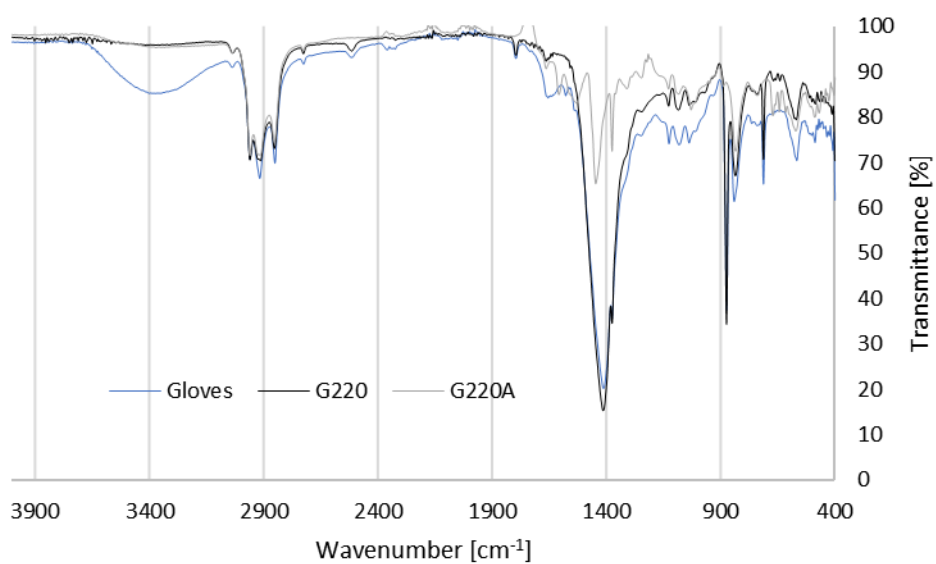
Figure S.29 – FTIR spectra of gloves and hydrochar produced at 220 °C for 3 h with and without the presence of acetic acid.
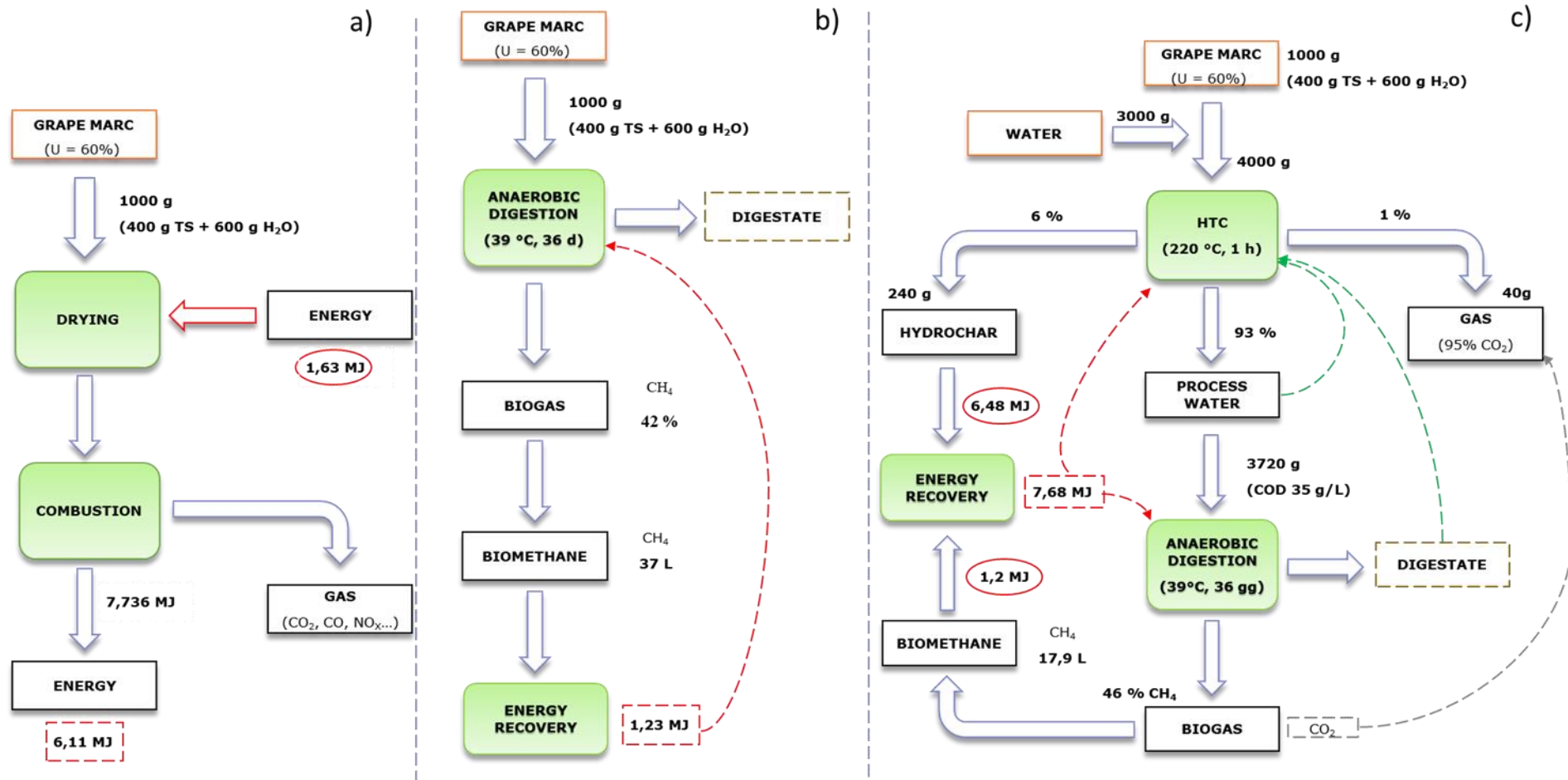
Figure S.30 - Simplified energy balance for the treatment of GM. a) Traditional combustion scheme where energy is lost due the humidity content; b) anaerobic digestion of GM; c) integration process scheme between HTC, AD, and combustion.